

# **Why do children with severe combined immunodeficiency get warts? The role of the common $\gamma$ -chain in skin immunity**

Thesis submitted for  
the Degree of Doctor of Philosophy  
in accordance with the requirements of the

**University College London, UCL**



**Karolin Nowak**

Molecular and Cellular Immunology Section  
Infection, Immunity, Inflammation and Physiological Medicine Programme  
Institute of Child Health

## Statement of declaration

I, Karolin Nowak, confirm that the work presented in this thesis is my own. Where information has been derived from other sources, I confirm that this has been indicated in the thesis.

A handwritten signature in blue ink, appearing to read 'K. Nowak', written in a cursive style.

## **Abstract**

X-linked severe combined immunodeficiency, caused by mutations in the common  $\gamma$ -chain, is characterized by absence of T and NK cells which leads to life-threatening infections. The disease can only be cured by bone marrow transplantation or gene therapy. Even after successful replacement of the T-cell compartment, patients display a persistent susceptibility to severe cutaneous human papillomavirus (HPV) infections. We hypothesized that persistent HPV susceptibility is due to residual  $\gamma$ -chain deficiency in keratinocytes.

The role of  $\gamma$ -chain in skin is unknown. In this thesis, we confirmed the expression of  $\gamma$ -chain in keratinocytes by reverse transcription PCR (RT-PCR) and flow cytometry and demonstrated that it is functional, mediating an increase in STAT5 and AKT phosphorylation in response to IL-2 and IL-15 stimulation. We then generated a  $\gamma$ -chain knock-down cell line which showed reduced levels of phospho-AKT after stimulation with IL-15 compared to control cells showing impaired signaling.

Using HPV pseudovirions, an increase of 50% in infectivity in knock-down cells compared to control cells was observed indicating an increase in initial infection. In an organotypic raft model using keratinocytes transfected with HPV18, we observed increased suprabasal DNA synthesis in knock-down cells indicating dysregulation of keratinocyte proliferation even though expression of HPV life cycle markers was unchanged.

Moreover, an increase in chemokine secretion after IL-15 stimulation was only observed in control but not in  $\gamma$ -chain deficient cells. These secreted levels of chemoattractants were able to induce migration of neutrophils, dendritic cells and CD4+ T cells. Using supernatants collected from keratinocytes transfected with HPV18 as chemoattractant, we saw altered migration towards supernatant from HPV18 positive  $\gamma$ -chain deficient cells compared to that of HPV18 positive control keratinocytes.

Together the results presented here suggest that  $\gamma$ -chain deficiency in keratinocytes leads to an increased susceptibility to HPV infection, altered regulation of infection and impaired immune cell recruitment.

## **Acknowledgements**

Three years and a tiny bit after I started working on this project, this thesis is finally done and now it is time to thank the following people without whom I would have never been able to do this project:

Number 1 has to be my amazing primary supervisor **Siobhan Burns** who has helped me so much during the whole PhD, who was always there to give advice and to listen when experiments were not working and to find a way to help me. Even though it was not always easy with working in two different places and everyone being busy, we always managed to find a way to make things work. Thank you so much!

A another huge thank you goes to my secondary supervisor **Wei Li Di** who taught me everything I needed to know about keratinocytes and who was also always there to listen to my experimental issues and gave me tips on how to solve my problems.

A big thank you also goes to **Adrian Thrasher** who was always supportive of and interested in my project and gave me interesting ideas for further experiments.

**Paul Lambert** and his lab members (especially Amy Liem, Aayushi Uberoi, Denis Lee and Kathleen Makielski) at the University of Madison-Wisconsin also deserve a big thank you for welcoming me so nicely, for teaching me so many things, for helping me all the time and for making my time in Madison so enjoyable and productive. Without them I would know significantly less about HPVs.

Further thanks go to **Daniela Linzner** who taught me how to isolate cells from blood, how to do neutrophil migration experiments and for making it so entertaining.

Thank you also to all the lovely healthy blood donors from the unit without whose cells I would not have been able to do so many experiments. Especially to **Roland, Kathryn, Yusuf** and **Dave** that gave me blood on multiple occasions.

Of course a big thank you to all the lovely people in MIU/MCI who had to deal with me and my occasional mood swings during this project and who helped to keep me sane, especially Miguel, Jo, Albert, Pili, Neelam and Marlene.

The very last but definitely not least thank you goes to **my parents** without whom I would not be who I am today, who are always supportive and who are the best parents anyone could ever wish for.

## TABLE OF CONTENTS

|   |           |
|---|-----------|
| Declaration   | 1         |
| Abstract  | 2         |
| Acknowledgements  | 3         |
| Table of Contents   | 4         |
| List of Figures   | 10        |
| List of Tables  | 12        |
| List of Abbreviations   | 13        |
| <br>  |           |
| <b>1. INTRODUCTION</b>  | <b>16</b> |
| <b>1.1 The skin</b>   | <b>17</b> |
| 1.1.1 Skin anatomy and skin cells   | 17        |
| 1.1.2 The differentiation programme of keratinocytes  | 19        |
| 1.1.3 The antigen-presenting cells of the skin  | 21        |
| 1.1.4 The immunological functions of keratinocytes  | 23        |
| <b>1.2 The human papilloma virus family</b>   | <b>25</b> |
| 1.2.1 Viral structure and genome  | 27        |
| 1.2.2 Papillomavirus life cycle   | 31        |
| 1.2.3 Mechanisms of HPV immune evasion  | 34        |
| 1.2.4 Regression, Persistence and Latency of HPV infections   | 37        |
| 1.2.5 The mouse papilloma virus   | 39        |
| <b>1.3 The common <math>\gamma</math>-chain and its cytokines</b>   | <b>42</b> |
| 1.3.1 The $\gamma$ -chain and its co-receptor   | 42        |
| 1.3.2 Signalling via the common $\gamma$ -chain   | 44        |
| 1.3.3 The effects of $\gamma$ -chain cytokines  | 47        |
| <b>1.4 Severe combined immunodeficiency (SCID) and other primary immunodeficiencies associated with <math>\gamma</math>-chain cytokines</b> | <b>49</b> |
| <b>1.5 HPV infections in SCID patients</b>  | <b>52</b> |
| <b>1.6 Hypothesis and Aim</b>   | <b>57</b> |

|  |           |
|--|-----------|
| <b>2. MATERIALS AND METHODS</b>  | <b>58</b> |
| <b>2.1 Materials</b>   | <b>59</b> |
| 2.1.1 General Supplies   | 59        |
| 2.1.2 Buffers and solutions  | 59        |
| 2.1.2.1 Commercial buffers   | 59        |
| 2.1.2.2 Buffers prepared in house  | 59        |
| 2.1.3 Antibodies   | 63        |
| 2.1.3.1 Antibodies for flow cytometry (FC)                                     | 63        |
| 2.1.3.2 Antibodies for Western Blot  | 65        |
| 2.1.3.3 Antibodies for Immunofluorescence                                      | 66        |
| 2.1.4 Enzymes  | 68        |
| 2.1.5 Cytokines  | 68        |
| 2.1.6 Primers  | 69        |
| 2.1.7 Probes and Standards   | 70        |
| 2.1.8 Tissue Culture   | 71        |
| 2.1.9 Cell lines   | 76        |
| 2.1.9.1 HEK 293T/17  | 76        |
| 2.1.9.2 293FT  | 76        |
| 2.1.9.3 ED-7R  | 76        |
| 2.1.9.4 NIKS   | 76        |
| 2.1.9.5 3T3  | 77        |
| 2.1.10 shRNA vectors   | 78        |
| 2.1.11 Others reagents   | 78        |
| <b>2.2 Methods</b>   | <b>80</b> |
| 2.2.1 Cell and tissue culture  | 80        |
| 2.2.1.1 Culturing of cells   | 80        |
| 2.2.1.2 Passaging cells  | 80        |
| 2.2.1.3 Isolation of primary keratinocytes                                     | 80        |
| 2.2.1.4 Lentiviral preparation   | 81        |
| 2.2.1.5 Titration of lentiviral particles by FC                                | 81        |
| 2.2.1.6 Lentiviral transduction of the NIKS cell line                          | 81        |
| 2.2.1.7 Puromycin selection of NIKS cells                                      | 82        |
| 2.2.1.8 Proliferation Assay using BrdU incorporation and FC                    | 82        |
| 2.2.1.9 Proliferation Assay using BrdU incorporation and a platereader         | 83        |
| 2.2.1.10 Production of HPV Virus-Like-Particles (VLP)                          | 83        |
| 2.2.1.11 Infectivity assay   | 84        |
| 2.2.1.12 Transfection of NIKS with HPV18wt vector                              | 85        |
| 2.2.1.13 Making organotypic rafts  | 85        |
| 2.2.1.14 Isolating peripheral blood mononuclear cells (PBMCs) from whole blood | 86        |
| 2.2.1.15 Isolation of CD14+ cells and differentiation to DCs                   | 86        |

|          |  |    |
|----------|--|----|
| 2.2.1.16 | Isolation of CD4+ and CD8+ T cells                             | 86 |
| 2.2.1.17 | Isolation of neutrophils                                       | 87 |
| 2.2.1.18 | Migration experiments using neutrophils                        | 87 |
| 2.2.1.19 | Migration experiments using DCs                                | 87 |
| 2.2.1.20 | Migration experiments using CD4+ and CD8+ T cells              | 88 |
| 2.2.2    | Protein Biology  | 89 |
| 2.2.2.1  | Cell lysis and sample preparation for Immunoblotting           | 89 |
| 2.2.2.2  | SDS-PAGE and Immunoblotting                                    | 89 |
| 2.2.2.3  | Surface Staining for FC  | 89 |
| 2.2.2.4  | Intracellular Staining for FC                                  | 90 |
| 2.2.2.5  | Analysis of JAK/STAT signalling by FC                          | 90 |
| 2.2.2.6  | Sample preparation for analysis of pAKT by immunoblotting      | 90 |
| 2.2.2.7  | Cytokine Array   | 91 |
| 2.2.2.8  | Luminex assay  | 91 |
| 2.2.3    | Molecular Biology  | 92 |
| 2.2.3.1  | Isolation of RNA   | 92 |
| 2.2.3.2  | Reverse transcription  | 92 |
| 2.2.3.3  | Polymerase chain reaction (PCR)                                | 92 |
| 2.2.3.4  | Quantitative PCR (qPCR)  | 93 |
| 2.2.3.5  | Agarose gels   | 93 |
| 2.2.3.6  | Plasmid DNA preparation  | 93 |
| 2.2.3.7  | Preparation of HPV18wt re-circularised plasmid                 | 93 |
| 2.2.3.8  | Isolating extrachromosomal DNA (HIRT-DNA)                      | 94 |
| 2.2.3.9  | Southern Blot  | 95 |
| 2.2.4    | Staining of paraffin embedded sections                         | 96 |
| 2.2.4.1  | Haematoxylin and Eosin staining                                | 96 |
| 2.2.4.2  | Immunofluorescent staining of paraffin embedded slides         | 96 |
| 2.2.4.3  | Making the probe for fluorescence in situ hybridisation (FISH) | 96 |
| 2.2.4.4  | FISH   | 97 |
| 2.2.5    | Animal experiments   | 98 |
| 2.2.5.1  | Infection with MmuPV1 particles                                | 98 |
| 2.2.5.2  | Grafting of ear skin onto the back of WT animals               | 98 |
| 2.2.6    | Data analysis and statistics                                   | 99 |

|            |  |            |
|------------|--|------------|
| <b>3.</b>  | <b>THE COMMON <math>\gamma</math>-CHAIN IS EXPRESSED AND FUNCTIONAL IN KERATINOCYTES</b> | <b>100</b> |
| <b>3.1</b> | <b>Introduction</b>  | <b>101</b> |
| <b>3.2</b> | <b>The <math>\gamma</math>-chain is expressed in keratinocytes</b>                       | <b>102</b> |
| <b>3.3</b> | <b>Multiple <math>\gamma</math>-chain co-receptors are expressed in keratinocytes</b>    | <b>104</b> |

|           |  |            |
|-----------|--|------------|
| 3.4       | Stimulation with $\gamma$ -chain cytokines induces phosphorylation of STAT5 in keratinocytes   | 107        |
| 3.5       | Stimulation with $\gamma$ -chain cytokines induces phosphorylation of AKT in keratinocytes   | 109        |
| 3.6       | Generation of a common $\gamma$ -chain knock-down cell line: Screening of shRNAs using the ED-7R cell line                                 | 110        |
| 3.7       | Generation of a common $\gamma$ -chain keratinocyte knock-down cell line   | 111        |
| 3.8       | Signalling mediated by $\gamma$ -chain is defective in knock-down keratinocyte cell line   | 114        |
| 3.9       | Discussion   | 116        |
| <b>4.</b> | <b>INFECTIVITY WITH PSEUDO- AND QUASIVIRIONS IS INCREASED IN <math>\gamma</math>-CHAIN DEFICIENT CELLS</b>                                 | <b>118</b> |
| 4.1       | Introduction   | 119        |
| 4.2       | Preparation of HPV18 wt plasmid  | 122        |
| 4.3       | Making HPV quasivirions  | 124        |
| 4.4       | Infectivity using pseudovirions is increased in $\gamma$ -chain deficient keratinocytes  | 127        |
| 4.5       | Proliferation is not changed between different NIKS cell lines   | 131        |
| 4.6       | Infectivity using quasivirions is increased in $\gamma$ -chain deficient keratinocytes   | 133        |
| 4.7       | Discussion   | 136        |
| <b>5.</b> | <b>CONTROL OF HPV IS ALTERED IN KERATINOCYTES LACKING FUNCTIONAL <math>\gamma</math>-CHAIN</b>   | <b>139</b> |
| 5.1       | Introduction   | 140        |
| 5.2       | $\gamma$ -chain deficiency in keratinocytes does not influence keratinocyte proliferation and differentiation in organotypic raft cultures | 142        |
| 5.3       | HPV genomes are maintained over multiple passages in scr control and KD NIKS   | 145        |
| 5.4       | HPV does not affect the proliferation in $\gamma$ -chain deficient keratinocytes cultured as a monolayer                                   | 147        |

|           |  |            |
|-----------|--|------------|
| 5.5       | Presence of HPV18 affects the differentiation and proliferation of rafts made with $\gamma$ -chain deficient keratinocytes     | 148        |
| 5.6       | $\gamma$ -chain deficiency in keratinocytes does not affect HPV18 life cycle in organotypic rafts                              | 153        |
| 5.7       | Discussion   | 155        |
| <b>6.</b> | <b>CHEMOKINE SECRETION IN <math>\gamma</math>-CHAIN DEFICIENT KERATINOCYTES IS ALTERED AND REDUCES IMMUNE CELL RECRUITMENT</b> | <b>157</b> |
| 6.1       | Introduction   | 158        |
| 6.2       | Cytokine and chemokine secretion is not changed after infection with HPV quasivirions  | 159        |
| 6.3       | Cytokine array shows cytokines and chemokines differentially secreted after IL-7 and IL-15 stimulation                         | 162        |
| 6.4       | IL-8, Mip-3 $\alpha$ and Gro- $\alpha$ are induced following stimulation with IL-15  | 166        |
| 6.5       | Levels of IL-8, Gro- $\alpha$ and Mip-3 $\alpha$ secreted by keratinocytes are able to attract neutrophils                     | 169        |
| 6.6       | Dendritic cell migration is stimulated by IL-8, Mip-3 $\alpha$ and Gro- $\alpha$   | 172        |
| 6.7       | IL-8, Mip-3 $\alpha$ and Gro- $\alpha$ are able to attract CD4+ T cells  | 174        |
| 6.8       | Gro- $\alpha$ secretion is increased in HPV18 positive control cells but not in $\gamma$ -chain deficient cells                | 176        |
| 6.9       | Higher Gro- $\alpha$ concentrations attract less CD4+ T cells  | 178        |
| 6.10      | HPV18 presence in control but not in $\gamma$ -chain deficient cells leads to increased attraction of CD4+ T cells             | 180        |
| 6.11      | HPV18 presence only in $\gamma$ -chain deficient but not in control cells leads to increased attraction of CD8+ T cells        | 182        |
| 6.12      | Discussion   | 184        |
| <b>7.</b> | <b>FINAL DISCUSSION</b>  | <b>188</b> |
| 7.1       | The absence of the common $\gamma$ -chain affects HPV infection at multiple stages   | 189        |
| 7.2       | Potential treatment options of X-SCID  | 193        |

|           |   |            |
|-----------|---|------------|
| 7.3       | Future experiments  | 195        |
| 7.4       | Relevance of this project to patients   | 197        |
| <b>8.</b> | <b>APPENDIX – USING MMUPV1 IN <math>\gamma</math>-CHAIN DEFICIENT MICE TO STUDY INFECTION</b> | <b>198</b> |
| 8.1       | Introduction  | 199        |
| 8.2       | MmuPV1 infection can successfully be established in $\gamma$ -chain KO mice                   | 200        |
| 8.3       | Skin grafting model for studying HPV infection in X-SCID skin                                 | 201        |
| 8.4       | No lesions develop using the initial skin graft model for MmuPV1 infection studies            | 202        |
| 8.5       | Discussion  | 203        |
| <b>9.</b> | <b>REFERENCES</b>   | <b>205</b> |

## List of Figures

|   |     |
|---|-----|
| Figure 1: Skin anatomy and cells  | 18  |
| Figure 2: Map of the circular HPV18 reference genome  | 28  |
| Figure 3: Effect of HPV16 E6 and E7 on cycle progression  | 30  |
| Figure 4: Life cycle of high-risk HPVs  | 33  |
| Figure 5: Receptors for $\gamma$ -chain cytokines   | 43  |
| Figure 6: Signalling via the common $\gamma$ -chain   | 46  |
| Figure 8: Expression of $\gamma$ -chain mRNA and protein in keratinocytes                       | 103 |
| Figure 9: Expression of $\gamma$ -chain co-receptors mRNA                                       | 105 |
| Figure 10: Expression of $\gamma$ -chain co-receptors   | 106 |
| Figure 11: Phosphorylation of STAT5 NIKS cells after stimulation with $\gamma$ -chain cytokines | 108 |
| Figure 12: Phosphorylation of AKT after stimulation with $\gamma$ -chain cytokines              | 109 |
| Figure 13: Knock-down of $\gamma$ -chain in ED-7R + $\gamma$ c cells                            | 110 |
| Figure 14: Knock-down of $\gamma$ -chain protein using shRNA3                                   | 112 |
| Figure 15: Knock-down of $\gamma$ -chain mRNA   | 113 |
| Figure 16: pAKT levels in $\gamma$ -chain knock-down and control cells after IL-15 stimulation  | 115 |
| Figure 17: Reconstruction of HPV18wt plasmid  | 123 |
| Figure 18: Identifying HPV18 quasivirions containing fractions                                  | 125 |
| Figure 19: Titering HPV18 quasivirions  | 126 |
| Figure 20: Levels of infectivity in NIKS cell lines 48 h post pseudovirion infection            | 127 |
| Figure 21: Levels of infectivity in NIKS cultured in different media                            | 129 |
| Figure 22: Infectivity with pseudovirions after stimulation with $\gamma$ -chain cytokines      | 130 |
| Figure 23: Proliferation of NIKS cell lines   | 132 |
| Figure 24: Validation of E1 <sup>4</sup> qPCR assay   | 134 |
| Figure 25: Infectivity in NIKS cell lines using HPV18 quasivirions                              | 135 |
| Figure 26: H&E staining of HPV negative rafts   | 143 |
| Figure 27: Keratin-10, Keratin-14, Loricrin and BrdU staining in HPV negative rafts             | 144 |
| Figure 28: Maintenance of HPV18 genomes in transfected NIKS cells                               | 146 |
| Figure 29: DNA synthesis in HPV18 positive NIKS cell lines infected with HPV18                  | 147 |
| Figure 30: H&E staining and Keratin-14 and Loricrin staining of HPV18 positive rafts            | 150 |
| Figure 31: Keratin-10 and BrdU staining of HPV18 positive rafts                                 | 151 |
| Figure 32: Quantification of BrdU positive cells in HPV18 positive rafts                        | 152 |

|  |     |
|--|-----|
| Figure 33: Expression of HPV markers E4 and MCM7 and fluorescent-in-situ hybridisation (FISH) for HPV18 genome expression in matured rafts | 154 |
| Figure 34: Secreted cytokines and chemokines after infection with HPV18 quasivirions   | 159 |
| Figure 35: Secretion of cytokines in untransduced NIKS after IL-7 and IL-15 stimulation  | 163 |
| Figure 36: Secretion of IP-10, IL-1 $\alpha$ and RANTES after different stimulations   | 167 |
| Figure 37: Secretion of Gro- $\alpha$ , IL-8 and Mip-3 $\alpha$ after IL-7 and IL-15 stimulation   | 168 |
| Figure 38: Neutrophil migration towards different chemoattractants   | 170 |
| Figure 39: Neutrophil migration towards different chemoattractants   | 171 |
| Figure 40: Dendritic cell migration towards Gro- $\alpha$ , IL-8 and Mip-3 $\alpha$  | 173 |
| Figure 41: CD4+ T cell migration towards different cytokines   | 175 |
| Figure 42: Secretion of Gro- $\alpha$ , IL-8 and Mip-3 $\alpha$ in HPV18 positive NIKS   | 177 |
| Figure 43: Migration of CD4+ T cells towards different concentrations of Gro- $\alpha$   | 179 |
| Figure 44: CD4+ T cell migration towards supernatants from HPV positive and negative NIKS  | 181 |
| Figure 45: CD8+ T cell migration towards supernatants from HPV positive and negative NIKS  | 183 |
| Figure 46: Model for the effect of $\gamma$ -chain deficiency on HPV infection   | 191 |
| Figure 47: Successful skin transplant on a mouse   | 201 |

## List of Tables

|   |     |
|---|-----|
| Table 1: Characteristics of immune cells in HPV regression vs. persistence      | 38  |
| Table 2: Commercial buffers used  | 59  |
| Table 3: Isotype controls for FC  | 63  |
| Table 4: Antibodies for specific immunogens for FC                              | 64  |
| Table 5: Primary antibodies for Western Blot                                    | 65  |
| Table 6: Secondary antibodies for Western Blot                                  | 66  |
| Table 7: Primary antibodies for Immunofluorescence                              | 67  |
| Table 8: Secondary antibodies for Immunofluorescence                            | 67  |
| Table 9: Enzymes  | 68  |
| Table 10: Cytokines   | 69  |
| Table 11: Primers   | 70  |
| Table 12: Tissue culture reagents   | 75  |
| Table 13: shRNA vectors   | 78  |
| Table 14: Other reagents  | 79  |
| Table 15: Chemokine and cytokine secretion after quasivirion infection          | 160 |
| Table 16: Quantification of the cytokine array after IL-7 and IL-15 stimulation | 164 |
| Table 17: Formation of wart lesions in mice                                     | 200 |

## List of abbreviations

|        |  |
|--------|--|
| ADA    | adenosine deaminase                              |
| BMT    | bone marrow transplantation                      |
| BPV    | bovine papilloma virus                           |
| CD     | Cluster of differentiation                       |
| cDC    | conventional dendritic cell                      |
| CDK    | cyclin-dependent kinases                         |
| CLL    | chronic lymphocytic leukaemia                    |
| COPV   | canine oral papilloma virus                      |
| CRPV   | cottontail rabbit papilloma virus                |
| DC     | dendritic cell                                   |
| dDC    | dermal dendritic cell                            |
| DNA    | deoxyribonucleic acid                            |
| dsDNA  | double-stranded DNA viruses                      |
| E6-AP  | E6-associated protein                            |
| EBV    | Epstein-Barr-virus                               |
| ECM    | extracellular matrix                             |
| EDC    | epidermal differentiation complex                |
| ELISA  | Enzyme-linked immunosorbent assay                |
| ERK    | extracellular signal regulated kinase            |
| EV     | Epidermodysplasia Verruciformis                  |
| FC     | Flow cytometry                                   |
| FDA    | Food and Drug Administration                     |
| fMLP   | N-Formylmethionyl-leucyl-phenylalanine           |
| GAG    | glycosaminoglycan                                |
| GAPDH  | Glyceraldehyde 3-phosphate dehydrogenase         |
| GFP    | green fluorescent protein                        |
| GM-CSF | Granulocyte-macrophage-colony-stimulating-factor |
| Gro    | Growth-regulated-protein                         |
| GSK    | GlaxoSmithKline                                  |
| GT     | gene therapy                                     |
| GVHD   | graft-versus-host-disease                        |
| FISH   | fluorescent-in-situ-hybridisation                |
| HLA    | human leukocyte antigen                          |
| HPKC   | human primary keratinocytes                      |
| HPV    | human papilloma virus                            |
| HSCT   | haematopoietic stem cell transplantation         |

|        |  |
|--------|--|
| HSPG   | heparin sulphate proteoglycans                                 |
| HSV    | herpes simplex virus   |
| ICAM   | intracellular adhesion molecule                                |
| IFN    | interferon   |
| Ig     | immunoglobulin   |
| IL     | interleukin  |
| IP-10  | interferon- $\gamma$ - inducible protein 10                    |
| JAK    | Janus-kinase   |
| K%     | keratin-%  |
| KD     | knock-down   |
| LC     | Langerhans cell  |
| LCR    | long control region  |
| LFA    | Lymphocyte-function-associated-antigen                         |
| LMP    | low molecular protein  |
| M&M    | Materials and Methods  |
| MAPK   | RAS-mitogen-activated protein kinase                           |
| MCP-1  | monocyte-chemoattractant-protein-1                             |
| McPV   | Mastomys coucha papilloma virus                                |
| MHC    | Major-histocompatibility-complex                               |
| Mig    | Monokine-induced-by-gamma-interferon                           |
| Mip    | Macrophage-inflammatory-protein                                |
| MmuPV  | Mus musculus papilloma virus                                   |
| MFD    | match family donor   |
| MSD    | Match-sibling donor  |
| NK     | natural killer   |
| ORF    | open-reading frame   |
| pAKT   | phosphorylated Akt   |
| PBMCs  | peripheral blood mononuclear cells                             |
| PCR    | polymerase chain reaction                                      |
| pDC    | plasmacytoid dendritic cell                                    |
| PI3K   | phosphoinositide 3-kinase                                      |
| pRB    | retinoblastoma protein   |
| PRR    | pattern-recognition receptors                                  |
| PV     | papilloma virus  |
| RANTES | Regulated-on-activation,-normal-T-cells-expressed-and-secreted |
| RLU    | relative light units   |
| RNA    | Ribonucleic acid   |
| ROPV   | rabbit oral PV   |
| RT-PCR | reverse transcription PCR                                      |

|        |  |
|--------|--|
| SCID   | Severe combined immunodeficiency                           |
| scr    | scrambled  |
| SH     | Scr-homology   |
| SCC    | squamous cell carcinoma                                    |
| STAT   | Signal-Transducers-and-Activators-of-Transcription         |
| TAP    | transporters of antigenic protein                          |
| TCGF   | T cell growth factor                                       |
| TG     | Transglutaminases  |
| Th     | T helper cell  |
| TLR    | Toll-like receptor   |
| TNF    | Tumor-necrosis-factor                                      |
| TSLP   | thymic stromal lymphopoietin                               |
| URR    | upstream regulatory region                                 |
| UV     | ultraviolet  |
| Vge    | viral-genome equivalents                                   |
| VLP    | virus-like particle  |
| WHIM   | Warts, Hypogammaglobulinemia, Infections and Myelokathexis |
| WHO    | World Health Organization                                  |
| wt     | wild-type  |
| XCR    | XC-chemokine receptor                                      |
| X-SCID | X-linked severe combined immunodeficiency                  |

# 1. Introduction

## 1.1 The skin

### 1.1.1 Skin anatomy and skin cells

The skin is the external cover of the body and one of its largest organs accounting for 15 – 20% of its mass. It has many essential functions as a barrier to the outside world. It is important to withstand chemical and physical traumas of everyday activities, e.g. as a mechanical barrier, permeability barrier and UV protection. It protects the host from harmful pathogens in the surrounding environment as an immune organ and against dehydration by retaining body fluids. It is also involved in sensation and homeostasis (e.g. thermoregulation) as well as excretion and endocrine functions (e.g. secretion of hormones, cytokines and growth factors).

The skin is made up of two distinct layers: the epidermis and the dermis which are separated by the basement membrane. The epidermis is further subdivided into multiple layers: the basal layer (stratum basale), spinous layer (stratum spinosum), granular layer (stratum granulosum) and the stratum corneum. Certain areas of the skin such as palms and soles (the so-called “thick” skin) also include a stratum lucidum (“clear layer”) which is also considered to be part of the stratum corneum (reviewed in (1-3) and compare with Figure 1).

The epidermis mainly consists of keratinocytes (~85%) but it also contains melanocytes (~5%), Langerhans cells (2-5%) and Merkel cells (6-10%) (3). It is not fully clear, yet, what the role of Merkel cells is. They are proposed to be important for somatosensation. As such they form slowly adapting touch receptors. They have also been considered to have endocrine functions and chemosensitive functions (4). Melanocytes are specialised cells that produce the pigment melanin which helps protect the body from UV radiation. The rate of melanin production determines the skin tone. They are mainly confined to the basal layer (5). Langerhans cells are specialised antigen-presenting cells of the epidermis and they are most prominent in the stratum spinosum (6).

The dermis is made up of connective tissue matrix and specialised immune cells such as dermal dendritic cells (dDCs) and T cells as well as mast cells and macrophages. It also contains fibroblasts, hair follicles, various glands as well as lymphatic and blood vessels (reviewed in (7)).

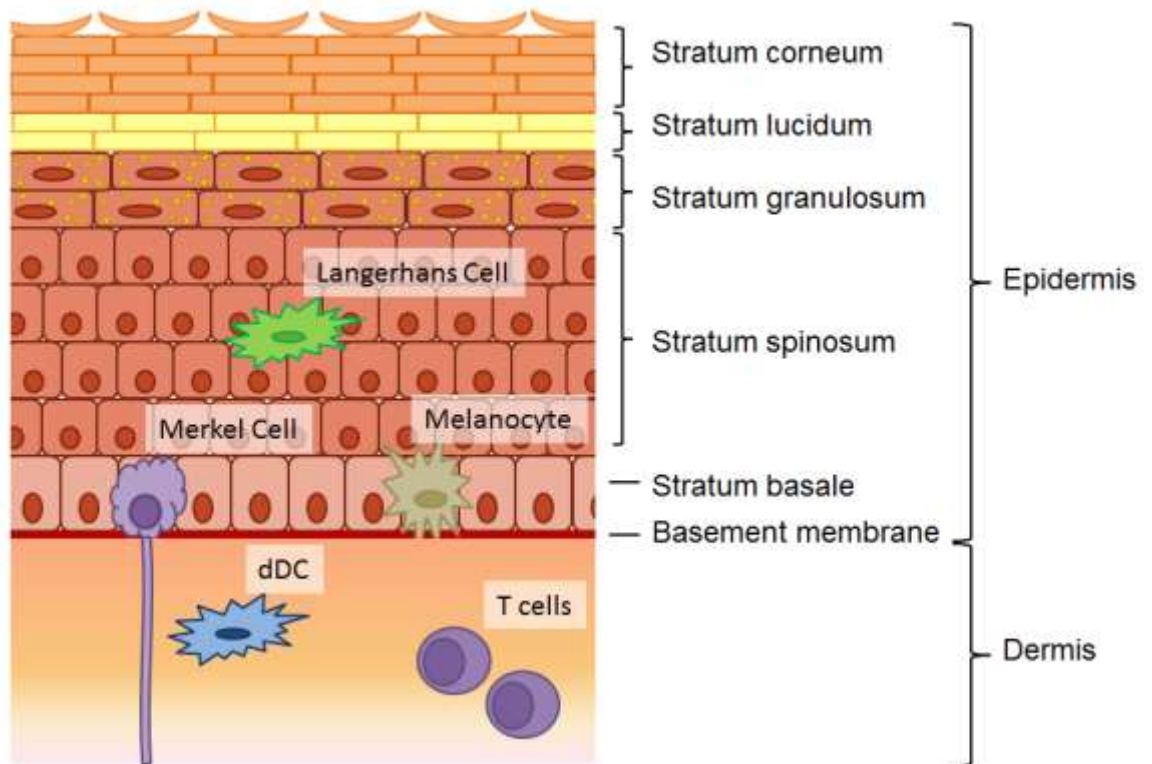


**Figure 1: Skin anatomy and cells**

The skin is made up of two distinct layers, the epidermis and the dermis which are separated by the basement membrane. The epidermis is further subdivided into four (“thin” epidermis) or five (“thick” epidermis, shown here) layers. It mainly consists of keratinocytes but Langerhans cells, melanocytes and Merkel cells are also present. The dermis consists of connective tissue matrix and contains immune cells such as dendritic cell (DC) subsets, e.g. dermal DCs, and different T cells subsets. Other cell types – which are not shown here – such as mast cells, macrophages and fibroblasts are also found in the dermis. Adapted from Nestle et. al., 2009, (7).

### 1.1.2 The differentiation programme of keratinocytes

One of the most important functions of the skin is its role as a protective barrier. The efficiency of the barrier formation depends on the correct execution of the differentiation programme of the keratinocytes in the epidermis.

In the epidermis only the basal layer contains stem cells or amplifying cells; incorporation of nucleotide analogues such as BrdU usually cannot be observed in any other layer. When keratinocytes start to leave this layer and move upwards, they lose their proliferative capabilities and begin terminal differentiation. As cells pass from the basal to granular layers, they increase in size, however, their nuclear size stays the same (8, 9).

The family of the 54 keratins accounts for some of the most important proteins inside keratinocytes. They constitute around 15-25% of the protein in basal cells but this number increases to more than 85% in the fully differentiated squamous cells (reviewed in (10)). During the course of terminal differentiation, there are changes in synthesis and therefore expression of different keratins. Inner layers (e.g. basal and spinous layers) only synthesize smaller keratins, whereas the outer layers of the epidermis express both large and small ones. In the stratum corneum there is no synthesis of keratins (9). Inside cells, keratins span the cytoplasm and anchor to the cytoplasmic plaques of desmosomes and hemi-desmosomes. That means that keratins are important for integrity and mechanical stability of single cells as well as epithelial tissues. They also provide attachment to the basement membrane (11).

There are two different groups of keratins: acidic type I keratins and basic type II keratins with heterodimers forming between a member of each group. Basal cells express the type II keratin keratin-5 (K5) and type I keratin K14. When the cells enter the suprabasal layers and become post-mitotic, expression of K5 and K14 ceases while type II K1 and type I K10 are induced. Their expression is an early indicator that a cell has undergone commitment for terminal differentiation. Filaments formed of K1 and K10 self-aggregate more than K5 and K14 filaments and they are less easily solubilised (9, 10, 12, 13). The epidermis also expresses other keratins such as K20 which is a marker for Merkel cells. A wide range of keratins (at least 26) is specifically expressed in hair-follicles and hair fibres (reviewed in (11, 14)).

During differentiation, a gene cluster named "epidermal differentiation complex" (EDC) is expressed. It encodes for the proteins involucrin, loricrin and filaggrin (15). Loricrin is a major component of the cornified envelope. It is highly insoluble and it is made during the later stages of terminal differentiation (16). Involucrin is synthesized when the cells

leave the basal layer and crosslinked by the enzyme transglutaminase (TG) in the later stages of differentiation (17, 18). Filaggrin is the main component of the keratohyalin granules which are the defining characteristic of the stratum granulosum. It enables the aggregation of keratin filaments into dense macrofibrils in the stratum corneum. It is also important for maintaining epidermal hydration as it is degraded to free amino acids in the upper stratum corneum (19-21).

In addition to changes and crosslinking of the protein filaments to form the cornified envelope, the organelles and the intracellular content of keratinocytes are replaced by a compact proteinaceous cytoskeleton and the resulting corneocytes are linked to a multicellular structure which is biologically dead. The process of cornification is a special type of cell death different from apoptosis and necrosis. Various anti-apoptotic and anti-necrotic mechanisms are employed by keratinocytes to avoid untimely death. What the intermediate stages of organelle breakdown look like is largely unknown (reviewed in (15)).

The skin continuously self-renews over the course of an individual's life and therefore, there must be different stem cell populations within the skin. The potential for long-term self-renewal differentiates a stem cell from a progenitor cell as the latter can only self-renew short-time. There are different stem cell populations in the skin. The hair follicle and melanocyte stem cells reside in the bulge of the hair follicle. In follicular epidermis, these hair follicle stem cells can also be mobilised to repair damaged epidermis (reviewed in (22) and (23)). In interfollicular epidermis, the basal epidermal layer is made up of self-renewing stem cells and progenitors which express K5 and K14. The progenitor cells receive pro-proliferative signals from the dermal fibroblast to give rise to the terminally differentiated cells that form the suprabasal layers and are eventually shed from the surface (24, 25).

The process from leaving the basal cell layer to desquamation and shedding from the skin surface takes around 2 – 4 weeks. This takes place throughout life and therefore, the cells of the adult epidermis are replaced every few weeks (14).

### 1.1.3 The antigen-presenting cells of the skin

The skin is not only a physical barrier to the outside world but it is also an important immune organ providing protection from pathogens in the surroundings. It is also home to around  $10^{12}$  bacteria per  $m^2$  which act a barrier against colonialization with pathogenic bacteria. In addition, there is continuous trafficking of immune cells between the skin, the draining lymph nodes and the periphery. The immune system of the skin is mainly formed of different DC population in dermis and epidermis, tissue resident T cells and keratinocytes (26).

The skin DC population can be divided into two main groups: LCs which are resident in the suprabasal layers of the epidermis and dermal DCs (dDCs) which are found just below the dermal-epidermal junction in the dermis (7).

LCs are characterised by the presence of Birbeck granules which are intracytoplasmic organelles. The expression of langerin in mice and CD1a in humans has been used to differentiate them from other cell types. They are derived from yolk-sac derived myeloid precursors and fetal liver derived monocytes. They acquire a mature morphology directly after birth and undergo extensive proliferation between day 2 and 7 after birth (27, 28). Afterwards, they self-renew in the skin under steady state conditions throughout life and are not replaced by bone marrow derived precursors cells (29).

LCs are radio-resistant and they have close interactions with the keratinocytes that surround them via E-cadherin. When LCs mature they downregulate E-cadherin to dissociate from keratinocytes and to be able to migrate across the basement membrane (30). LCs have the ability to take up antigens, migrate to local draining lymph nodes and prime naïve T cells, especially CD8+ T cells. In addition, they are able to secrete chemokines and cytokines (31). It has mostly been suggested that LCs have immunosuppressive or tolerance-inducing functions, e.g. antigen-specific contact hypersensitivity responses are enhanced in the absence of LCs and they protect mice from allergic contact dermatitis by inducing tolerance, deletion of allergen-specific T cells and activation of Tregs (32, 33). They might also have functional plasticity inducing activation of T cells depending on the signal they detect (34).

There are different types of dermal DCs in the dermis including plasmacytoid DCs (pDCs), conventional DCs (cDCs) and monocyte-derived DCs. Of these three types, pDCs are only found in the dermis during inflammation (34). dDCs and monocyte-derived DCs are found in the healthy dermis and in contrast to LCs, have short life-span and are replaced by bone-marrow derived precursors in around 7 days. cDCs

originate from a subpopulation called pre-cDCs and monocyte-derived DCs are derived from blood LYC6<sup>hi</sup> monocytes (35-37).

cDCs can transport cutaneous antigens to the T cell zones of the draining lymph nodes and present to and activate naïve T cells, leading to clonal expansion and acquisition of T cell effector functions. Monocyte-derived DCs are very similar to cDCs. They are also able to present antigens to naïve T cells, however, they have poor migratory ability and are therefore more suited to activate skin-tropic T cells (reviewed in (34)). Overall, dDCs have higher migratory abilities than LCs and they arrive earlier in the draining lymph nodes than LCs and both groups colonise distinct areas (30).

In conclusion, the presence of different types of antigen-presenting cells in the skin is probably due to functional specialisation of the different cell types. They continuously patrol both epidermis and dermis to detect incoming pathogens and to be able to activate T cell immune responses. However, important immune modulatory functions are provided not only by the skin-resident DCs and LCs, but also the keratinocytes.

#### 1.1.4 The immunological functions of keratinocytes

Keratinocytes are often considered to be the first immune sentinel that is encountered by pathogens when they enter the skin. They as such play an important role in immune responses as they express various pattern-recognition receptors (PRRs), have the ability to secrete immune modulatory molecules and can present antigens.

Various studies have shown that keratinocytes express many different Toll-like receptors such as TLR-1, 2, 4, 5 and 6 on their cell surface and TLR-3 and TLR-9 in their endosomes. TLR expression can be regulated by mycobacteria, viruses or other pathogen related products. Their activation leads to activation of the nuclear factor B and interferon regulatory factor pathways resulting in secretion of type I interferons (IFN) and tumour necrosis factor (TNF)  $\alpha$ . The expression of other surface PRR such as the C-type lectin dectin-1 is inducible on keratinocytes. Keratinocytes also express cytosolic PRRs such as NOD-like receptors and the RIG-like helicase receptors such as RIG-I, MDA-5 and protein kinase R, which are important for detection of intracellular pathogens such as viruses (26, 38-42). As keratinocytes express a variety of PRRs, they can screen and recognise pathogens when they enter the skin. PRR ligation activates innate immune responses resulting in secretion of chemotactic and proinflammatory molecules and thereby activation of other immune cells (43).

One consequence of keratinocyte stimulation by pathogens or wounding of the skin barrier is the secretion of a wide range of chemokines which can attract various professional immune cells such as DCs, LCs and T cells. These chemokines include Interferon- $\gamma$ -inducible protein 10 (IP-10) / CXCL-10, Monokine-induced-by-gamma-interferon (Mig) / CXCL-9 and Regulated-on-activation,-normal-T-cells-expressed-and-secreted (RANTES) / CCL5 which can attract T cells, Macrophage-inflammatory-protein 3 $\alpha$  (Mip-3 $\alpha$ ) / CCL20 which attracts LCs and DCs, and Interleukin (IL) 8 and Growth-regulated-protein  $\alpha$  (Gro- $\alpha$ ) to attract neutrophils. Apart from chemokines, inflammatory and immunological mediators such as TNF- $\alpha$ , IFN- $\gamma$  and Granulocyte-macrophage-colony-stimulating-factor (GM-CSF) are also released (44-46). TNF- $\alpha$  is a cytokine of the acute phase reaction, it induces apoptosis and inflammation and can inhibit viral replication and tumourigenesis (47). IFN- $\gamma$  has antiviral, immunoregulatory and anti-tumour properties, e.g. it promotes NK cell activity, promotes differentiation of CD4+ T cells to Th1 cells and increases antigen presentation of macrophages (48). GM-CSF is leukocyte growth factor as it stimulates the production of granulocytes and monocytes from stem cells (49). As a consequence of the secretion of these various cytokines and chemokines neutrophils, macrophages and T lymphocytes are recruited

and infiltrate the affected tissue leading to an orchestrated immune response against pathogens or induction of wound repair (26).

While keratinocytes clearly have role in recruiting professional immune cells, they can also act as antigen-presenting cells. Keratinocytes express various molecules that are necessary for antigen-presentation to T cells. They constitutively express major-histocompatibility-complex (MHC) class I and they can be stimulated by IFN- $\gamma$  to express MHC class II (50, 51). They also express low levels of the co-stimulatory molecule CD86 (51). However, the other co-stimulatory molecule, CD80 cannot be detected on keratinocytes unless stimulated with allergens or irritants (52). Keratinocytes also express Intracellular-adhesion-molecule (ICAM) 1 which is a component of the immune synapse required for intercellular interactions (53).

Initial studies of the antigen-presenting potential of keratinocytes showed induction of tolerance or anergy but did not show activation of T cells (reviewed in (43) and in (7)). Keratinocytes are therefore considered to be non-professional antigen-presenting cells and can only re-activate T cells that have been primed by professional antigen-presenting cells (51). However, in an *in vivo* model, LCs and dDCs cells were dispensable for the induction of keratinocyte-directed CD8+ T cell responses suggesting that keratinocytes might be able to prime naïve T cells as the two professional antigen-presenting cell subsets were absent (54). In any case, activation of T cells by keratinocytes is not as efficient as activation by DCs.

In conclusion, keratinocytes provide not only a physical protection from the outside world but they are also important to mount an immune response against pathogens. They are able to not only sense them but also recruit immune cells by secretion of chemokines. Keratinocytes also act as antigen-presenting cells. However, many aspects about the interaction between keratinocytes and the immune system remain unknown and require further study.

## 1.2 The human papilloma virus family

Papilloma viruses (PV) are a family of small, non-enveloped, double-stranded DNA viruses with a circular genome of approximately 8 kb. More than 170 human papilloma virus (HPV) genotypes have been identified of which many have been found in clinical lesions. In addition, over 60 animal PVs have been sequenced, infecting e.g. cow (*Bos Taurus*, bovine PVs, 13 types), dog (*Canis familiaris*, canine PVs, 15 types), horse (*Equus caballus*, 7 types), dolphin (*Tursiops truncatus*, 7 types), mouse (the newly discovered MmuPV1), different bird and different turtle species and a variety of other species (Papillomavirus Episteme (PaVE), <http://pave.niaid.nih.gov/>) and it is hypothesized that PVs are ubiquitously present in all present day amniotes (55). In fact, they are so widely expressed that porcine PVs can be found in ground pork purchased from supermarkets (56).

Different HPVs are associated with disease manifestations ranging from causing benign epithelial proliferation such as warts to different forms of cancer (55, 57). In fact, HPVs are associated with causing nearly all cervical cancers and HPVs can also be causative for cancers of the head and neck, penis, vagina, vulva and anus. Cervical cancer is one of the most common cancers with an estimated 530,000 new cases in 2012 and one of the cancers leading to most deaths in women, with 270,000 deaths in 2012, most of them (85%) in developing countries (<http://www.who.int/mediacentre/factsheets/fs380/en/>).

PVs are divided into 29 different genera based on DNA sequence analysis of the L1 protein which is well conserved and can be aligned for the known PVs. HPVs have been divided into five groups while other mammalian PVs occupy 20 genera, avian three and reptile PVs one. Most PV types in one genus have less than 60% of L1 sequence identity with PVs from other genera. These groups are associated with different life cycle characteristics, target tissue and pathogenicity (58, 59).

Supergroup A or  $\alpha$ -papillomaviruses contains mucosal and cutaneous HPV types, including the high-risk mucosal HPV types whose DNA are found in nearly all cases of cervical cancers. They initially cause mucosal lesions that can progress to high-grade neoplasia and cancer in some individuals. HPV16 and HPV18 are the two high-risk viruses which are found in more than 70% of all cervical cancers. HPV31, HPV33, HPV45 and HPV58 account for a further 15% of cervical cancer cases with no HPV type identified in just 5% of affected individuals. In total, 12 HPV types have been defined by the World Health Organization (WHO) as being cancer-causing (the six mentioned before above along with 35, 39, 51, 52, 56 and 59) (55, 60, 61). Moreover,

HPVs are also the causative agent in 90% of anal cancer cases, 40% of vaginal, vulvar and penile cancers as well as 35% of oropharyngeal and 25% of oral cavity cancers. Again, HPV16 and HPV18 are the main HPV types found in these HPV positive cancers ranging from 60% for penile cancers to more than 90% for anal, oropharyngeal and oral cavity cancers (62). The  $\alpha$ -PV group also contains the low-risk mucosal types that cause benign lesions such as genital warts. HPV6 and 11 are causative in 90% of cases but they are generally not considered to cause cancer (60). In addition, low-risk cutaneous HPV types such as HPV2 and HPV57 which cause common warts and HPV3 and HPV10 causative of flat warts are also part of supergroup A (55, 63).

The second major group are the  $\beta$ -papilloma viruses or the supergroup B. It includes high-risk and low-risk cutaneous types and is typically associated with inapparent or latent infections in the general population (55). However, immunocompromised individuals and Epidermodysplasia Verruciformis (EV) patients are more susceptible to infections with these viruses where they can proliferate and form open infections (64). Persistent infections with  $\beta$ -types are associated with development of squamous cell carcinoma (SCC) of the skin especially in immunosuppressed individuals and EV patients but the link has also been shown in immunocompetent people (65). HPV types such as HPV5, HPV14 and HPV36 are members of this group (58).

The third group are the  $\gamma$ -papillomaviruses which cause benign lesions in the general population and the resulting warts resemble those caused by  $\alpha$ -PVs but their DNA is only very rarely detected in skin cancers. HPV4 belongs to this group (55, 58).

Mu- and Nu-papillomaviruses make up the final two HPV groups. They usually cause benign cutaneous infections in the general population. Mu-PV lesions are usually found at palmar and plantar epithelial sites and they are not associated with cancer. So far, the two members of this group are HPV1 and HPV63. Even though it is mostly found in benign infections, Nu-PV DNA is occasionally found in skin cancers and its only member is HPV41 (55, 58).

### 1.2.1 Viral structure and genome

HPVs belong to the Virus Group I after the Baltimore classification which describes double-stranded DNA viruses (dsDNA virus). They contain a circular, double-stranded relatively small genome of 8 kb (66). The genome can be divided in three main parts: the non-coding upstream regulatory region (URR) which is also known as long control region (LCR) and the “early” and the “late” region (see Figure 2).

The URR contains the viral origin of replication, sequences required for genome maintenance and transcriptional enhancers and promoters. This region is highly conserved between different PVs (67, 68).

The late region contains the genes for L1 and L2 which code for the structural HPV proteins (the major and minor capsid proteins). They are expressed in the late stages of the viral life cycle. L1 is the major capsid protein; the capsid contains 360 copies of L1 organised into 72 pentamers called capsomeres (69). Up to 72 copies of L2 are contained within the capsid mostly hidden inside the virus lumen (70). Together they form a so-called T = 7 icosahedral capsid of approximately 55 – 60 nm which surrounds the viral DNA which is organised in chromatin form (69).

In contrast to the late region, the early region codes for the non-structural proteins. It contains six to seven open-reading frames (ORFs). It generally codes for the early genes E1, E2, E4, E5, E6 and E7 but some PVs contain an extra ORF for a small E8 protein. The early genes are important for replication, immune evasion and enhancing proliferation of the infected keratinocytes (63).

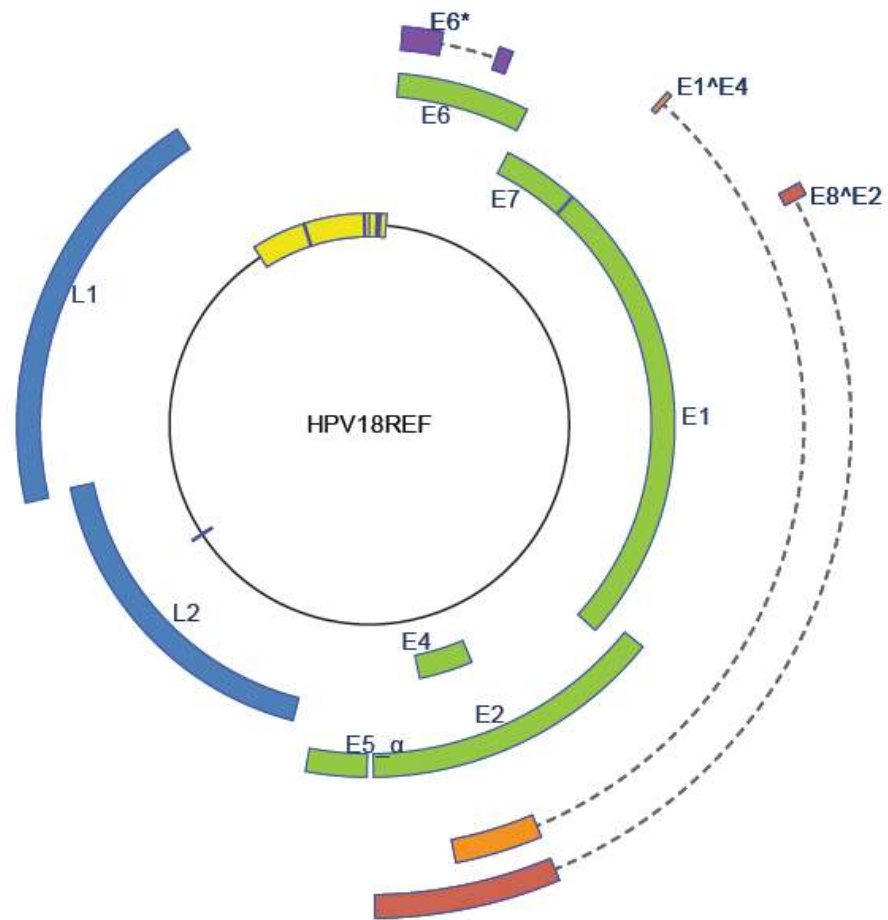


**Figure 2: Map of the circular HPV18 reference genome**

HPV18 was chosen as a typical example of a high-risk  $\alpha$ -type HPV genome. The early region of the HPV18 genome encodes for six ORFs E1, E2, E4, E5, E6 and E7 (shown in green) and the late region encodes the two capsid proteins L1 and L2 (shown in blue). Also shown are the spliced variants for E1 $\wedge$ 4 (orange), E8 $\wedge$ 2 (red) and E6\* (purple). The upstream regulatory region (URR) is shown in yellow, taken from PaVE (<http://pave.niaid.nih.gov/>).

HPV replication is dependent on the cellular DNA synthesis machinery as the virus itself does not encode any polymerases. PVs are able to re-programme the cell's DNA replication machinery to serve for their own replication. The early proteins E6 and E7 are importantly involved in these processes. E6 and E7 of high-risk HPV types are oncogenes that can interfere with the cell cycle control. These processes are best studied in HPV16 (71).

HPV E7 shares functional and structural similarities with oncogenes from other small DNA viruses such as the polyomavirus SV40 large tumour antigen and adenovirus E1A. They all contain a LXCXE motif which is the canonical binding site for retinoblastoma protein Rb (pRB). HPV E7 can bind pRB and its related pocket proteins p107 and p130 and lead to their degradation (72, 73). This leads to the aberrant expression of the transcription factor E2F and as result E2F-mediated activation of cyclin A and E and therefore activation of the cell cycle (74, 75). In addition, HPV E7 prevents p21<sup>Cip1</sup>-and p27<sup>Kip1</sup>-mediated inhibition of cyclin-dependent kinases (CDK) such as CDK2 and induces S phase entry by bypassing the G0/G1 arrest (76, 77). These effects are important for carcinogenic progression and are pronounced in high-risk HPV types such HPV16 but markedly reduced in non-oncogenic types such as HPV6 (76).

The E7-induced activation of E2F also leads to stabilisation of p53 via activation of p14<sup>ARF</sup>. Stabilisation of p53 would normally induce cell cycle arrest or apoptosis (71). Here however, HPV E6 protein plays its role in cellular transformation as it induces ubiquitination-dependent degradation of p53 through interaction with the cellular protein E6-associated protein (E6-AP) (78, 79).

Together these abilities of high-risk HPV E6 and E7 are sufficient to override the G1/S checkpoint which allows viral DNA replication in non-dividing cells. This can also lead to deregulation of growth control and the development of cancer.

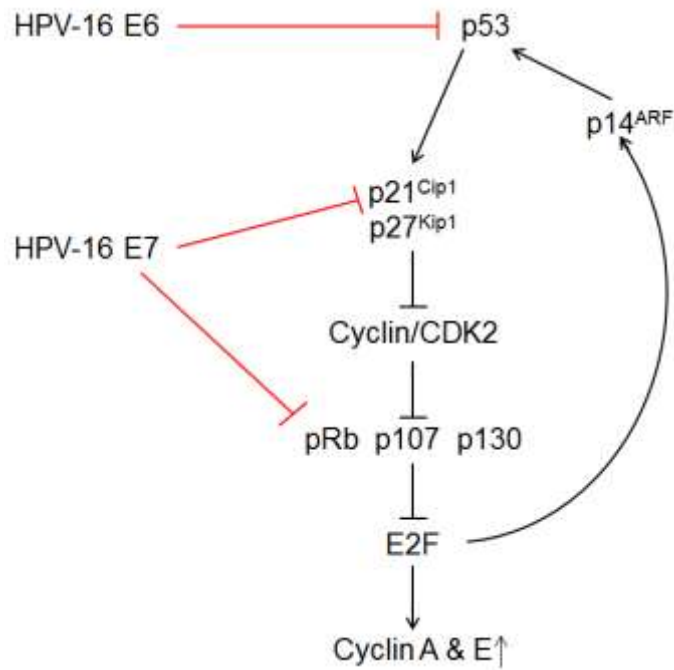


**Figure 3: Effect of HPV16 E6 and E7 on cycle progression**

HPV16 E6 and E7 can affect cell cycle progression. HPV16 E6 binds and degrades p53 and HPV16 E7 degrades pRb and the other pocket proteins, p107 and p130. As a result, E2F-mediated activation of cyclin A and E leads to cycle progression without passing through the appropriate cell cycle checkpoints (adapted from (71)).

### 1.2.2 Papillomavirus life cycle

HPVs are very successful pathogens. They usually induce chronic infections that rarely kill the host but shed large amounts of infectious virions. Moreover, the virus is very effective at evading the host's immune system which it manages by employing different mechanisms. One of the main reasons for its success is the exclusively intraepithelial nature of its life cycle. Infection and growth are dependent on complete keratinocyte differentiation and there is no evidence that viral genes are expressed in any other cell type than keratinocytes (reviewed in (80)).

Even though there are different HPV genera showing different pathogenicity and tropism, general principles of the life cycle are the same for all types (81). The virus life cycle begins by infection of the basal layer cells of the epidermis or the mucosal epithelium as a consequence of abrasion, wounding or microtrauma which exposes areas of the extracellular matrix (ECM), e.g. the basement membrane. It is generally thought that infection begins in epithelial stem cells (82, 83). For cutaneous HPV types it is thought that they enter via hair follicles infecting stem cells in this location and forming reservoirs which can be reactivated. HPV DNA has been found in plucked hair from both immunosuppressed individuals as well as healthy controls (84).

In order to enter the cell, PVs initially bind to cell surface receptors and to the ECM via the glycosaminoglycan (GAG) chains of heparin sulphate proteoglycans (HSPG). Different PV types (e.g. cutaneous vs. mucosal) recognise different forms of HSPGs (85, 86). For certain HPV types binding to the ECM can also occur via laminin 332 but this interaction is not conserved, e.g.  $\alpha 9$  types such as HPV16 use laminin 332 but  $\alpha 7$  members such as HPV18 do not (87). These pre-entry requirements might explain site preferences of HPV types.

After binding to the ECM, the PV particle changes conformation (88). These changes include exposure of the L2 protein which is usually found inside the virus lumen and its cleavage at the N-terminus by furin at sequence conserved amongst PVs. This cleavage is essential for successful infection (89).

The virus is then taken up into the cell and it is thought that a secondary receptor may trigger this uptake. However, no receptor has been identified so far and it has been suggested that in fact PVs do not bind to just one but multiple molecules (90). In addition, it is thought that the binding to the secondary receptor happens via L1 through a binding site that is only exposed after furin cleavage of L2 (82). After binding, PVs are taken up by endocytosis. It was initially thought that the endocytosis was clathrin- or caveolin-mediated, however, for HPV16 pseudovirions it was shown the process is clathrin-, caveolin-, flotillin-, cholesterol- and dynamin-independent but rather

dependent on actin dynamics. It is suggested that PV particles are taken up by a novel, ligand-activated pathway (91, 92).

After endocytosis, PVs are transported to endosomes where the virus is uncoated. The PV genome is then transported by the L2 protein into the nucleus via a currently unknown mechanism and the L1 protein is degraded in the lysosome (68, 90, 93). Inside the nucleus, transcription is initiated and the viral proteins are made.

Once the virus has entered the nucleus it is replicated in three different stages: establishment, maintenance and amplification (68).

Establishment is the replication process during which HPVs establishes itself as a multi-copy extrachromosomal replicon (= nuclear plasmid) in basal cells. The viral proteins E1 and E2 are required for this process (94, 95). After initial establishment, the infected cell undergoes cell division. During this process, the HPV genome is replicated and partitioned to daughter cells. In this maintenance phase, HPV is replicated at a constant copy number between 50 – 200 copies per cell. HPV E2 is important for the attachment of the genome to host cell chromatin and therefore necessary for maintenance (96). Depending on the HPV type, the expression of E6 and E7 proteins are also important for maintenance. For example, HPV16 and HPV31 E6 are essential for maintenance, while HPV18 is maintained without the presence of HPV18 E6 albeit at lower levels (97).

The final stage of replication is called amplification, vegetative replication or productive phase of the replication. It is restricted to the differentiated layers of the skin. At this stage, the viral genome is amplified to a high copy number and each cell can contain many thousands of virus copies (98).

After the viral genome is successfully amplified, it is packaged into the capsid. The late proteins L1 and L2 are expressed and the icosahedral capsid is assembled in the nucleus. The virus matures in the superficial, dying keratinocytes which involves formation of disulphide bonds between the L1 monomers (99, 100). The virions are shed from dying cells and released into the surroundings in a passive manner.

The viral life cycle dictates where certain viral components can be detected: viral DNA and E4 are detected in the suprabasal layers, whereas E6 and E7 are expressed throughout the epithelium. L1 and L2 proteins are only expressed in the superficial layer of the epithelium (compare with Figure 4 and (55, 101)).

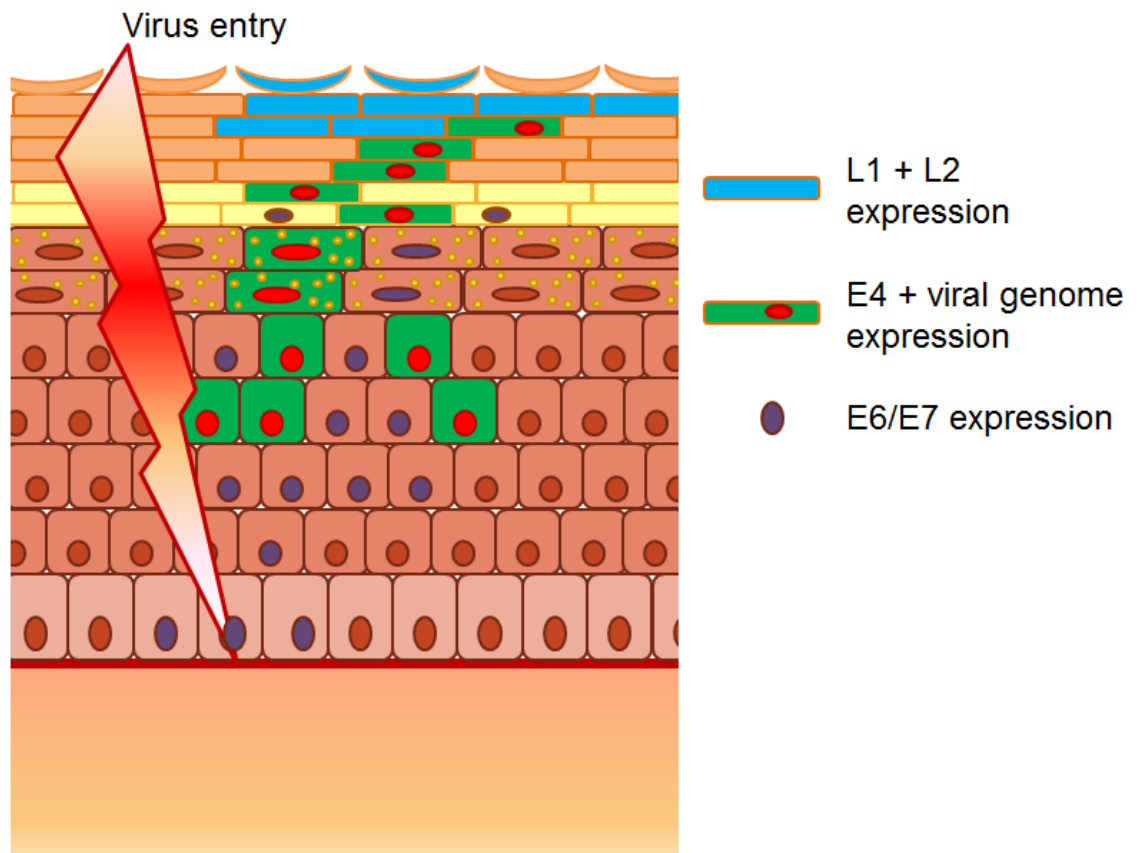


**Figure 4: Life cycle of high-risk HPVs**

HPVs enter via a micro-wound and infect basal cells of the epidermis. The genome is maintained at low copy number there. As cells divide the genomes are distributed between the daughter cells which will undergo their normal life cycle and move up inside the layers. Different virus proteins are expressed in different layers of the skin. Viral genomes are amplified in suprabasal layers where normally no DNA synthesis occurs. Virions are formed in the upper layers and shed from there. Adapted from Doorbar et.al. 2012 (55).

### 1.2.3 Mechanisms of HPV immune evasion

As previously mentioned, HPVs are very successful pathogens. They have developed multiple strategies to evade the immune system.

One of the strategies employed by HPVs is to keep a “low profile” as it is exclusively intra-epithelial. Viral particles are only formed and shed from external and differentiated cells that are destined to die, thereby reducing the exposure to the host immune system. The life cycle is non-lytic and does not induce any inflammatory signals to activate an immune response. The E proteins which are present in lower layers of the epidermis are expressed at low levels and mainly in the cell nuclei. In addition, the highly immunogenic L1 and L2 proteins are only expressed in the outer layers and therefore “hidden” from the immune system meaning that presentation of viral peptides to the immune cells is very limited. There is also no blood-borne or viremic phase of the infection leaving HPV essentially invisible to the immune system as most of the life cycle takes place in relative distance to the immune cells of the dermis. In addition, even though LCs can detect presence of the virus, HPV has developed multiple strategies to avoid their recruitment (80, 102, 103).

HPV is not only “hidden” from the immune system but its proteins directly affect the activation of the innate immune system. As already described keratinocytes express a range of TLRs that can detect viral DNA and RNA whose activation lead to production of type I interferons and to Th1-type cytotoxic responses via activation of interferon regulatory factor (IRF) and nuclear factor of  $\kappa$ -light chain enhancer of activated B cells (NF $\kappa$ B) pathways. Type I interferons (e.g. IFN- $\alpha$ , - $\beta$  and - $\lambda$ ) have antiviral, antiproliferative and immunostimulatory properties, e.g. stimulation of DCs. In addition keratinocytes are able to secrete chemokines and cytokines to recruit and activate other immune cells (7, 44-46, 104, 105).

High risk HPVs are able to influence innate immune signalling, e.g. interferon and IRF signalling as well as the NF $\kappa$ B and inflammasome pathways. They can also affect the adaptive immune response by changing MHC surface expression and peptide presentation. In addition, HPV alters the normal growth and apoptosis programmes of keratinocytes after infection ((106) and reviewed in (107)).

In particular, IFN-inducible genes and TLRs are downregulated or their activation inhibited. HPV16 and to a lesser extent HPV18 are able to downregulate the expression of TLR9 (108). HPV16, 18 and 31 inhibit the expression of antiviral genes such as IFIT1 and MX1, IFN signalling components such as STAT1, pathogen recognition receptors such as TLR3, RIG-I and MDA5 as well as the proapoptotic genes TRAIL and XAF1. This correlates with a reduction in the induction of IFN- $\beta$  and the different IFN- $\lambda$ s after stimulation (109).

In addition, the high-risk HPV oncoproteins can also inhibit the production and the effects of different type I interferons, especially those of HPV16 and 18. HPV16 and 18 E7 interact with IRF-1 thereby inhibiting IRF-1 mediated activation of IFN- $\beta$ . E7 is also able to induce recruitment of histone deacetylases to the IFN- $\beta$  promoter interfering with IRF-1's trans-activating functions (110, 111).

HPV16 E6 protein (but not HPV18 E6) can bind to IRF-3 inhibiting its trans-activation function and thereby inhibiting IFN- $\beta$  transcription and its secretion after viral infection (112). High-risk HPV E2 reduces the expression of STING which is activated by DNA sensors of the cell usually activating IRF-3 signalling also reducing IFN- $\beta$  transcription and both E2 and E6 reduce the expression of the type I interferon IFN- $\kappa$  (113, 114).

High-risk HPVs also interfere with signalling downstream of interferon receptors. Binding of HPV18 E6 occurs to Tyk2 which inhibits phosphorylation of Tyk2 resulting in reduced phosphorylation of STAT-1 and STAT2 impairing JAK-STAT signalling after IFN- $\alpha/\beta$  stimulation ((112) and reviewed in (80, 115)). HPV16, 18 and 31 E6 are further able to reduce the transcription and translation of STAT1. IFN- $\alpha/\beta$  mediated signalling is also inhibited by HPV E7 via binding to IRF-9 which prevents its translocation to the nucleus and therefore formation of the ISGF-3 transcription complex. As a consequence IFN-inducible genes are not transcribed (116).

Another important signalling pathway other than the IFN pathways that is activated after stimulation of PRRs is the NF $\kappa$ B signalling pathway leading to production of immune modulatory cytokines. High-risk HPVs also have various effects on the NF $\kappa$ B signalling pathway. After activation of both the canonical and non-canonical NF $\kappa$ B pathways by PRRs and CD40 or TNFR2 and CD40, respectively, NF $\kappa$ B1 and 2 translocate to the nucleus where they bind to DNA and initiate gene transcription. High-risk HPVs impair NF $\kappa$ B translocation into the nucleus and its function there at multiple stages of the signalling pathway by, e.g. sequestering NF $\kappa$ B family members in the cytoplasm or reducing their transcriptional activity as well as using endogenous proteins to prevent ubiquitination and therefore degradation of I $\kappa$ B $\alpha$ , an inhibitor of the NF $\kappa$ B pathway. E7 is also able to block NF $\kappa$ B DNA binding activity (106, 107, 117-119). This leads to decreased production of pro-inflammatory cytokine and recruitment of immune cells (120).

Another effect of HPV is the global downregulation of cytokine responses in keratinocytes. Activation of NOD-like receptors leads to activation of pro-inflammatory signalling pathways, e.g. the inflammasome. This is essential for the activation of tissue-resident immune cells such as LCs and recruitment of effector T cells (121). HPV E6 as previously described binds to E6-AP and p53 leading to degradation of pro-

IL-1 $\beta$  in the proteasome and therefore a significantly reduced IL-1 $\beta$  secretion but cannot completely abolish it (122, 123).

Via interfering with the NF $\kappa$ B and IFN pathway, high-risk HPVs inhibit induction of chemokines, e.g. secretion of Mip-3 $\alpha$  and IL-8 after stimulation with TLR9 ligands is inhibited by expression of HPV16, 18 and 31, as are basal levels of these cytokines (108, 109, 124). Reduced expression of Mip-3 $\alpha$  leads to a reduction in LC migration (125) and IL-8 is important for attraction of T cells and neutrophils (126). This might explain the reduced numbers of LCs found in lesions infected with high-risk mucosal types such as  $\alpha$ 7 and  $\alpha$ 9 and low-risk cutaneous types such as  $\gamma$  and Nu (127).

HPVs do not only affect the chemoattraction of immune cells but also proteins important for antigen presentation. HPV E7 proteins are able to down-regulate the expression of MHC class I molecules by repressing the promoter activity of the heavy chain. Some of the E7 proteins are also able to repress the expression of low molecular protein (LMP) 2 and TAP-1 which are important for the transport of MHC molecules to the cell surface (128). E7 as described above interferes with IRF-1 signalling and thereby reducing IFN- $\gamma$  mediated upregulation of MHC class I molecules via the JAK1/STAT1/IRF-1 pathway and E5 is able to retain MHC class I in the Golgi and therefore hampering its transport to the cell surface. E5 also blocks peptide-loading of MHC class II and reduces MHC II surface expression after IFN- $\gamma$  stimulation (129-131).

In summary, HPVs employ a wide range of strategies to successfully evade the immune system and induce infection by a) "hiding" from the immune system, b) interfering with pathways that would induce an anti-viral state inside keratinocytes, c) reducing the production of cytokines and chemokines for recruitment of immune cells and d) inhibiting parts of the antigen machinery (also reviewed in (115) and (107)).

However, all these mechanisms have only been studied in detail using high-risk mucosal HPV types and not all are not found in low-risk HPV types.

#### 1.2.4 Regression, Persistence and Latency of HPV infections

Virus infection of a host with a virus can have multiple outcomes. An acute infection can develop which is associated with open symptoms and signs of disease. It is often followed by recovery or complete elimination of the virus. However, it can also result in chronic infection or latent infection. During a chronic infection the host is still infectious but there are usually no overt signs of disease. A latent infection is associated with no clinical signs of disease and no production or release of infectious particles. The disease can, however, be reactivated leading to synthesis of new virions. A typical example of a latent infection is the infection with herpes simplex virus 1 (HSV-1) (132).

Most HPV infections spontaneously regress and eventually get cleared by the immune system. However, in certain cases they persist and this persistence can enable the formation of cancer. It is not yet fully understood which immune cells are important for regression and control of HPV infection. Regression of HPV-induced lesions is usually associated with infiltration of T lymphocytes. Most studies describe a mixed lymphocyte population consisting of both CD4+ and CD8+ cells, e.g. in animal studies using canine oral PV (COPV), rabbit oral PV (ROPV) and bovine PV (BPV) 4 (133-135) with initially an influx of mainly CD4+ T cells. This correlation between regression and a high CD4:CD8 cell ratio has also been described in humans (136).

In contrast, in cottontail rabbit PV (CRPV)-induced papillomas regression was associated with an influx of CD8+ T cells and only few CD4+ cells but viral DNA persisted for months after clearance of the overt infection (137). It is, therefore, possible that different PV infections are cleared in different ways.

Following initial clearance, viruses can enter a latent state. For HPVs this is suggested as often overt papillomatosis can be seen in immunosuppressed patients such as people on immunosuppressive treatment following a transplant or in the context of HIV infection (138, 139). This correlation is seen for a variety of HPV types such as the high-risk mucosal types but also for certain  $\beta$ - and  $\gamma$ -HPV types (140).

It is thought that HPVs persists in the form of viral genomes in the basal layers (suggested to be epithelial stem cells) with little or no expression of viral genes. For ROPV it has been shown that viral copy number decreases from 50 copies per cell during active infection to less than one copy per cell in latency. During this time no evidence of productive infection can be found (141). In animal models, viral DNA is found in cells months after immune regression and in sites adjacent to the regressed papillomas. Reactivation of the virus can again lead to wart formation (142).

**Table 1: Characteristics of immune cells in HPV regression vs. persistence**

Adapted from Hibma, 2012 (143)

| <b>Regression</b>  | <b>Persistence</b>   |
|--|--|
| Increased TLR expression                                   | Reduced TLR expression   |
| TNF- $\alpha$ production by infiltrating mononuclear cells | Chronic inflammation in the epidermis  |
| CD4 and CD8 infiltrate                                     | Impaired natural killer (NK) cell function and IFN pathways                  |
| High CD4:CD8 ratio   | Low CD4:CD8 ratio with few or no CD4 cells present at site                   |
| Infiltration of antigen-presenting cells                   | Reduced number of antigen-presenting cells and impaired antigen presentation |

### 1.2.5 The mouse papilloma virus

For many decades papilloma virus research was limited to using tissue culture methods as well as transgenic mice that were modified to express viral oncogenes of BPVs or HPVs such as E6 and E7 of HPV16. Lacking a PV that infected the laboratory strain mice (*Mus musculus*) naturally significantly limited the research as the full power of mouse genetics and available knock-out and knock-in strains could not be used to study PV infections. Available animal models for PV infection studies included dogs using COPV, rabbits using CRPV and cows using BPV 1, 2 and 4 (133, 144, 145).

In 2011, the Sundberg group identified a novel mouse papilloma virus (initially called MusPV, later renamed to MmuPV1). Papillomatosis occurred in a closed colony of NMRI-*Foxn1<sup>nu</sup>/Foxn1<sup>nu</sup>* mice at the Advanced Centre for Treatment Research and Education in Cancer (ACTREC) in Kharghar, Navi Mumbai, India. Papillomas mainly appeared around the mouth and nose and in low numbers in other haired skin sites but they were limited to cutaneous surfaces. Histological analysis showed a phenotype similar to koilocytes which are found in many productive PV infections. Sequencing analysis identified a virus with 65% genomic and 83% L1 amino acid similarity to the *Mastomys coucha* (Southern multimammate mouse) PV, McPV2. Using cell-free suspensions from these papillomas, they could be transferred onto other immunocompetent laboratory mice (*S/RV/Cri-ba/ba*) (146). Following the discovery of this novel PV, another variant of it was discovered a year later (147).

The complete MmuPV1 sequence is 7510 nt and it is classified as a member of the  $\pi$ -genus as it has around 60% similarity with rodent PVs from this genus which includes McPV2. It has seven ORFs coding for the early proteins E1, E2, E4, E6 and E7 and L1 and L2. No E5 ORF has been identified. A binding site for pRb has been found on E6 and not on E7 like in other PVs. In addition, it has multiple binding sites for other transcription factors such as AP1 and GATA1, a p53 (TRP53) binding site and a C-terminal PDZ binding domain in E7 usually found in E6 (147, 148).

Even though the initial study showed development of papillomas in immunocompetent *S/RV/Cri-ba/ba* mice, in other studies immunocompetent hosts such as wild type FVB/NCr, C57BL/6J or BALB/c mice did not develop papillomas when scarified and inoculated with MmuPV1 and no MmuPV1 DNA could be detected in swabs taken from these animals 1 months post-inoculation (149-151). Lesions can be induced in some immunocompetent strains when they are treated with immunosuppressive drugs such as ciclosporin A which inhibits T cell activation and cytokine production. However, different strains show different susceptibilities with FVB/NCr and SENCAR being highly susceptible, BALB/c intermediately susceptible and C57BL/6J mice being relatively

resistant to lesion formation after MmuPV1 infection. In addition, all lesions that develop regress once the ciclosporin A treatment is stopped indicating that their formation is due to the induced immunosuppression. If ciclosporin A treatment was started a few months after inoculation no lesion formation was observed showing that the initial infection was effectively cleared (151).

Lesions develop in immunocompromised animals when scarified sites are inoculated with either live virus isolated from other lesions, MmuPV1 DNA encapsidated into L1/L2 capsids of either MmuPV1 or HPV16, or naked MmuPV1 DNA. In some cases, they appear as early as 2 to 3 weeks after application of the virus or viral DNA. Secondary infections have also been observed that developed after around 3 to 4 months and they show broadened tissue tropism being present at tail, face, back, urethra, anus and vagina. This indicates that infectious virions are shed from the surface of lesions (150, 152).

Interestingly, different skin sites on the body of the mice show different susceptibility to lesion formation after MmuPV1 infection. Whereas at muzzle, tail and ear effective lesion formation can be observed, the skin of the back is relatively resistant even though all three sites are permissive for transduction with MmuPV1. The formation of papillomas is related to the amount of E1<sup>4</sup> transcript copies and therefore viral transcription found in the inoculated site (150). This seems to indicate that there are region-specific factors that are responsible for the resistance to papilloma formation in the back.

MmuPV1 can also be used to assess the immune response following infection with a PV. Both CD4<sup>+</sup> and CD8<sup>+</sup> T cells infiltrate MmuPV1 infected tissue (more than 10-fold increase compared to mock infected sites) with CD4<sup>+</sup> T cells being present in the epithelium and the underlying dermis whereas CD8<sup>+</sup> T cells are mainly present in the epithelium only (151).

CD3<sup>+</sup> T cell depletion before infection from immunocompetent hosts such as SENCAR and C57BL/6 leads to efficient formation of papillomas. Whether single depletion of CD4<sup>+</sup> and CD8<sup>+</sup> T cells is sufficient to induce papilloma formation depends on the background strain: in highly susceptible SENCAR mice single depletion is sufficient whereas in C57BL/6 mice both CD4<sup>+</sup> and CD8<sup>+</sup> T cells need to be depleted (151).

C57BL/6 knock-outs for either CD4<sup>+</sup> or CD8<sup>+</sup> T cells alone do not develop papillomas after MmuPV1 infection. However, in CD4<sup>+</sup> T cell single knock-outs the levels of E1<sup>4</sup> transcripts peak at 2 weeks post-infection which does not happen in wild type or CD8<sup>+</sup> T cells knock-outs indicating that CD4<sup>+</sup> T cells are responsible for early viral gene expression control. CD1d-deficient mice lacking NKT cells or B-cell deficient mice

strains do not form lesions suggesting that these cells do not play a critical role in MmuPV1 control (151, 153).

Overall, it is clear from the initial MmuPV1 studies that T cell immunity is essential for the control of PV infections. However, different mouse strains show different susceptibility to MmuPV1 infection which needs to be taken in consideration when working with this system (151, 153).

Most of the initial studies were done on scarified skin and proved cutaneous tropism of MmuPV1. At the beginning of 2015, Cladel et al. also confirmed its mucosal tropism. The vaginal canal and cervix of *Foxn1<sup>nu</sup>/Foxn1<sup>nu</sup>* are susceptible to MmuPV1 infection as well as cutaneous and mucosal tissues of the anal canal (154). Therefore, MmuPV1 can potentially also be employed to further the research done on the cancer-inducing properties of PVs on mucosal surfaces.

In fact, malignant potential of MmuPV1 at cutaneous sites has already been shown as not only papillomas but also trichoblastomas (benign neoplasm of follicular germinative cells) were identified in some animals (153) and pre-malignant lesions were found in others (152).

## 1.3 The common $\gamma$ -chain and its cytokines

### 1.3.1 The $\gamma$ -chain and its co-receptor

The common  $\gamma$ -chain, also known as IL-2R $\gamma$  or CD132, is a cytokine receptor subunit which is encoded by the IL2RG gene located on the long (q) arm of the X chromosome. The gene consists of eight exons and seven introns and spans only 4.2 kb. It shows many genetic features characteristic for a member of the cytokine receptor superfamily, e.g. two pairs of conserved cysteines in exon 2 and 3 and a WSXWS motif in exon 5. Exon 6 encodes the transmembrane domain and the entire cytoplasmic domain is encoded in exons 7 and 8 (155).

The common  $\gamma$ -chain was originally detected as co-precipitate of IL-2R $\beta$ . It was also bound to IL-2 and identified to be a part of the high-affinity IL-2 receptor together with the  $\beta$ -chain and IL-2R $\alpha$  – these three chains forming a heterotrimer (156). It was subsequently identified that the amount of  $\gamma$ -chain co-precipitated with IL-2R $\beta$  was proportional to numbers of IL-2 binding sites and that it is essential for the transduction of intracellular signals as a complex formed of IL-2R $\alpha$  and IL-2R $\beta$  can bind IL-2 with high affinity but does not activate downstream signals (157, 158).

The subunits of the IL-2 receptor have different binding affinities for IL-2. IL-2R $\alpha$  alone has low binding affinity ( $K_d \approx 10$  nM) and is not involved in signal transduction. IL-2R $\beta$  alone has a very low affinity ( $K_d \approx 100$  nM) whereas  $\gamma$ -chain cannot bind IL-2 on its own. A complex formed of IL-2R $\beta$  and  $\gamma$ -chain has an intermediate affinity ( $K_d \approx 100$  pM) and it is the receptor which is usually found on macrophages, NK cells and resting T cells. The heterotrimer with IL-2R $\alpha$  forms a high affinity receptor ( $K_d \approx 10$  pM) and is found on activated T cells. The IL-2R $\beta$  and the  $\gamma$ -chain are sufficient and necessary for IL-2 signal transduction, which does not depend on IL-2R $\alpha$  (159, 160).

It was subsequently identified that the common  $\gamma$ -chain is part of a number of different cytokine receptors including those for the interleukins (IL) IL-2, IL-4, IL-7, IL-9, IL-15 and IL-21 (161-166). The majority of these receptors are heterodimers (IL-4, IL-7, IL-9 and IL-21), which are formed of a specific  $\alpha$ -chain and the common  $\gamma$ -chain. The IL-15R, however, like IL-2R forms a heterotrimer formed of a private  $\alpha$ -chain (IL-15R $\alpha$ ), the  $\beta$ -chain shared with IL-2R (IL-2R $\beta$ ) and the common  $\gamma$ -chain (163, 167). For all these receptors the  $\gamma$ -chain is essential for signalling processes.

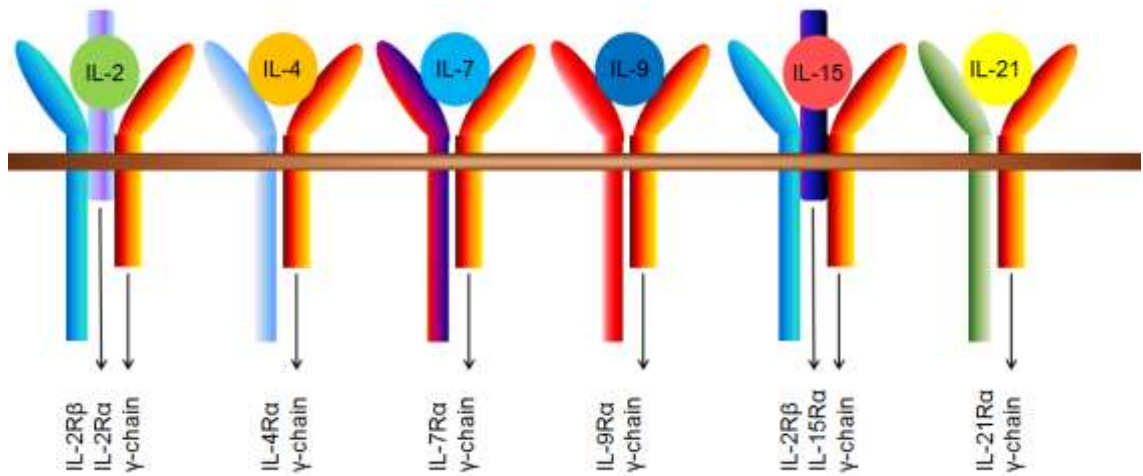


**Figure 5: Receptors for  $\gamma$ -chain cytokines**

The common  $\gamma$ -chain is part of the receptors for six different cytokines. Four of these receptors – for IL-4, IL-7, IL-9 and IL-21 – are heterodimers formed of a specific  $\alpha$ -chain and the  $\gamma$ -chain. The two other receptors – for IL-2 and IL-15 – are formed of their private  $\alpha$ -chains (IL-2R $\alpha$  and IL-15R $\alpha$ ), a shared  $\beta$ -chain (IL-2R $\beta$ ) and the  $\gamma$ -chain. These receptor chains hetero-dimerise or hetero-trimerise when the respective cytokines bind and activate downstream signals. Adapted from Rochman et al, 2009 (168).

### 1.3.2 Signalling via the common $\gamma$ -chain

The receptors of the common  $\gamma$ -chain family lack intrinsic tyrosine kinase activity and therefore transmit signals via the Janus-kinase (JAK) and Signal-Transducers-and-Activators-of-Transcription (STAT) pathway: the carboxyl-terminal region of the  $\gamma$ -chain is associated with the N-terminal region of JAK3; the cytoplasmic part of the  $\alpha$ -chains (except IL-2R $\alpha$  and IL-15R $\alpha$ ) and IL-2R $\beta$  are bound to JAK1 (169, 170). When the respective cytokines bind to their receptors, the receptor chains hetero-dimerise or hetero-trimerise, which leads to catalytic activation of the receptor-associated JAKs. In addition, JAK1 and JAK3 trans-activate each other. JAK1 is essential for further downstream signalling even though it is not directly associated with  $\gamma$ -chain, e.g. cells from JAK1 knock-out mice do not show any responses to  $\gamma$ -chain cytokines (171). The trans-activation of JAK1 and JAK3 creates interaction sites for proteins with phosphotyrosine-binding Src-homology 2 (SH2) domains. STATs contain these motifs and are then recruited to the cell membrane and are phosphorylated by the JAKs on conserved tyrosine residues. Phosphorylated STATs dimerise and acquire high-affinity DNA-binding activity. They translocate into the cell nucleus and function there as nuclear transcription factors and activate downstream targets. IL-2, IL-7, IL-9 and IL-15 mainly signal via STAT5A and STAT5B, IL-4 via STAT6 and IL-21 via STAT3 (cytokine signalling and the JAK-STAT pathway are reviewed in (172, 173)).

In addition to the JAK/STAT pathway, common  $\gamma$ -chain cytokines also activate other pathways such as the phosphoinositide 3-kinase (PI3K/Akt) pathway, e.g. binding of IL-2 to its receptor leads to activation of PI3K which results in phosphorylation of Akt. Activated Akt translocates to the cytosol and the cell nucleus where it activates its targets resulting, e.g. in a block of apoptosis and induction of cell cycle progression. These distinct outcomes differ from the results of the activation of STAT proteins (174-176). Different RAS-mitogen-activated protein kinase (MAPK) pathways are activated by common  $\gamma$ -chain cytokines as well (177). The combination of these different pathways leads to the specific effects of the different cytokines.

However, there is one receptor in the  $\gamma$ -chain family that exists in two forms, one of which does not rely on the common  $\gamma$ -chain for its signalling function – the receptor for IL-4. One of its forms is made up of the IL-4R $\alpha$  and the common  $\gamma$ -chain and the other one of IL-4R $\alpha$  and IL-13R. In certain cells, e.g. colon cancer cell lines, IL-4 does not signal via the common  $\gamma$ -chain but instead via its complex with IL-13R $\alpha$ . In this case, different downstream molecules are activated namely JAK1, JAK2 and Tyk2 whereas no changes in phosphorylation of JAK3 are observed (178, 179).

Moreover, the receptor for IL-15 is the only receptor from the  $\gamma$ -chain family that is known to be able to trans-present and this accounts for most IL-15 signalling. The IL-15R $\alpha$  and IL-15 form high-affinity interactions and so the receptor can present the cytokine in cis or trans to the  $\beta/\gamma$ -complex. Cis-presentation means that the quaternary complex made of IL-15 and the three receptor chains is assembled on the surface of the same cell, whereas trans-presentation happens between two different cells. This allows cytokine signalling through cell contact rather than usual soluble messenger mechanisms and presentation of IL-15 to cells that only express the  $\beta/\gamma$ -complex but not IL-15R $\alpha$ , e.g. the presentation by monocytes to CD8<sup>+</sup> T cells upon cell-cell interaction (180, 181).

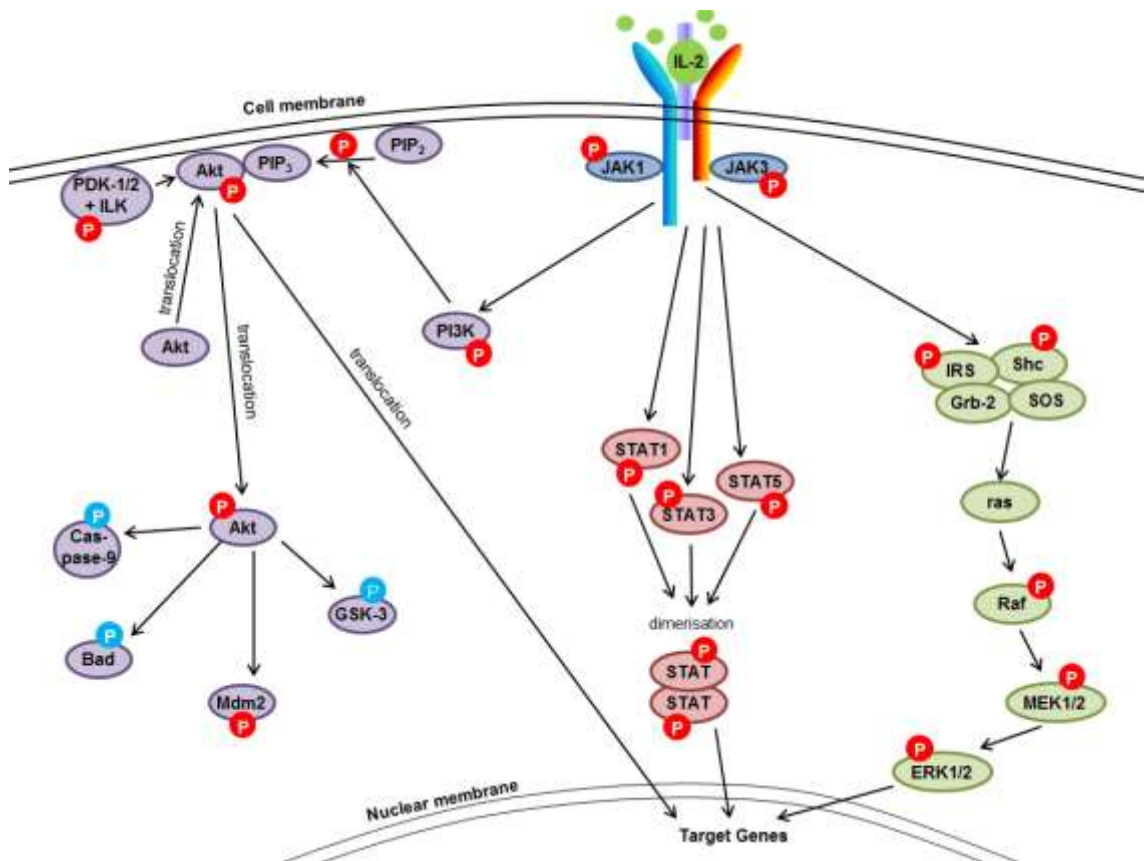


**Figure 6: Signalling via the common  $\gamma$ -chain**

When the respective cytokine binds to its receptor – here shown for IL-2 – and the single receptor chains dimerise or trimerise, JAK3 (bound to the  $\gamma$ -chain) and JAK1 (bound to the  $\alpha$ -chains of the heterodimers or IL-2R $\beta$  of the heterotrimers) are activated and phosphorylate each other. This leads to activation of different downstream pathways such as the STAT pathway, the MAPK pathway via ERK1/2 and the PI3K/Akt pathway. This activation and translocation of transcription factors to the nucleus leads to the activation and transcription of target genes. Activating phosphorylations are shown in red, inhibitory phosphorylation in blue.

### 1.3.3 The effects of $\gamma$ -chain cytokines

The common  $\gamma$ -chain cytokines can induce various effects on different cell types but their effects have only been thoroughly examined in cells of the immune system, such as T, B and NK cells.

IL-2 was initially identified by Morgan et al. in 1976 as a glycoprotein present in conditioned media from phytohemagglutinin stimulated lymphocytes that induced a selective growth advantage of the T lymphocyte fraction of bone marrow cells (182). It was initially also known as 'T cell growth factor' (TCGF) and its cDNA was cloned in 1983 (183). IL-2 was subsequently shown to also increase the cytolytic activity and IFN- $\gamma$  production of NK cells (184), to enhance proliferation of NK and activated B cells (184, 185) and to be important for the differentiation of Th cells (186, 187). Even though IL-2 has various effects *in vitro*, in *in vivo* systems it is implied to be more important for immune tolerance as it is involved in the development of regulatory T cells (188-190).

IL-2 deficient mice present with generalised autoimmune diseases and show symptoms such as inflammatory bowel disease or haemolytic anaemia (191, 192). IL-2R $\alpha$  deficient mice have normal T and B cell development at young age but later on present with enlargement of secondary lymphoid organs, lymphoproliferative disorder, haemolytic anaemia and inflammatory bowel disease (191). This data shows the importance of IL-2 for immune tolerance.

IL-4 is involved in the development and function of Th2 cells, it is a T cell growth factor and it is involved in class switching of immunoglobulins especially for IgE and IgG1 and it is therefore involved in allergic reactions (193). IL-4 is also a survival factor for dendritic cells and is used *in vitro* in combination with GM-CSF to induce DCs from human CD14+ monocytes (194).

IL-4 deficient mice show normal T and B cell development but IgG1 and IgE serum levels are greatly reduced. In addition, IgE secretion cannot be induced in these animals and IgG1 levels remain low even after T cell activation. Their ability to secrete Th2 derived cytokines is reduced as well. (195, 196). IL-4R $\alpha$  knock-out mice are very similar to IL-4 knock-out mice (197).

IL-7 was identified in the late 1980s as a novel haematopoietic growth factor (198). It is involved in stimulating the proliferation of pre-B cells, thymocytes and mature T cells (199). It is constitutively expressed by epithelial and stromal cells in the primary lymphoid organs – bone marrow and thymus – as well as the T cell zones in the

secondary lymphoid organs (200, 201). The IL-7R $\alpha$  is mainly expressed on naïve and memory T cells but not on activated T cells (202).

IL-7 deficient mice are highly lymphopenic in both blood and lymphoid organs, and splenic T and B cellularity as well as thymic cellularity are reduced (203). This shows that IL-7 is important in mice for the development of both B and T cells. In addition, IL-7R $\alpha$  deficient mice have reduced thymic and peripheral lymphoid cellularity (204).

IL-9 was identified in 1988 as a murine Th cell-derived T cell growth factor and it was initially called P40 (205, 206). The human homologue was identified two years later (207). IL-9 is correlated with activation of B cells, mast cells and eosinophils (208). It enhances the production of IgE and IgG in presence of IL-4, but has no effect on IgM production (209).

IL-9 deficient mice do not display changes in T cell development or differentiation or antigen-driven antibody responses. They show differences in specific Th2 responses to lung challenges with allergens underlining IL-9's importance in allergic reactions (210).

IL-15 was identified in 1994 as a cytokine that was able to induce T cell proliferation and that was similar in its activities to IL-2 and used components of the IL-2 receptor (211). IL-15 signalling is essential for NK cell development and survival as well as the long-term survival of CD8<sup>+</sup> memory T cells (212, 213).

IL-15R $\alpha$  deficient mice are lymphopenic due to reduced proliferation and decreased homing of lymphocytes to peripheral lymph nodes. IL-15 is important for the development of NK cells as IL-15R $\alpha$  deficient mice are deficient in this cell type. They also lack NKT cells and CD8<sup>+</sup> T cells (214). Similarly, IL-15 knock-out mice have a greatly reduced NK cell and CD8<sup>+</sup> memory T cell pools (215).

IL-21 is the member of the  $\gamma$ -chain cytokine family that was found the latest (in 2000) and it is closely related to IL-2 and IL-15 (216). IL-21 is able to induce proliferation of B cells, differentiation of plasmablasts and antibody secretion (217). IL-21 is not only important for the regulation of B cell development, but it is also involved in the proliferation and maturation of NK and T cells. (218, 219).

The roles of  $\gamma$ -chain cytokines are also reviewed in (168). The role of the common  $\gamma$ -chain cytokines in other cell types has not been widely examined and is therefore largely unknown. For keratinocytes, it has been shown that they express IL-7, IL-15 and IL-21 and that these cytokines have pro-proliferative effects on keratinocytes (220-222). In addition, they express IL-9R and IL-9 signalling can induce secretion of cytokines such as IL-8 (223).

## **1.4 Severe combined immunodeficiency (SCID) and other primary immunodeficiencies associated with $\gamma$ -chain cytokines**

Severe combined immunodeficiency (SCID) is a group of primary immunodeficiencies which are characterised by the absence of a functional adaptive immune system mainly due to lack of T cells. The immunodeficiencies are relatively similar in all cases of SCID regardless of the underlying genotype. The prevalence of SCID is 1 in 100,000 live births even though it is higher in certain ethnic groups. Patients suffer from severe opportunistic infections such as pneumocystis, adenoviruses, EBV and *Candida albicans*. Due to the absence of a functional adaptive immune system, children need to live in an enclosed sterile environment. The risk of mortality within the first years of life due to recurrent infections is very high if patients are not treated (224, 225).

The proportions of different types of SCID vary between different cohorts. For example, the numbers of autosomal recessive forms are higher in countries with higher consanguinity. The most widely cited study about percentages for SCID cases is from a single-centre study in the United States where data from 170 SCID patients was analysed in a retrospective study. There, the majority of genes responsible for SCID regulated cytokine signalling and antigen receptor recombination, processes which are important for the development of lymphocytes and their metabolism. The SCID types associated with defective cytokine signalling are: a) X-linked SCID (X-SCID), the most common type of SCID is caused by mutations in the common  $\gamma$ -chain, characterised by an absence of T and NK cells and B cells are present but dysfunctional. It accounted for 46% of cases. b) Mutations in JAK3, which signals downstream of the common  $\gamma$ -chain, accounted for 7% of SCID cases and patients are phenotypically identical to X-SCID boys. c) Mutations in IL-7R $\alpha$  are the third group of SCID cases with an involvement of cytokine signalling and were present in 10% of patients. In these patients only T cells are absent (225).

The second most common (17%) SCID type is due to defective metabolism: ADA SCID is caused by mutations in adenosine deaminase (ADA) which leads to cellular accumulation of adenosine and its derivatives resulting in lymphocyte apoptosis and an absence of T, B and NK cells. The other types of SCID are due to problems in antigen receptor recombination and are characterised by an absence of T and B cells, but NK cells are present. They are caused by mutations in T- and B-cell receptor arrangement associated ARTEMIS (1.2%) and RAG (2.9%) genes. For a small percentage of patients the underlying mutations remain unknown (225).

In a London cohort of 117 patients, the numbers differed from the ones presented in the US study: the percentages for X-SCID (17%), ADA-SCID (19%) and RAG-deficiency (15%) were nearly identical with 17% of patients not having been diagnosed at the time of transplant (226).

The only curative treatment available for all types of SCID is bone marrow transplantation (BMT). Its outcome varies depending on the type of transplant, the type of underlying SCID, preceding comorbidity and the age at transplant. Match sibling donors (MSD) and match family donors (MFD) usually show a high survival rate. Nowadays, there is over 85% overall survival for MSD or MFD but only around 55% for haploidentical donors. Moreover, generally, B- SCID types are associated with lower survival rates than B+ SCID types (226, 227).

Moreover, it is important to consider whether conditioning regimes should be used prior to transplantation as they are associated with short- and long-term toxicity. For SCID an unconditioned transplant can be performed due to the lack of significant host adaptive immunity reducing the risk of rejection. Studies have shown that T-B+ forms of SCID (such as X-SCID, JAK3 and IL-7R $\alpha$  deficiency) and ADA-deficiency show excellent outcomes after unconditioned, matched transplants. However, it has also been described that for certain types of SCID, e.g. T-B-NK+ SCID, the survival is higher after unconditioned transplants, but the immune reconstitution is lower and further treatment is more often needed. In general, for X-SCID, unconditioned BMT is performed when there is a MSD or MFD available, otherwise patients will undergo conditioning (226, 227).

As unmatched or haploidentical transplants are still associated with a high mortality rate, gene therapy (GT) has been developed in the past decades for patients who lack an optimal donor. SCID forms are ideal diseases for GT due to their monogenetic nature, the fact that BMT has been successful at curing the disease and that the genetic correction of the cells gives them a positive selective advantage over non-corrected cells. GT has been successfully developed for X-SCID showing good engraftment and reconstitution of the immune system (228). However, in early GT trials 5 patients developed T-cell leukaemia due to insertional mutagenesis (229). New clinical trials using self-inactivating vectors have shown promising results, however, it is too early to make a final statement about their safety (230). GT for X-SCID is performed without any conditioning and adds the significant advantage that autologous cells are utilised thereby removing the risk of graft-versus-host-disease (GVHD).

There are three forms of SCID associated with the  $\gamma$ -chain pathway (X-SCID, JAK3 and IL-7R $\alpha$  deficiency) as described. In addition, there are also other immunodeficiencies associated with this pathway which are even rarer. IL-2RA or CD25 deficiency in

humans is a primary immunodeficiency showing decreased numbers of peripheral T cells with abnormal proliferation but B cell development is normal. Absence of CD25 interferes with thymocyte differentiation and apoptosis resulting in elevated numbers of auto-reactive cells (231). In a few cases, the disease manifests with chronic infections and severe autoimmunity and a similar phenotype as IPEX syndrome caused by mutations in FOXP3 (232). This shows that IL-2 is important for T cell development and immune regulation.

In 2013, two kindreds with loss-of-function mutations in the IL-21R were identified with two affected individuals each. A lack of phosphorylation of STAT1, STAT3 and STAT5 after IL-21 stimulation was observed in these patients. Impaired IL-21 signalling in these patients led to reduced class-switching and proliferation of B cells, defective cytotoxicity in NK cells and reduced cytokine secretion in T cells highlighting the role of IL-21 for immune cell development (233).

Very recently, a family with a mutation in the IL-7 gene was identified. Patients presented with severe CD4<sup>+</sup> T cell lymphopenia in their adult age. This is in contrast to IL-7R $\alpha$  patients which present with SCID early on. It was hypothesized that the milder phenotype in IL-7 deficient patients results from substitution of some of the effects of IL-7 by thymic stromal lymphopoietin (TSLP). IL-7R $\alpha$  is part of the receptor for TSLP which is the potential reason for the more severe phenotype of IL-7R $\alpha$  deficiency compared to IL-7 deficiency in humans (234).

Mutations of IL-4 or IL-4R $\alpha$ , IL-9R or IL-9, IL-15R $\alpha$  nor IL-15 have not been identified in human patients so far.

## 1.5 HPV infections in SCID patients

BMT is a curative treatment for all forms of SCID and GT is available for some types of SCID. However, there is evidence that even after otherwise successful BMT and GT, a persistent selective immunodeficiency remains, which leads to a high susceptibility of patients to HPV infections.

In a single-centre cohort at Hôpital Necker in Paris, 90 SCID patients were examined several years after BMT. Among them, 22 patients had mutations in  $\gamma$ -chain, 16 had mutations in JAK3 and the other patients had different mutations in other genes. In this cohort, 23 out of 90 patients presented with HPV infections. 9 of these patients had severe HPV infection with persistence of more than 30 lesions for more than 2 years. Of these nine severely infected patients, 3 were  $\gamma$ -chain- and 6 JAK3-deficient. The median disease onset was 7 years and ranged from 4 to 15 years after BMT. Fourteen patients in this cohort had mild HPV infections (less than 20 lesions over 2-year period) with 8 having  $\gamma$ -chain deficiency and 2 of them JAK3 mutations. The third group of patients that developed mild HPV infections had mutations in IL-7R $\alpha$  indicating the potential importance of the  $\gamma$ -chain cytokine IL-7 in this pathology. The median onset of disease in this group was 10 years and ranged from 5 to 19 years. In this cohort 50% (11/22) of patients with mutations in  $\gamma$ -chain and 50% (8/16) of patients with JAK3-deficiency and 33% (2/6) of patients with IL-7R $\alpha$  mutations developed HPV infections of the skin compared to no HPV infections in other SCID types. The HPV types were mainly from the  $\beta$ 1 (e.g. HPV5, HPV14 and HPV36) and  $\alpha$ 4 (e.g. HPV2 and HPV57) HPV classes even though members of other genera were also isolated. Multiple individuals were affected by more than one HPV type (235, 236).

In another cohort study in London, 9 SCID patients developed severe HPV infections with 7 of those patients having mutations in  $\gamma$ -chain and 2 having JAK3 mutations. A total of 14 patients with either mutations in JAK3 or  $\gamma$ -chain were alive at the time of the study and therefore 64% (9/14) of patients with  $\gamma$ -chain or JAK3 mutations developed HPV infections (237). Again, patients with other forms of SCID did not present with severe HPV infections. In this cohort, HPVs also mainly from  $\beta$ 1 (e.g. HPV5, HPV14, HPV21, HPV24 and HPV36) and  $\alpha$ 4 (HPV2, HPV27 and HPV57) families were isolated from lesions as well as members of the  $\gamma$ 1 (HPV4) and  $\mu$ 2 (HPV63) classes (personal communication, C. Harwood). In addition, a female patient with JAK3 deficiency presented with severe cervical dysplasia associated with HPV16 and 18 in early adulthood (237).

In both studies, patients with other forms of SCID such as ADA and RAG1/2 deficiencies did not develop HPV infections and therefore, there seems to be a distinct defect in  $\gamma$ -chain and JAK3 deficient patients that is not cured with BMT. Moreover, both studies could not demonstrate any significant differences in transplant specific or immunological parameters such as CD4+ T cell counts, NK cell counts or NK cell cytotoxicity in patients that presented with HPV infections and those without. The occurring HPV infections were difficult to treat and the usual therapy options such as the use of TLR agonists had hardly any effect. However, in a few cases the disease spontaneously regressed without any further treatment ((236, 237) and personal communication S. Burns).

However, recently, a paper published by Kamili et al. argued that poor NK cell engraftment is the reason for the observed HPV susceptibility of X-SCID patients. They performed a retrospective study of 65 SCID patients treated between 1981 and 2012 in their centre. Six patients developed severe cutaneous HPV infections defined as 2 or more locations and resistant to more than 3 forms of treatment. Four patients with chronic HPV infections were followed up for more than 10 years and they had good engraftment with normal T cell function and three of them had normal B cell function. They all had X-SCID and did not receive conditioning prior to transplant and the mean disease onset was 7.4 year post-BMT. In these four patients the NK cell count remained low post-transplant and did not change significantly from pre-transplant numbers whereas HPV negative patients showed good NK cell restoration. When only X-SCID and JAK3 patients' NK cell numbers were compared, there was a significant difference between HPV positive and negative patients. In addition, NK cell cytotoxicity was reduced in HPV patients.

However, this study had a few limitations such as that there was no data was available for 5 patients of which 2 had evidence of HPV disease. Moreover, all SCID cases without HPV disease received myeloablative conditioning in contrast to the HPV positive cases indicating that the engraftment of immune cells including antigen-presenting cells in the skin might have been different between the two groups. In addition, the mean follow-up in the HPV negative group was only 6.5 years post-BMT, a time point at which in the majority of patients no indication of HPV disease has been detected in other studies. This might also explain why their numbers of HPV positive cases was lower (19%) than in other studies (50% and 64%) (238). This study, however, shows again the link between mutations in  $\gamma$ -chain- and JAK3-deficiency and HPV infections of the skin.

Further indication for a link between JAK3 and  $\gamma$ -chain mutations and HPV infections comes from individuals suffering from milder immunodeficiency forms. Members of a

family with a mutation in  $\gamma$ -chain that only led to decreased numbers and not absence of T cells, presented with bacterial infection of the respiratory tract, herpes simplex infections and chronic HPV infections located at the hands. In the oldest member of this kindred the chronic papillomatosis progressed to fatal squamous cell carcinoma (SCC) (239). In a family with a mutation in JAK3 associated with persistence of circulating T cells, one of the siblings presented with recurrent cutaneous warts at 9 years of age that spontaneously regressed when she was 14 (240).

Interestingly, this susceptibility to infections with papilloma viruses in  $\gamma$ -chain deficient individuals has also been observed in other species.

Canine X-SCID is a naturally occurring disease and it has been identified in Cardigan Welsh Corgis and Basset Hounds (241, 242). Its clinical and immunological phenotypes are virtually identical to the human disease and it arises due to naturally occurring mutations of  $\gamma$ -chain. At the University of Pennsylvania, Philadelphia, an X-SCID dog colony was established which harbours a 4-bp deletion in exon 1 resulting in a frame shift with a premature stop codon. The colony was established using a single female carrier (243). X-SCID dogs present with a failure to thrive and a small, dysplastic thymus. Recurrent or chronic infections start from 8 weeks of age and the affected dogs do not usually survive past 3 to 4 months of age. New born dogs present with normal or elevated levels of B cells and significantly reduced or absent T cells which is identical to the presentation of the majority of human X-SCID patients (242, 244, 245). X-SCID dogs have been used for BMT and GT studies and they achieve full immunologic reconstitution and engraftment of donor B and T cells without cytoablative therapy. Typically, the T cell compartment is exclusively of donor origin whereas the B cell compartment shows mixed chimerism after BMT studies (246).

In a study using X-SCID dogs, 71% of dogs developed severe chronic cutaneous papilloma virus infections at 8 to 15 months post-BMT, whereas papillomas were not present in healthy male dogs or female carriers. All dogs that developed the disease showed a normally reconstituted immune function after transplant with normal levels of naïve T cells, normal IgG levels and a normal response to immunization. Moreover, the papillomas were unusual in their location on feet, especially affecting footpads. Canine papillomas usually spontaneously regress within 6 to 8 weeks but were persistent in the X-SCID dogs suggesting that the development of papillomas in SCID dogs is similar to the disease affecting SCID patients. In addition, studies have also shown that a high percentage (67%) of dogs with papillomas developed invasive SCC 3½ years after transplantation, with 75% of these dogs developing metastatic disease. A 3 ½ year dog is equivalent to a 30-year old human based upon aging studies (247).

As already indicated earlier in this chapter, not only JAK3- and  $\gamma$ -chain-deficiency are associated with severe cutaneous HPV infections, but also individuals with mutations in IL-7R $\alpha$  present with HPV infection albeit with a milder form (235). In addition, patients of the kindred with the IL-7 mutation presented with verrucous skin lesions in their twenties due to infection with  $\alpha$ 2-type HPV3. One patient suffered from recurrent SCC since early adulthood on sun-exposed areas (234). This suggests that IL-7 signalling is important for the protection from HPV infections. However, as disease phenotypes for both IL-7 and IL-7R $\alpha$  deficiency were milder than for patients with X-SCID or JAK3 deficiency, another  $\gamma$ -chain cytokine is likely to play a role in the protection from HPV infections.

Whether IL-21 signalling is important cannot be deduced from the study of the IL-21R-deficient kindreds. For one family, patients were still young when they were identified and described (8 and 13 years) and unfortunately, all patients from the other kindred died due to infections or therapy-associated complications (233).

All described studies indicate that the susceptibility for HPV infections may be linked to the common  $\gamma$ -chain pathway and to cells, which are not or only insufficiently replaced by BMT. In experiments using parabiotic mice, Merad et al. presented data showing that certain skin-resident immune cells such as LCs are not replaced by BMT (29). In parabiotic mice that shared a single blood circulation, complete mixing of granulocytes, T and B cells was observed after 10 days, whereas mixing of LCs was not observed even after 6 months. Similarly, dermal DCs (dDC) remained to > 80% of host origin. In lethally irradiated mice, that were transplanted with unfractionated bone marrow, >90 % of donor engraftment in the blood was achieved after 8 weeks, whereas less than 3 % of LCs in the skin were of donor origin but only 25% of dDCs remained of host origin (29, 248). This shows that whereas LCs are radio-resistant only a small subset of dDCs are radio-resistant and proliferative. Human LCs are able to survive conditioning therapy in significant numbers, e.g. in the lowest intensity non-myeloablative transplantation 100% of LCs and 75% of dDCs remain of host origin despite complete donor-derived leukocyte chimerism (249). In a double human hand allograft, results showed that 4.5 years after transplantation, the LCs in the allograft remained of donor origin (250), indicating as well that LCs self-renew in the skin under steady state conditions.

These studies indicate that due to the conditioning protocol used for transplanting X-SCID patients, it is very likely that myeloid cells such dDC and LCs are not replaced and  $\gamma$ -chain and JAK3 mutations in those cells could lead to the susceptibility to HPV infections.

In a  $\gamma$ -chain deficient mouse model, it has been shown by our group that the common  $\gamma$ -chain was required for effective antigen-induced CD4<sup>+</sup> T cell activation by DCs (251, 252). In this mouse model, the optimal CD4<sup>+</sup> T cell activation by DCs was shown to be dependent on trans-presentation of IL-15, which requires the expression of the common  $\gamma$ -chain. Therefore, absence of the common  $\gamma$ -chain leads to functional defects in DCs. It is, however, unknown if these defects are responsible for the susceptibility to HPV infections. As proposed by Kamili et al., limited NK cell reconstitution might explain the disease seen in X-SCID and JAK3-deficient patients, however, this correlation has not been observed in other studies where there was no difference between HPV negative and positive patients in their NK cell levels.

A different possibility is that the susceptibility is due to a defect in keratinocytes as they cannot be replaced by BMT or GT and HPV infections are limited to these cells. Moreover, keratinocytes have multiple immune functions which are altered by HPV in a normal infection making them a likely target for the increased susceptibility.

## 1.6 Hypothesis and Aim

As keratinocytes are not replaced by BMT or GT and HPV infection is limited to these cells, we hypothesise that common  $\gamma$ -chain deficiency in keratinocytes could result in persistent HPV susceptibility in treated SCID patients due to influences on the anti-HPV immunity by one or more of the following mechanisms:

- The lack of the  $\gamma$ -chain could influence initial infectivity of keratinocytes with HPV particles leaving patients more permissive to HPV infections.
- The  $\gamma$ -chain could have an impact on the interferon response of keratinocytes, which would lead to a decrease in the direct effects on the virus and dampen the first line of the immune response.
- The absence of the  $\gamma$ -chain might lead to the virus having a greater influence on the keratinocyte differentiation programme leading to increased hyperproliferation or increased copy number in the patients' cells.
- The secretion of cytokines and chemokines from  $\gamma$ -chain deficient keratinocytes might be reduced decreasing the chemoattraction of professional immune cells.
- The direct cell-cell interaction of keratinocytes with immune cells might be altered in  $\gamma$ -chain deficient cells similar to the effects seen in  $\gamma$ -chain deficient dendritic cells.

We, therefore, aimed to analyse the expression of the common  $\gamma$ -chain and its co-receptors in keratinocytes as well as signalling pathways via  $\gamma$ -chain in the skin. As X-SCID skin samples are in short supply, we generated a common  $\gamma$ -chain knock-down cell line to analyse the effect of the common  $\gamma$ -chain on:

- Keratinocyte infectivity of HPV virus-like particles
- Secretion of cytokines and chemokines from keratinocytes after stimulation with  $\gamma$ -chain cytokines and the effect of these chemokines on immune cell migration
- HPV life cycle in skin raft cultures

From these experiments, we wished to determine whether keratinocyte defects result in increased HPV susceptibility or whether it is more likely that DCs and LCs play a role. This will be important for the design of future therapies for HPV in SCID patients and refinement of BMT/GT protocols.

Moreover, we will generate information about the  $\gamma$ -chain signalling pathway in keratinocytes, which has not been – to our knowledge – studied before.

## **2. Materials and Methods**



|                            |   |
|----------------------------|---|
| Destain solution           | 50% (v/v) methanol<br>10% (v/v) glacial acetic acid   |
| 5x SDS Page Loading Buffer | 10% (w/v) SDS<br>30% (v/v) Glycerol<br>0.001 % (w/v) Bromphenol blue<br>In 0.5 M Tris/HCl, pH 0.5<br>Add 100 mM DTT fresh on the day of use |
| TBS-T                      | 150 mM NaCl<br>10 mM Tris/HCl, pH = 7.0<br>0.1% (v/v) Tween-20  |

#### **2.1.2.2.2 Fluorescent in situ hybridisation**

|                            |   |
|----------------------------|---|
| 10 x NT buffer             | 0.5 M Tris-HCl pH 8.0<br>50 mM MgCl <sub>2</sub><br>0.5 mg/ml BSA |
| Denaturation solution      | 70% (v/v) formamide<br>10% (v/v) 20x SSC, pH 5.3                  |
| FISH wash                  | 4x SSC<br>0.05% (v/v) triton X-100                                |
| FISH detection solution    | 1% (v/v) streptavidin-Cy3 (Sigma)<br>in STM solution              |
| Pre-hybridisation solution | 2x SSC<br>0.5 % NP-40<br>Adjust pH to 7.0                         |
| STM solution               | 5% (w/v) non-fat dried milk<br>0.05% (v/v) Tween-20<br>4x SSC     |

### 2.1.2.2.3 HIRT DNA preparation and Southern Blot

HIRT DNA lysis buffer                    1.25 M NaCl  
    10 mM EDTA pH 7.4  
    20 mM Tris HCl pH 7.4  
    0.75% (w/v) SDS  
    add Proteinase K to 100 µg/ml on the day of use

HIRT DNA resuspension buffer        150 mM NaCl  
    10 mM EDTA pH 7.4  
    20 mM Tris HCl pH 7.4

Depurination buffer                    0.24 N HCl

Denaturation buffer                    0.5 N NaOH  
    1.5 M NaCl

Neutralisation buffer                    0.5 M Tris pH 7.4  
    1.5 M NaCl

Church Hybridisation buffer        0.25 M Na<sub>2</sub>HPO<sub>4</sub>, pH 7.2  
    1 % (w/v) BSA  
    7 % (w/v) SDS  
    50 µM EDTA pH 8.0

Church Wash buffer                    1% (w/v) SDS  
    0.02 M Na<sub>2</sub>HPO<sub>4</sub>, pH 7.2  
    1 µM EDTA pH 8.0

### 2.1.2.2.4 Others

6x Agarose loading dye                0.25% (v/v) bromophenol blue  
    0.25% (v/v) xylene cyanol  
    50% (v/v) glycerol

20x SSC                                    3 M NaCl  
    0.4 M monosodium citrate  
    adjust pH to 7.0

|                    |   |
|--------------------|---|
| Alcoholic HCl      | 1 % HCl<br>70 % ethanol   |
| HindIII ladder     | 20% (v/v) $\lambda$ DNA-HindIII Digest<br>1x Agarose loading dye<br>in TE |
| LB Medium          | 20 g LB Broth in 1 L water<br>Autoclave before use                        |
| TAE solution       | 40 mM Tris<br>20 mM acetic acid<br>1 mM EDTA                              |
| TE buffer          | 10 mM TrisCl<br>1 mM EDTA<br>adjust pH to 7.4 or 8.0                      |
| Virus lysis buffer | 0.5 % (w/v) SDS<br>25 mM EDTA<br>1 mg/ml Proteinase K                     |

### 2.1.3 Antibodies

#### 2.1.3.1 Antibodies for flow cytometry (FC)

##### 2.1.3.1.1 Isotype controls

| Species + Isotype | Clone    | Company + Catalogue Number | Dilution        | Conjugation |
|-------------------|----------|----------------------------|-----------------|-------------|
| Mouse, IgG1, κ    | MOPC-21  | BioLegend<br>400111        | 1 µl per test   | PE          |
| Mouse, IgG2a, κ   | MOPC-173 | BioLegend<br>400213        | 2.5 µl per test | PE          |
| Mouse, IgG2b, κ   | MPC-11   | BioLegend<br>400313        | 2.5 µl per test | PE          |
| Rat, IgG2b, κ     | RTK4530  | BioLegend<br>400612        | 5 µl per test   | APC         |

**Table 3: Isotype controls for FC**

### 2.1.3.1.2 Antibodies for specific immunogens

| Immunogen                      | Species + Isotype | Clone   | Company + Catalogue Number | Dilution        | Conjugation     |
|--------------------------------|-------------------|---------|----------------------------|-----------------|-----------------|
| Human Stat5 (pY694)            | Mouse, IgG1, k    | 47      | BD Pharmingen<br>612599    | 5 µl per test   | Alexa Fluor 647 |
| Human CD25 (IL-2R $\alpha$ )   | Mouse, IgG1, k    | BC96    | BioLegend<br>302605        | 2.5 µl per test | PE              |
| Human CD124 (IL-4R $\alpha$ )  | Mouse, IgG2a, k   | G077F6  | BioLegend<br>355003        | 2.5 µl per test | PE              |
| Human CD129 (IL-9R)            | Mouse, IgG2b, k   | AH9R7   | BioLegend<br>310403        | 2.5 µl per test | PE              |
| Human CD215 (IL-15R $\alpha$ ) | Mouse, IgG2b, k   | JM7A4   | BioLegend<br>330207        | 10 µl per test  | PE              |
| Human CD360 (IL-21R)           | Mouse, IgG1, k    | 2G1-K12 | BioLegend<br>347805        | 10 µl per test  | PE              |
| Human CD132 ( $\gamma$ -chain) | Rat, IgG2b, k     | TUGh4   | BioLegend<br>338608        | 5 µl per test   | APC             |

**Table 4: Antibodies for specific immunogens for FC**

### 2.1.3.2 Antibodies for Western Blot

#### 2.1.3.2.1 Primary Antibodies

| Immunogen         | Species + Clonality | Company + Catalogue Number           | Dilution | Size of protein (kDa) |
|-------------------|---------------------|--------------------------------------|----------|-----------------------|
| p-Akt (Ser473)    | rabbit, monoclonal  | Cell Signaling<br>#4060              | 1:2000   | 60                    |
| Akt (pan) (C67E7) | rabbit, monoclonal  | Cell Signaling<br>#4691              | 1:1000   | 60                    |
| GAPDH (6C5)       | mouse, monoclonal   | Santa Cruz Biotechnology<br>Sc-32233 | 1:1000   | 37                    |
| IL-2RB (C-20)     | rabbit, polyclonal  | Santa Cruz Biotechnology<br>Sc-671   | 1:200    | 70-75                 |
| IL-7R (H-215)     | rabbit, polyclonal  | Santa Cruz Biotechnology<br>Sc-25475 | 1:200    | 76                    |

**Table 5: Primary antibodies for Western Blot**

### 2.1.3.2.2 Secondary Antibodies

| Antibody  | Company + Catalogue Number           | Dilution |
|---|--------------------------------------|----------|
| Anti-mouse IgG, HRP-linked whole antibody<br>(from sheep)   | GE Healthcare Life Sciences<br>NA931 | 1:3000   |
| Anti-rabbit IgG, HRP-linked whole antibody<br>(from donkey) | GE Healthcare Life Sciences<br>NA934 | 1:1000   |

**Table 6: Secondary antibodies for Western Blot**

### 2.1.3.3 Antibodies for Immunofluorescence

#### 2.1.3.3.1 Primary antibodies

| Immunogen  | Species + Clonality | Company + Catalogue Number  | Dilution |
|------------|---------------------|---|----------|
| BrdU       | Mouse, monoclonal   | Calbiochem<br>NA61  | 1:100    |
| E4         | Rabbit              | Provided by Dr. John Doorbar<br>Department of Pathology<br>University of Cambridge<br>Tennis Court Road<br>Cambridge, CB2 1QP | 1:100    |
| Keratin-10 | Rabbit, polyclonal  | Covance<br>PRB-159P   | 1:1,000  |
| Keratin-14 | Rabbit, polyclonal  | Covance<br>PRB-155P   | 1:1,000  |

|                             |                          |                        |       |
|-----------------------------|--------------------------|------------------------|-------|
| Loricrin                    | Rabbit, polyclonal       | Covance<br>PRB-145P    | 1:500 |
| MCM7                        | Mouse, monoclonal        | NeoMarkers<br>MS-862-P | 1:200 |
| Streptavidin,<br>conjugated | Cy3<br>Mouse, monoclonal | Sigma<br>S6402-1ml     | 1:100 |

**Table 7: Primary antibodies for Immunofluorescence**

#### 2.1.3.3.2 Secondary antibodies

| Antibody                             | Company + Catalogue<br>Number | Dilution | Conjugation |
|--------------------------------------|-------------------------------|----------|-------------|
| Anti-mouse IgG (H+L)<br>from donkey  | Invitrogen<br>A31571          | 1:500    | Alexa-647   |
| Anti-rabbit IgG (H+L) from<br>donkey | Invitrogen<br>A21206          | 1:500    | Alexa-488   |

**Table 8: Secondary antibodies for Immunofluorescence**

### 2.1.4 Enzymes

| Enzyme              | Company + Catalogue Number    |
|---------------------|-------------------------------|
| E.coli polymerase I | New England Biolabs<br>M0209S |
| DNase I             | Roche<br>04716728001          |
| HindIII             | New England Biolabs<br>R0104S |
| NcoI                | New England Biolabs<br>R0193S |
| PlasmidSafe (ExoV)  | Epicentre<br>E3105K           |
| Proteinase K        | Roche<br>03 115 879 001       |
| RNase A             | Roche<br>10 109 142 001       |
| T4 ligase           | New England Biolabs<br>M0202M |
| T4 PNK              | New England Biolabs<br>M0201S |
| Xmnl                | New England Biolabs<br>R0194S |

**Table 9: Enzymes**

### 2.1.5 Cytokines

| Cytokine             | Company + Catalogue number |
|----------------------|----------------------------|
| Fractalkine (CX3CL1) | PeptoTech<br>300-31        |
| GM-CSF               | PeptoTech<br>300-03        |
| Gro- $\alpha$ /CXCL1 | PeptoTech<br>300-11        |
| IFN- $\beta$         | PeptoTech<br>300-02BC      |

|                       |                      |
|-----------------------|----------------------|
| IFN- $\gamma$         | PeptoTech<br>300-02  |
| IL-2                  | PeptoTech<br>200-02  |
| IL-4                  | PeptoTech<br>200-04  |
| IL-7                  | PeptoTech<br>200-07  |
| IL-8/CXCL8            | PeptoTech<br>200-08  |
| IL-9                  | PeptoTech<br>200-09  |
| IL-15                 | PeptoTech<br>200-15  |
| IL-21                 | PeptoTech<br>200-21  |
| Mip-3 $\alpha$ /CCL20 | PeptoTech<br>300-29A |

**Table 10: Cytokines**

### 2.1.6 Primers

All primers were purchased from Life Technologies.

| Name              | Forward primer            | Reverse primer           | Product length |
|-------------------|---------------------------|--------------------------|----------------|
| E1 <sup>4</sup>   | TGTGCATCCCAGCAGTAAG       | GGTGCTGGAATACGGTGA       | 116            |
| $\gamma$ -chain   | ACAGGCCACACAGATGCTAA      | CTATGCTGGTTGCATGGGG<br>A | 645            |
| IL-2R $\alpha$ I  | CATTTTCGTGGTGGGGCAGAT     | CCGTGTCCTGTGATGTGAC<br>T | 557            |
| IL-2R $\alpha$ II | AATGCAAAGTCCAATGCAGC<br>C | TGTATCCCTGGACGCACTG<br>A | 146            |
| IL-2R $\beta$     | TATGAGTTTCAGGTGCGGGT<br>C | GAGCCACGGAATGGTGTCC      | 123            |
| IL-4R             | AATGGGGTGGCTTTGCTCTG      | GCTCATGTAGTCGGAGACG<br>C | 121            |

|                 |                       |                           |     |
|-----------------|-----------------------|---------------------------|-----|
| IL-7R $\alpha$  | CTCTGTCGCTCTGTTGGTCAT | ATCTGGCAGTCCAGGAAAC<br>T  | 171 |
| IL-9R           | ATGTGGTAGAGGAGGAGCGT  | CGACAGCTTGAACAGGAGG<br>T  | 182 |
| IL-15R $\alpha$ | GTCTCTCCTGGCATGCTACC  | GCTGGTTTCCCCGAGTTTC<br>A  | 159 |
| IL-21R          | CCCGGTCATCTTTCAGACCC  | TGCACCCACCCATTTCTTGA      | 226 |
| GAPDH           | CCCATCACCATCTTCCAGGA  | CCAGTGAGCTTCCCGTTCA<br>GC | 473 |

**Table 11: Primers**

### 2.1.7 Probes and Standards

E1<sup>4</sup>: Probe: [DFAM]AACAAATGGCTGATCCAGAAGTACCAGTGACGACA[DTAM]

E1<sup>4</sup> Standard:

ccg tgg tgt gca tcc cag cag taa gca aca atg gct gat cca gaa gta cca gtg acg aca cgg tat  
ccg cta ctc agc ttg tta aac agc tac agc aca ccc cct cac cgt att cca gca ccg tgt ccg t

### **2.1.8 Tissue Culture**

All media and supplements were purchased from Gibco® (Life Technologies) if not stated otherwise.

#### **E-medium (keratinocyte growth medium)**

- 44.5% (v/v) DMEM/F-12, GlutaMAX™ (31331-028)
- 44.5% (v/v) DMEM, high glucose, pyruvate (41966-029)
- 10% (v/v) Fetal Calf Serum (FCS)
- 1% (v/v) Penicillin-Streptomycin (P/S; 10,000 U/mL; 15140-122)
- 0.4 µg/ml hydrocortisone
- 10<sup>-10</sup> M cholera toxin
- 1.8 x 10<sup>-4</sup> M adenine
- 5 µg/ml insulin
- 10ng/ml EGF

#### **1:3 medium**

- 50% (v/v) DMEM/F-12, GlutaMAX™ (31331-028)
- 50% (v/v) DMEM, high glucose, pyruvate (41966-029)

#### **DMEM + FCS**

- 89% (v/v) DMEM, high glucose, GlutaMAX™ (61965-026)
- 10% (v/v) FCS
- 1% (v/v) P/S

#### **RPMI**

- 89% (v/v) RPMI 1640 Medium, GlutaMAX™ (61870-010)
- 10% (v/v) FCS
- 1% (v/v) P/S

#### **Optimem (31985-070)**

#### **KSFM (10744-019)**

**Keratinocyte plating medium**

48.75 % F-12 (21765-029)  
48.75 % DMEM/F-12, GlutaMAX™ (31331-028)  
0.5 % FCS  
1 % P/S  
0.4 µg/ml hydrocortisone  
10<sup>-10</sup> M cholera toxin  
1.8 x 10<sup>-4</sup> M adenine  
5 µg/ml insulin  
10ng/ml EGF

**Cornification medium**

Keratinocyte plating medium  
Add FCS to 5% FCS  
10 µM C8:0

**EF-1-F medium**

94 % F-12 (21765-029)  
5 % FCS  
1 % P/S

**293FT medium**

89 % DMEM (11965-092)  
10 % FCS  
1x sodium pyruvate (11360-070)  
1x MEM Non-Essential Amino Acids (11140-035)  
1 % P/S  
500 µg/ml G418

**10x DME salts**

53.7 mM KCl  
10 mM NaH<sub>2</sub>PO<sub>4</sub>  
2.5 µM Fe(NO<sub>3</sub>)<sub>3</sub> \* 9 H<sub>2</sub>O  
1.1 M NaCl  
0.25 M Dextrose  
0.4 mM g Phenol Red

**Calcium-free DMEM**

1x DME salts  
1x Glycine  
1x MEM Amino Acids Solution (11130-036)  
1x MEM Non-Essential Amino Acids (11140-035)  
1x MEM Vitamin Solution (11120-037)  
1.45 mM MgSO<sub>4</sub>  
4 mM sodium bicarbonate  
Adjust pH to 7.2  
1x glutamine

**Low Ca<sup>2+</sup> medium**

70.5% Calcium-free DMEM  
23.5% F-12 medium  
5% Chelex-treated FCS  
1% P/S  
0.4 µg/ml hydrocortisone  
10<sup>-10</sup> M cholera toxin  
1.8 x 10<sup>-4</sup> M adenine  
5 µg/ml insulin  
10ng/ml EGF

| <b>Reagent</b>                              | <b>Company + Catalogue Number</b>                  |
|---|--|
| μ-Slide Chemotaxis 3D<br>Collagen IV coated | Ibidi<br>80322                                     |
| Accutase Solution                           | Sigma-Aldrich<br>A6964                             |
| Blasticidin                                 | Gibco<br>A11139-03                                 |
| BrdU Reagent                                | Sigma-Aldrich<br>B5002                             |
| CD4+ T Cell Isolation Kit                   | Miltenyi Biotec<br>130-096-534                     |
| CD8+ T Cell Isolation Kit                   | Miltenyi Biotec<br>130-096-496                     |
| CD14 MicroBeads, human                      | Miltenyi Biotec<br>130-050-201                     |
| CyQuant NF Cell Proliferation Assay Kit     | LifeTechnologies<br>C35007                         |
| CellTiter-Glo®                              | Promega<br>G7570                                   |
| Chelex-100 Resin                            | Biorad<br>142-2842                                 |
| C8:0  | Santa Cruz<br>Sc-202397A                           |
| Collagen I<br>Cell Matrix type I-P          | Wako Chemicals<br>634-00663                        |
| Deep Well Plate<br>6-Well-Plate             | Corning<br>355467                                  |
| Dunn Chamber                                | Hawksley, Medical & Laboratory Equipment<br>DCC100 |
| Fibrinogen                                  | Sigma-Aldrich<br>#F3506                            |
| fMLP  | Sigma-Aldrich<br>#F3879                            |
| FuGENE® HD                                  | Promega<br>E2311                                   |

|  |                                |
|--|--------------------------------|
| Luciferase Assay System  | Promega<br>E1500               |
| Mitomycin C  | Sigma-Aldrich<br>M0503         |
| MS Columns   | Miltenyi Biotec<br>130-042-201 |
| Neutrophil Isolation Kit, MACSexpress                                    | Miltenyi Biotec<br>130-604-434 |
| OptiPrep™ Density Gradient Medium  | Sigma-Aldrich<br>D1556-250ML   |
| Polyethylenimine (PEI)   | Sigma-Aldrich<br>872-7         |
| Puromycin  | LifeTechnologies<br>A1113803   |
| Transwell, 0.4 µm polyester membrane,<br>24 mm insert, 6 well plate      | Costar<br>3450                 |
| Transwell, 5.0 µm polycarbonate<br>membrane, 6.5mm insert, 24 well plate | Costar<br>3421                 |

**Table 12: Tissue culture reagents**

## **2.1.9 Cell lines**

All cell lines were routinely tested for mycoplasma contamination before they were used for experiments.

### **2.1.9.1 HEK 293T/17**

HEK 293T/17 (ATCC®, catalogue: CRL-11268™) are a variant of the 293 cell line. The 293 cell line was established from primary embryonal human kidney cells which were transformed using sheared human adenovirus type 5 DNA which leads to expression of adenoviral E1A in these cells. 293T is a derivative of the 293 cell line into which the gene for SV40 T-antigen was inserted (293tsA1609neo). These cells were cloned and the clones tested for their capability of producing high titres of infectious virus. This cell line was purchased from ATCC.

### **2.1.9.2 293FT**

293FT cells (Invitrogen, catalogue: R700-07) are another variant of the 293 cell line. The 293-FT cell line was derived from the 293F cell line (Invitrogen) – a fast-growing variant of the 293 cell line – by stably transfecting it with SV40 large T antigen from the pCMVSPORT6Tag.neo plasmid. This cell line was used for the production of papilloma virus stocks and it expresses a neomycin resistance gene. It was purchased from Invitrogen.

### **2.1.9.3 ED-7R**

ED-7R cells are a subline of a human T cell line derived from the peripheral blood of a patient with adult T cell leukaemia. They express IL-2R $\alpha$ , IL-2R $\beta$  but they lack the  $\gamma$ -chain (253). For some experiments, a genetically modified ED-7R line (ED-7R +  $\gamma$ c) was used which expresses the wild-type  $\gamma$ -chain (254).

### **2.1.9.4 NIKS**

Normal Immortalised KeratinocyteS (NIKS) are a spontaneously immortalised keratinocyte cell line derived from neonatal human foreskin. It is negative for HPV16 and HPV31 as well as HIV provirus sequences. The cell line is not tumorigenic in athymic nude mice. It is morphologically the same as normal human keratinocytes and it has keratinocyte cell-type specific growth requirements, e.g. dependence on EGF. They contain 47 chromosomes due to an extra copy of the long arm of chromosome 8. The cell line is able to form fully stratified squamous epithelium in organotypic cultures (255). This cell line was kindly provided by Dr. John Doorbar, Department of Pathology,

University of Cambridge, Tennis Court Road, Cambridge, CB2 1QP at passage number 60. It was generally co-cultured with irradiated 3T3 cells.

#### **2.1.9.5 3T3**

3T3 are an immortalized fibroblast cell line that originated from Swiss albino mouse embryos and was established in 1962 by George Todaro and Howard Green. 3T3 cells were  $\gamma$ -irradiated or mitomycin C treated and used as a bed of feeder cells for culturing primary keratinocytes and NIKS (256).

### 2.1.10 shRNA vectors

All vectors were obtained from UCL Openbiosystems. Vectors have a pGIPZ backbone which contains an ampicillin resistance cassette, a puromycin resistance cassette and a turbo-GFP marker.

| Name                    | Oligo_ID     | Sequence            |
|-------------------------|--------------|---------------------|
| Scrambled (scr) control | V3LHS_314459 | TGAACTCATTTTTCTGCTC |
| shRNA1                  | V2LHS_77306  | ATGTCTATAATCCACTGAT |
| shRNA2                  | V3LHS_330322 | TCAAGAATCTGTTGTTCCA |
| shRNA3                  | V3LHS_330320 | TCAGTAACAAGATCCTCTA |
| shRNA4                  | V3LHS_330321 | TGGGCGTCAGAATTGTCGT |

Table 13: shRNA vectors

### 2.1.11 Others reagents

| Reagent  | Company + Catalogue Number            |
|--|---------------------------------------|
| $\lambda$ DNA-HindIII Digest                                     | New England Biolabs<br>N3012S         |
| 1 Kb Plus DNA ladder   | LifeTechnologies<br>10787-026         |
| Amersham Full-Range Rainbow Molecular Weight Marker              | GE Healthcare Life Science<br>RPN800E |
| Biotin-16-dUTP   | Roche<br>110 93 070 910               |
| BD Vacutainer® K2E (EDTA)  | BD Biosciences<br>367525              |
| BrdU Cell Proliferation Assay Kit                                | Cell Signaling<br>#6813               |
| Donkey serum   | Sigma Aldrich<br>D9663-10ML           |
| EasyTides® Adenosine-5'-triphosphate [ $\gamma$ <sup>32</sup> P] | Perkin Elmer<br>BLU502Z250UC          |
| GeneAmp® RNA PCR Core Kit  | Life Technologies<br>N808-0143        |
| Human Cot I DNA  | Gibco<br>15279-011                    |

|  |                                    |
|--|------------------------------------|
| Hybond™ N <sup>+</sup>                                     | GE Healthcare<br>RPN303B           |
| Immobilon-P Membrane, PVDF, 0.45 µm                        | Millipore<br>IPVH00010             |
| ODN 2216 (TLR9 ligand)                                     | Miltenyi Biotec<br>130-100-243     |
| Protease Inhibitor Cocktail                                | Roche<br>1 697 498                 |
| QIAGEN Plasmid Maxi Kit                                    | QIAGEN<br>12163                    |
| QIAPrep Spin Miniprep kit                                  | QIAGEN<br>27106                    |
| NuPAGE® Novex® 4-12% Bis-Tris Gels,<br>1.0 mm, 10 well     | LifeTechnologies<br>NP-0321BOX     |
| Proteome Prolifer™<br>Human Cytokine Array Panel A         | R&D Systems<br>ARY005              |
| Salmon sperm DNA, sheared                                  | LifeTechnologies<br>AM9680         |
| Sso Fast™ Probes<br>Supermix with ROX                      | Biorad<br>100-19549                |
| SuperSignal® West Pico Chemiluminescent<br>Substrate (ECL) | Thermo Scientific Fisher<br>#34087 |
| Taq DNA polymerase   | Roche<br>11 145 173 001            |
| TRizol Reagent   | LifeTechnologies<br>15596-018      |

**Table 14: Other reagents**

## **2.2 Methods**

### **2.2.1 Cell and tissue culture**

#### **2.2.1.1 Culturing of cells**

Primary keratinocytes as well as keratinocyte cell lines were cultured in E-medium. 60 Gy irradiated or mitomycin C treated 3T3 cells were added as feeder. 293T, 3T3 cells and primary skin fibroblasts were cultured in DMEM with 10% FCS. 293FT cells were cultured in DMEM with 10% FCS, 1x non-essential amino acids, 1x sodium pyruvate and 500 µg/ml G418. EF-1-F cells were cultured in F-12 medium with 10% FCS. ED-7R cells with and without  $\gamma$ -chain were cultured in RPMI medium with 10% FCS. All cells were kept at 37 °C in an incubator with 5% CO<sub>2</sub>.

#### **2.2.1.2 Passaging cells**

To split adherent cells when they reached confluence, they were detached from cell culture flasks/dishes and re-seeded. The culture media were removed and the cells were washed once with PBS without calcium and magnesium. 0.05% trypsin/EDTA solution was added and cells were incubated with trypsin at 37 °C with 5% CO<sub>2</sub> until cells started to detach. Once the cells detached, culture medium was added and cells were washed from the plate and transferred to a Falcon tube and pelleted. The medium was removed and cells were resuspended in appropriated media. Cells were counted using a haemocytometer and seeded as required.

#### **2.2.1.3 Isolation of primary keratinocytes**

Patient skin biopsies were obtained with consent from procedures carried out at Great Ormond Street Hospital. Sterile skin biopsies were wrapped in the gauze soaked with saline and put in a container and transported from the theatre to the lab. In the hood, the biopsy was removed from the container and placed onto a 10 mm dish containing PBS. Excess dermis and connective tissue underneath the epidermis were removed using a sterile blade. The epidermis was cut into smaller pieces and transferred into a tube containing 0.25% trypsin-EDTA and incubated for 3 – 4 hours at 37 °C in a 10% CO<sub>2</sub> incubator. During this time, the tube was shaken every 30 minutes. After the incubation, the contents in the tube were transferred into a tube with DMEM + 10% FCS. The mixture was filtered through a 100 µm cell strainer into a fresh tube. The resulting suspension was centrifuged for 10 minutes at 590 x G. The cells were resuspended in E-medium, 60 Gy irradiated 3T3 cells were added and they were cultured as previously described (2.2.1.1).

#### **2.2.1.4 Lentiviral preparation**

293T cells were seeded the day before transfection to reach approximately 90% confluency on the day of transfection. For transfection, two mixes were prepared in two separate tubes. 1  $\mu$ l of PEI (10 mM) per flask was added to 5 ml of Optimem. In another tube 17.5  $\mu$ g pMD.g2 vector (PlasmidFactory), 32.5  $\mu$ g p8.74 vector (PlasmidFactory) and 25  $\mu$ g of the vector construct (2.1.10) were mixed with 5 ml Optimem. The two mixes were filtered separately through 0.22  $\mu$ m filters. They were mixed at equal volumes and incubated at room temperature for 20 minutes.

The 293T cells were washed once with Optimem, the medium was removed and 9 ml of the transfection mix was pipetted into each flask. Flasks were topped up with 2 ml of Optimem to ensure full coverage of the bottom of the flask. 5 hours later the transfection mix was removed and replaced with 17 ml of DMEM + FCS.

24 hours after transfection the medium was replaced with 17 ml of fresh DMEM + FCS. A further 24 hours later the medium was collected and replaced with fresh DMEM + FCS. The virus containing medium was centrifuged for 5 minutes at 2360 x g and filtered through 0.22  $\mu$ m filters. Subsequently, the supernatant was aliquoted into centrifuge tube and left to spin for 2 hours at 4 °C at 50,000 x g. The supernatant was then removed and 100  $\mu$ l of Optimem was added to the virus pellet and left on ice for 30 minutes. The pellet was then resuspended in the Optimem and the concentrated virus was aliquoted at 20  $\mu$ l each. The procedure was repeated the next day.

#### **2.2.1.5 Titration of lentiviral particles by FC**

293T cells were seeded at  $1 \times 10^5$  cells/well on a 24-well plate. 24 hours after seeding, the concentrated virus was serially diluted five-fold in DMEM + FCS and the different virus concentrations were added to the cells. 5 hours after transduction the virus-containing medium was replaced with fresh DMEM + FCS.

72 hours after transduction the 293T cells were detached from the plate by trypsinising them. They were washed with PBS and then analysed by FC. The sample where the amount of GFP positive cells was between 1 – 5% was used to calculate the titre.

#### **2.2.1.6 Lentiviral transduction of the NIKS cell line**

NIKS cells were seeded at a concentration of  $1 \times 10^5$  cells per well on a 12 well plate. The following day, virus was added with defined number of virus particles in 300  $\mu$ l of E-medium. 6 hours later, the media containing virus was removed and replaced with 1 ml of fresh medium. 72 hours post transduction, the cells were trypsinised and seeded

into a T25 flask and grown to confluency before they were FACS sorted according to GFP intensity to enrich transduced cells. If the vector contained a puromycin resistance gene, cells were selected as in 2.2.1.7.

#### **2.2.1.7 Puromycin selection of NIKS cells**

To assess the correct puromycin concentration, untransduced (UT) NIKS were seeded on 12 well plate and different concentrations of puromycin were added to the wells. The cells were assessed every other day to check for cell death. The concentration was chosen as the one where all cells were dead after 4 days which was equivalent to 2 µg/ml puromycin.

If the vector contained a puromycin resistance gene, the cells were selected 72 hours after transduction using puromycin at the determined concentration of 2 µg/ml. The medium was changed every 3 days and cells were selected for a week. Then the media containing puromycin was removed and the cells were grown normally in E-medium.

#### **2.2.1.8 Proliferation Assay using BrdU incorporation and FC**

Cells were incubated for 1 hour with 20 µM BrdU at 37 °C. Then they were detached from the plate and pelleted at 250 x g for 5 minutes. Cells were resuspended in 1 ml of ice-cold 90% ethanol and incubated in the fridge overnight. Cells were washed in PBS and pelleted at 300 x g for 5 minutes. To release the nuclei and remove the RNA, cells were treated with 2N HCl containing 0.5% triton x-100 for 30 minutes and 0.1 M sodium tetraborate was added to neutralise the acid. Cells were pelleted at 600 x g for 10 minutes and washed twice with PBS with 0.5% Tween-20 and 1% BSA (PBS-TB). Tween-20 prevents the nuclei and BSA prevents the DNA from clumping. To remove RNA, the released nuclei were resuspended in 1 ml RNase A (10 µg/ml) in PBS-TB and incubated for 30 minutes at 37 °C. They were pelleted at 600 x g for 5 minutes and washed with PBS-TB once. To stain the nuclei, they were resuspended in 100 µl of a 1:50 dilution of the anti-BrdU antibody and either incubated for 90 minutes at room temperature or overnight at 4 °C. They were washed with PBS-TB and resuspended in 1:250 dilution of anti-mouse-Alexa-488 antibody and incubated in the dark at room temperature for 30 – 45 minutes. They were washed again in PBS-TB and resuspended in PBS. They were filtered through mesh prior to analysing them by FC.

### **2.2.1.9 Proliferation Assay using BrdU incorporation and a platereader**

NIKS cells were seeded at 10,000 cells per well on a 96-well plate. They were left overnight to adhere, the following day they were starved in 1:3 medium for 6 hours before 100 ng/ml IL-7 and IL-15, respectively, were added as well as 10  $\mu$ M BrdU. 16 hours later they were analysed with the BrdU Cell Proliferation Kit

The cell proliferation kit was used according to the manufacturer's instructions. In brief, the medium was removed and cells were fixed for 30 minutes at room temperature using the provided Fixing/Denaturing Solution. The solution was removed and 1x Detection Antibody as added and the plate was kept for 1 hour at room temperature. It was washed three times with washing buffer before 1x HRP-conjugated secondary antibody was added. After a 30 minute incubation at room temperature, the antibody was removed and the wells were washed three times with washing buffer. The TMB Substrate was added and the plate was incubated for 20 – 30 minutes at room temperature while the colour change was observed. To stop the reaction STOP Solution was added. Colour change was analysed with a plate reader. The absorbance was read at 450 nm. Differences in proliferation were calculated as differences in absorbance.

### **2.2.1.10 Production of HPV Virus-Like-Particles (VLP)**

293FT cells were seeded on 10cm dishes at a density of  $5.6 \times 10^6$  cells per plate in DMEM with 10% FCS without antibiotics the day before transfection. Per plate, 15  $\mu$ g pShell and 15  $\mu$ g of expression plasmid, e.g. pLuc or recircularised HPV18 plasmid (see 2.2.3.7), were mixed in 750  $\mu$ l Optimem. In a second tube, 750  $\mu$ l Optimem was mixed with 65  $\mu$ l Lipofectamine. Both tubes were incubated at room temperature for 5 minutes, then they were mixed and incubated a further 30 minutes at room temperature. The medium was removed from the 293FT cells and replaced with 1.5 ml of transfection mix per plate. The cells were incubated for 5 hours at 37 °C and then 5 ml fresh 293FT medium was added. 48 hours after transfection, cells from 6 plates were harvested and pooled together, washed with DBPS with 9.5 mM MgCl<sub>2</sub> and transferred to siliconised tubes. For the maturation, the cells were pelleted, the size of the cell pellet estimated and supplemented with 1.5 times the volume of DPBS with 9.5 mM MgCl<sub>2</sub>, 1/25<sup>th</sup> of the volume of 10% Brij-58, 1/40<sup>th</sup> of the volume of 1 M ammonium sulfate pH 9.1 and 5 units of RNase A. The mix was incubated at 37 °C for 24 hours under rolling conditions. The following day, the matured cell lysate was cooled to 4 °C for at least 10 minutes and the cells pelleted by centrifugation at 8.000 x g at 4 °C for 10 minutes. The supernatant was added to a three-step Optiprep gradient, which was prepared 2 – 4 hours prior and it was centrifuged for 3.5 hours at

235,000 x g at 16 °C. The tube was punctured using a 23G needle and different fractions were collected whereby the first fraction was made up of approximately 600 µl and fractions 2 – 16 of 200 µl, the remaining volume was discarded. The virus particles were stored at -80 °C.

To analyse in which fractions contained the virus particles, 10 µl of each virus fraction were mixed with 2 µl 6x SDS loading dye, boiled for 5 minutes and then separated on an SDS PAGE. The gel was stained with Coomassie stain overnight and de-stained for several hours the following day until bands became visible. The fractions containing a band of 55 kD (corresponding to the size of L1) were further analysed by Southern blot. For the blot, 10 µl of virus lysis buffer were mixed with 10 µl of virus fractions and incubated at 56 °C for 30 minutes. 1 µl of loading dye was added and the lysate was added to a 0.6 % agarose gel together with weight standards and separated by electrophoresis, the gel was stained with SYBR green and used for a Southern blot analysis (2.2.3.9) to estimate viral concentration.

#### **2.2.1.11 Infectivity assay**

Cells were seeded at a density of 10,000 cells per well on two 96 well plates. The following day they were infected with HPV pseudovirions at an virus concentration of 1 and 10 viral genome equivalents (vge) per cell in quadruplets. Four wells of each cell type were left uninfected as control. 48 hours after infection, one plate was used for the Luciferase Assay (E1500, Promega) and the other plate was used for the viability assay using CellTiter-Glo® (G7570, Promega). Both assays were carried out following the manufacturer's instructions. In brief, for the luciferase assay the medium was removed, the cells were washed with PBS and then lysed in 20 µl of 1x lysis reagent per well. They were briefly frozen at -80 °C to ensure cell lysis and then read using the Microumat Plus (Perkin Elmer instruments) which injected 100 µl of Luciferase Assay Reagent per well. Luminescence was read for 3 s per well. For the cell viability assay, a volume of CellTiter-Glo® reagent equal to the volume of cell culture medium present was added to each well and the sample was incubated for 10 minutes at room temperature. Luminescence was measured for 1 s.

For the infectivity assay with cytokine stimulation, cells were seeded at a density of 10,000 cells per well in E-medium. The following day, the medium was changed to Optimem and the cells were incubated for 6 hours at 37 °C. The medium was changed to Optimem containing the indicated amounts of cytokines. Cells were infected 24 hours after addition of the cytokines by adding virus containing medium to the cytokine containing medium. The luminescence was read 48 hours after adding the virus.

#### **2.2.1.12 Transfection of NIKS with HPV18wt vector**

NIKS were seeded at  $5 \times 10^5$  on 6-well plates the day before transfection. On the day of transfection, the medium was changed to low  $\text{Ca}^{2+}$  medium and the cells were incubated for 4 hours. For transfection, pcDNA1 (which contains a blasticidin resistance cassette) and HPV18wt plasmid were mixed at a weight ratio of 1.2 to 3 in a total volume of 155  $\mu\text{l}$  Optimem. 10  $\mu\text{l}$  of Fugene HD® reagent were added and mixed by pipetting. The mix was incubated for 10 minutes at room temperature. The medium was removed from the cells and replaced with 3 ml of fresh low  $\text{Ca}^{2+}$  medium. 150  $\mu\text{l}$  of transfection mix were added to each well and incubated overnight. The following day, the cells were transferred to 10 cm dish feeder plates. 48 hours after transfection, selection with Blasticidin was started at a concentration of 7  $\mu\text{g}/\text{ml}$ . Selection was carried out for 96 hours before cells were grown in normal E-medium. Mitomycin C treated 3T3 cells were added to the cells when needed.

#### **2.2.1.13 Making organotypic rafts**

In order to make organotypic rafts, first a collagen raft was made using transwell inserts with a 0.4  $\mu\text{m}$  polyester membrane placed into deep well plates. A collagen premix to make six rafts was prepared by mixing 2.5 ml 10X F-12 media, 6  $\mu\text{l}$  10 N NaOH, 250  $\mu\text{l}$  P/S, 2.5 ml FCS and 20 ml collagen I solution. Everything was mixed carefully to avoid bubbles and centrifuged for 5 minutes at 4 °C. 1 ml of collagen premix was added to each transwell insert and incubated for 5 – 10 minutes at 37 °C. 600  $\mu\text{l}$  of a  $7.5 \times 10^5$  cell/ml EF-1-F fibroblast solution was added to the remaining collagen mixture and mixed carefully. 2.5 ml of the collagen-cell-suspension was added to the transwells and incubated until gelled (approx. 30 – 60 minutes) in an incubator at 37 °C. 20 ml of EF-1-F medium was added to the outer well and the collagen rafts were incubated at 5%  $\text{CO}_2$  and 37 °C for 6 days. After the gels had contracted to the appropriate shape, 150  $\mu\text{l}$  of a  $1.4 \times 10^6$  cells/ml solution of NIKS in keratinocyte plating medium was layered onto the collagen raft. The rafts were incubated for 2 hours at 37 °C to allow the cells to attach, then 20 ml of keratinocyte plating medium were added to the outer well. After two days, the medium was removed from the outer and inner well and replaced by fresh keratinocyte plating medium. On day 4 after plating the keratinocytes, the medium was removed and the transwell inserts were lifted onto three cotton pads. Cornification medium was added to the outer well so that the inner well was left dry and the cotton pads were soaked in medium. The rafts were fed every other day with cornification medium. At day 15 after plating the keratinocytes, the medium was supplemented with 10  $\mu\text{M}$  BrdU and the rafts incubated for 8 hours. They were

harvested and embedded in 2% agar/1% formalin and incubated overnight at 4 °C. The agar blocks were transferred into 10 % buffered formalin overnight at 4 °C, followed by an incubation at 4 °C overnight in 70% ethanol. After fixation they were embedded in paraffin by the Histology department, cut and stained appropriately (see section 2.2.4).

#### **2.2.1.14 Isolating peripheral blood mononuclear cells (PBMCs) from whole blood**

CD4+ and CD8+ T cells and CD14+ cells were isolated from PBMCs purified from whole blood. Blood was obtained from healthy volunteers with consent and collected into a BD Vacutainer® tube which contained EDTA to stop coagulation. The blood was diluted with 1 part of medium. To separate the PBMCs, the same amount of Ficoll as blood obtained was pipetted into a tube and the diluted blood was slowly layered on top. The tube was centrifuged for 25 minutes, 400 x g using no brake at the centrifuge. The middle white layer of PBMCs was removed carefully and the remaining liquid was discarded. The suspension containing the PBMCs was washed with medium and the cells pelleted at 300 x g for 7 minutes and used for further isolations.

#### **2.2.1.15 Isolation of CD14+ cells and differentiation to DCs**

CD14+ cells were isolated from PBMCs using CD14+ MicroBeads and following the manufacturer's instructions. In brief, cells were resuspended in cold MACS buffer, CD14+ selection beads were added and the mix incubated in the fridge for 15 minutes. MACS buffer was added, the cells were washed, centrifuged at 300 x g for 5 minutes and then resuspended in 500 µl of MACS buffer. In the meantime, an MS MACS column placed in an MACS magnet was calibrated using 3 ml of MACS buffer. The cell suspension was added and the flow through discarded. The column was washed three times and the flow through discarded. The column was then removed from the magnet and placed above a fresh 15 ml tube, 1 ml of MACS buffer was added and the plunger was rapidly pushed down to harvest the positive cells and counted.

To induce dendritic cells,  $1 \times 10^6$  cells were seeded per well of a 6 well plate. They were grown in RPMI supplemented with 100 ng/ml GM-CSF and 25 ng/ml IL-4. Fresh medium was added on Day 3 after harvest. They were used for experiments on Day 6.

#### **2.2.1.16 Isolation of CD4+ and CD8+ T cells**

CD4+ and CD8+ T cells were isolated from PBMCs using the CD4+ or CD8+ T cell isolation kit, respectively, and following the manufacturer's instructions. In brief, cells were resuspended in cold MACS buffer, CD4+/CD8+ T Cell Biotin-Antibody Cocktail was

added and the mix incubated in the fridge for 5 minutes. Additional MACS buffer and CD4+/CD8+ T Cell MicroBead Cocktail were added and the mix incubated in the fridge for 10 minutes. An additional 500  $\mu$ l of MACS buffer were added and the mix used for magnetic separation. The cell suspension was added to a calibrated MS column and the flow through collected as this represented the enriched CD4+/CD8+ cells. The column was washed once using 500  $\mu$ l MACS buffer and this flow through collected as well. The cells were then used for experiments.

#### **2.2.1.17 Isolation of neutrophils**

Neutrophils were isolated for migration assays from 4 ml blood collected into an EDTA tube. They were then isolated using the MacsXpress Separator kit following the manufacturer's instructions. In brief, to 4 ml of EDTA blood 2 ml of MACS bead cocktail were added and incubated at room temperature for 5 minutes using a MACSmix Tube rotator. The tube was then placed into a MACSxpress Separator for 15 minutes. Leaving the tube inside the separator, the supernatant was removed and washed by adding fresh RPMI medium and spinning them down at 300 x g for 7 minutes. The cells were then resuspended in RPMI, counted and used for further experiments.

#### **2.2.1.18 Migration experiments using neutrophils**

For migration experiments with neutrophils, Dunn Chambers (Hawksley, Medical & Laboratory Equipment) were used. Coverslips were coated with fibrinogen at 25 mg/ml and incubated for 1 hour at 37 °C. The fibrinogen was removed and  $1 \times 10^5$  neutrophils were seeded onto each coverslip and incubated for further 1 hour at 37 °C to allow for adherence of neutrophils. The outer ring of the Dunn chamber was filled with 100  $\mu$ l of chemoattractant solution prepared in a 1% solution of low melting agarose. The inner ring was filled with 50  $\mu$ l of chemoattractant-free solution. Coverslips were carefully placed on top of the Dunn chambers with the cell-side facing down. The edges of the coverslip were sealed using hot wax. The chambers were imaged using the Zeiss Axiovert 135 time-lapse microscope for 1 hour at 37 °C taking images every minute. fMLP was used at 100 nM as positive control. Analysis was carried out using Icy (257).

#### **2.2.1.19 Migration experiments using DCs**

Migration experiments with dendritic cells were carried out using the  $\mu$ -Slide Chemotaxis 3D (Ibidi) according to the manufacturer's instructions. In brief, 6  $\mu$ l of a  $3 \times 10^6$  cells/ml cell suspension was seeded per slide and the cells left to adhere for 4-5 hours. Then, 65  $\mu$ l of chemoattractant-free medium was filled into one side first and sealed. Into the other side, first 65  $\mu$ l of chemoattractant-free medium was filled and

then  $2 \times 15 \mu\text{l}$  of a 2x chemoattractant solution. All ports were sealed and the slide imaged overnight using the time-lapse microscope at  $37^\circ\text{C}$  taking pictures every 5 minutes. Migration was analysed using the Manual Tracking plugin from ImageJ.

#### **2.2.1.20 Migration experiments using CD4+ and CD8+ T cells**

Isolated CD4+ and CD8+ T cells were used for transwell migration experiments using transwells with a  $5.0 \mu\text{m}$  polycarbonate membrane. The chemoattract solution was filled into the bottom of the wells and  $100 \mu\text{l}$  of a  $1 - 2 \times 10^6$  cells/ml suspension was plated on top of the insert membrane. The plate was incubated at  $37^\circ\text{C}$  for 2 hours. The inserts were removed and placed into a separate plate filled with PBS to wash their bottoms and then transferred into a trypsin filled plate. The plate was incubated to detach cells that were attached to the bottom of the insert. The chemoattractant solution which contained migrated cells was pooled with the trypsin solution which contained cells detached from the membrane. Cells were centrifuged at  $300 \times g$  for 5 minutes and the supernatant removed. The cell number was determined using the CyQUANT® NF cell proliferation assay kit following the manufacturer's instructions. In brief, cell pellets were resuspended in  $50 \mu\text{l}$  of  $1 \times$  HBSS buffer and transferred to a black-bottom 96-well plate. Then,  $50 \mu\text{l}$  of 2x dye binding solution was added to each well and the plate was incubated at  $37^\circ\text{C}$  for 1 hour before fluorescence was read using  $490 \text{ nm}$  as excitation wave length and  $540 \text{ nm}$  at emission detection. Fold-migration was calculated using relative fluorescence levels.

## **2.2.2 Protein Biology**

### **2.2.2.1 Cell lysis and sample preparation for Immunoblotting**

Depending on the experiment, cells were either pelleted after harvesting them from their plate using trypsin or scraped off the plate in lysis buffer using cell scrapers. For cell pellets, approximately 100 µl lysis buffer per  $1 \times 10^6$  cells were used to lyse the cells. For cells in plates, 100 µl per well of a 12 well plate and 200 µl per well of a 6 well plate were used. Cells were resuspended in cold lysis buffer and incubated on ice for 10 minutes. They were then centrifuged at 14,000 x g for 10 minutes at 4 °C. The supernatant was transferred into a new tube and the pellet was discarded. The appropriate volume of 5x SDS Page Loading Buffer was added to the supernatant and the sample was boiled for 5 minutes at 95 °C and was used for electrophoresis or stored at -20 °C for future use.

### **2.2.2.2 SDS-PAGE and Immunoblotting**

SDS-PAGE gels were purchased at a Bis-Tris concentration of 4-12% from LifeTechnologies. Samples were loaded onto the gel and separated for 45 minutes at 200 V. The gel cast was removed and a blot sandwich consisting of two blot papers soaked in transfer buffer, a PVDF membrane, the gel and another two blot papers soaked in transfer buffer was prepared. A wet transfer was carried out for 75 minutes at 25 V. The membrane was then incubated in 5% BSA in TBS-T for 60 minutes and then the appropriate antibody (see 2.1.3.2.1) was added and the blot was incubated overnight at 4 °C. The following day the blot was washed three times for five minutes with TBS-T and then the secondary antibody (see 2.1.3.2.2) was added and incubated for 1 hour. Afterwards the blot was again washed three times for five minutes in TBS-T and then developed using ECL solution. For loading control antibodies such GAPDH, the incubation with the primary antibody was reduced to 2 – 3 hours at room temperature.

### **2.2.2.3 Surface Staining for FC**

If cell surface markers were stained, cells were detached from the flask by using trypsin or accutase. When trypsin was used, it was neutralised using DMEM + FCS. PBS was used to dilute the accutase. The cells were pelleted at 250 x g for 5 minutes and resuspended in PBS. They were pelleted again and resuspended in 100 µl PBS per sample and the appropriate amount of antibody (see 2.1.3.1.1 for isotype controls and 2.1.3.1.2 for specific immunogens) was added. The samples were incubated on ice, in the dark for 45 to 60 minutes. Afterwards, they were washed once in PBS and

resuspended in 150 µl of PBS to run on the FC. All FC data was analysed using FlowJo.

#### **2.2.2.4 Intracellular Staining for FC**

If samples were analysed for the expression of intracellular markers, cells needed to be permeabilised before staining with antibodies. Cells were detached and washed as described as before (2.2.2.3). After washing the PBS supernatant was discarded and the cells were resuspended in 2 ml warm 1x Lyse-Fix buffer and incubated at 37 °C for 10 minutes. The tube was topped up with 3 ml of PBS and the cells were pelleted by centrifugation for 5 minutes at 250 g. Afterwards, 1 ml of ice-cold Perm Buffer III was added and the cells were incubated on ice for 30 minutes. The cells were then washed in 3 ml PBS and pelleted again, the supernatant was discarded and the cells were resuspended in the remainder of the liquid. Just as staining for surface molecules, antibodies were added and cells were incubated for 45 to 60 minutes on ice, then washed again and resuspended in PBS and analysed by FC.

#### **2.2.2.5 Analysis of JAK/STAT signalling by FC**

To test STAT5 phosphorylation NIKS cells were seeded onto 6 plates and were grown until they were approximately 80% confluent. They were then starved overnight in 1:3 medium without any supplements. The following day the cells were used for the pSTAT5-assay. In order to detach the cells, they were washed once with PBS and then 1 ml of accutase solution was added per well. The cells were incubated at 37 °C until they detached. 1 ml of PBS was added and the cells were pelleted at 250 x g for 5 minutes. They were then resuspended in 100 µl of 1:3 medium and transferred to FC tubes. The interleukins were added to these tubes and the cells were incubated for 10 minutes at 37 °C. Directly to these tubes 2 ml of 1x Lyse-Fix buffer was added. The cells were then prepared as described in 2.2.2.4 intracellular staining for FC.

#### **2.2.2.6 Sample preparation for analysis of pAKT by immunoblotting**

Cells were seeded onto 12 well plates and grown in the incubator until they were 80% confluent. They were then starved overnight in 1:3 medium. The following day, the cells were washed once in PBS and then 300 µl of 1:3 medium supplemented with different concentrations of the appropriate interleukin were added. One well was left unstimulated. The cells were incubated for 10 minutes at 37 °C. The medium was removed and the cells were washed once with 500 µl ice cold PBS, the PBS was removed and 100 µl of ice-cold lysis buffer was added. The cells were scraped off the plate using cell scrapers. The samples were incubated for 15 minutes on ice and then

they were centrifuged 2 min at 14,000 x g to pellet cell debris. The supernatants were transferred to a new tube and stored at – 20 °C until they were used for immunoblot analysis (2.2.2.2).

#### **2.2.2.7 Cytokine Array**

The supernatants were collected from cells after 24 hours under the appropriate culture conditions and used for the Proteome Prolifer™ Assay. The assay was carried out according to the manufacturers' instructions. In brief, the membranes from the kit were incubated for 1 hour at room temperature in Array Buffer 4 on a rocking shaker. The 800 µl of the supernatant were added to 200 µl Array Buffer 5 and 500 µl Array Buffer 4. 15 µl of Detection Antibody Cocktail was added to the prepared samples. They were mixed and incubated at room temperature for 1 hour. Array Buffer 4 was removed from the membranes and the samples were added and incubated overnight at 4 °C on a rocking shaker. The following day, the membranes were washed three times with 1x wash buffer before the 1x Streptavidin-HRP antibody added. The membranes were incubated 30 minutes at room temperature on a rocking shaker. They were washed again three times with 1x wash buffer and then developed with Chemi Reagent Mix using autoradiography film in a dark room.

#### **2.2.2.8 Luminex assay**

Cells were seeded at  $3 \times 10^5$  on 6-well plates and grown to confluency. They were grown under the appropriate culture conditions. The supernatants were collected after 24 hours in culture, centrifuged to remove cell debris and stored at -20 °C until they were used. The Luminex assay was carried out according to the manufacturer's protocol. In brief, supernatants and standards were mixed with the microparticles and incubated for 2 hours in the dark under shaking. The plate was washed and the biotin antibody cocktail was added and the mix incubated for 1 hour in the dark under shaking. The plate was washed again and then streptavidin-PE was added and incubated for 30 minutes. The plate was washed again and the beads were resuspended in wash buffer and it was read with a Luminex 100 analyser. Values were calculated using the standard curve.

### **2.2.3 Molecular Biology**

#### **2.2.3.1 Isolation of RNA**

Isolation of RNA was carried out using TRIzol reagent following the provided protocol. In brief, cells were trypsinised and pelleted. 1 ml TRIzol reagent was added per  $1 \times 10^6$  cells and the pellet was homogenised by pipetting up and down multiple times. Afterwards, the sample was incubated for 5 minutes at room temperature and then 0.2 ml chloroform were added and the tube was shaken for 15 seconds and then further incubated for 2 minutes at room temperature. The sample was centrifuged at  $12,000 \times g$  for 15 minutes at  $4^\circ\text{C}$ . It then separated into three layers. The top layer was transferred to a new tube and 0.5 ml of 100% isopropanol were added and incubated for 10 minutes at room temperature before the sample was centrifuged at  $12,000 \times g$  for 10 minutes at  $4^\circ\text{C}$ . The supernatant was removed and the pellet was washed with 1 ml of 75% ethanol. The tube was centrifuged at  $7,500 \times g$  for 5 minutes at  $4^\circ\text{C}$ . The supernatant was discarded, the pellet was air dried and then resuspended in water.

#### **2.2.3.2 Reverse transcription**

Reverse transcription of RNA samples was carried out using the GeneAmp® RNA PCR Core Kit following the provided protocol. In brief, the provided chemicals were mixed to the following final concentrations: 5 mM  $\text{MgCl}_2$ , 1x PCR buffer, 1 mM of dGTP, dATP, dCTP and dTTP each, 1 U/ $\mu\text{l}$  RNA inhibitor, 2.5 U/ $\mu\text{l}$  MuLV reverse transcriptase, 2.5 mM random hexamer primers and 1  $\mu\text{g}$  isolated RNA in 20  $\mu\text{l}$  total volume. Everything was mixed and incubated for 10 minutes at room temperature. Afterwards, the tubes were placed in a thermocycler and run for one cycle at  $42^\circ\text{C}$  for 45 minutes,  $99^\circ\text{C}$  for 5 minutes and  $5^\circ\text{C}$  for 5 minutes. Once the run was completed, samples were either stored at  $-20^\circ\text{C}$  or used for PCR.

#### **2.2.3.3 Polymerase chain reaction (PCR)**

To amplify the reverse transcribed cDNA PCR was carried out using Taq polymerase and PCR buffer from Roche. Reagents were mixed in 22.5  $\mu\text{l}$  total volume to the following final concentrations: 1X PCR buffer, 100  $\mu\text{M}$  dNTPs, 0.15  $\mu\text{M}$  forward primer, 0.15  $\mu\text{M}$  reverse primer and 0.625 U Taq DNA polymerase. To this mix 2.5  $\mu\text{l}$  of the prepared cDNA were added. Tubes were placed in the thermocycler and amplified using the following protocol:  $94^\circ\text{C}$  for 2 min, then 30 cycles of  $94^\circ\text{C}$  for 30 s,  $55^\circ\text{C}$  for 30 s,  $72^\circ\text{C}$  for 30 s, followed by a final annealing step of  $72^\circ\text{C}$  for 10 minutes.

#### **2.2.3.4 Quantitative PCR (qPCR)**

RNA Samples that were to be used for qPCR were isolated and 1 µg of total RNA was reverse transcribed as previously described. Primers were used at a final concentration of 1 µM and the probe at 500 nM. The standards were prepared to contain  $1 \times 10^8$  to  $1 \times 10^1$  copies of the product of interest. Primers and probe were mixed with the Sso Fast™ Supermix to make up a mastermix and 19 µl was pipetted into each well. 1 µl of the reverse transcription reaction was added per well. The run was carried out with the following programme: 50 °C for 2min followed by 95 °C 10min and 40 cycles of 95 °C 15 s and 60 °C 1 min. All results were normalized to the GAPDH values and presented as copies of the product of interest compared to 1,000 copies of GAPDH.

#### **2.2.3.5 Agarose gels**

DNA samples were separated using 1% agarose gels in 1x TAE. Ethidiumbromide was added to the agarose solution at a concentration of 0.5 µg/ml. 15 µl of each sample were loaded alongside 10 µl of DNA ladder and separated at 100 V.

#### **2.2.3.6 Plasmid DNA preparation**

Plasmid DNA was obtained from Open Biosystems UCL shRNAmir clone service, which provides shRNA already cloned into a pGIPZ vector. The samples were bought as GIPZ hairpin containing bacteria streaked onto a solid LB agar stab culture containing 100 µl/ml carbenicillin. A pipette tip was used to streak bacteria from the top of the stab culture onto an LB agar plate which contained ampicillin (100 µg/ml). The plate was cultured at 37 °C in an incubator overnight. The following day, colonies were picked and then transferred into 5 ml of LB medium with ampicillin (100 µg/ml) and grown at 37 °C with shaking overnight. Afterwards, plasmid mini preps were performed using the QIAprep Spin Miniprep kit following the manufacturer's instructions. The isolated plasmid DNA was sequenced to check if it contained the right hairpin. If it did, bigger overnight cultures (250 ml) were grown in LB medium with ampicillin (100 µg/ml) and plasmid DNA was isolated using the QIAGEN Plasmid Maxi Kit. The isolated DNA was used for lentiviral preparations.

#### **2.2.3.7 Preparation of HPV18wt re-circularised plasmid**

For experiments with the HPV18wt vector, the bacterial backbone needs to be removed from the HPV18 plasmid. The plasmid then needs to be re-circularised and the bacterial backbone needs to be removed, before the plasmid is purified again. The normal protocol (<http://home.ccr.cancer.gov/Lco/production.asp>) was modified for preparation of larger quantities of plasmid.

In order to obtain enough re-circularised plasmid, the HPV18wt vector was maxi-prepped as previously described. 50 µg of the plasmid was restriction digested with 20 U NcoI as the bacterial backbone is flanked by NcoI sites at 37 °C overnight in 250 µl total volume. It was checked the following day for the presence of two bands at 3,000 bp and 7,900 bp indicating complete digestion of the plasmid. The whole mix was used for the ligation. It was diluted to a final volume of 6 ml (<10 ng/µl of DNA) to enhance the chances that particles would only self-ligate and the appropriate volumes of T4 ligase buffer and 2,000 U T4 ligase were added and the sample was incubated overnight at 16 °C. It was checked for the presence of re-circularised plasmid by agarose gel electrophoresis. Then, 6 ml 5 M ammonium acetate and 22.5 ml 95% ethanol were added to the sample and it was incubated overnight at 4 °C to allow for efficient DNA precipitation. The following day, the mix was centrifuged for 1 hour at room temperature and 5.000 x g, the supernatant was removed and the pellet was washed once with 2 ml of 70% ethanol and centrifuged again for 10 min at 5.000 x g. The pellet was air-dried and resuspended in 100 µl of TE and 100 µl of water. 22 µl of NEB buffer 4 and 60 U XmnI were added and the sample was incubated 45 minutes at 37 °C. This was done as only the bacterial backbone has an XmnI restriction site whereas the HPV18 genome does not contain such a restriction site. ATP was added to a final concentration of 1 mM as well as 30 U PlasmidSafe DNase (Exonuclease V = ExoV) and incubated for 45 minutes at 37 °C. PlasmidSafe only digests linearized DNA but not circularized plasmids. Then 1200 U T4 DNA ligase were added and the sample was incubated for 1 hour at room temperature. To inactivate the present enzymes, 3 µl each of 0.5 M EDTA, 10% SDS and 20 mg/ml proteinase K were added and the sample was incubated for 20 min at 56 °C. 1 ml of buffer PB from the Qiagen mini-prep kit was added to the sample. The sample was split in two parts and each part was put onto a miniprep column. It was centrifuged, the flow through was discarded and the column washed with buffer PE. Then the column was spun without adding any further buffer to remove residual wash buffer. The DNA was eluted in 50 µl of sterile water. It was checked for successful removal of the bacterial backbone by test digesting 1 µl of sample with NcoI and running it on an agarose gel.

#### **2.2.3.8 Isolating extrachromosomal DNA (HIRT-DNA)**

Cells were trypsinised, counted and spun down. The resulting cell pellet was either stored at -20 °C or directly resuspended in 600 µl Hirt Resuspension Buffer. 2.4 ml of Hirt Lysis buffer was added and the cell suspension was incubated at 37 °C for 3 hours. The tube was then incubated at 4 °C overnight. The following day the solution was centrifuged at 65,000 x g for 30 minutes at 4 °C. The supernatant was collected

and 2.5 x volume of cold 100% ethanol were added and the solution was incubated at -20 °C overnight. The next day, the DNA solution was centrifuged for 30 minutes at 7.000 x g and 4 °C. The supernatant was removed and the cell pellet dried at room temperature and then resuspended in 300 µl TE. 60 µg RNase A were added and incubated at room temperature for an hour. To extract the DNA, an equal volume of phenol was added and the mix centrifuged for 4 minutes at 20,000 x g. The top layer was transferred into a new tube and an equal volume of chloroform-isoamylalcohol (24:1) was added, mixed and then centrifuged for 4 minutes at 20,000 x g. To precipitate the DNA, 2.5x volumes of 100% cold ethanol and 0.1x volumes of 3 M sodium acetate were added and the solution was incubated at -20 °C overnight. The following day, it was centrifuged for 30 minutes at 4 °C and 20,000 x g. The pellet was washed once with 70% ethanol followed by another centrifugation for 10 minutes. The pellet was dried at room temperature and resuspended in 50 µl TE.

#### **2.2.3.9 Southern Blot**

The isolated HIRT DNA samples were adjusted for their cell number so that equal amounts of cells were used for digestion. The samples were digested with DpnI and a single cutter (NcoI) or a non-cutter (HindIII) of HPV18 DNA overnight at 37 °C. The DNA as well as HPV18 standards were separated on a 0.8% agarose gel and the gel was stained to check for successful DpnI digestion and DNA separation. The DNA was depurinated by incubating the gel for 15 minutes in Depurination buffer, then it was denatured by in Denaturation buffer twice or 45 minutes and then naturalized twice for 45 minutes in Neutralisation buffer. The Hybond membrane was activated and then washed in 2x SSC buffer. A blot sandwich was assembled by first putting a filter paper bridge as a connection to a reservoir of 10x SSC, followed by the gel, the Hybond membrane and two filter papers. Paper towels were placed on top of the filter papers as well as a weight. The transfer was carried out overnight at room temperature. The following day, the southern blot probe was made by mixing 5 mM DTT, 0.5 µM HPV18 fistful, 1x T4 PNK buffer, <sup>32</sup>P labeled ATP (Perkin Elmer) and 15 U T4 PNK. The mix was incubated for 5 hours at 37 °C. After the transfer, the membrane was crosslinked with UV light of 254 nm and 2 x 120 mJ using the UV Stratalinker 2400 (Stratagene) and then prehybridised at 48 °C for 15 minutes in 10 ml Church Hybridisation buffer. The probe was added directly to the hybridization buffer and the membrane incubated overnight at 48 °C. The next day, the membrane was washed three times for 15 minutes with 20 ml Church Wash buffer at 52 °C before it was transferred into a Storage Phosphor Screen (Molecular Dynamics) developing cassette for 2 days. It was then read with a Typhoon 8610 Variable Mode Imager (GE Health Care).

## **2.2.4 Staining of paraffin embedded sections**

### **2.2.4.1 Haematoxylin and Eosin staining**

Slides were deparaffinized in three changes of xylene for two minutes each. They were rehydrated by dipping them slowly 30 times in two changes of absolute ethanol followed by 15 dips and 30 second incubations in 80% ethanol and 70% ethanol each. They were washed four times for 1 minute in water and transferred to Shandon Instant Hematoxylin for 10 minutes. They were washed under running tap water for 3 minutes and differentiated by dipping them three times in 1.0% alcoholic HCl and rinsed again. The sections were blued in 0.4% sodium acetate, pH 7.25 for 3 minutes, rinsed by dipping them 30 times in three changes of water each and incubated for 30 seconds in 50% ethanol. They were incubated in Eosin-multichrome stain for 2 minutes and washed by dipping them 30 times slowly into three changes of absolute ethanol. They were then dehydrated by incubating them 2 minutes in three changes of xylenes before a coverslip was mounted onto them.

### **2.2.4.2 Immunofluorescent staining of paraffin embedded slides**

The slides were de-paraffinised using xylenes and rehydrated through a graded series of ethanols as for the haematoxylin staining (2.2.4.1). They were then soaked in PBS for 5 minutes followed by microwaving the slides in 10 mM citrate buffer pH 6.0 for 20 minutes. After letting the slides cool, they were washed twice for 3 minutes with PBS. They were incubated at room temperature for 1 hour using 5% serum of the species in which the secondary antibody was raised. The primary antibodies were added at appropriate dilutions in 5% serum and incubated overnight at 4 °C (2.1.3.3.1). The following day, the slides were washed twice for 3 minutes with PBS before 1:500 dilutions of fluorescently-labelled secondary antibodies were added for 60 minutes. The slides were stained with Hoechst dye for 5 minutes at room temperature, washed three times for 3 minutes with PBS before coverglasses were mounted onto the slides.

### **2.2.4.3 Making the probe for fluorescence in situ hybridisation (FISH)**

To make the probe for FISH 1x NT buffer, 0.01 M beta-mercaptoethanol, 0.05 mM dATP, dGTP and dCTP each, 20 U E.coli polymerase, 0.02 U DNase I, 0.02 mM DTT, 0.04 mM Biotin-16-dUTP and 1 µg recircularised HPV18 wt genome as template DNA were mixed and made up to a final volume of 100 µl. The mix was incubated for 2 hours at 15 °C, denatured at 70 °C for 10 minutes and then kept at 4 °C. It was analysed for the presence of 300 – 600 bp fragments. If fragments were present, the

probe was precipitated, if not the mix was further incubated at room temperature for up to 30 minutes after another 0.01 U of DNase I were added.

To precipitate the probe, to 20 µl of mix 4 µg Human Cot I DNA and 6 µg salmon sperm DNA were added and the final volume adjusted to 60 µl. 1/10<sup>th</sup> of the volume of 3 M sodium acetate and 2.75x the volume of cold ethanol were added and the tube centrifuged for 20 minutes at room temperature and 20,000 x g. The supernatant was removed and the pellet air-dried.

The pellet was resolubilised in 21 µl CEP hybridization buffer for every 20 µl used in the precipitation. The probe was denatured at 70 °C for 10 min, 4 °C for 5 minutes and then kept at 37 °C until it was used.

#### **2.2.4.4 FISH**

For FISH, the slides with the rafts were baked overnight at 65 °C. The following day, they were cooled to room temperature and then deparaffinised by incubating them three times 5 minutes in Xylene and rehydrated twice for 5 minutes in 100 % ethanol and air dried. They were boiled 25 minutes with 10 mM sodium citrate and cooled to room temperature. The slides were incubated in pre-hybridisation solution for 30 minutes at room temperature and then dehydrated through an ethanol series by incubating them for 2 minutes each in ice cold 70%, 80% and 95% ethanol. They were then incubated for 5 minutes at 50 °C before they were transferred for 2 minutes into denaturation solution at 72 °C and the ethanol series was repeated as before. The slides were air dried and then 7 µl probe per slide were added and sealed by using a coverslip and parafilm. The slides were incubated overnight at 37 °C in a moist warming chamber. The following day, the coverslip and parafilm were removed and the slides were incubated in 50% formamide, 2x SSC for 30 minutes at 50 °C to remove unbound probe. They were then transferred to 2x SSC for another 30 minutes at 50 °C. Both washes were repeated once. A drop of Detection reagent was applied and covered with parafilm and the slides were incubated for 30 minutes at 37 °C. They were washed three times in 4x SSC, 0.05% triton-x100 for 5 minutes, they were then stained with Hoechst dye for 10 minutes and washed three times for 5 minutes in PBS before a coverslip was mounted onto the slides. They were kept at -20 °C until images were acquired.

## **2.2.5 Animal experiments**

All animal experiments were carried out in the animal facilities at the University of Wisconsin-Madison under the animal licence of Prof. Paul Lambert and under the supervision of Amy Liem or Aayushi Uberoi. Theoretical and practical courses were carried out at the university to obtain approval to work with animals. All animal experiments were performed using B6.129S4-*I2rg<sup>tm1Wjl</sup>/J* (The Jackson Laboratory, Stock: 003174,  $\gamma$ -chain knock-out mice) and C57/BL6 as WT control.

### **2.2.5.1 Infection with MmuPV1 particles**

MmuPV1 particles were isolated from wart lesions by homogenising the tissue and purifying virions by gradient-centrifugation as described for VLP in 2.2.1.10. Infections were carried out in a bio-safety level 2 facility. Mice were anaesthetised using isoflurane. The skin on tail, ears and/or grafts was abraded using the tip of a needle to create micro-abrasion but not going below epidermis and without causing bleeding. MmuPV1 solution was applied onto the abraded site and allowed to dry before the animal was revived. During the procedure, reflexes were tested to ensure that the animal was in a state of anaesthesia, breathing was monitored and the animal was kept warm and its eyes moist. Infected animals were monitored for general health according to local protocols and were examined weekly to detect and measure wart lesion formation.

### **2.2.5.2 Grafting of ear skin onto the back of WT animals**

Graft donors were euthanized using CO<sub>2</sub>, both ears were excised, dorsal and ventral surfaces separated and underlying cartilage scraped off using a scalpel. The tissue was kept in PBS until it was used for grafting. The graft recipients (WT mice) were anaesthetised using ketamine (80-100 mg/kg)/xylazine (5-10 mg/kg), their backs shaven and sterilised using ethanol. The epidermis and dermis were incised down to the panniculus carnosus which was conserved. The recipient skin was removed. Donor skin was fitted onto the graft site and surgical cement was applied. The graft was covered with Vaseline gauze and held in place with stretch adhesive tape. Each recipient received two grafts with one being placed on each side of the back and one of a WT donor and one from a knock-out donor. During the procedure, reflexes were tested to ensure that the animal was in a state of anaesthesia, breathing was monitored and the animal was kept warm and its eyes moist. After the procedure, mice were monitored twice a day for signs of distress or ill health and the adhesive tape loosened if they showed signs of distress or breathing difficulties. Seven days post-transplant, the dressing was removed by anaesthetising the animals using isoflurane

and cutting off the bandages using curved scissors. The graft was infected with MmuPV1 one month post-transplantation.

### **2.2.6 Data analysis and statistics**

Images of agarose gels, immunoblots and the cytokine array were analysed by densitometry using ImageJ. Number of BrdU positive cells, FISH positive cells and total number of nuclei in organotypic rafts were counted using the ImageJ “Analyze Particles” feature. FC data was analysed using FlowJo. Migration for neutrophils was tracked using Icy. Migration of DCs was manually tracked using ImageJ. The manual tracking data was analysed using a previously created Matlab template (258). All graphs were plotted using GraphPad Prism 5, shown are mean  $\pm$  SEM if not indicated otherwise. Data was analysed using statistical tests according to data-sets, e.g. Kruskal-Willis test for multiple groups and Mann-Whitney test to compare two groups.

**3. The common  $\gamma$ -chain is expressed and functional in keratinocytes**

### 3.1 Introduction

Keratinocytes are the main cell type affected by HPV infections and they are not replaced by BMT or GT which is why they are one of the most likely cell types to play a role in the greater susceptibility of X-SCID patients to HPV. However, the role of the common  $\gamma$ -chain has only been studied in detail in haematopoietic cells where it has been shown to be expressed in T, NK and B cells as well as DCs. At the beginning of this project, there was limited data showing whether keratinocytes express  $\gamma$ -chain and whether signalling mediated by  $\gamma$ -chain takes place in these cells. Moreover, as signals via the common  $\gamma$ -chain can only be transmitted when it forms one of its heterodimers and heterotrimers, the expression of these receptors also needed to be examined in detail, which had not been done before. There were only a few reports of single studies showing that  $\gamma$ -chain signalling played a role in keratinocyte biology and no systemic study had been done. Specifically, it was shown that the PI3K and ERK1/2 pathways are activated after stimulation with IL-15 leading to increased proliferation (259). Expression of IL-7R has been shown as well as IL-21R expression and the pro-proliferative effect of IL-21 (221, 222). IL-9 signalling in keratinocytes was reported very recently leading to an increase in secretion of IL-8 (223). IL-4 signalling is also present in keratinocytes, however, this can occur by two separate pathways (260), making it difficult to distinguish between  $\gamma$ -chain dependent and independent IL-4 signalling. Various JAK and STAT molecules are expressed in keratinocytes which is important as  $\gamma$ -chain signals via the JAK-STAT pathway (261).

To examine which interleukin signals mediated by  $\gamma$ -chain are present in keratinocytes and to analyse the effects of the common  $\gamma$ -chain in keratinocytes, it was a crucial step to generate a cell model with common  $\gamma$ -chain knock-down or knock-out when the project started. As primary keratinocytes have a limited life-span and there are few samples available from X-SCID patients due to the low patient number and young age at transplant, we chose a keratinocyte cell line known as NIKS, a commonly used cell line in HPV research in this study (255). In order to establish the vital knock-down cell line for this project without which no further studies into the role of the common  $\gamma$ -chain would have been possible, an shRNA approach was used to knock-down  $\gamma$ -chain in NIKS cells using lentiviral vectors.

### **3.2 The $\gamma$ -chain is expressed in keratinocytes**

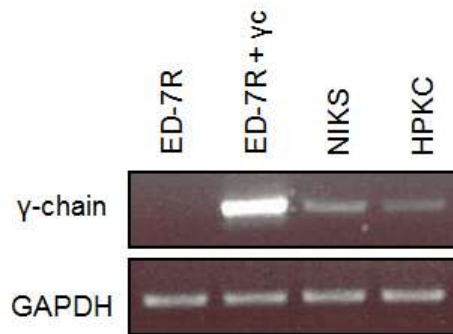
Haematopoietic cells are known to express the common  $\gamma$ -chain confirmed at both mRNA and protein levels. There is no previous data showing whether keratinocytes express  $\gamma$ -chain. To confirm  $\gamma$ -chain expression in keratinocytes, human primary keratinocytes (HPKC) and the keratinocyte cell line NIKS were analysed by reverse transcription PCR (RT-PCR) for mRNA expression and by flow cytometry (FC). ED-7R cells were used as negative control as they do not express the common  $\gamma$ -chain. We also used an ED-7R +  $\gamma$ c cell line which was genetically modified to express  $\gamma$ -chain as a positive control (see 2.1.9).

RT-PCR was carried out using a primer set specific for the common  $\gamma$ -chain. No band was detected in the negative control, but a strong band in the positive control and bands with the same size as the positive control in both NIKS and HPKC. No other bands were detected on the gel. GAPDH expression was used as internal control (Figure 7a). The results indicate that  $\gamma$ -chain mRNA is expressed in HPKC and NIKS.

To assess surface expression of the common  $\gamma$ -chain protein, NIKS and HPKCs were stained with a specific antibody for  $\gamma$ -chain conjugated with APC. Histogram analysis showed that there was a clearly shifted trace in NIKS and HPKC compared to the isotype control. HPKC and NIKS both expressed  $\gamma$ -chain, with HPKC  $\gamma$ -chain expression at a higher level. In contrast, there was no difference in negative control ED-7R cells which do not express  $\gamma$ -chain (Figure 7b).

In summary, common  $\gamma$ -chain is expressed in human keratinocytes at both protein and mRNA level.

a)



b)

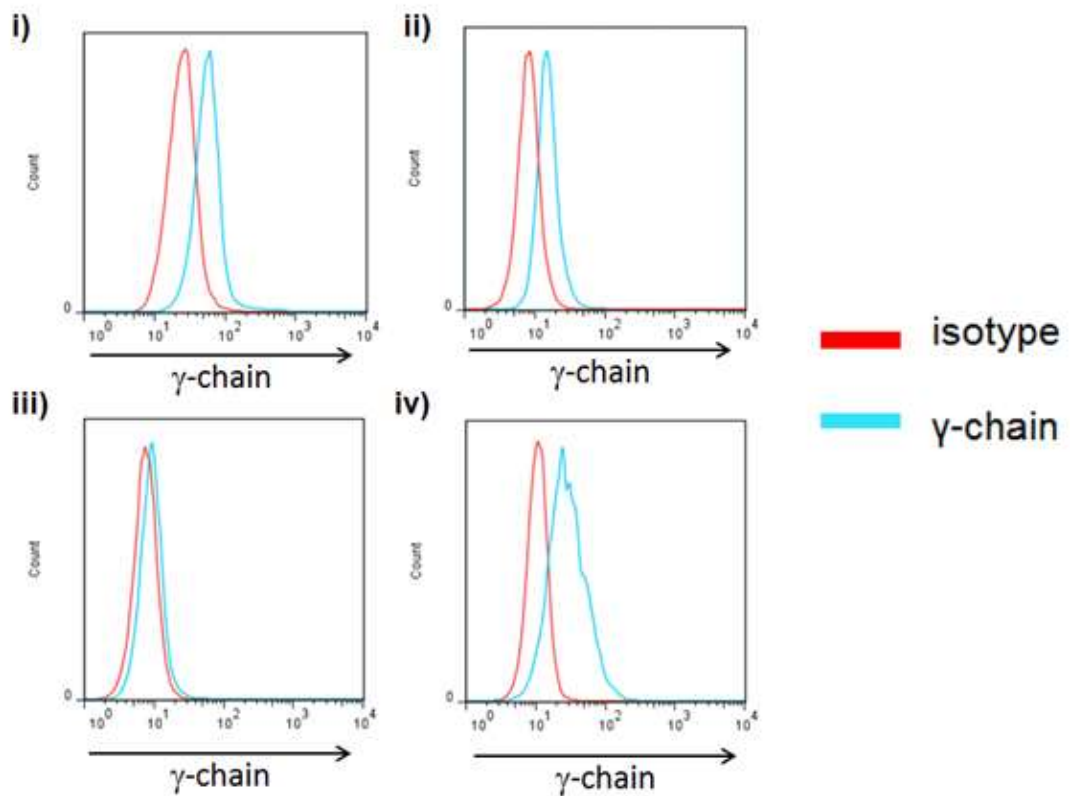


**Figure 7: Expression of  $\gamma$ -chain mRNA and protein in keratinocytes**

RNA of NIKS and primary keratinocytes was isolated and RT-PCR was performed using  $\gamma$ -chain specific primers; GAPDH RNA was amplified as internal control (a);  $\gamma$ -chain was stained and analysed by FC in i) HPKC, ii) NIKS cells, iii) ED-7R and (iv) ED-7R +  $\gamma$ c, representative pictures from  $n = 4$  (b).

### **3.3 Multiple $\gamma$ -chain co-receptors are expressed in keratinocytes**

There is not only a lack of previous data showing the expression of the common  $\gamma$ -chain in keratinocytes but it has also not been examined whether keratinocytes express all  $\gamma$ -chain co-receptors, such as the specific  $\alpha$ -chains for IL-2R, IL-4R, IL-7R, IL-9R, IL-15R and IL-21R and IL-2R $\beta$ . Therefore, NIKS and HPKC were examined for the expression of these co-receptors by RT-PCR, FC and immunoblotting.

RNA was isolated from HPKC and NIKS, and RT-PCR was carried out with specific primers for the different co-receptors. It was found that the PCR products generated by the primers specific for IL-2R $\beta$ , IL-4R, IL-7R $\alpha$ , IL-9R, IL-15R $\alpha$  and IL-21R showed a band in both NIKS and HPKC of the same size as the positive control. This suggests that these receptors were expressed in both HPKC and NIKS. There were no bands observed in the PCR product generated by IL-2R $\alpha$ -specific primers in HPKC and NIKS. This was confirmed by a second pair of primers which also showed no band, suggesting that IL-2R $\alpha$  is not expressed in HPKC and NIKS (Figure 8).

The expression of IL-2R $\alpha$ , IL-2R $\beta$ , IL-4R, IL-7R $\alpha$ , IL-9R, IL-15R $\alpha$  and IL-21R co-receptors in keratinocytes was further analysed by FC and/or western blot. NIKS were stained with antibodies for IL-2R $\alpha$ , IL-4R, IL-9R, IL-15R $\alpha$  and IL-21R and analysed by FC. Histogram analysis showed that there was a clearly shifted trace in NIKS for IL-4R, IL-9R, IL-15R $\alpha$  and IL-21R compared to the isotype control. No shift was observed for IL-2R $\alpha$ . These results illustrate that keratinocytes express IL-4R, IL-9R, IL-15R $\alpha$  and IL-21R but not IL-2R $\alpha$  (Figure 9a).

The expression of IL-2R $\beta$  and IL-7R $\alpha$  was analysed by western blot in both HPKC and NIKS. Corresponding bands of IL-2R $\beta$  and IL-7R $\alpha$  could be detected in both cell lysates (Figure 9b).

In summary, common  $\gamma$ -chain co-receptors IL-2R $\beta$ , IL-4R, IL-7R $\alpha$ , IL-9R, IL-15R $\alpha$  and IL-21R are expressed on keratinocytes, which was confirmed for both mRNA and protein, whereas there is no IL-2R $\alpha$  expression indicating that keratinocytes can only assemble a low affinity IL-2R and not the high affinity heterotrimer.

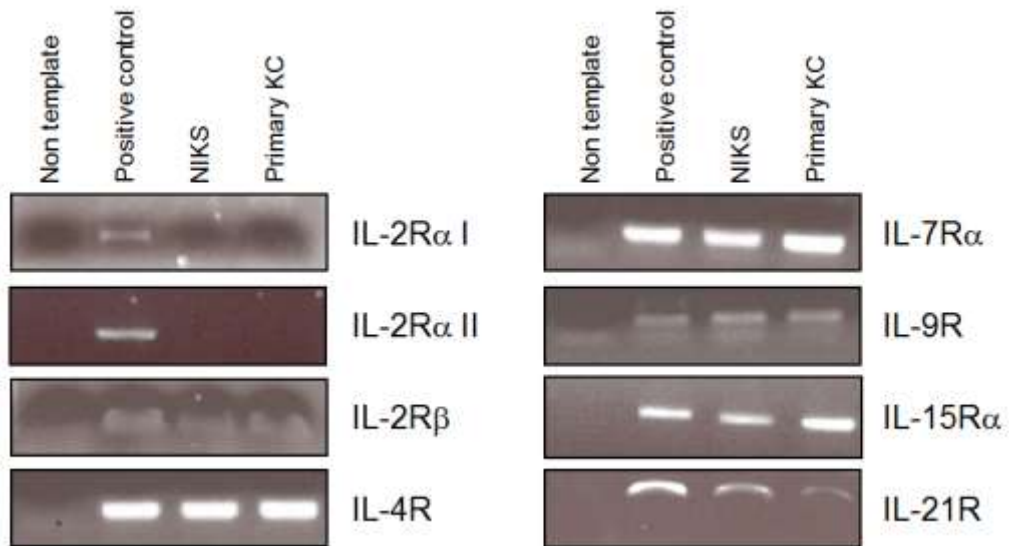
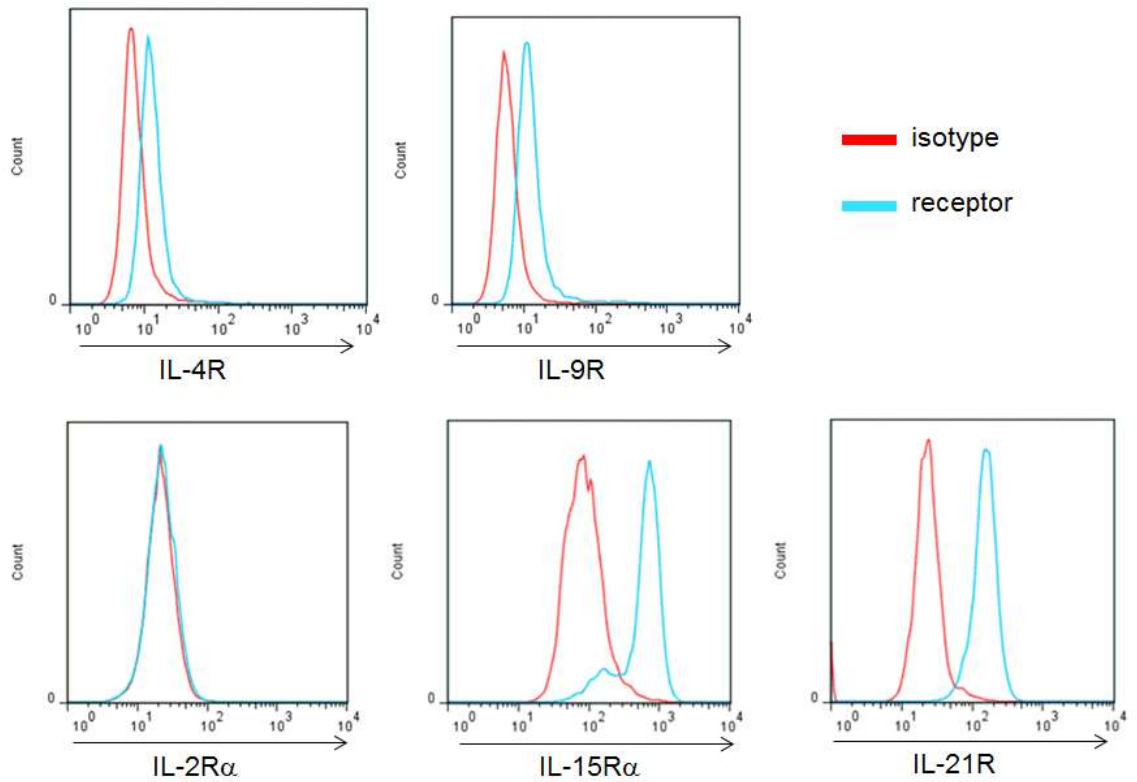


**Figure 8: Expression of  $\gamma$ -chain co-receptors mRNA**

RNA of ED-7R (positive control), NIKS and HPKC was isolated and RT-PCR was performed with primers specific for IL-2R $\alpha$ , IL-2R $\beta$ , IL-4R, IL-7R $\alpha$ , IL-9R, IL-15R $\alpha$  and IL-21R. The RT-PCR products were separated on a 1% agarose gel.

a)



b)

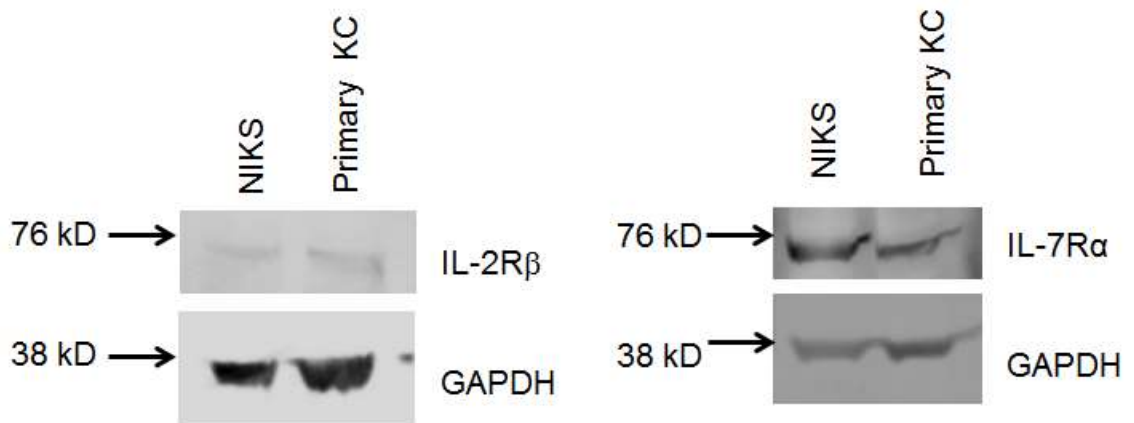


**Figure 9: Expression of  $\gamma$ -chain co-receptors**

NIKS were stained with antibodies for IL-2R $\alpha$ , IL-4R, IL-9R, IL-15R $\alpha$  and IL-21R and analysed by FC; representative pictures from  $n = 4$  (a); cell lysates of NIKS and HPKC were run in SDS-PAGE, transferred onto PVDF membranes and detected by anti-IL-2R $\beta$  and -IL-7R $\alpha$  antibodies, GAPDH was used as internal control (b).

### **3.4 Stimulation with $\gamma$ -chain cytokines induces phosphorylation of STAT5 in keratinocytes**

To further understand, which interleukins play a role in skin immunity, interleukin signalling mediated by  $\gamma$ -chain in keratinocytes was analysed by FC. The signalling pathway linked to common  $\gamma$ -chain signalling is the JAK-STAT pathway with STAT5 being the most commonly phosphorylated STAT protein. As STAT5 phosphorylation can also be induced by other factors such as growth hormone and prolactin which are present in FCS, cells were cultured in serum-free medium overnight to eliminate this influence on phospho-STAT5 levels. The following day, the cells were stimulated with IL-2 (200 ng/ $\mu$ l) for 10 minutes and then harvested and stained with a STAT5 (pY694) antibody for FC analysis.

Analysis showed a small but significant increase in the median fluorescence intensity after stimulation with IL-2, indicating that IL-2 signalling occurs in keratinocytes albeit at lower levels than seen in leukocytes which express the high affinity receptor for IL-2 (Figure 10a+b).

As keratinocytes do not express IL-2R $\alpha$  and cannot form the high-affinity IL-2R, IL-2 may not be the best cytokine to stimulate STAT5 phosphorylation mediated by  $\gamma$ -chain. Therefore, phosphorylation of STAT5 following stimulation with other  $\gamma$ -chain cytokines such as IL-7, IL-9, IL-15 and IL-21 was examined.

The same experiment was performed in NIKS cells following stimulation with IL-7, IL-9, IL-15 and IL-21. Compared to the IL-2 study described above, the challenge levels of these cytokines were 200-fold lower (1 ng/ $\mu$ l). Stimulation with IL-7, IL-15 and IL-21, but not IL-9 induced a small but significant increase in median fluorescence intensity (Figure 10c+d). There was a small increase in phospho-STAT5 after stimulation with IL-9 which was, however, not significant.

In summary, stimulation with multiple common  $\gamma$ -chain cytokines led to a small increase in phosphorylation of STAT5 in NIKS. A significant change could be seen in NIKS with IL-2, IL-7, IL-15 and IL-21. This indicates that the  $\gamma$ -chain is functional on keratinocytes.

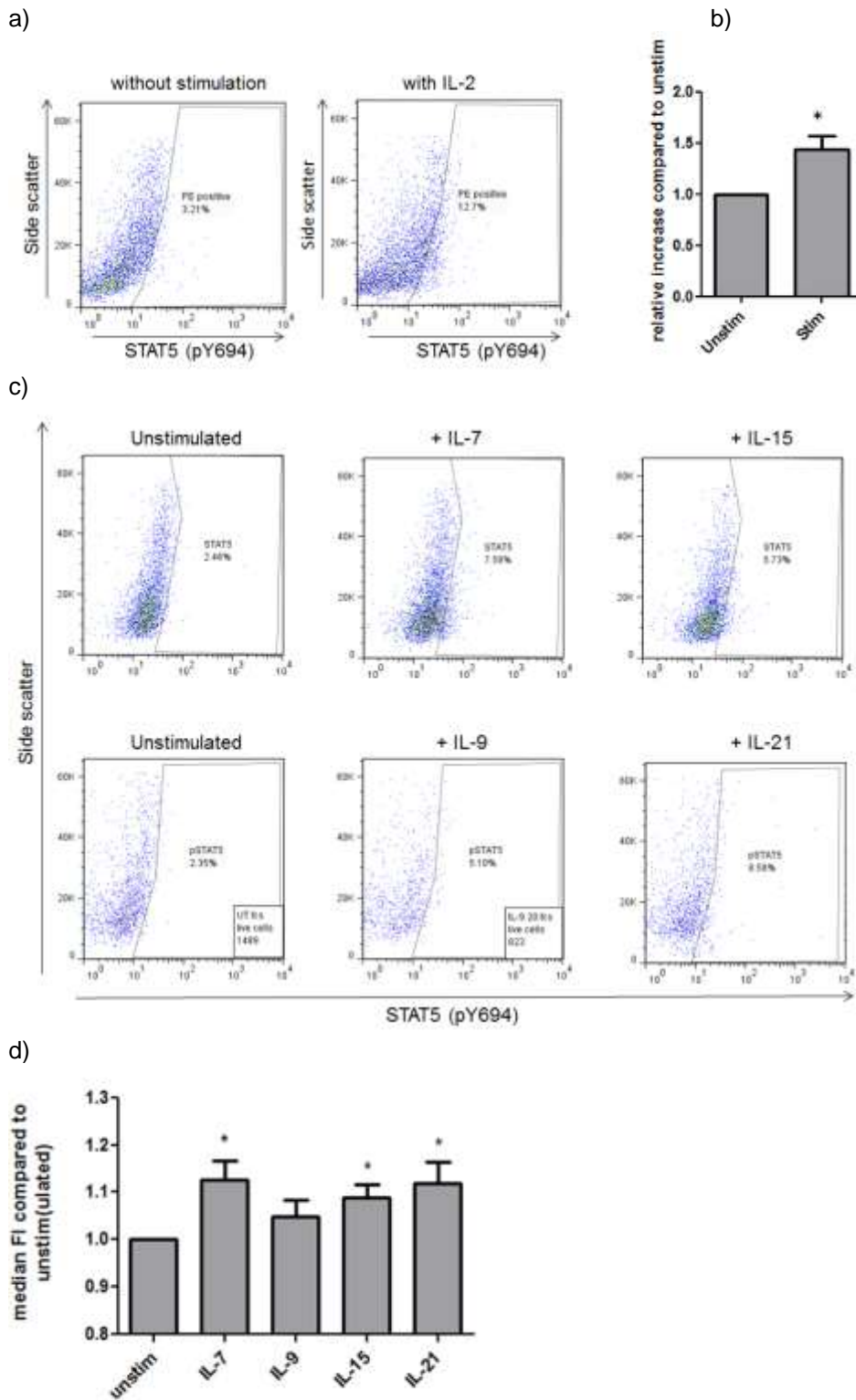


**Figure 10: Phosphorylation of STAT5 NIKS cells after stimulation with  $\gamma$ -chain cytokines**  
 NIKS were cultured in serum-free media overnight and then stimulated for 10 minutes with different cytokines, stained with a STAT5 (pY694) antibody and analysed by FC, representative FC plots for stimulation with 200 ng/μl IL-2 are shown in a), mean  $\pm$  SEM of changes in median FI for IL-2 stimulation in b), \*p < 0.05, Mann-Whitney test, n = 5; c) representative FC plots for stimulation with 1 ng/μl of IL-7, IL-9, IL-15 and IL-21, respectively and d) increase in median FI, mean  $\pm$  SEM, \*p < 0.05, Kruskal-Willis, followed by Dunn's multiple comparison test, n = 6.

### 3.5 Stimulation with $\gamma$ -chain cytokines induces phosphorylation of AKT in keratinocytes

As pSTAT5 levels induced by  $\gamma$ -chain cytokines were relatively low, we wanted to measure a second readout for  $\gamma$ -chain signalling to confirm our results. As it had been published before, that IL-15 stimulation leads to phosphorylation of AKT (pAKT) in a dose-dependent manner (259), we wanted to test whether this was true for different  $\gamma$ -chain cytokines in our study.

NIKS were cultured in serum-free medium overnight and stimulated with different  $\gamma$ -chain cytokines at 100 ng/ml for 10 minutes the following day. Post stimulation, cells were lysed and analysed by western blot for the expression of pAKT and GAPDH as an internal control.

An increase of pAKT levels by 2- to 3-fold compared to unstimulated was observed in cells challenged with IL-7, IL-9, IL-15 or IL-21 (Figure 11). This indicates again that the  $\gamma$ -chain is functional in keratinocytes.

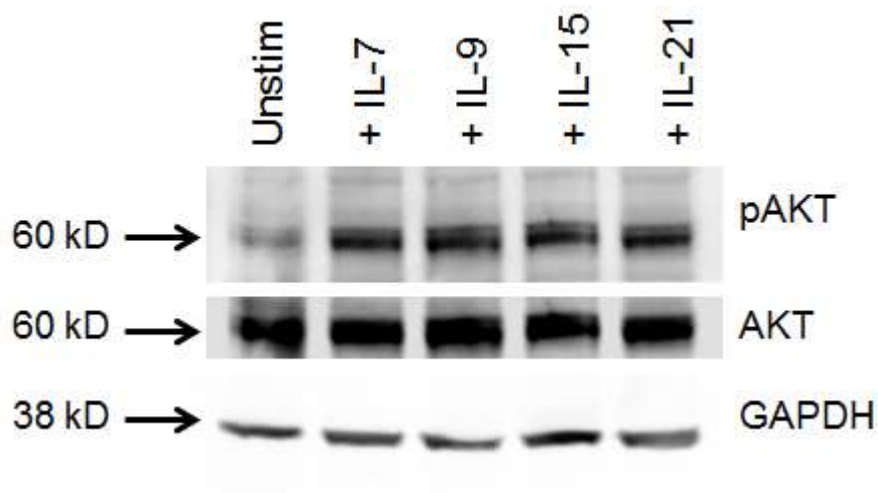


**Figure 11: Phosphorylation of AKT after stimulation with  $\gamma$ -chain cytokines**

NIKS were cultured in serum-free medium overnight, the following day they were stimulated with 100 ng/ml of the different cytokines for 10 min at 37 degrees, lysed and analysed by Western blot for the expression of pAKT. AKT and GAPDH were analysed as an internal controls, representative image from n = 4.

### 3.6 Generation of a common $\gamma$ -chain knock-down cell line: Screening of shRNAs using the ED-7R cell line

To examine the effects of the common  $\gamma$ -chain in keratinocytes, a keratinocyte cell line with loss of  $\gamma$ -chain function was generated. An shRNA approach was used to knock-down  $\gamma$ -chain in NIKS cells. Four shRNAs with complimentary sequences to  $\gamma$ -chain in pGIPZ lentiviral vector were obtained from UCL Open Biosystems. The pGIPZ lentiviral vector contains a puromycin resistance cassette to select positive cell clones and a Turbo-GFP marker to fluorescently mark the transduced cells.

The four shRNAs were tested in ED-7R +  $\gamma$ c cells to screen the most potent shRNA. 72 hours post transduction, the expression of  $\gamma$ -chain was assessed by FC in the GFP positive cells. shRNA2, 3 and 4 showed a clear reduction of  $\gamma$ -chain expression. Compared to the scrambled (scr) control, the greatest knock-down (KD) of  $\gamma$ -chain was seen in the cells transduced with shRNA3, followed by shRNA4 and shRNA2. shRNA1 only showed a small change (Figure 12). As shRNA3 and 4 showed the most potent effect, these two shRNAs were further used in NIKS cells.

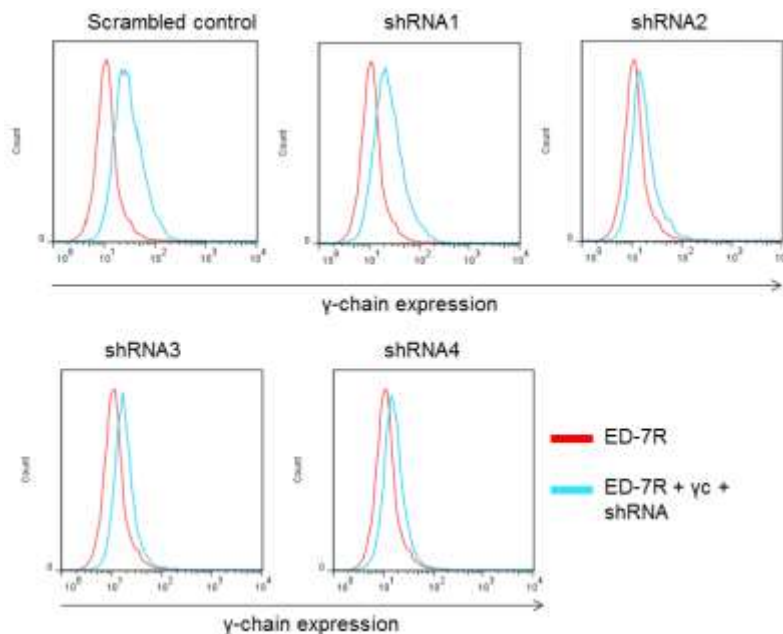


**Figure 12: Knock-down of  $\gamma$ -chain in ED-7R +  $\gamma$ c cells**

ED-7R +  $\gamma$ c were transduced with lentiviruses coding for shRNAs against  $\gamma$ -chain as well as a scr control, 72 hours after transduction the cells were stained with a  $\gamma$ -chain specific antibody and analysed by FC, expression of  $\gamma$ -chain in ED-7R +  $\gamma$ c transduced with different shRNAs are compared to ED-7R ( $\gamma$ -chain negative population).

### **3.7 Generation of a common $\gamma$ -chain keratinocyte knock-down cell line**

NIKS were transduced with the lentiviruses encoding shRNA3 and shRNA4 to knock-down  $\gamma$ -chain; the scrambled shRNA was used as control. 72 hours after transduction, NIKS cells were treated with puromycin for a week to select positively transduced cells (see 2.2.1.7). FC analysis showed >95% GFP positive cells after one week of puromycin selection. Selected cells were stained with anti  $\gamma$ -chain antibody and analysed by FC to confirm common  $\gamma$ -chain expression.

Transduction with the scr control did not alter the expression of  $\gamma$ -chain compared to untransduced cells, whereas cells transduced with shRNA3 showed clear reduction in  $\gamma$ -chain expression compared to that in untransduced cells. However, cells transduced with shRNA4 did not show a reduction in  $\gamma$ -chain expression in NIKS cells (Figure 13).

To further confirm the reduction of  $\gamma$ -chain expression after shRNA3 transduction, the expression of  $\gamma$ -chain mRNA was also examined by RT-PCR. RNA was isolated from cells transduced with scr control or shRNA3 and for untransduced cells. RT-PCR was performed with  $\gamma$ -chain primers used before. The intensity of the bands was compared using ImageJ and normalised to the intensity of the band obtained from untransduced cells.

The results showed a significant reduction of the band intensity by more than 75% compared to untransduced cells and scr control cells (Figure 14).

In summary, cells expressing shRNA3 show a reduction of  $\gamma$ -chain mRNA and protein expression confirmed by RT-PCR and FC.

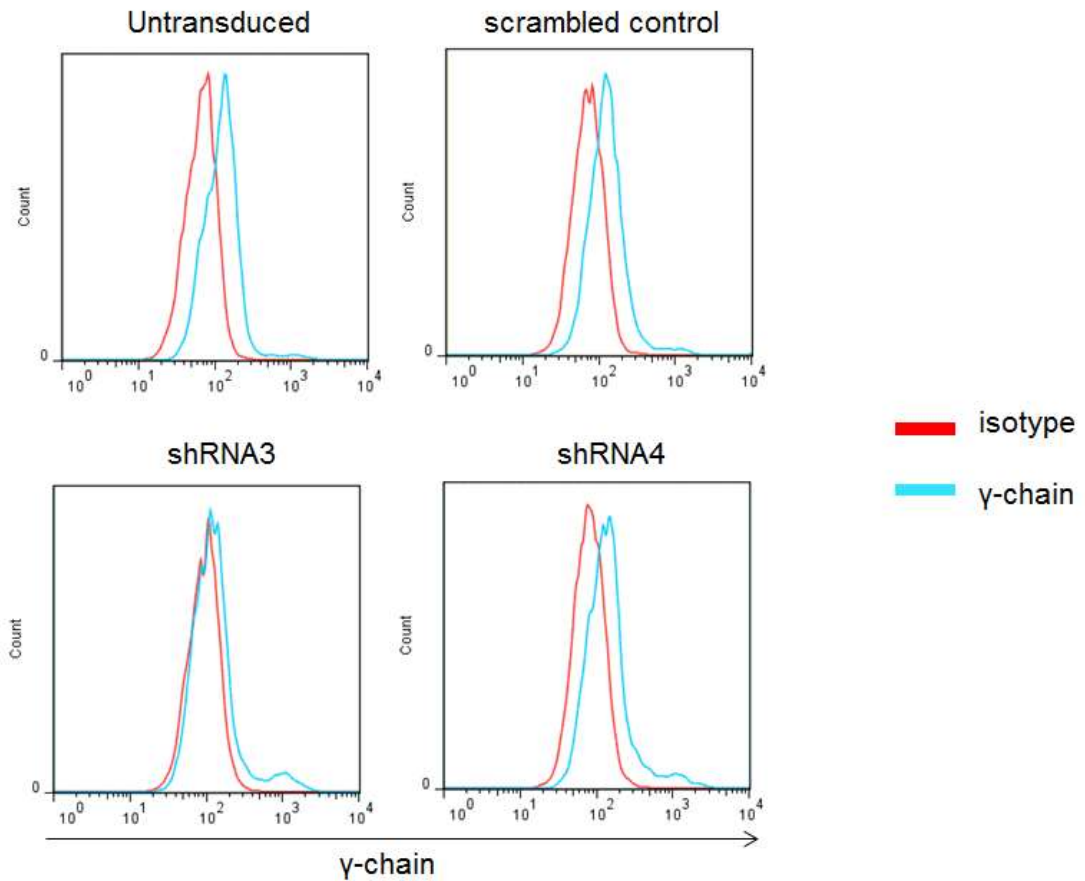


**Figure 13: Knock-down of  $\gamma$ -chain protein using shRNA3**

NIKS were transduced with shRNAs against  $\gamma$ -chain and selected with puromycin for a week starting 72 hours after transduction;  $\gamma$ -chain expression in untransduced (UT) and cells transduced with scr control shRNA or shRNAs 3 and 4 were analysed by FC, representative images from, n = 8.

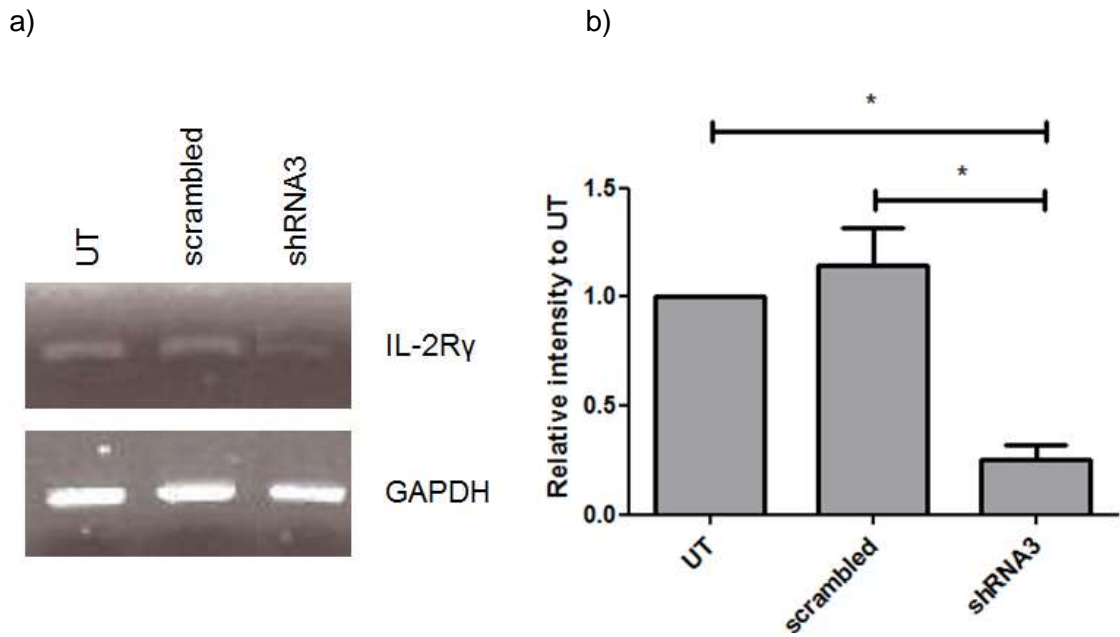


**Figure 14: Knock-down of  $\gamma$ -chain mRNA**

RNA was isolated from different NIKS cell lines and RT-PCR was performed using  $\gamma$ -chain specific primers, GAPDH RNA was amplified as internal control, representative image (a) and bar charts showing the compared intensities of the bands obtained using ImageJ compared to UT (b), mean  $\pm$  SEM, \* $p < 0.02$ , Mann-Whitney test,  $n = 4$ .

### **3.8 Signalling mediated by $\gamma$ -chain is defective in knock-down keratinocyte cell line**

To test, if the reduction in  $\gamma$ -chain expression led to a functional change, phosphorylation of AKT after stimulation with IL-15 was analysed as we saw previously that pAKT gives a clearer and stronger signal than pSTAT5.

Untransduced NIKS and NIKS transduced with either scr control or shRNA3 were cultured in serum-free medium overnight and then stimulated with IL-15 (10 ng/ml) for 10 minutes the following day. The samples were analysed for the expression of pAKT by Western blot. The protein bands in the blot were analysed by densitometry and the relative pAKT expression in unstimulated and IL-15 stimulated samples was calculated by normalising to the total protein levels using GAPDH as internal control.

A significantly increased pAKT level after IL-15 stimulation was observed in untransduced samples and scr control as expected. In contrast, cells transduced with shRNA3 demonstrated no change in pAKT levels, indicating absence of IL-15 signalling in these cells (Figure 15).

In summary, the expression of  $\gamma$ -chain mRNA and protein were reduced in the cells with  $\gamma$ -chain knock-down. The reduced expression further led to significantly impaired  $\gamma$ -chain signalling capability as shown by reduced levels of phosphorylated AKT after IL-15 stimulation. Cells transduced with shRNA3 were used for further experiments and are referred to in future chapters as “KD cells”.

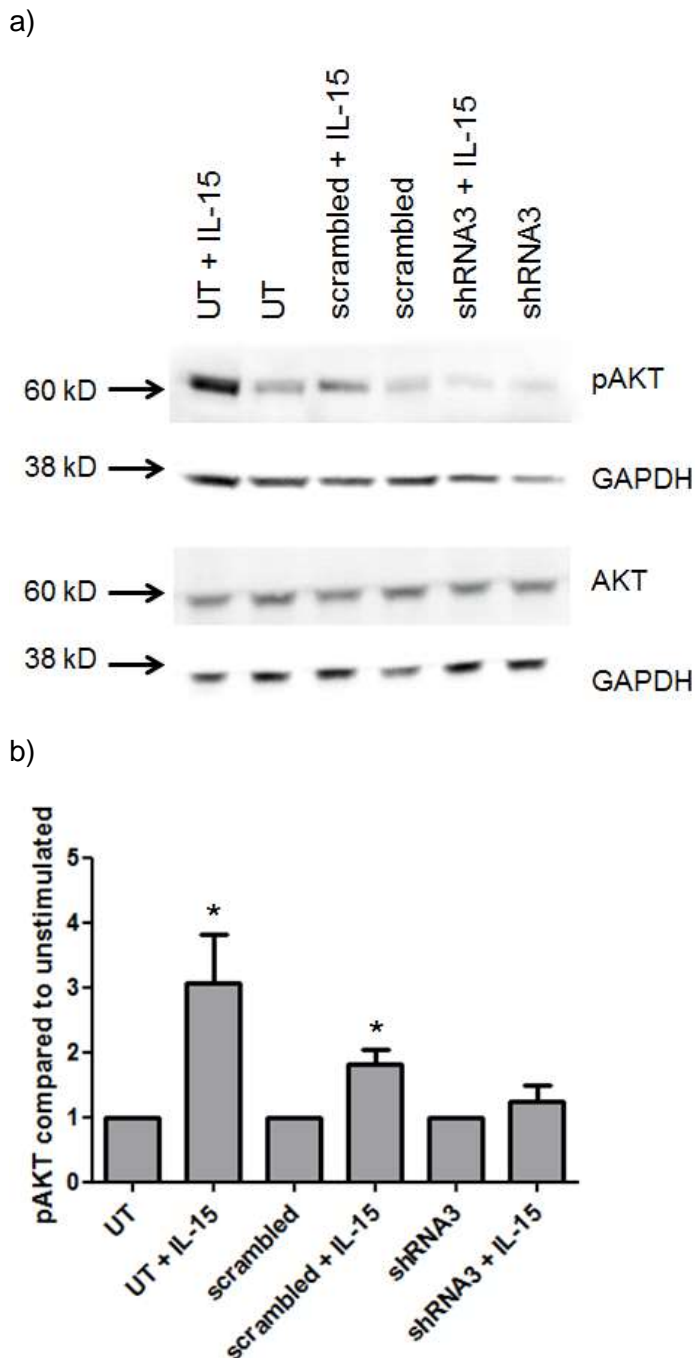


**Figure 15: pAKT levels in  $\gamma$ -chain knock-down and control cells after IL-15 stimulation**

Untransduced NIKS and cells transduced with scr control or shRNA3 were cultured in serum-free medium overnight and then stimulated for 10 minutes with 10 ng/ml IL-15. Cell lysates were analysed by western blot for the expression of pAKT. AKT (run on a second gel) and GAPDH were used as internal controls, representative western blot images (a) and densitometry results normalised to GAPDH (b) showed the relative increase of pAKT in untransduced and scr control cells after stimulation with IL-15 but not in cells with shRNA3 expression, mean  $\pm$  SEM, \* $p < 0.05$ , Kruskal-Willis test, followed by Dunn's multiple comparison test,  $n = 6$ .

### 3.9 Discussion

To analyse the role of  $\gamma$ -chain in keratinocytes, it first needed to be confirmed that  $\gamma$ -chain and its co-receptors are expressed in keratinocytes, as limited literature existed. Kagami et al. showed the expression of  $\gamma$ -chain at mRNA level in the HaCaT keratinocyte cell line but no data has shown the expression of  $\gamma$ -chain protein in primary keratinocytes and other cell lines (262). In addition, from the  $\gamma$ -chain co-receptors, the expression of IL-4R, IL-9R, IL-15R $\alpha$  and IL-21R in different human keratinocyte cell lines or primary keratinocytes has been described mainly as single reports (223, 260, 263, 264). However, our study is the first to test the expression of all common  $\gamma$ -chain receptors in one study and to examine their expression in the NIKS cell line.

RT-PCR and FC were used to show the expression of  $\gamma$ -chain in HPKC and the NIKS cell lines at mRNA and protein levels. The specificity of these tests was shown by using the ED-7R cell line which does not express  $\gamma$ -chain and a genetically modified ED-7R cell line which overexpresses  $\gamma$ -chain. In addition, expression of all  $\gamma$ -chain co-receptors except IL-2R $\alpha$  was also shown in HPKC and NIKS. This confirmed that a broad range of  $\gamma$ -chain receptors are expressed in both cell types and suggests that the high affinity IL-2 receptor cannot be formed on keratinocytes although the low affinity IL-2R $\beta$ / $\gamma$ -chain heterodimer can be assembled.

While this project was undertaken, Luff et al. published a paper about the expression of  $\gamma$ -chain and its co-receptors in canine keratinocytes. They observed the expression of IL-4R, IL-7R, IL-15R $\alpha$  and low levels of IL-2R $\alpha$ . However, in contrast with the results shown here, IL-9R and IL-21R were not expressed in their study (265). This may be explained by different species which might have different expression profiles of certain receptors. Technical limitations could also give rise to discrepancies but in support of the data shown here, expression of IL-9R and IL-21R has been described in human keratinocytes in other studies (223, 264).

As  $\gamma$ -chain and most of its co-receptors were expressed in keratinocytes, it seemed very likely that there would be a relationship between  $\gamma$ -chain containing-receptors, keratinocyte function and possibly immunity in the skin. We, therefore, went on to test whether we could detect signalling via the common  $\gamma$ -chain in keratinocytes. As in haematopoietic cells, signalling pathways activated by  $\gamma$ -chain cytokines are the JAK3/STAT-pathway, the PI3K/Akt and the RAS-mitogen-activated MAPK pathways, we decided to analyse the phosphorylation of downstream molecules of these pathways (168, 266).

When cells were stimulated with different  $\gamma$ -chain dependent cytokines, phosphorylation of downstream signalling molecules was observed. A small but significant increase in pSTAT5 levels was observed after stimulation with IL-2, IL-7, IL-15 and IL-21. The change seen with IL-9 was not significant. That means that even though IL-2R $\alpha$  was not expressed in keratinocytes, signalling via IL-2 was still possible because the IL-2R $\beta$  and  $\gamma$ -chain receptors form an intermediate receptor, which can transduce signals. The magnitude of pSTAT5 was relatively low compared with published results for leukocytes stimulated with the same cytokines (233, 267, 268). There may be a number of reasons for this, e.g. that the expression of  $\gamma$ -chain is lower in keratinocytes than in leukocytes.

It has been previously reported that IL-15 stimulation leads to an increase in phosphorylation of AKT and ERK1/2 in HaCaT cells (259). Therefore, we went on to measure pAKT levels which are downstream of JAK/STAT signalling and could benefit from amplification of the signalling pathway. In support of the pSTAT5 data, IL-7, IL-9, IL-15 and IL-21 led to robust and significant increases in pAKT levels. This suggests that signalling via different  $\gamma$ -chain dependent receptors is present in keratinocytes.

Even though, we detected IL-4R mRNA and protein in keratinocytes, we decided to exclude IL-4 from further analysis as it has been described that many effects of IL-4 in keratinocytes are independent of JAK3 as IL-4R can additionally heterodimerise with IL-13R $\alpha$  and signal through JAK1 and STAT6 (260, 262).

In conclusion, these experiments suggest that  $\gamma$ -chain is not only expressed in keratinocytes but is also functional and can transmit signals to downstream target genes, although these target genes in keratinocytes remain to be identified.

In order to analyse the effects of  $\gamma$ -chain in human keratinocytes, it was crucial to generate a keratinocyte cell line with  $\gamma$ -chain knock-down. In order to establish this important tool for this project, an shRNA approach was used to knock-down  $\gamma$ -chain in NIKS. FC and RT-PCR analysis showed that cells transduced with one of the shRNAs led to a significant decrease in  $\gamma$ -chain expression by at least 75% compared to untransduced cells and cells transduced with scr control. This resulted in almost complete abrogation of signalling in these cells, evidenced by failure to increase pAKT levels after stimulation with IL-15. These results show that we successfully created a common  $\gamma$ -chain knock-down keratinocyte cell line which has not been done before. This cell line as our most important tool for this project was used in all further chapters to examine the role of the  $\gamma$ -chain in the keratinocytes in HPV-related immunity.

**4. Infectivity with pseudo- and quasivirions is increased in  $\gamma$ -chain deficient cells**

## 4.1 Introduction

One of our hypotheses to explain the increased susceptibility of patients with X-SCID to severe HPV infections after BMT or GT, even with successful restoration of T cell compartment, is that patients' keratinocytes are more easily infected than those of healthy individuals. A higher infection rate could explain the higher number of affected individuals as well as the high number of affected sites seen in X-SCID patients compared to the rest of the population.

In order to test this hypothesis, live HPV virions needed to be prepared for cell infections. It is difficult to isolate live virus as it can only be obtained from wart lesions where it can only be retrieved in relatively small amounts (269, 270). In addition, only certain low risk HPV types such as HPV1 and HPV2 can be isolated from warts but not high-risk  $\alpha$ -types HPV such as HPV16 and 18. Therefore, researchers have attempted to make virus *in vitro*.

Initially, PV virus-like particles (VLP) were produced *in vitro* using vaccinia virus recombinants expressing L1 and L2 capsid proteins and plasmid DNA containing an SV40 origin of replication. When PV DNA was transfected and the cells infected with the vaccinia virus, the DNA was successfully encapsidated into particles inside the cells. The resulting particles were shown to be infectious as they could transport the encapsidated DNA into a number of different cell types. This process was used to make HPV16, 18, 33 and BPV1/2 VLPs (271-273).

It is also possible to harvest virions from organotypic rafts made with HPV transfected cells as they provide the level of epithelial differentiation that is needed for the synthesis of virions. These virions have the typical virion morphology which has been shown by electron microscopy for HPV18 and HPV31. However, when isolating virions from rafts, a high number of rafts are needed to provide sufficient quantity of PV particles for experiments (274-276). Thus the *in vitro* production of virions is not very efficient and is very laborious and technically demanding.

In the past decade, more efficient methods were developed for intracellular production of HPV VLPs using 293 cells. Two different plasmids are required to make the HPV VLPs: a plasmid coding for HPV L1 and L2, e.g. the pShell plasmid and the recircularised full-length HPV genome. The pShell plasmids are bicistronic L1/L2 expression plasmids which contain stuffer DNA to increase their size to 10.8 kb. In order to make replication deficient virions, the pShell plasmid must not be packaged in to the PV particle after co-transfection. The packaging process is a promiscuous process which is sequence-independent, however, efficient packaging occurs only with

plasmid DNA with a size smaller than 8 kb. Therefore, pShell which is 10.8 kb is inefficiently packaged into PV particles. The size restriction makes it essential to remove the bacterial insert from PV plasmids prior to vector production to reduce its size to < 8kb (277). After transfection, the Shell plasmid is transcribed and translated inside the 293 cells, separately from the PV plasmid. The proteins L1 and L2 are produced and form a capsid for encapsidating the plasmid DNA (278).

As HPVs are not actively released from keratinocytes but shed from dying cells the 293 cells need to be lysed in order to obtain the virus. The resulting cell lysate contains immature HPV virions which need to be incubated overnight at 37 °C for maturation. Maturation is associated with an increase in multimeric L1 forms and loss of L1 monomers due to the formation of disulphide bonds. Mature virions are smaller in size and more regular than immature particles as observed by electron microscopy. Overall, the maturation process of PVs takes several hours compared to seconds or minutes for most other viruses (99, 277).

The resulting virion containing supernatant also contains cell debris and proteins. Therefore, it needs to be further purified to obtain high quality virions to use for experiments. There are two ways for purification of the cell lysate:

- a) density-gradient centrifugation using iodixanol (sold as OptiPrep™) or caesium chloride
- b) size exclusion chromatography using agarose gel filtration.

A single partially diffused iodixanol gradient is efficient at separating virions from cellular proteins in 293 lysates. In addition, separation of empty capsids and DNA-containing capsids is achieved with good recovery of viral titre (277).

Size exclusion chromatography relies on the fact that the produced VLP capsids are larger than all other complexes in the clarified lysate. A pore size of 50- to 150-µm can be used as this is slightly smaller than the VLP capsids and the capsids are excluded and directly eluted. Using ultracentrifugation higher purity can be achieved but it is more technically challenging (278).

VLPs were subsequently used for experiments investigation the early steps in PV infection, examining for example which cell surface receptors mediate the uptake of PVs into cells, whether certain cytokines affect infectivity with PVs and which downstream molecules are activated after infection.

No published studies have analysed whether the common  $\gamma$ -chain or its cytokines have any influence on the uptake of PVs into keratinocytes and therefore, we set out to test

this using both VLPs containing a reporter gene and ones containing a HPV plasmid. In addition, the influence of  $\gamma$ -chain and some of its cytokines on proliferation was examined as the level of proliferation can alter infectivity.

X-SCID patients are often affected by infections with the cutaneous HPV  $\beta$ 1 types HPV5, HPV14 and HPV36 or the  $\alpha$ 4 type HPV2. Shell plasmids for HPV14 and HPV36 are currently not available. For virions made with HPV5 pShell a high particle to infectivity ratio and for virions made with HPV2 pShell essentially no infectivity on tested keratinocyte cell lines was described (<http://home.ccr.cancer.gov/lco/plasmids.asp>). In addition, in a publication from 2014 the cutaneous VLPs used had lower infectivity than mucosal types in 293TT cells. However, in skin cell lines, the cutaneous types showed minimal or undetectable signals (279). As VLPs made with capsid proteins from mucosal types show more robust infection, we decided to use the previously successfully used pShell plasmid from HPV16 for our experiments to ensure that we would observe infection. Moreover, we used HPV18 plasmid in our quasivirion experiments and later transfection experiments because it is an easily detectable HPV type as it is usually replicated in high quantities in transfected or infected cells.

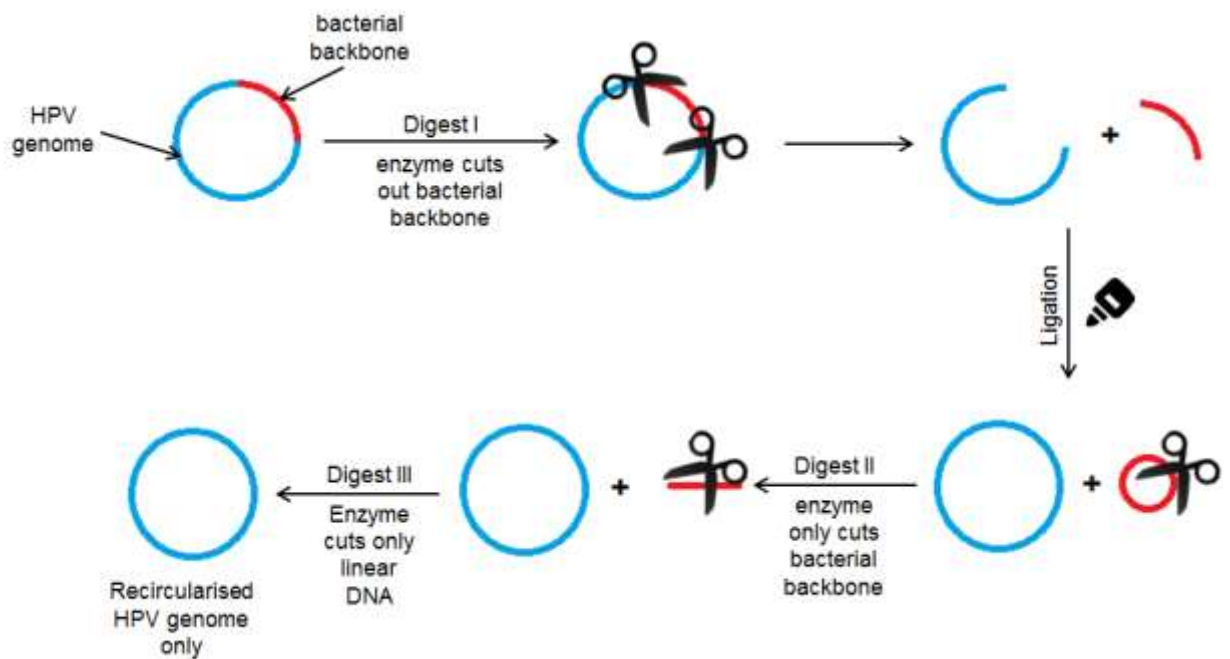
In this chapter, “pseudovirions” refer to VLPs comprising the capsid formed of L1 and L2 and Luciferase as a reporter gene and “quasivirions” to particles containing the full-length HPV18 genome. The Luciferase plasmid codes for firefly luciferase under the control of the CMV promoter leading to constitutive expression in cells when the plasmid has entered the cell. As this type of work is not done at ICH, I spent five months in the laboratory of Prof. Paul Lambert at the University of Wisconsin-Madison where I obtained the following results.

## 4.2 Preparation of HPV18 wt plasmid

For transfection with the HPV18 wild-type (wt) genome as well as to produce VLPs, the bacterial sequences need to be removed from the HPV18 plasmid. In order to do this, the original protocol from C. Buck (<http://home.ccr.cancer.gov/Lco/production.asp>) was modified and optimised to increase the amount of recircularised vector obtained and to reduce the amounts of enzymes used (see 2.2.3.7).

First, the HPV18 plasmid was digested with NcoI to remove the bacterial sequences. Before digestion, the supercoiled and open circular circularized plasmid at around 6.2 kb and > 16 kb was observed, respectively (Figure 16b, Lane 1). Following digestion, two bands could be seen. From previous work, the band at 7.9 kb is known to be the HPV genome and 3.0 kb the bacterial sequences (Lane 2). After re-ligation the re-circularised genomes could be seen as multiple bands. The sizes around 6.2 kb and >16 kb corresponded to the supercoiled and open circular forms of the HPV genome plasmid and the sizes between 1.8 kb and 3.2 kb to the supercoiled and open circular forms of the bacterial sequences (Lane 3). The bands around 23 kb were head to tail concatomers of the HPV genome. The re-ligated sample was precipitated (Lane 4) and digested with XmnI, an enzyme which only linearised the bacterial backbone (Lane 5). After digestion, bands which were same size as the HPV18 genome after ligation (6.2 kb and >16Kb) and the linearised bacterial backbone (3.0 kb) were obtained (Lane 5). This sample was digested with Exonuclease V which only digested the linearized bacterial backbone but not circularized HPV18 genome. After digestion, the HPV18 genome was still present whereas the linearised bacterial backbone at 3.0 kb disappeared (Lane 6). The sample was further incubated with ligase to re-seals nicks in the open circular HPV18 genomes. The size of the product after ligation was same as lane 6 (Lane 7). The sample was then purified to remove enzyme and salts using a Qiagen Miniprep column. During the purification, concatomers were also partly removed as the miniprep column only allows <30kb DNA to pass through (Lane 8). To confirm, whether the product contained only HPV18 genomes, a restriction enzyme (NcoI) that only cuts the HPV18 genome once was used. After digestion, only a band at 7.9 kb was observed suggesting that the sample contained only HPV18 genomes (Lane 9). These recircularised HPV18 genomes were used for further studies.

a)



b)

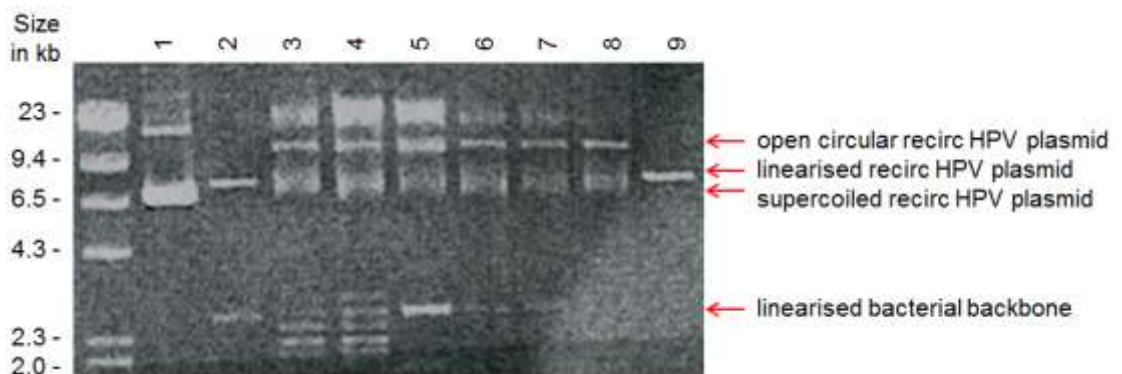


**Figure 16: Reconstruction of HPV18wt plasmid**

The HPV18wt plasmid was digested with NcoI, to remove the bacterial backbone, re-ligated, precipitated, digested with XmnI which only cuts the bacterial backbone and treated with ExoV which only digests linearised DNA, a) flow-chart showing the process, b) agarose gel picture showing in Lane 1) uncut HPV18wt plasmid including bacterial backbone; Lane 2) after digest with NcoI; Lane 3) after religation; Lane 4) after precipitation; Lane 5) after digest with XmnI; Lane 6) after digest with ExoV; Lane 7) after T4 ligase treatment; Lane 8) after purification; Lane 9) test digest with NcoI to confirm the product was HPV18 wt plasmid.

### 4.3 Making HPV quasivirions

Using the recircularised HPV18 plasmid HPV quasivirions were made for further experiments. The virus was produced as described in 2.2.1.10 and then purified using an iodixanol gradient. The separation was done in two separate tubes to test the effect of benzoase treatment prior to purification (tube B). Benzoase removes any residual DNA that had bound to the capsids. 15 fractions were collected from each tube by puncturing the tube and collecting eluent drops.

To identify which fractions contained the virus particles, the expression of L1 protein around ~55 kD was checked as L1 is the only protein present in abundance in HPV virions. In addition, the presence of other proteins representing cellular protein impurities was examined. A small aliquot was used for an SDS-PAGE and stained with Coomassie blue. A single protein band of 55 kD corresponding to L1 was observed in fractions 2 – 6 of tube A and fractions 2 – 4 of tube B and no additional bands were seen (Figure 17). The difference in the number of fractions containing the virus particles is due to the fact that the first fractions of tube A were smaller in volume than for tube B. The total virus containing volume was similar for both tubes.

As the virions had to consist of both the capsid particles and the HPV DNA, the fractions were further examined for presence of HPV18 DNA. The particles from each fraction were lysed and run on an agarose gel. Linearised HPV18 plasmids with various dilutions were used as standards. Due to high viscosity of the DNA samples extracted from virus particles, these samples ran differently from the pure linearised HPV18 plasmid DNA. Therefore the observed sizes did not accurately reflect the size of HPV18 DNA. The results from the gel showed that tube B fractions contain only two bands which are the supercoiled and open circular circularized forms of the HPV plasmid, whereas tube A contains additional DNA bands (Figure 18a). As Tube B was treated with Benzoase prior to gradient centrifugation, this result indicated that nuclease treatment was efficient at removing DNA bound to the virus particles. These results suggested A2 – A6 and B2 – B4 contained viral quasivirions.

The viral titre was assessed using Southern Blot. Two bands representing the supercoiled and open circular circularized plasmid forms could be observed in tube A and B fractions. The titre was calculated based on the intensity of bands by densitometry and compared to the standards. It was around  $2 \times 10^7$  viral genome equivalents (vge) per  $\mu\text{l}$  (Figure 18b). As fractions from tube B were cleaner they were used for subsequent experiments. For most experiments, fraction B2 was used as it showed the highest viral titre.

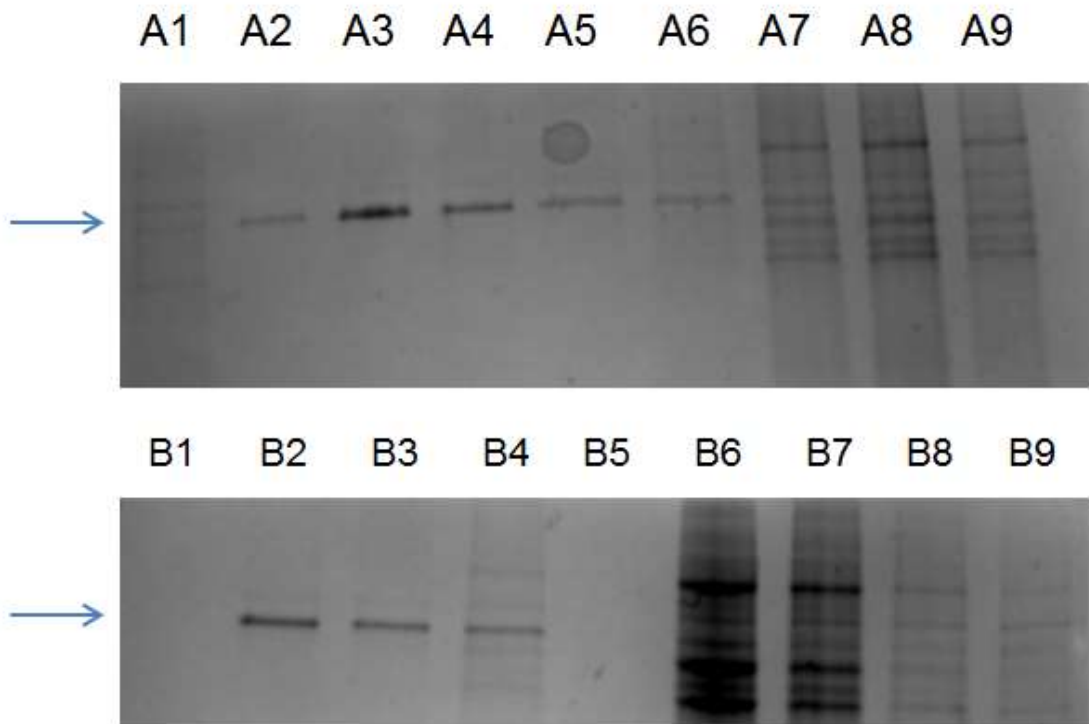
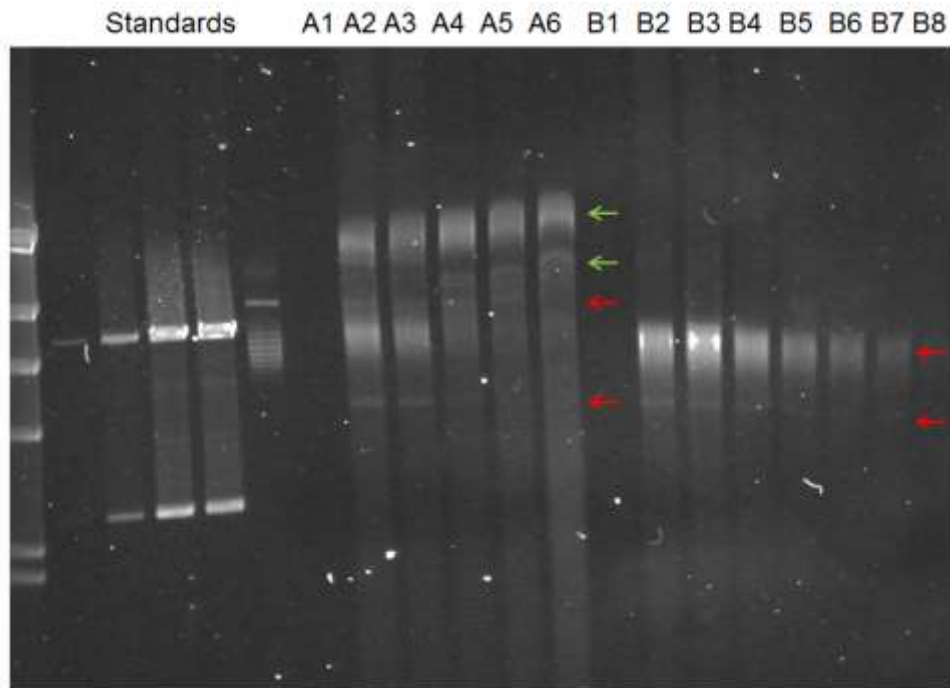


**Figure 17: Identifying HPV18 quasivirions containing fractions**

HPV18 quasivirions were purified using an Optiprep gradient. For two different sets, 15 fractions each were collected. 10  $\mu$ l of each fraction were supplemented with SDS loading dye and boiled to lyse virus particles and separated on an SDS-PAGE gel. The gel was stained for Coomassie blue and bands were visualised after destaining. The size of the L1 protein (55 kD) is indicated by arrows.

a)



b)

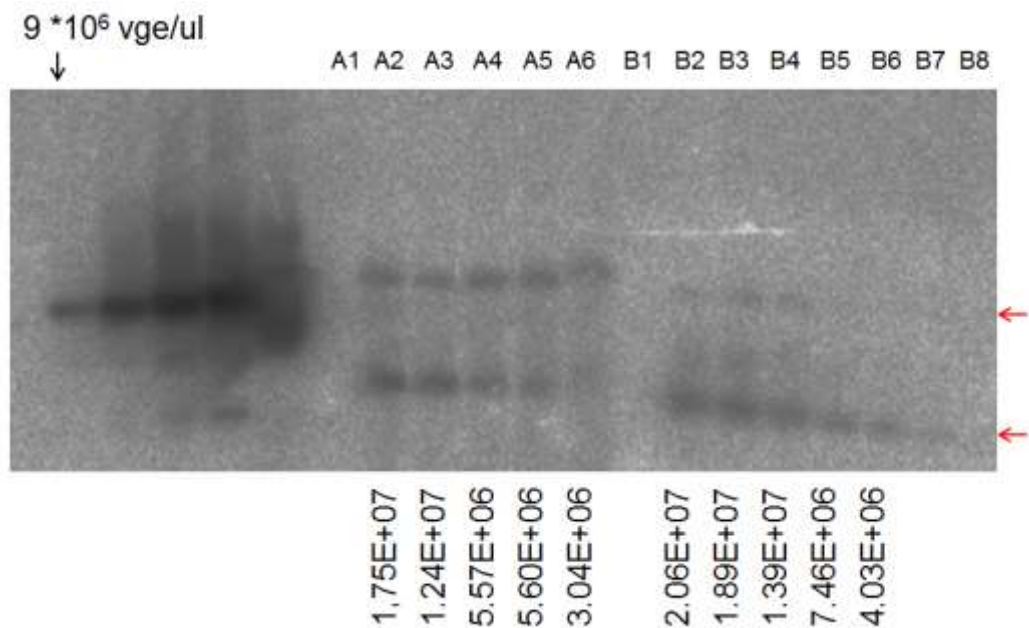


**Figure 18: Titering HPV18 quasivirions**

HPV quasivirions were lysed using proteinase K, SDS and EDTA. These were run, along with standards of different concentrations on a 0.6% agarose gel; HPV18 bands are indicated with red arrows, additional bands with green arrow; fractions B were treated with Benzoase prior to quasivirions purification (a). The gel was used for Southern blot and the blot was probed using an anti-HPV18 probe (b). Viral-genome equivalents (vge) per  $\mu$ l are shown beneath each fraction as calculated compared to the indicated standard using densitometry.

#### 4.4 Infectivity using pseudovirions is increased in $\gamma$ -chain deficient keratinocytes

To examine whether absence of the common  $\gamma$ -chain in keratinocytes changes the initial phase of the HPV infectious life cycle, infectivity in scr control NIKS and KD NIKS was analysed using pseudovirions. As the pseudovirions expressed the reporter gene luciferase, the infectivity was evaluated by luciferase activity 48 hours post infection. NIKS cell lines were infected with the pseudovirions at a virus concentration of 1 and 10 vge/cell.

An increase in luciferase activity of 60% was observed with both viral concentrations in the KD cells compared to scr control cells (Figure 19). This suggests that reduction of  $\gamma$ -chain expression could cause an increased susceptibility to HPV virion infection.

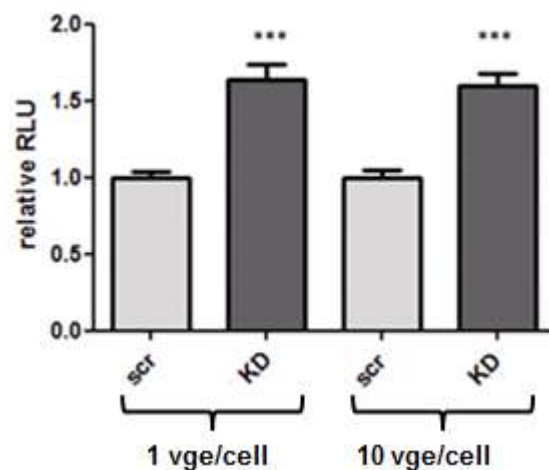


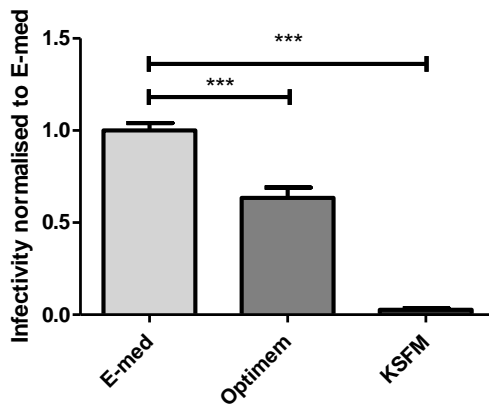
**Figure 19: Levels of infectivity in NIKS cell lines 48 h post pseudovirion infection**

Scr control and KD NIKS cell lines were seeded on 96 well plates, infected with pseudovirions at viral concentrations of 1 or 10 vge/cell. Luciferase activity was measured 48 hours later. Relative light units (RLU) were normalised to cell numbers and to scr control values, mean  $\pm$  SEM, \*\*\*  $p < 0.001$ , Kruskal-Wallis test, followed by Dunn's multiple comparison test,  $n = 4$ , each in quadruplets.

To further examine whether signalling mediated by the  $\gamma$ -chain can influence infectivity with HPV virions, cells were stimulated with IL-7 and IL-15 prior to the virion infection. Before carrying out the study, a serum free culture system was established because i) components in FCS such as prolactin can activate  $\gamma$ -chain related signalling pathways (such as the STAT5 pathway) and ii) excluding serum from the normal growth medium ("E-med") leads to significant cell death in less than 24 hours. Two serum-free media were tested – Optimem and Keratinocyte SFM. Untransduced NIKS were seeded in E-med. The medium was removed the following day and cells were washed with PBS to remove traces of media. The medium was replaced with Optimem or KSFM or remained in E-med. 6 hours later pseudovirions were added at a viral concentration of 1 vge/cell and luciferase activity measured 48 hours later.

Luciferase activity was reduced in both Optimem and KSFM compared to E-med. However, it was noticed that proliferation rates were also reduced in cells cultured with Optimem and KSFM compared to E-med. Therefore, the luciferase activity was recalculated after normalisation for cell number. The results showed similar levels of luciferase activity for cells cultured with E-med and Optimem. In contrast, the luciferase activity was still significantly reduced when cells were grown in KSFM (Figure 20). Based on these results, Optimem medium was chosen for the study.

a)



b)

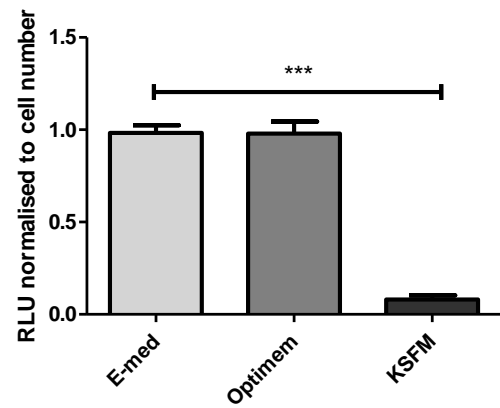


**Figure 20: Levels of infectivity in NIKS cultured in different media**

Cells were seeded in E-medium onto 96 well plates, the following day the medium was changed and pseudovirions were added 6 hours later at a concentration of 1 vge/cell. Luciferase activity was measured 48 hours later; shown are RLU normalised to E-medium in a) and normalised to cell number in b), mean  $\pm$  SEM, \*\*\* $p < 0.001$ , Kruskal-Wallis test, followed by Dunn's multiple comparison test,  $n = 3$  in quadruplets.

To analyse the effect of pre-stimulation with IL-7 and IL-15 on infectivity, control cells were seeded in E-medium and the medium was changed to Optimem the next day. After 6 hours, the cytokines were added at 100ng/ml to the Optimem. 24 hours post-stimulation, the cells were infected with pseudovirions at a concentration of 5 vge/cell. Luciferase activity was measured 48 hours post-infection. Cells challenged with IFN- $\beta$  were used as a positive control as infectivity with HPV pseudovirions is reduced by this stimulation (280).

The results showed that infectivity was reduced following stimulation with IFN- $\beta$ . In contrast, no differences in infectivity were observed in cells challenged with IL-7 or IL-15 compared to unchallenged cells (Figure 21), suggesting that neither IL-7 nor IL-15 provided a protective effect from HPV infection.

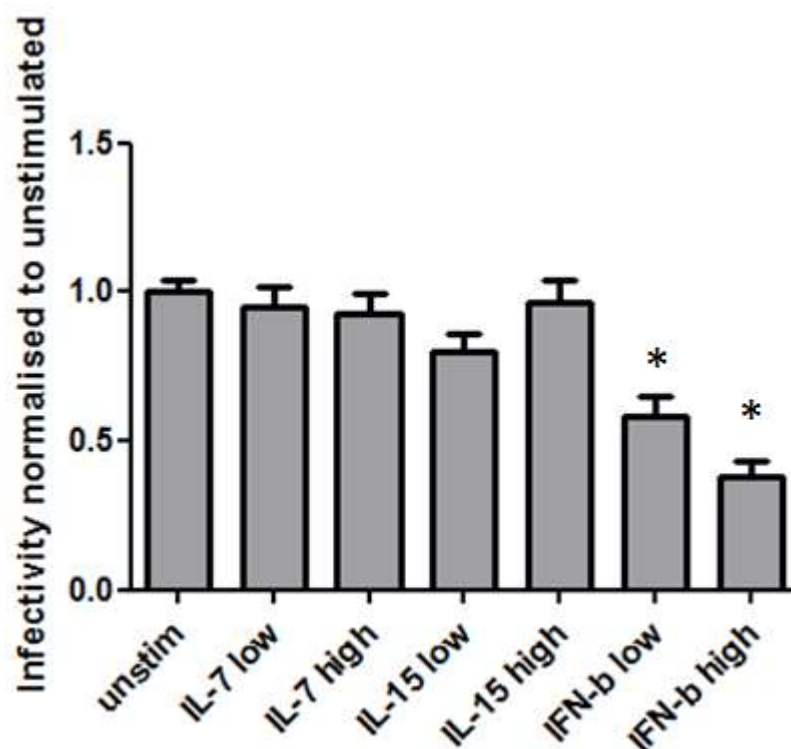


**Figure 21: Infectivity with pseudovirions after stimulation with  $\gamma$ -chain cytokines**

Control cells were seeded onto 96 well plates, the following day the medium was changed to Optimem and cytokines were added at 10 ng/ml (low) and 100 ng/ml (high) 6 hours later, the following day cells were infected with a concentration of 5 vge/cell and luciferase activity was measured 48 hours later, values were normalised to unstimulated, mean  $\pm$  SEM, \*  $p < 0.01$ , Kruskal-Wallis test, followed by Dunn's multiple comparison test,  $n = 3$ , in quadruplets.

## **4.5 Proliferation is not changed between different NIKS cell lines**

As cells need to be proliferating in order for a PV infection to be established (281), it was possible that differences in proliferation might explain infectivity differences. To test this, cell proliferation was compared between the scr control cells and KD cells. BrdU – a synthetic analogue of thymidine – incorporation assays were carried out as these are indicative of DNA synthesis (see 2.2.1.8 and 2.2.1.9).

There were no differences in proliferation rate between the scr control and KD cells, as seen in two different BrdU incorporation assays lasting for 1 and 18 hours, respectively. There was also no difference in proliferation rate in cells stimulated with IL-7 or IL-15 (Figure 22). This suggested that the differences in viral susceptibility in KD cells with  $\gamma$ -chain deficiency are not due to hyper-proliferation of the cells.

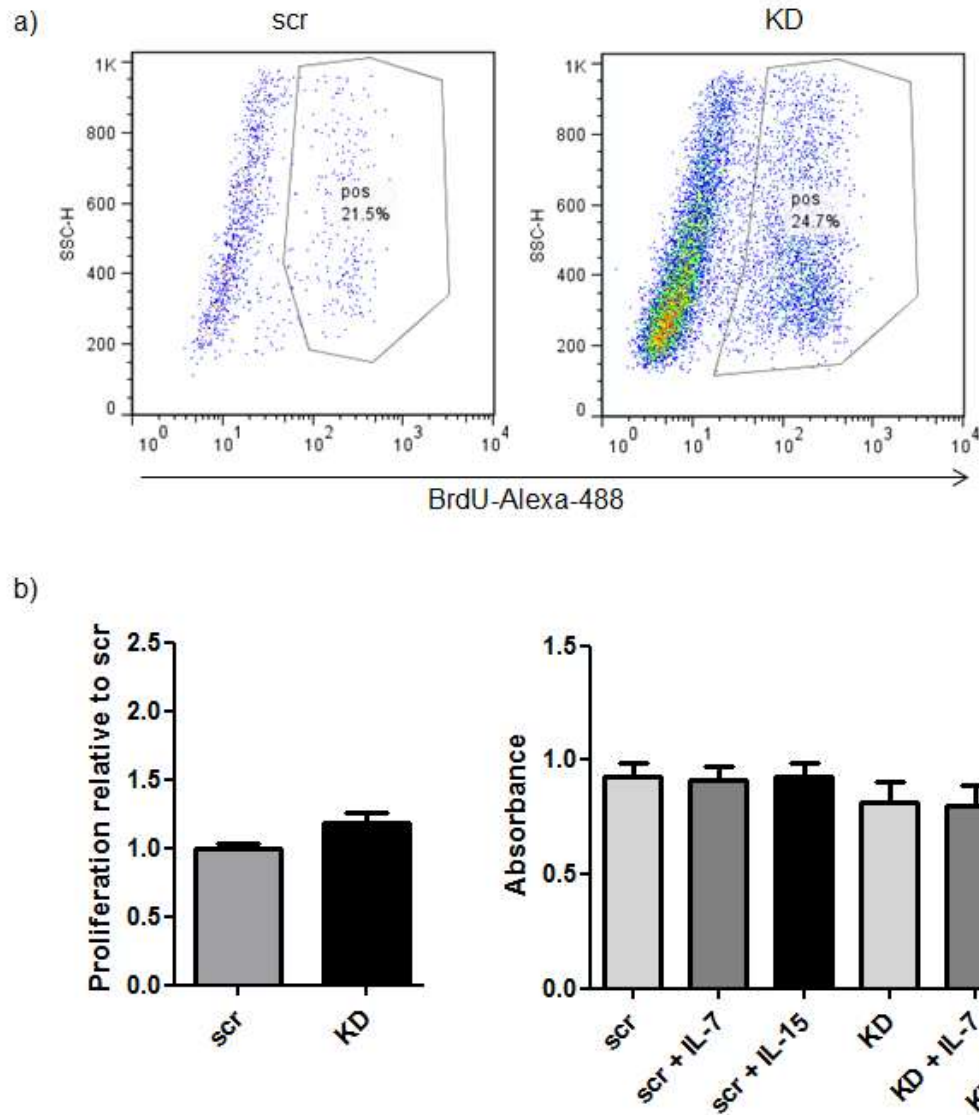


**Figure 22: Proliferation of NIKS cell lines**

Monolayer NIKS were incubated with BrdU for 1 h, fixed and stained with an anti-BrdU-Alexa-488 antibody, representative FC plots (a) and quantification of FC experiments (b), mean  $\pm$  SEM,  $n = 6$ , in duplicates; NIKS were seeded on 96 well plates, cultured under serum-free conditions for 6 hours and then 100 ng/ml IL-7 and IL-15, respectively, were added as well as BrdU. Incorporation of BrdU was detected 18 hours later using a colorimetric reaction measured using a plate reader (c), mean  $\pm$  SEM,  $n = 3$  in quadruplets.

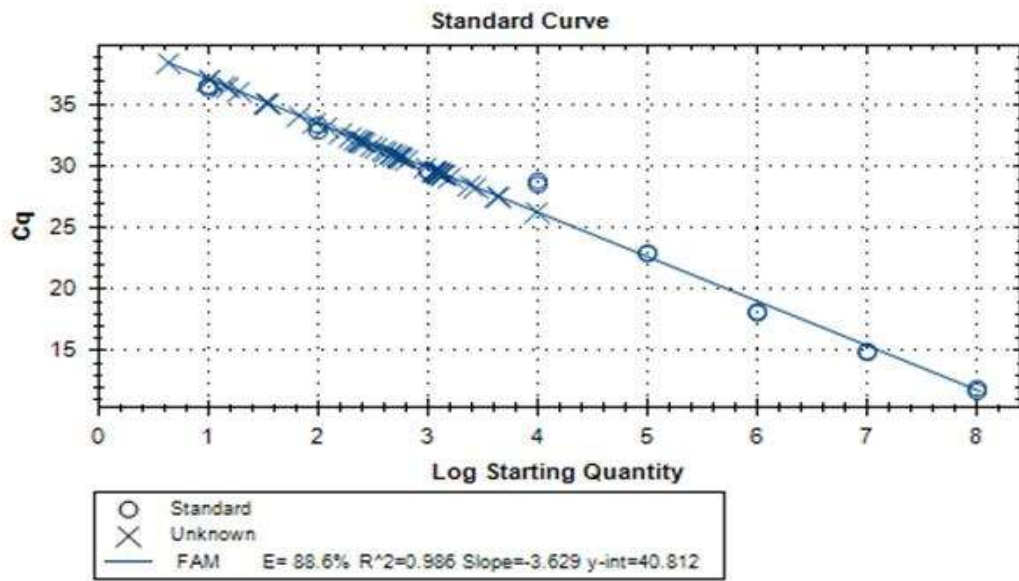
## **4.6 Infectivity using quasivirions is increased in $\gamma$ -chain deficient keratinocytes**

Following the result of the increased infectivity in KD NIKS by pseudovirions, the infectivity in KD NIKS by quasivirions was investigated for further confirmation. The quasivirions contained the full-length HPV18 genome but no reporter genes such as luciferase or eGFP. Therefore, the infectivity cannot be assessed by simple reporter gene assays or using GFP expression. One possibility would be to analyse HPV genome copy number. However, it is difficult to exclude virions bound to rather than contained within the cell using this method. Therefore, the expression of the early transcript E1<sup>4</sup> was analysed by qPCR and used as a read-out for HPV infection.

For the qPCR, a standard was used which corresponded to the 130 bp sequence of the HPV18 genome that is flanked by the designed qPCR primers and where the probe binds. Serial dilutions of this standard were used to generate a standard curve with an R-value of 0.986 and used for determination of E1<sup>4</sup> copy number by qPCR (Figure 23a).

To validate the assay, untransduced NIKS were infected with HPV18 quasivirions using three different viral concentrations (10, 50 and 100 vge/cell). RNA was collected 48 hours post infection, reverse transcribed and used for qPCR. The results showed increasing E1<sup>4</sup> copies with an increase in viral concentration used (4.9, 14.7 and 35.7 E1<sup>4</sup> copies per 1,000 GAPDH for concentrations 10, 50 and 100 vge/cell, respectively) (Figure 23b). No copies (< 0.3) were detected in the negative, uninfected control samples.

a)



b)

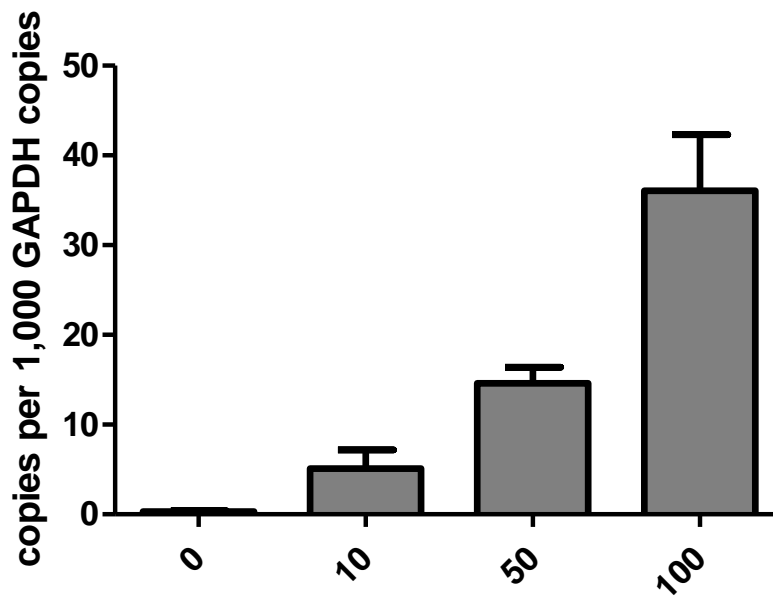


**Figure 23: Validation of E1<sup>4</sup> qPCR assay**

E1<sup>4</sup> primers and a probe were designed and tested using a geneBLOCK standard; the standard curve is showing: standards as open circles and tested samples as crosses (a); untransduced NIKS were infected with HPV18 quasivirions at concentrations of 10, 50 and 100 vge/cell, RNA was isolated 48 hours later and used for qPCR, shown are E1<sup>4</sup> copy numbers per 1,000 GAPDH copies (b), mean ± SEM, n = 4.

The validated qPCR was used to assess infectivity using HPV18 quasivirions. Scr control and KD cells were seeded onto 96 well plates and infected with HPV18 quasivirions. Samples were collected 48 hours later for qPCR analysis.

There was a significant increase of copy number (34%) in the KD cells compared to scr control cells (Figure 24). These results, along with the results obtained from pseudovirion infection suggested that  $\gamma$ -chain KD cells are more easily infected than scr control cells.

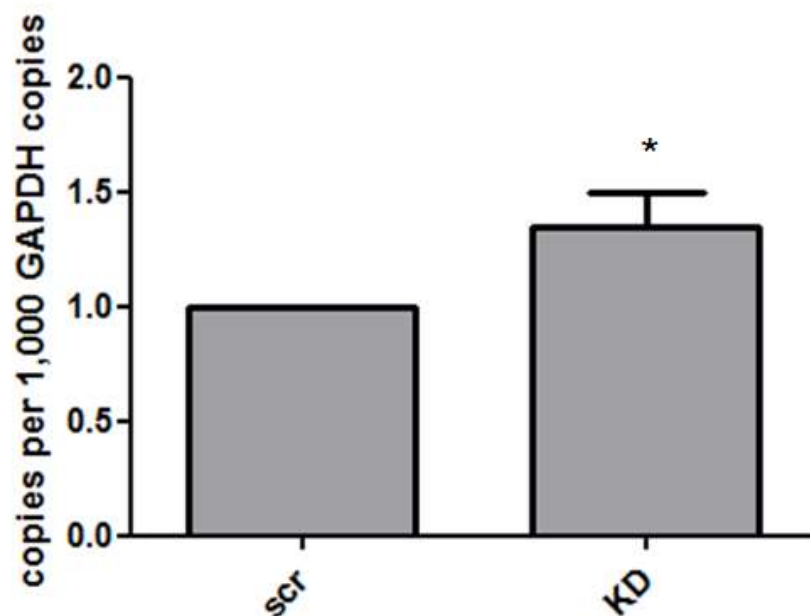


**Figure 24: Infectivity in NIKS cell lines using HPV18 quasivirions**

Scr control cells and KD cells were infected with HPV18 quasivirions; 48 hours post infection, RNA was isolated and the copy number of E1<sup>4</sup> versus GAPDH were assessed by qPCR, mean  $\pm$  SEM, \*p = 0.03, Wilcoxon matched-pairs signed rank test, n = 6, run in duplicates.

## 4.7 Discussion

Even though extensive research has been done to understand how PVs enter the cell, the process of infection has still not been fully understood, in particular which receptors and mechanisms are involved in the procedure. Pseudovirions and quasivirions have been a useful tool for PV research as they enable investigation of the initial stages of PV infection such as attachment and entry into the cells. For example, they have been used to analyse which cellular factors and receptors are necessary for the infectivity of papillomaviruses. It is known that differences in proliferation or autophagy, stimulation with IFN- $\beta$  and blocking certain signalling pathways can affect infectivity. For example, an increase in proliferation leads to increased infectivity whereas stimulation with IFN- $\beta$  decreases it. Blocking autophagy also enhances infectivity whereas blocking EGFR, PKC and PI3K completely or partially blocked infection (91, 280-282).

In this chapter, we set out to test whether  $\gamma$ -chain knock-down alters HPV infectivity. Infectivity with VLPs was analysed in control and  $\gamma$ -chain deficient keratinocytes. Increased infectivity in KD cells infected with pseudovirions was confirmed by measuring luciferase activity. Similar results were observed in KD cells infected with quasivirions assessed by the copies of the E1<sup>4</sup> mRNA. This suggests that absence of  $\gamma$ -chain leads to an increase in HPV infectivity in keratinocytes. We, next, carried out experiments to identify the reasons for the differences in infectivity seen. We initially postulated that cytokine signalling through the  $\gamma$ -chain could alter HPV infectivity but, pre-stimulation with IL-7 and IL-15 did not affect the infectivity in WT KC.

Differences in proliferation can account for differences in infectivity as cell cycle progression is necessary for viral establishment in cells (281). However, we did not observe any differences in proliferation rate as measured by BrdU incorporation between scr control and KD cells in our system. In addition, we also did not see any changes of BrdU incorporation after IL-7 or IL-15 stimulation in our study. This is in agreement with results from Ruckert et al., who saw that IL-15 stimulation did not affect proliferation but inhibited apoptosis in primary human foreskin keratinocytes (283). However, Yano et al. reported that stimulation of the keratinocyte cell line HaCaT with IL-15 for 24 hours led to a significant increase in BrdU incorporation (259). They further found that the use of inhibitors MEK or PI3K could block the effect of IL-15 stimulation, so concluded that the effect on cell proliferation was due to the activation of the MEK/ERK1/2 and PI3K/AKT pathway. The different results might be explained by the use of different cell lines in both studies. Here, we used NIKS and Yano et al. employed HaCaT. Both cell lines are spontaneously immortalised keratinocytes but they have distinct genetic changes from wild-type cells and are derived from different

parts of the body: HaCaT cells were isolated from full thickness adult male human skin and NIKS transformed from new-born human foreskin (255, 284). Therefore, both cell lines are genetically different and these differences might lead to differences in the response to IL-15 stimulation.

Although our data suggests increased infectivity in  $\gamma$ -chain deficient keratinocytes, the mechanism for this could not be determined within the time frame of this project. Potential mechanisms could be that  $\gamma$ -chain affects a) uptake or one of the signalling pathways involved, b) autophagy or c) regulation of expression of receptors that are important for HPV uptake.

For HPV16, whose capsid was used in the pseudovirions experiments, it was shown that entry is clathrin-, caveolin-, flotillin-, cholesterol- and dynamin-independent but rather dependent on actin dynamics and tyrosine and serine/threonine kinase signalling. In addition, PAK-1, PKC and PI3K signalling was required for the endocytic internalisation (91). Signalling via the  $\gamma$ -chain can impact signalling of PI3K and other kinases, therefore, this might be the link with the increase of infectivity in KD cells. In addition, an increased host autophagy leads to a reduction in infectivity (282). No link has been described between  $\gamma$ -chain signalling and autophagy but this is a potential route of experiments that can be followed in future work.

As it is not known which secondary receptor is necessary for successful entry of HPV (90) a potential involvement of the  $\gamma$ -chain and its co-receptors on the level of binding and/or entry cannot be ruled out. Therefore, it would be of interest to examine HPV surface binding and internalisation into the endocytic compartment using fluorescently labelled PV pseudovirions and super resolution microscopy (91, 285).

In addition, as briefly mentioned in the introduction to this chapter, we used the pShell plasmid of a mucosal HPV type for these experiments and not of a cutaneous HPV type. Therefore, the results obtained here cannot be directly translated to cutaneous HPV types. The number of experiments done with cutaneous HPV types especially in comparison to mucosal types is limited. In a recent publication, Kwak et al. compared different mucosal and cutaneous HPV types and different inhibitors and their effect on infectivity using pseudovirions (279). They identified differences between mucosal and cutaneous HPV types in response to various inhibitors using 293TT cells. This potentially explains the different tissue tropism of the HPV genera due to potentially different cell surface receptor interactions. As these variations in interactions might impact the results obtained in this chapter, it will be necessary to repeat experiments

using different types of packing plasmids even though there are still difficulties using VLP made with capsid proteins from cutaneous HPV types in keratinocyte cell lines.

As the main effect analysed here is due to the packing plasmids and therefore cell entry, the use of the HPV18 plasmid in the quasivirion experiments compared to using a cutaneous type virus might be negligible. Here, we did not analyse the effect of HPV18 expression on the cell itself. However, HPV18 – as a strong mucosal type – might be more highly expressed than cutaneous HPV types therefore making detection easier. To rule out any effects the use of the HPV18 genome might have had, it would be best to repeat these experiments using both pseudovirions made with pShell plasmids from cutaneous types and with quasivirions expressing both packing and expression plasmids from cutaneous types.

In conclusion, this chapter shows first evidence that the absence of the  $\gamma$ -chain can lead to an increased infectivity with HPV particles. This result is interesting, as increased infectivity in X-SCID patients could explain the high number of patients affected compared to healthy populations as well as give an explanation for the great number of affected sites. However, further work needs to be done in order to understand the mechanisms of this defect.

**5. Control of HPV is altered in  
keratinocytes lacking  
functional  $\gamma$ -chain**

## 5.1 Introduction

The HPV life cycle is closely linked to the differentiation programme of keratinocytes (55). In order to investigate the influence of HPV on keratinocyte biology, it is therefore necessary to use systems which allow for keratinocyte proliferation and differentiation to recapitulate the full viral life cycle.

The use of organotypic rafts generated using the immortalised NIKS keratinocyte cell line has made this possible. NIKS are a spontaneously immortalised human foreskin keratinocyte cell line that displays normal differentiation properties. They can be cultured in the organotypic raft system which allows cells to undergo proliferation and differentiation processes. These processes have been shown to support the life cycle of different HPV types including HPV16, 18 and 58 (101, 255, 286). In addition, it was confirmed that NIKS cells express wild-type p53 and pRb which are two of the main cellular proteins influenced by HPV (287).

In order to mimic skin using raft cultures, a collagen-fibroblast matrix is used to represent the dermis (“dermal equivalent”) onto which keratinocytes are seeded. Once the keratinocytes reach confluency to form a continuous layer representing the basal skin layer, the raft is lifted so that the keratinocytes are exposed to an air/liquid interface. This leads to cell differentiation and two weeks post lifting, a cornified layer is formed (287).

To examine the HPV life cycle, rafts can be stained for different HPV life cycle markers such as the surrogate marker for HPV E6/E7 minichromosome maintenance protein (MCM) 7 and the HPV proteins L1 and E4 using immunofluorescence techniques. Presence of the capsid protein L1 detects the virus assembly. Alternatively, fluorescent-in-situ-hybridisation (FISH) can be used to detect the onset of HPV genome amplification. In addition, parameters for HPV activity such as suprabasal DNA synthesis can be examined. Clinically, tissues from patients can be stained in the same way and the expression of these markers used to examine disease severity. E4 expression declines when lesions progress to higher severity and can be absent in high-grade clinical lesions, but E7 expression and therefore MCM7 and p16 are still present or increased (55, 288, 289).

As we hypothesized that absence of  $\gamma$ -chain has an influence on HPV *in situ*, we examined whether the HPV life cycle in rafts made with  $\gamma$ -chain deficient cells differs from the life cycle in rafts made with control cells. The rafts in this chapter were made according to the protocol by Lambert et al. (287). As for the VLP experiments in the previous chapter, we used HPV18 for the experiments using rafts. This is because

NIKS do not always maintain the cutaneous HPV types when they are transfected which is a vital requirement for raft studies (personal communication P.F. Lambert). In addition, HPV18 – as previously mentioned – is an easily tractable system as it is usually replicated in high quantities in transfected cells and antibodies for its E4 protein and probes for its detection by Southern blot and FISH were available for this project.

## **5.2 $\gamma$ -chain deficiency in keratinocytes does not influence keratinocyte proliferation and differentiation in organotypic raft cultures**

Before analysing the effects of HPV on keratinocyte growth in organotypic rafts, proliferation and differentiation markers were first examined to see whether there were any differences between rafts using scr control or  $\gamma$ -chain deficient keratinocytes.

Rafts were made, harvested and H&E stained to check for correct tissue processing and differentiation of keratinocytes (Figure 25). They were then immunofluorescence stained with antibodies for BrdU, Keratin-10 (K10), Keratin-14 (K14) and Loricrin (see 2.2.1.13 and 2.2.4).

Keratinocyte proliferation and differentiation markers K14, K10 and Loricrin were expressed in the rafts within their expected localisation (Figure 26a). K10 staining was evenly distributed throughout all layers except the basal layer as it is a marker for commitment to differentiation. K14 staining was strong in the basal layer and its intensity decreased towards more differentiated layers. Loricrin – a marker for terminal differentiation – was expressed in the upper layers of the rafts. No differences were observed between the control and the KD cells indicating that  $\gamma$ -chain deficiency does not affect keratinocyte differentiation without HPV present (Figure 26a).

In addition, rafts were stained with an anti-BrdU antibody as their culture medium was supplemented with BrdU 8 hours prior to harvesting. The results showed that only cells in the basal and parabasal layers were positively stained for BrdU incorporation but no BrdU positive cells were found in the suprabasal layers as proliferation under normal circumstances only occurs in the basal layer. There was no significant difference in terms of BrdU positive cells between rafts made with scr control cells or KD cells (Figure 26b).

These results suggested that  $\gamma$ -chain does not affect keratinocyte proliferation and their differentiation process.

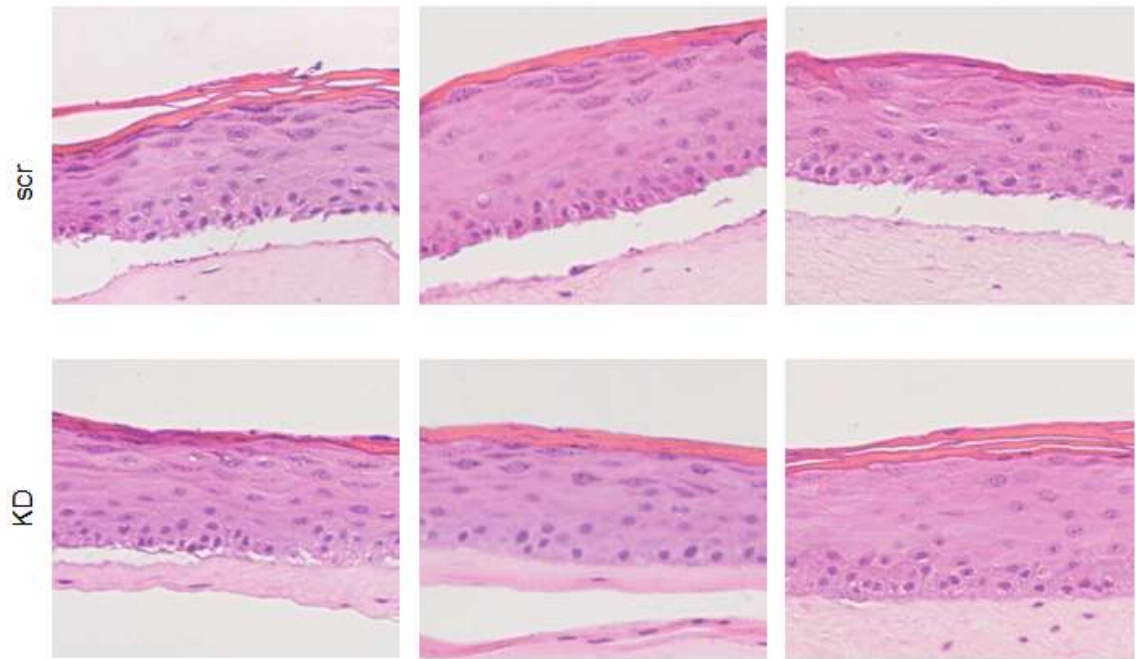
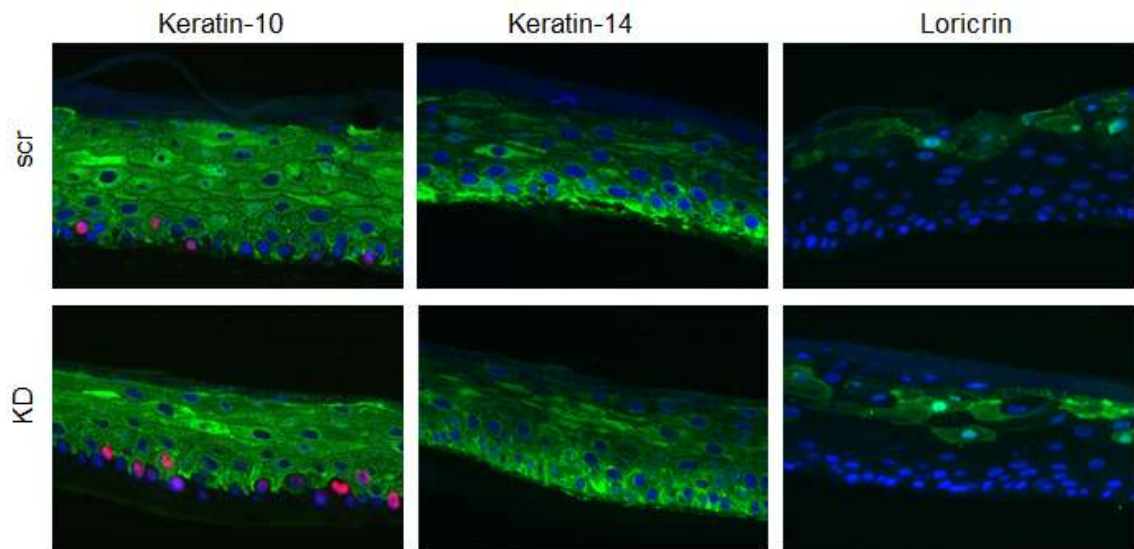


**Figure 25: H&E staining of HPV negative rafts**

Scr control and KD cells were used to make organotypic raft cultures. Rafts were harvested and H&E stained, representative image for each raft.

a)



b)

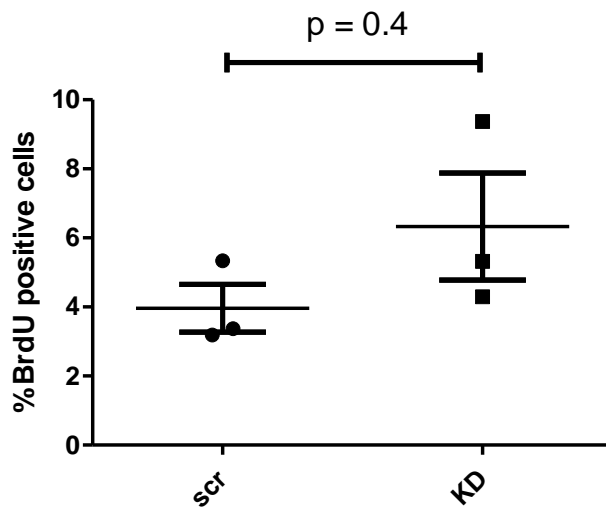


**Figure 26: Keratin-10, Keratin-14, Loricrin and BrdU staining in HPV negative rafts**

Scr control and KD cells were used to make organotypic raft cultures. 8 hours before harvesting, growth medium was supplemented with BrdU. Rafts were harvested and stained for K10, K14 and Loricrin (green), BrdU (red on the images with K10) and DAPI (blue), representative images (a) and quantification of BrdU positive cells (b), six images per raft were analysed, n = 3.

### **5.3 HPV genomes are maintained over multiple passages in scr control and KD NIKS**

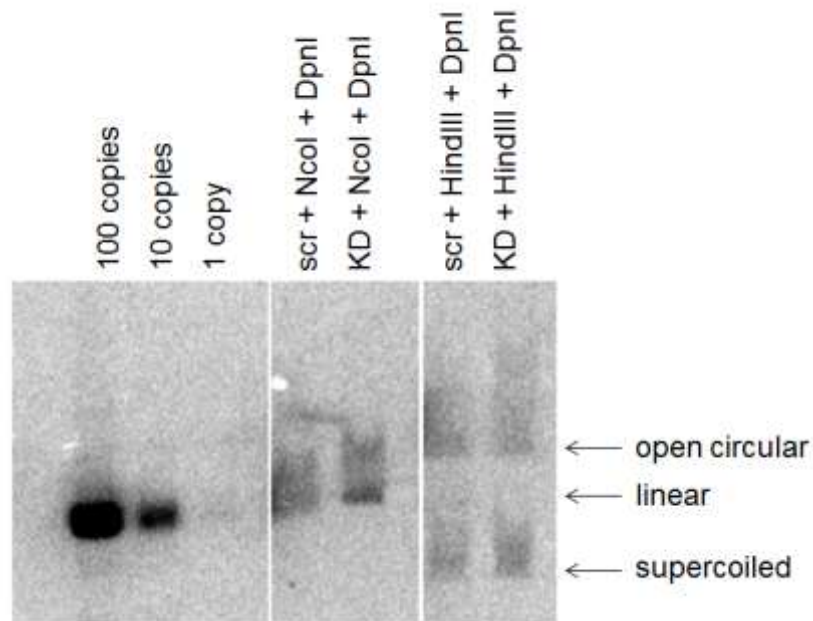
Once HPV infects cells, HPV genomes are maintained in cells as episomes. For research purposes, keratinocytes are transfected with HPV genomes in order to mimic this phenotype. In order to establish HPV genomes in NIKS, cells were transfected with the recircularised HPV18 genome (see Chapter 4.2) as well as a blasticidin plasmid to enable selection. Extrachromosomal DNA was extracted from blasticidin-selected cells and analysed for the presence of HPV genomes by Southern blot (see 2.2.3.8 and 2.2.3.9).

For both the scr control and the KD cells presence of HPV genomes were shown by Southern blot. The HPV18 genome is replicated extrachromosomally as indicated by the presence of the open circular and supercoiled forms in both samples (Figure 27a, HindIII digested samples showing the plasmid in undigested forms as HindIII does not cut the HPV genome). The linearised sample (NcoI digested) was used to calculate the copy number compared to the loaded standards. For both control and KD cells, the copy number was approximately 5 copies per cell (Figure 27a).

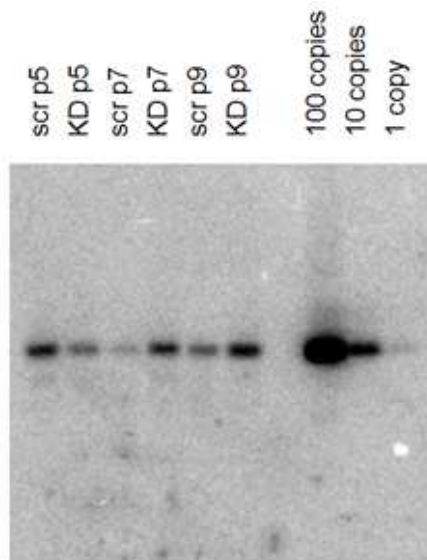
To examine whether the HPV genome was maintained in transfected cells over a prolonged period of time, NIKS were cultured with mitomycin C treated 3T3 feeder cells and propagated for 9 passages. Extrachromosomal DNA was isolated from cells at each passage and subjected to Southern blot analysis. HPV18 genomes were maintained in transfected cells for at least 9 passages. The copy numbers were around 5 copies per cells for all samples tested. No differences were observed between scr control and KD cells. Variation in the band intensities were due to differences in DNA amount loaded as seen on the agarose gel (Figure 27b).

In conclusion, HPV18 genomes were maintained in both control and KD cells at similar levels for prolonged time periods. This result suggests that  $\gamma$ -chain deficiency does not influence HPV maintenance in cells under these conditions.

a)



b)



c)

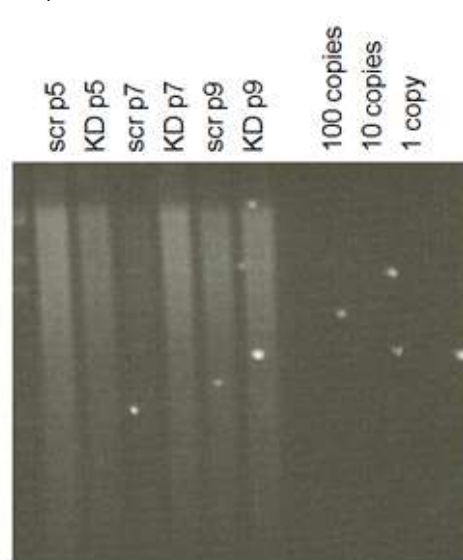


**Figure 27: Maintenance of HPV18 genomes in transfected NIKS cells**

Scr control and KD NIKS were transfected with recircularised HPV18 genomes and a blasticidin resistance plasmid and selected with blasticidin. Blasticidin resistant cells were used for experiments. Extrachromosomal DNA was isolated and digested with NcoI which cuts the HPV18 genome once or HindIII which does not cut the HPV18 genome. Samples were also digested with DpnI which cuts only bacterial DNA. Digested DNA samples were separated by agarose gel electrophoresis and further used for Southern blot with a probe against the HPV18 genome. Linearised plasmid DNA was used as standards (labelled with copy number), shown are passage 0 (a) and multiple passages (b, only digested with NcoI + DpnI), (c) shows agarose gel for (b).

## 5.4 HPV does not affect the proliferation in $\gamma$ -chain deficient keratinocytes cultured as a monolayer

HPV infection of keratinocytes can affect cell proliferation and therefore, we wanted to test if presence of HPV can affect the proliferation of cells in monolayer. Similarly to the experiment in Chapter 4.5., a BrdU incorporation assay was performed to analyse DNA synthesis in NIKS grown in monolayers.

No difference was seen between scr and KD cells transfected with HPV18 (Figure 28), suggesting that at least in cells grown in monolayers, which would be representative of the basal cells in the skin,  $\gamma$ -chain absence does not affect cell proliferation.

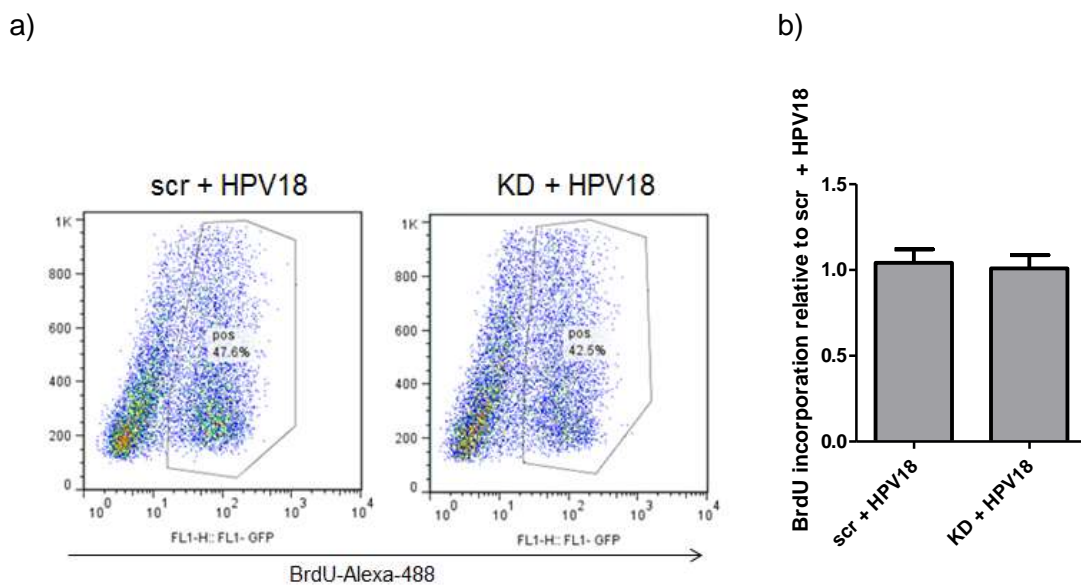


**Figure 28: DNA synthesis in HPV18 positive NIKS cell lines infected with HPV18**

NIKS cells cultured as monolayer were incubated with BrdU for 1 h, fixed and stained with an anti-BrdU-Alexa-488 antibody. Representative FC plots (a) and quantification of FC experiments are shown (b), mean  $\pm$  SEM, n = 6, in duplicates.

## **5.5 Presence of HPV18 affects the differentiation and proliferation of rafts made with $\gamma$ -chain deficient keratinocytes**

We, then, used the HPV18 positive NIKS cells to make organotypic rafts. They were used to assess differentiation and proliferation using immunofluorescence staining for BrdU, K10, K14 and loricrin in the same way as for HPV negative rafts.

The rafts generated using HPV18 positive NIKS showed similar morphology to HPV negative rafts as seen from H&E stained sections. In addition, no obvious differences in morphology were observed between scr control and KD cells (Figure 29a).

In order to assess, proliferation and differentiation markers, we stained for K10, K14, Loricrin and BrdU. K14 staining seemed to be more intense in HPV18 positive rafts compared to HPV18 negative rafts (Figure 29b compared to Figure 26) but there were no differences between the scr control and KD rafts. For Loricrin, the staining seemed to be in fewer cells in HPV18 positive cells compared to HPV negative cells, but again there were no differences between the scr control and KD rafts. This suggests that differentiation occurs in rafts despite presence of HPV18 but that HPV is able to disturb this process. However, absence of  $\gamma$ -chain does not affect expression of these two markers.

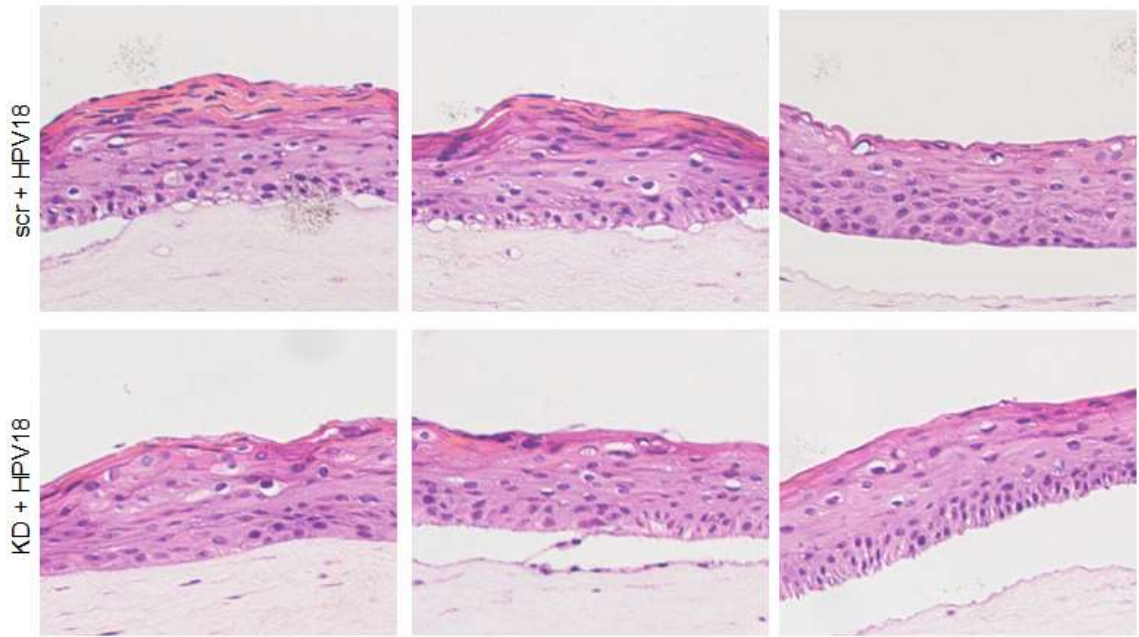
We then analysed the expression of K10 in these rafts. Similarly to K14 and Loricrin, K10 expression differed in HPV18 positive rafts. Here, it was not as even as seen in HPV negative rafts showing again HPV18's ability to disturb the differentiation of keratinocytes (Figure 30 compared to Figure 26). When examining the images in more detail, it became apparent that in KD rafts the staining was more disturbed than in control rafts. The different staining patterns were grouped into three categories: i) "organised" which meant even staining similar to the staining observed in HPV negative rafts; ii) "slightly disorganised" where strong staining was present throughout the rafts but differed in the different layers and was generally patchy and iii) "extremely disorganised" which meant staining that was very weak or missing in large part of the images analysed. The differences between the images grouped into each category was significantly different indicating that differentiation is more disturbed by the presence of HPV genomes in the absence of  $\gamma$ -chain compared to the control cells (Figure 30 a + b).

The number of BrdU positive nuclei was analysed to see actively proliferating cells. In contrast to HPV negative rafts where no positive nuclei were seen in suprabasal layers, a high proportion of them was seen in the HPV positive rafts. This shows how the

presence of HPV dysregulates the normal life cycle of keratinocytes. When the total number of BrdU positive cells was compared, no differences were seen between the control and the KD cells. However, when we compared suprabasal DNA synthesis, a significantly higher number of BrdU positive nuclei was present in KD cells compared to control cells ( $1.96 \pm 0.25\%$  vs.  $3.18 \pm 0.54\%$ ) (Figure 31).

In conclusion, in  $\gamma$ -chain deficient cells suprabasal DNA synthesis is increased and differentiation is more disturbed than in control cells which suggests that  $\gamma$ -chain in cells is important for the control of HPV induced effects.

a)



b)

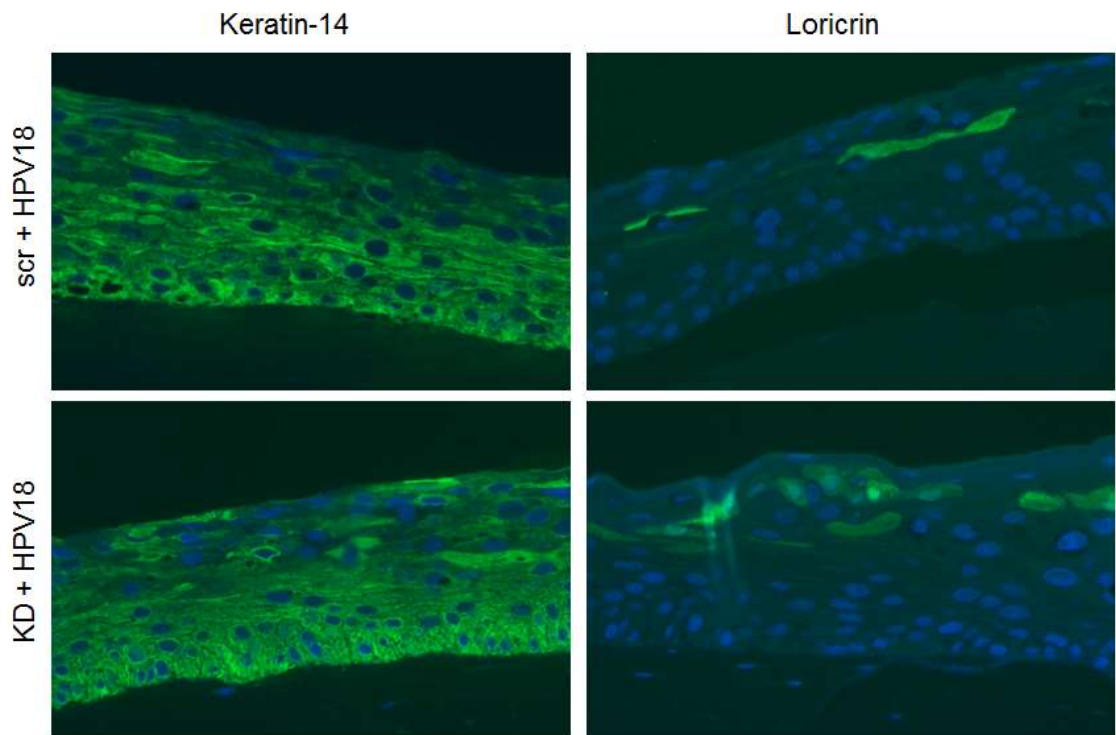
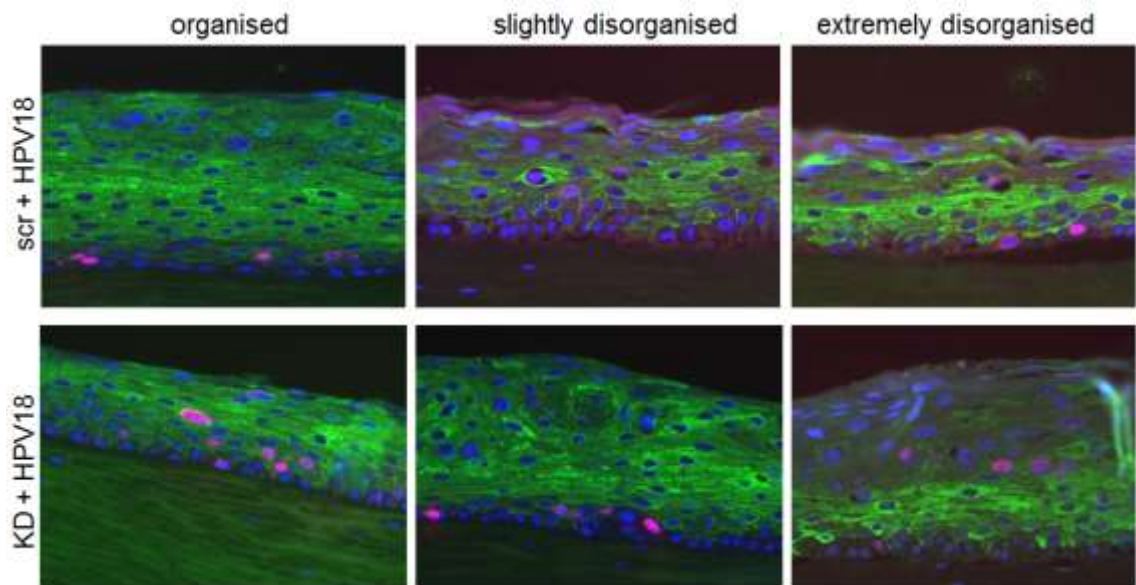


**Figure 29: H&E staining and Keratin-14 and Loricrin staining of HPV18 positive rafts**

Scr control and KD cells transfected with HPV18 were used to generate organotypic raft cultures. Rafts were harvested and a) H&E stained and b) stained for K14 and Loricrin (green) and DAPI (blue), representative images, six images per raft were analysed, n = 4.

a)



b)

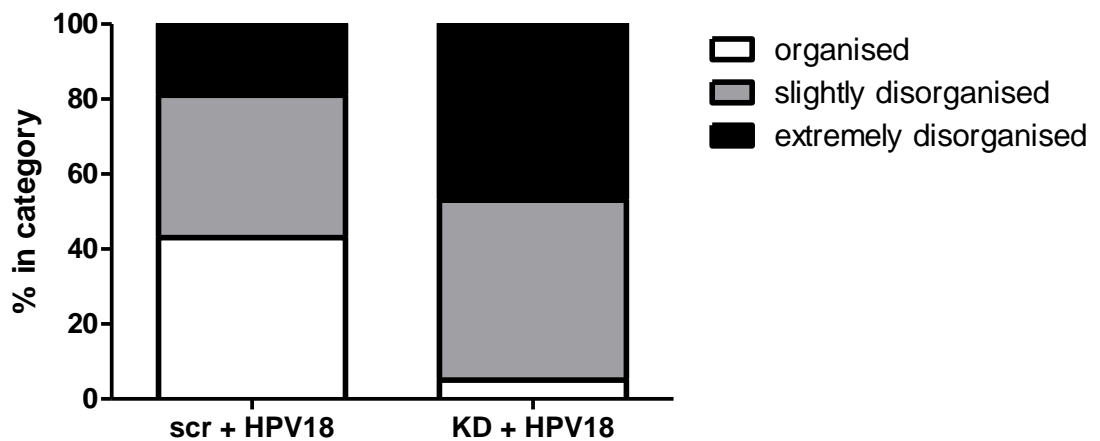
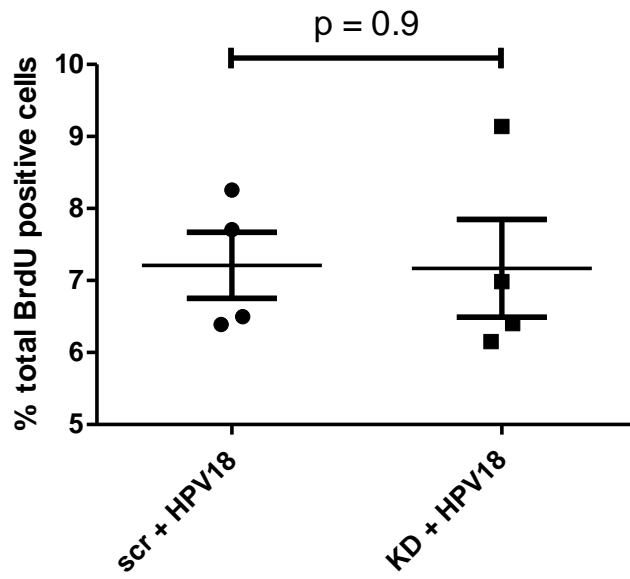


**Figure 30: Keratin-10 and BrdU staining of HPV18 positive rafts**

Scr control and KD cells transfected with HPV18 were used to generate organotypic raft cultures. 8 hours before harvesting, growth medium was supplemented with BrdU. Rafts were harvested and stained for K10 (green), BrdU (red) and DAPI (blue), representative images for each of the three categories (a) and categorisation of K10 staining (b), six images per raft were analysed, n = 4.

a)



b)

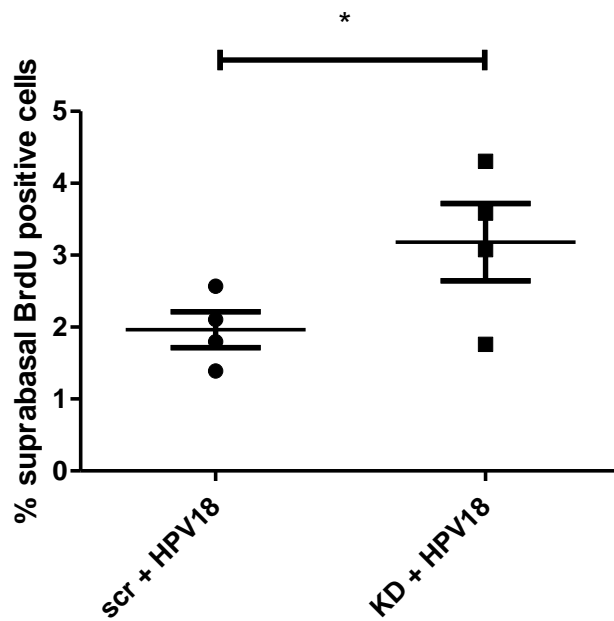


**Figure 31: Quantification of BrdU positive cells in HPV18 positive rafts**

The number of BrdU positive nuclei was counted and compared to the total number of cells, for all layers (a) and for the suprabasal layers only (b), \* $p < 0.05$ , Mann-White test, six images per raft were analysed,  $n = 4$ .

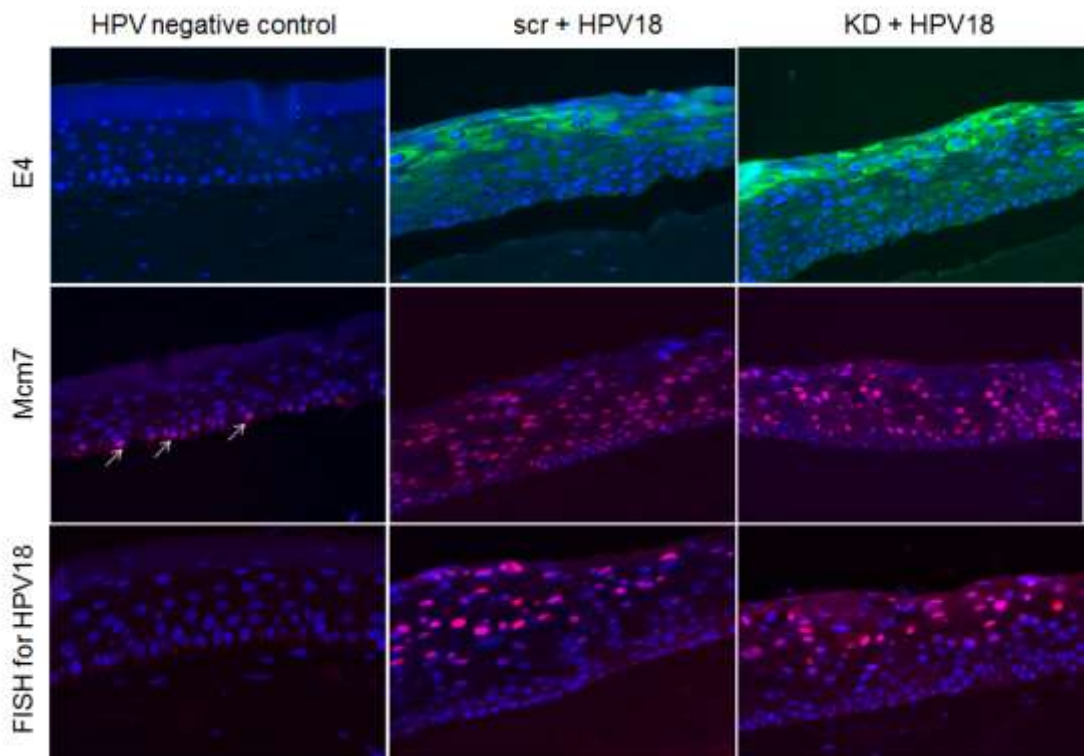
## **5.6 $\gamma$ -chain deficiency in keratinocytes does not affect HPV18 life cycle in organotypic rafts**

After seeing differences in the differentiation marker K10 and suprabasal DNA synthesis between rafts made with  $\gamma$ -chain deficient and scr control NIKS, we wanted to confirm whether HPV could undergo its normal life cycle in cultured rafts and whether any changes were observed here. To do this, matured rafts were stained for MCM7 and E4 protein expression and FISH for HPV18 genome amplification was performed.

E4 protein was expressed in the upper layers of the HPV18 positive rafts whereas MCM7 (a surrogate marker for expression of the HPV E7 protein) was expressed in these rafts through all layers in the cell nuclei. MCM7 is a cellular protein which is upregulated by the expression of HPV and very faint expression of it was also seen in the nuclei of cells in the lower layers of HPV negative rafts (shown with white arrows pointing to positive cells). There were no differences in the expression of HPV18 E4 as well as MCM7 between the scr control and KD rafts (Figure 32a).

As HPV DNA synthesis is strongly upregulated in the upper layers of the skin shortly before virions are packaged and shed, FISH positive cells were detected in the suprabasal layers of the rafts. This indicates presence of HPV genomes in many cells in the upper layers of the raft. The number of FISH positive cells was counted and compared to the number of total cells. There was no significant difference between the control and KD cells ( $15.25 \pm 1.08\%$  vs.  $12.97 \pm 1.19\%$ ,  $p = 0.2$ ), suggesting  $\gamma$ -chain deficiency does not affect HPV life cycle (Figure 32b) under these conditions.

a)



b)

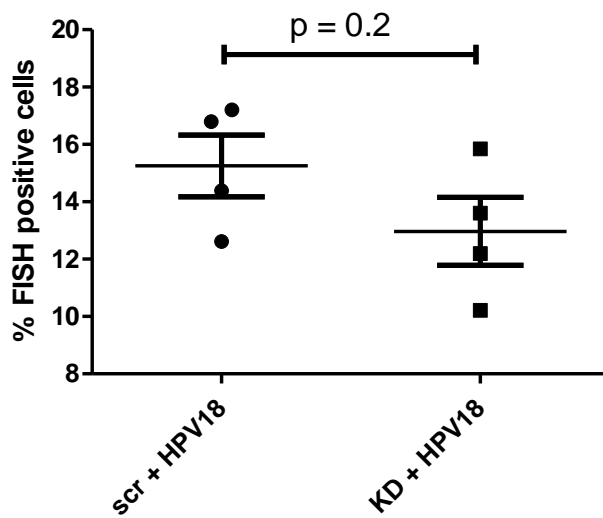


**Figure 32: Expression of HPV markers E4 and MCM7 and fluorescent-in-situ hybridisation (FISH) for HPV18 genome expression in matured rafts**

Organotypic raft cultures were generated using HPV18 positive or HPV negative NIKS cells as control. Matured rafts were stained with antibodies against HPV18 E4 (green, a) and MCM7 (red, white arrows pointing to positive cells in negative control, a). FISH assay was performed using a probe against HPV18 (red, a). The number of FISH-positive cells was counted and calculated as a percentage of all cells in the optical image (b), six images per raft were analysed, n = 4.

## 5.7 Discussion

Rafts are a useful tool to analyse the complete HPV life cycle in a 3D setting and have led to vital discoveries about the role of the HPV oncogenes E6 and E7 and their ability to influence the host cells. They were, for example, used to show that the E7 protein of HPV16 is important for the productive stage of the HPV life cycle (290).

Here, we show that in rafts made using  $\gamma$ -chain deficient cells or control cells without HPV expression, there are no differences in differentiation and proliferation markers tested. In contrast, when  $\gamma$ -chain deficient cells transfected with HPV18 are used to make rafts, suprabasal DNA synthesis is increased and normal expression patterns of K10 are more disturbed than in rafts made with HPV18 positive control cells. In contrast, neither K14 and Loricin nor any of the HPV markers analysed (E4 expression, MCM7 as marker for E6/E7 expression and FISH for HPV genome amplification) showed any differences. These results suggest that even though the life cycle of HPV18 itself is not different in  $\gamma$ -chain deficient keratinocytes, its presence leads to a more pronounced effect on keratinocyte proliferation and differentiation.

It has been long known that HPV16 and 18 in particular are able to alter the expression of proliferation and differentiation markers in raft cultures but that the effect was also dependent on the cell line used for the study (291). Especially the function of E7 has been linked to the uncoupling of differentiation and proliferation leading to suprabasal DNA synthesis which is not observed in HPV negative rafts (292).

However, there are – to our knowledge – no previous studies looking at the effect of the  $\gamma$ -chain or any of its associated cytokines in organotypic rafts. In fact, cytokine signalling has not been studied using organotypic rafts. Therefore, no comparisons with other publications can be made.

There are a few studies looking at the changes of differentiation using rafts but mostly both K10 and K14 expression are disturbed. Interestingly, in a study using primary keratinocytes transduced with E7 proteins of the low-risk HPV types such as HPV1, 4 and 38, rafts displayed changes in K10 expression but K14 expression was normal. In addition, they also observed an increase in the proliferation of the basal layer using these cells. However, the paper did not make any statements about the reasons for the changes in differentiation (293).

It is important to also consider that NIKS are spontaneously immortalised cells. That means even though they are very similar to primary foreskin keratinocytes in many aspects, it is still unknown which cellular processes are disrupted and are contributing to their immortalisation. Therefore, it would be necessary to use primary keratinocytes

to repeat this experiment to rule out any influences of the used cell line. In addition, it would be useful to obtain tissue samples from X-SCID patients, especially from areas affected by warts and stain them. Doing so was initially planned for this project. However, due to difficulties, the previously collected patient samples were not available for staining until the end of this project.

In addition, whereas the use of the HPV18 plasmid in the VLP experiments might have low impact on the comparability with cutaneous HPV types, it is important in the organotypic rafts as here the effects of the virus on the cell itself were analysed. The mucosal types, especially HPV16, 18 and 31, have been widely studied and most effects of the HPV E6 and E7 proteins on cellular proteins such as p53 and pRb are only observed using the high risk mucosal types but not low risk mucosal HPV types or cutaneous HPV types. This means that the results obtained in this chapter are only true in the context of HPV18 infection and cannot directly be transferred to cutaneous HPV types and therefore infections in X-SCID patients. As it can be assumed that the effect of cutaneous types would be reduced compared to HPV18 and as some of the effects seen here were relatively mild, the effects of cutaneous HPV types in  $\gamma$ -chain deficient cells compared to healthy control cells might be negligible and not relevant in a patient setting. However, this remains to be tested.

This means that further work is needed to confirm the results and to identify potential reasons for the changes in proliferation and differentiation observed, e.g. which of the HPV proteins is responsible. To test this, it would be possible to transduce keratinocytes with retroviral or lentiviral vectors expressing either E6 or E7 oncoproteins to identify the effects they have on these processes.

In conclusion, we observed changes in proliferation and differentiation in rafts made using  $\gamma$ -chain deficient HPV18 positive compared to control cells. This could explain a more severe phenotype seen in patients as the disruption of normal skin morphology was more disturbed in the  $\gamma$ -chain deficient setting.

**6. Chemokine secretion in  $\gamma$ -chain deficient keratinocytes is altered and reduces immune cell recruitment**

## 6.1 Introduction

Keratinocytes are important immune sentinels and they are able to secrete a variety of chemokines and cytokines when they are stimulated. These chemokines, e.g. IP-10, Mig, RANTES and Mip-3 $\alpha$ , can recruit a wide range of immune cells to the site of infection (45).

Chemokines and cytokines are important to fight infection and HPVs have developed strategies to interfere with their secretion. It has been shown for HPV16, 18 and 31 that they can repress the secretion of IL-8 and Mip-3 $\alpha$  after stimulation with TLR9 ligands (108, 109, 124) resulting in reduced numbers of immune cells in HPV positive lesions.

The involvement of common  $\gamma$ -chain cytokines in the stimulation of chemokine and cytokine secretion has been shown for other cell types. In a patient with a mutation in IL-21R, the secretion of GM-CSF, IFN- $\gamma$ , IL-10, Mip-3 $\alpha$  and TNF- $\alpha$  from T cells was reduced compared to healthy control cells after stimulation with IL-21 (233). Studies have also shown that IL-15 signalling induces MCP-1, TNF- $\alpha$  and RANTES secretion in myeloid cells (294). Therefore, changes in the secretion of cytokines and chemokines might be of importance in X-SCID patients leading to their susceptibility to HPV infections.

Regressing wart lesions are usually associated with an influx of T cells. In various animal models (BPV-4, CRPV-2 and COPV), both CD4+ and CD8+ T cells are present in regressing lesions with CD4+ T cells being the dominant type and double knock-out of CD4+ and CD8+ T cells is required for formation of wart lesions in all mouse models (133-135, 144, 151). In humans, CD4+ T cells have also been reported to be the cell type associated with mucosal wart regression (136, 295-297).

We, therefore, hypothesized that there are changes in chemokine and cytokine secretion either after infection with HPV quasivirions, after stimulation with  $\gamma$ -chain dependent cytokines or in cells stably transfected with HPV18. These changes might lead to differences in migration of various immune cells such as neutrophils, dendritic cells and T cells. We used cytokine arrays and Luminex assays to assess the secretion of chemokines and cytokines from control and KD cells after various stimuli and examine their influence on immune cell migration.

## 6.2 Cytokine and chemokine secretion is not changed after infection with HPV quasivirions

First, cytokine secretion in NIKS cell lines 24 hours post infection with HPV quasivirions was tested. The quasivirions described in Chapter 4.3 were used for this experiment. To identify potential target cytokines for further experiments, the Proteome Prolifer™ assay which includes a membrane upon which 36 different capture antibodies have been spotted in duplicate was used. The intensity of the detected spots was analysed by ImageJ using densitometry. The media from scr control cells infected with quasivirions at a viral concentration of 100 vge/cell or uninfected cells was collected 24 hours post-infection. The collected supernatants were analysed for cytokine secretion (Table 15).

MIF, IL-8, Gro- $\alpha$ , Serpin E1 and low levels of IL-1ra were detected in the supernatant of the keratinocytes. However, none of these cytokines showed a different secretion pattern in the virus infected cells compared to the uninfected cells (Figure 33). Therefore, initial virus infection was not shown to alter cytokine secretion at early time points.

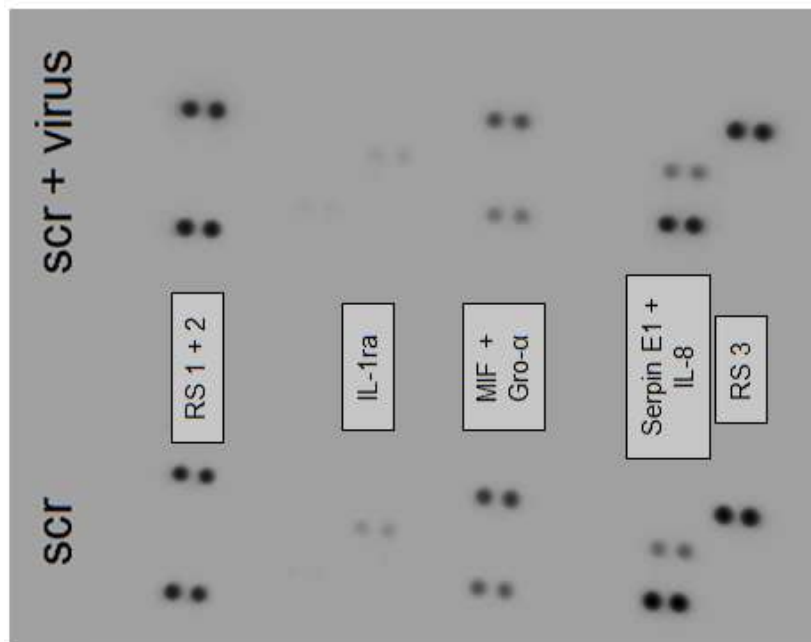


**Figure 33: Secreted cytokines and chemokines after infection with HPV18 quasivirions**

Scr control cells were infected with HPV18 quasivirions at a viral concentration of 100 vge/cell. 24 hours after infection, cell culture supernatants were collected and used for a cytokine array according to suppliers guidelines, RS = reference spot.

**Table 15: Chemokine and cytokine secretion after quasivirion infection**

Full list of cytokines tested in the cytokine array. Y = yes, N = No.

| Coordinate | Target/Control                 | Present? (Y/N) | Differences |
|------------|--------------------------------|----------------|-------------|
| A1, A2     | <b>Positive Control</b>        | <b>Y</b>       | N           |
| A3, A4     | C5/5a                          | N              | --          |
| A5, A6     | CD40 Ligand                    | N              | --          |
| A7, A8     | G-CSF                          | N              | --          |
| A9, A10    | GM-CSF                         | N              | --          |
| A11, A12   | <b>Gro-<math>\alpha</math></b> | <b>Y</b>       | N           |
| A13, A14   | I-309                          | N              | --          |
| A15, A16   | sICAM-1                        | N              | --          |
| A17, A18   | IFN- $\gamma$                  | N              | --          |
| A19, A20   | <b>Positive Control</b>        | <b>Y</b>       | N           |
| B3, B4     | IL-1 $\alpha$                  | N              | --          |
| B5, B6     | IL-1 $\beta$                   | N              | --          |
| B7, B8     | <b>IL-1ra</b>                  | <b>Y</b>       | N           |
| B9, B10    | IL-2                           | N              | --          |
| B11, B12   | IL-4                           | N              | --          |
| B13, B14   | IL-5                           | N              | --          |
| B15, B16   | IL-6                           | N              | --          |
| B17, B18   | <b>IL-8</b>                    | <b>Y</b>       | N           |
| C3, C4     | IL-10                          | N              | --          |
| C5, C6     | IL-12 p70                      | N              | --          |
| C7, C8     | IL-13                          | N              | --          |
| C9, C10    | IL-16                          | N              | --          |
| C11, C12   | IL-17                          | N              | --          |
| C13, C14   | IL-17E                         | N              | --          |
| C15, C16   | IL-23                          | N              | --          |
| C17, C18   | IL-27                          | N              | --          |

|          |                         |          |          |
|----------|-------------------------|----------|----------|
| D3, D4   | IL-32 $\alpha$          | N        | --       |
| D5, D6   | IP-10                   | N        | --       |
| D7, D8   | I-TAC                   | N        | --       |
| D9, D10  | MCP-1                   | N        | --       |
| D11, D12 | <b>MIF</b>              | <b>Y</b> | <b>N</b> |
| D13, D14 | Mip-1 $\alpha$          | N        | --       |
| D15, D16 | Mip-1 $\beta$           | N        | --       |
| D17, D18 | <b>Serpin E1</b>        | <b>Y</b> | <b>N</b> |
| E1, E2   | <b>Positive Control</b> | <b>Y</b> | <b>N</b> |
| E3, E4   | RANTES                  | N        | --       |
| E5, E6   | SDF-1                   | N        | --       |
| E7, E8   | TNF- $\alpha$           | N        | --       |
| E9, E10  | sTREM-1                 | N        | --       |
| E19, E20 | Negative Control        | N        | --       |

### **6.3 Cytokine array shows cytokines and chemokines differentially secreted after IL-7 and IL-15 stimulation**

Because changes in cytokine secretion after infection with HPV quasivirions were seen, we decided to test whether stimulation with  $\gamma$ -chain cytokines would lead to changes in secretion. This is particularly relevant as in a model for epidermal injury upregulation of IL-15 was shown and HPV is only able to enter the skin via micro-injuries (298). Therefore, it is likely that there would be an increase in the IL-15 concentration at the site of viral entry.

Untransduced NIKS were cultured for 6 hours in serum free medium and then stimulated with 100 ng/ml IL-7 and IL-15, respectively, in serum free medium for 24 hours. The supernatants were analysed using the same Proteome Prolifer™ assay as in the previous experiment.

On all membranes we detected – similarly to the previous experiment – Gro- $\alpha$ , IL-1ra, IL-8, MIF and Serpin E1 as well as the three positive reference spots after short exposure times indicating high concentrations of these cytokines present. Out of these five cytokines, IL-1ra increased 1.2-fold following IL-7 and 1.3-fold following IL-15 stimulation. Gro- $\alpha$  was increased 1.3-fold and IL-8 1.2-fold in IL-15 stimulated cells but no change was seen in IL-7 stimulated cells. MIF and Serpin E1 did not show any differences in the secreted levels following stimulation (Figure 34 and Table 16).

In order to detect cytokines that were present at lower levels, we developed the membrane longer to increase the intensity of detected spots. CD40 ligand, sICAM-1, IL-1 $\alpha$ , IL-6, IL-13 and IP-10 were detected in all samples. IL-13 was not influenced by any of the stimuli whereas the other cytokines were increased to varying extents following stimulation (Table 16).

IL-23, IL-27, RANTES and TNF- $\alpha$  were not detected in the unstimulated samples but they were detected after both IL-7 and IL-15 stimulation, while GM-CSF, I-309, IL-16 and I-TAC were only detected in IL-15 stimulated samples.

These results suggest that stimulation of keratinocytes with  $\gamma$ -chain cytokines can induce changes in cytokine and chemokine secretion.

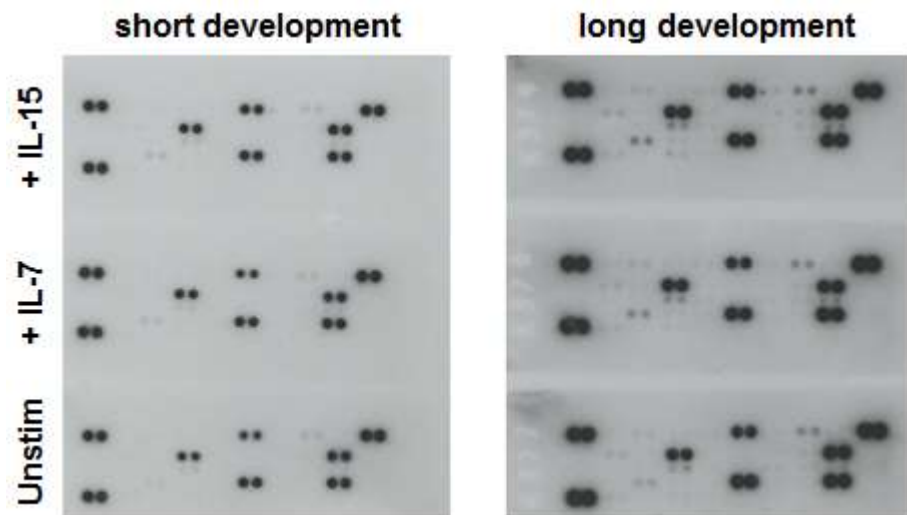


**Figure 34: Secretion of cytokines in untransduced NIKS after IL-7 and IL-15 stimulation**

NIKS cells were cultured in serum-free medium for 6 hours and then stimulated with 100 ng/ml IL-7 and IL-15, respectively. The samples were analysed using a cytokine array. Shown are cytokine arrays developed for 1 minute (left) or 10 minutes (right).

**Table 16: Quantification of the cytokine array after IL-7 and IL-15 stimulation**

The cytokine array was analysed with densitometry using ImageJ; N = not present, Y = present; if present in unstimulated samples the fold change for stimulated samples are shown in the respective fields of the table; cytokines secreted following stimulation but not present in unstimulated cells are indicated with a Y in the relevant column, cytokines increased following stimulation are marked with a green square; marked in bold are strongly expressed cytokines.

| Coordinate | Target/Control                 | Unstim | IL-7   | IL-15  |
|------------|--------------------------------|--------|--|--|
| A1, A2     | <b>Positive Control</b>        | Y      | Y  | Y  |
| A3, A4     | C5/5a                          | N      | N  | N  |
| A5, A6     | CD40 Ligand                    | Y      | 2.3x <span style="color: green;">▣</span>        | 1.6x <span style="color: green;">▣</span>        |
| A7, A8     | G-CSF                          | N      | N  | N  |
| A9, A10    | GM-CSF                         | N      | N  | Y <span style="color: green;">▣</span>           |
| A11, A12   | <b>Gro-<math>\alpha</math></b> | Y      | <b>1.0x</b>                                      | <b>1.3x</b> <span style="color: green;">▣</span> |
| A13, A14   | I-309                          | N      | N  | Y <span style="color: green;">▣</span>           |
| A15, A16   | sICAM-1                        | Y      | 1.1x <span style="color: green;">▣</span>        | 1.4x <span style="color: green;">▣</span>        |
| A17, A18   | IFN- $\gamma$                  | N      | N  | N  |
| A19, A20   | <b>Positive Control</b>        | Y      | Y  | Y  |
| B3, B4     | IL-1 $\alpha$                  | Y      | 1.1x <span style="color: green;">▣</span>        | 1.6x <span style="color: green;">▣</span>        |
| B5, B6     | IL-1 $\beta$                   | N      | N  | N  |
| B7, B8     | <b>IL-1ra</b>                  | Y      | <b>1.2x</b> <span style="color: green;">▣</span> | <b>1.3x</b> <span style="color: green;">▣</span> |
| B9, B10    | IL-2                           | N      | N  | N  |
| B11, B12   | IL-4                           | N      | N  | N  |
| B13, B14   | IL-5                           | N      | N  | N  |
| B15, B16   | IL-6                           | Y      | 1.0x   | 1.3x <span style="color: green;">▣</span>        |
| B17, B18   | <b>IL-8</b>                    | Y      | <b>1.0x</b>                                      | <b>1.2x</b> <span style="color: green;">▣</span> |
| C3, C4     | IL-10                          | N      | N  | N  |
| C5, C6     | IL-12 p70                      | N      | N  | N  |
| C7, C8     | IL-13                          | Y      | 1.0x   | 1.0x   |
| C9, C10    | IL-16                          | N      | N  | Y <span style="color: green;">▣</span>           |

|          |                         |          |                   |                   |
|----------|-------------------------|----------|-------------------|-------------------|
| C11, C12 | IL-17                   | N        | N                 | N                 |
| C13, C14 | IL-17E                  | N        | N                 | N                 |
| C15, C16 | IL-23                   | N        | Y <sub>-</sub>    | Y <sub>-</sub>    |
| C17, C18 | IL-27                   | N        | Y <sub>-</sub>    | Y <sub>-</sub>    |
| D3, D4   | IL-32 $\alpha$          | N        | N                 | N                 |
| D5, D6   | IP-10                   | Y        | 1.7x <sub>-</sub> | 2.4x <sub>-</sub> |
| D7, D8   | I-TAC                   | N        | N                 | Y <sub>-</sub>    |
| D9, D10  | MCP-1                   | N        | N                 | N                 |
| D11, D12 | <b>MIF</b>              | <b>Y</b> | <b>1.0x</b>       | <b>1.0x</b>       |
| D13, D14 | Mip-1 $\alpha$          | N        | N                 | N                 |
| D15, D16 | Mip-1 $\beta$           | N        | N                 | N                 |
| D17, D18 | <b>Serpin E1</b>        | <b>Y</b> | <b>1.0x</b>       | <b>1.0x</b>       |
| E1, E2   | <b>Positive Control</b> | <b>Y</b> | <b>Y</b>          | <b>Y</b>          |
| E3, E4   | RANTES                  | N        | Y <sub>-</sub>    | Y <sub>-</sub>    |
| E5, E6   | SDF-1                   | N        | N                 | N                 |
| E7, E8   | TNF- $\alpha$           | N        | Y <sub>-</sub>    | Y <sub>-</sub>    |
| E9, E10  | sTREM-1                 | N        | N                 | N                 |
| E19, E20 | Negative Control        | N        | N                 | N                 |

## **6.4 IL-8, Mip-3 $\alpha$ and Gro- $\alpha$ are induced following stimulation with IL-15**

To confirm the cytokine array results, the expression and changes detected in the screen were assessed further using a Luminex assay.

We chose to analyse Gro- $\alpha$  and IL-8 as they were highly expressed in keratinocytes and upregulated by IL-15 stimulation. The other two strongly expressed chemokines, MIF and Serpin E1 were not further tested as we did not see a change after stimulation in the cytokine array.

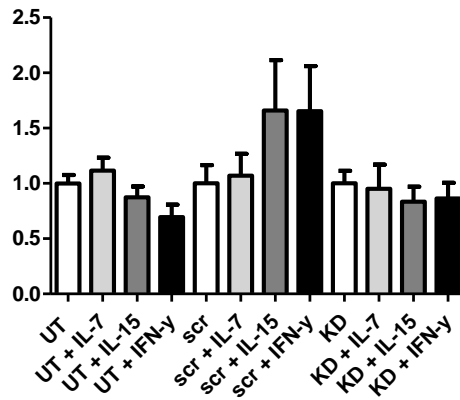
From the lower expressed molecules, we picked GM-CSF and TNF- $\alpha$  for further analysis as these two are important immune cell regulators and their expression was induced by stimulation with  $\gamma$ -chain cytokines. RANTES – a T cell and monocyte attractant – which was induced by  $\gamma$ -chain cytokines and IP-10 which was the most highly induced chemokine after stimulation were also evaluated. IL-1 $\alpha$  was chosen as it is often implied to play a role in keratinocyte biology. Additionally, we included Mip-3 $\alpha$  which was not part of the screen but is known to be released by keratinocytes, modified in HPV infection and has been implied to be  $\gamma$ -chain dependent in other cell types (45, 125, 233).

Initially, untransduced, scr control and KD cells were used. They were cultured in serum-free medium for 24 hours and then stimulated with 100 ng/ml IL-7, IL-15 and IFN- $\gamma$  for 24 hours. Supernatants were collected and analysed for cytokine presence using the Luminex system.

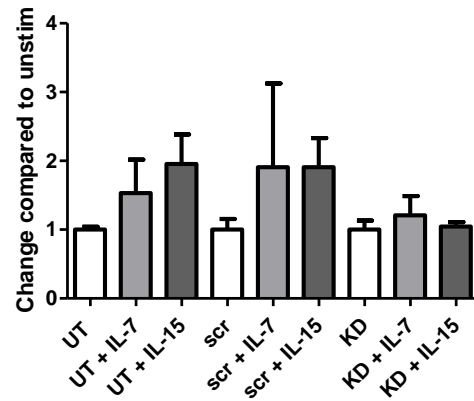
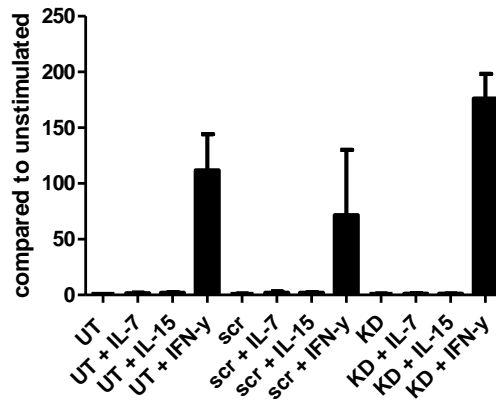
The levels of GM-CSF and TNF- $\alpha$  were below the detection limit in this experiment and were therefore defined as not present. Expression of IL-1 $\alpha$  was not significantly changed by any of the stimuli whereas IP-10 and RANTES were upregulated by IFN- $\gamma$  but not by IL-7 or IL-15 (Figure 35).

IL-8, Gro- $\alpha$  and Mip-3 $\alpha$  were analysed in scr control cells and KD cells after stimulation with 100 ng/ml IL-7 and IL-15 for 24 hours. All three chemokines were significantly induced after IL-15 stimulation in scr control cells. In contrast, no change was observed in KD cells. IL-7 stimulation did not lead to a significant increase in the secretion of these chemokines (Figure 36).

a) IL-1 $\alpha$



b) IP-10



c) RANTES

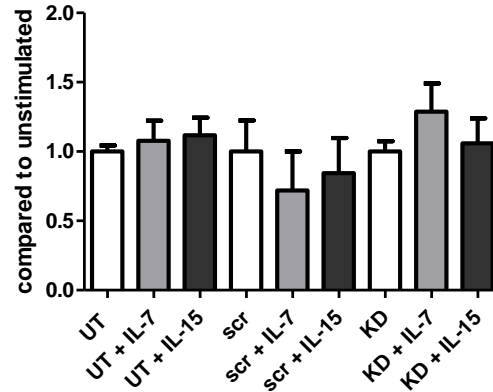
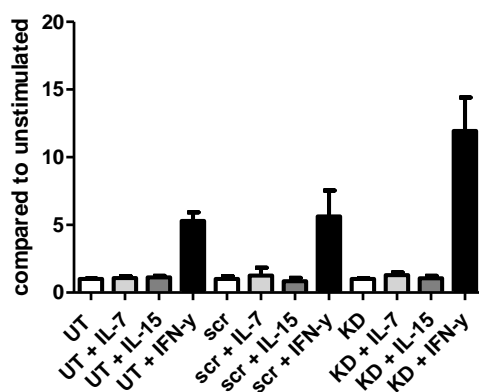
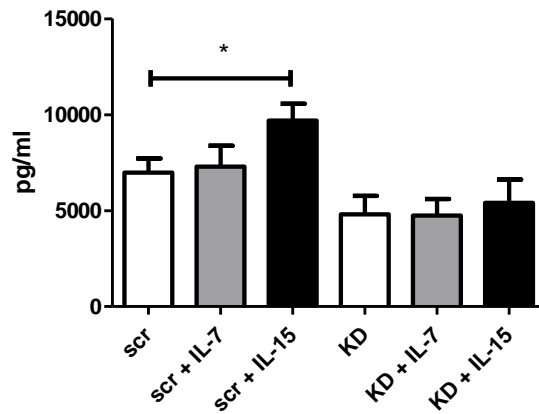


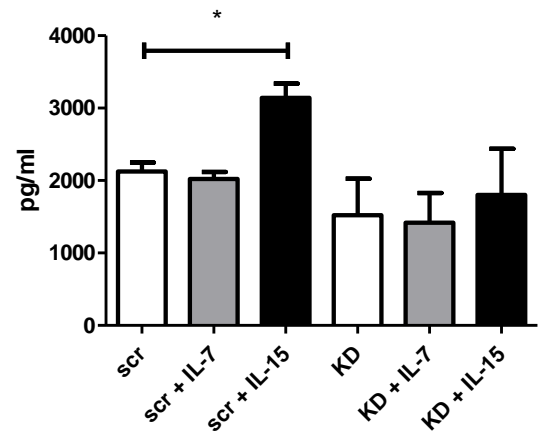
**Figure 35: Secretion of IP-10, IL-1 $\alpha$  and RANTES after different stimulations**

Untransduced, scr control and KD NIKS were cultured in serum-free medium for 24 hours, before they were stimulated with 100 ng/ml of IL-7, IL-15 and IFN- $\gamma$  for a further 24 hours, supernatants were collected and analysed for the expression of IL-1 $\alpha$  (a), IP-10 (b) and RANTES (c) using a Luminex bead assay. Results for IP-10 and RANTES are plotted with and without IFN- $\gamma$ , mean  $\pm$  SEM, n = 3.

a) Gro- $\alpha$



b) IL-8



c) Mip-3 $\alpha$

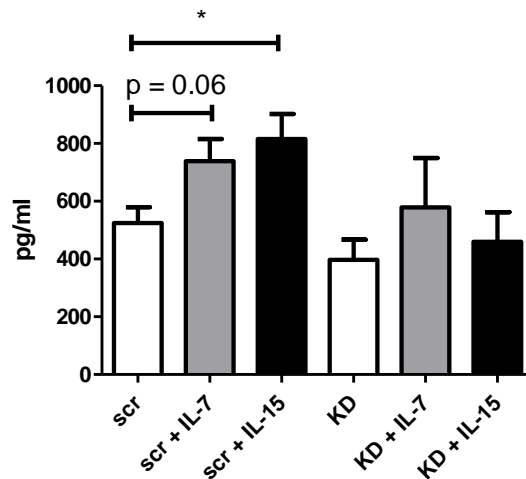


**Figure 36: Secretion of Gro- $\alpha$ , IL-8 and Mip-3 $\alpha$  after IL-7 and IL-15 stimulation**

Scr control and KD NIKS were cultured in serum-free medium for 24 hours, before they were stimulated with 100 ng/ml of IL-7 or IL-15 for a further 24 hours, supernatants were collected and analysed for the expression of Gro- $\alpha$  (a), IL-8 (b) and Mip-3 $\alpha$  (c) using a Luminex bead assay, mean  $\pm$  SEM, \* $p$ <0.05, Kruskal-Wallis test, followed by Dunn's multiple comparison test,  $n = 6$ .

## **6.5 Levels of IL-8, Gro- $\alpha$ and Mip-3 $\alpha$ secreted by keratinocytes are able to attract neutrophils**

As cytokine secretion is reduced after IL-15 stimulation in knock-down cells, it is possible that immune cells are attracted to a lesser extent to the site of infection which might explain the increased susceptibility of X-SCID patients to HPV infections. It is not fully understood which immune cell types are important for the regression of HPV induced lesions. From animals models it is known, that the influx of T cells is important for lesion clearance and recently, in a patient with Warts, Hypogammaglobulinemia, Infections and Myelokathexis (WHIM) syndrome the importance of the myeloid lineage was shown (151, 299). Therefore, migration of both myeloid and lymphoid immune cells towards the secreted cytokines was analysed.

As the neutrophil migration assay is the best established migration experiment in our laboratory, we first wanted to examine if the secreted levels of IL-8, Gro- $\alpha$  and Mip-3 $\alpha$  were sufficient to attract neutrophils.

Neutrophils were isolated from healthy donor blood and used in Dunn Chamber experiments (see 2.2.1.18). Migration of neutrophils was tested towards the levels of cytokines released from control cells after stimulation with IL-15 (Gro- $\alpha$ : 10  $\mu$ g/ml, IL-8: 3  $\mu$ g/ml and Mip-3 $\alpha$ : 1  $\mu$ g/ml in one mix). fMLP (N-Formylmethionyl-leucyl-phenylalanine) was used as a positive control for chemoattraction of neutrophils. Data was analysed using Icy software, which automatically detects neutrophils as white dots over the black background, measures distances travelled and calculates speed and directionality.

The migratory speed of the neutrophils was significantly increased in the presence of the cytokine mix compared to no chemoattractant present to similar levels as seen with the positive control fMLP. Moreover, the chemotactic index describing the directionality of migration was also significantly increased suggesting that the neutrophils migrated in a more directional manner (i.e. "in a straight line") towards the chemokine source (Figure 37 and Figure 38).

This result suggests that the levels of IL-8, Mip-3 $\alpha$  and Gro- $\alpha$  secreted by keratinocytes are physiologically relevant and are able to significantly attract immune cells.

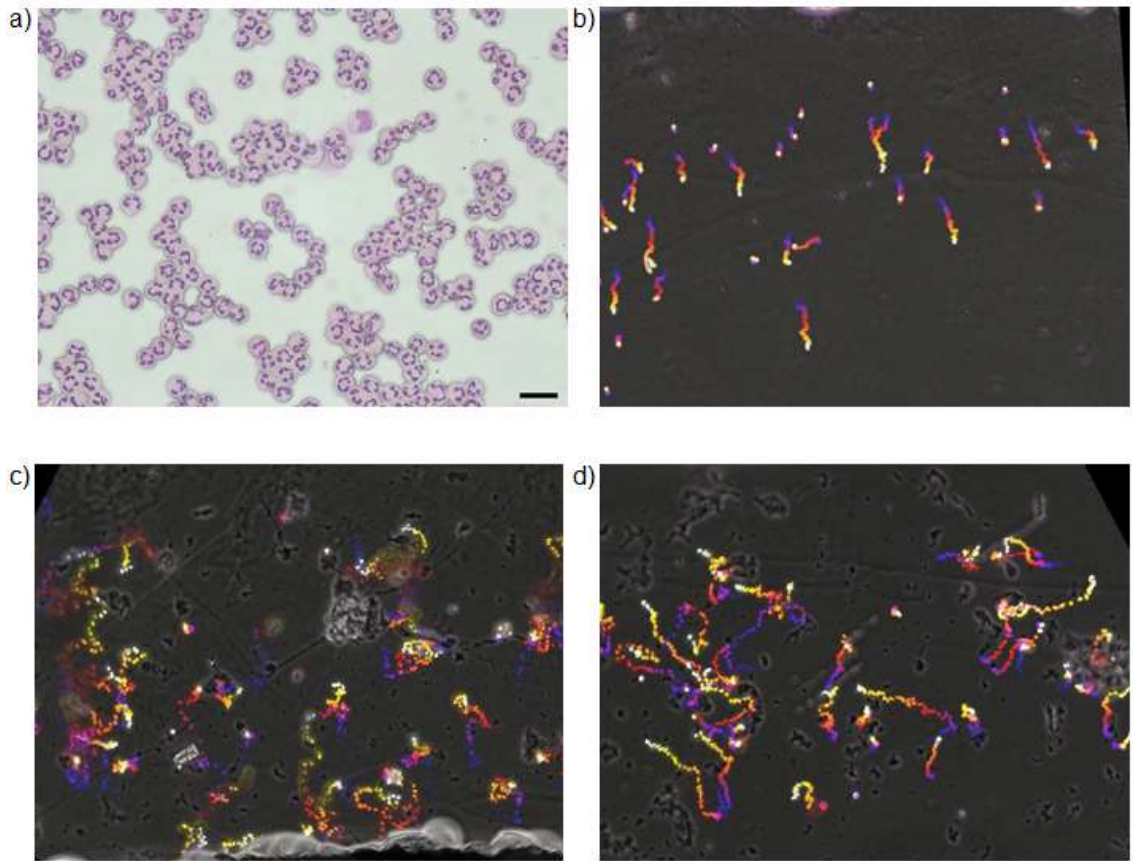


**Figure 37: Neutrophil migration towards different chemoattractants**

Neutrophils were used for migration experiments using Dunn chambers. Cells were imaged every minute for an hour. a) Cytopsin of neutrophils before plating them on coverslip, black scale bar equivalent to 25  $\mu\text{m}$ . The other images show overlays made using ImageJ of all captured images with blue being the first image and white being the last image in the time series. The highest chemoattractant concentration is located at the top of picture. b) control without chemoattract added, c) positive control fMLP used at 100 nM, d) neutrophils migrating towards the cytokine mix of 10  $\mu\text{g/ml}$  Gro- $\alpha$ , 3  $\mu\text{g/ml}$  IL-8 and 1  $\mu\text{g/ml}$  Mip-3 $\alpha$ . Representative images from  $n = 4$  are shown.

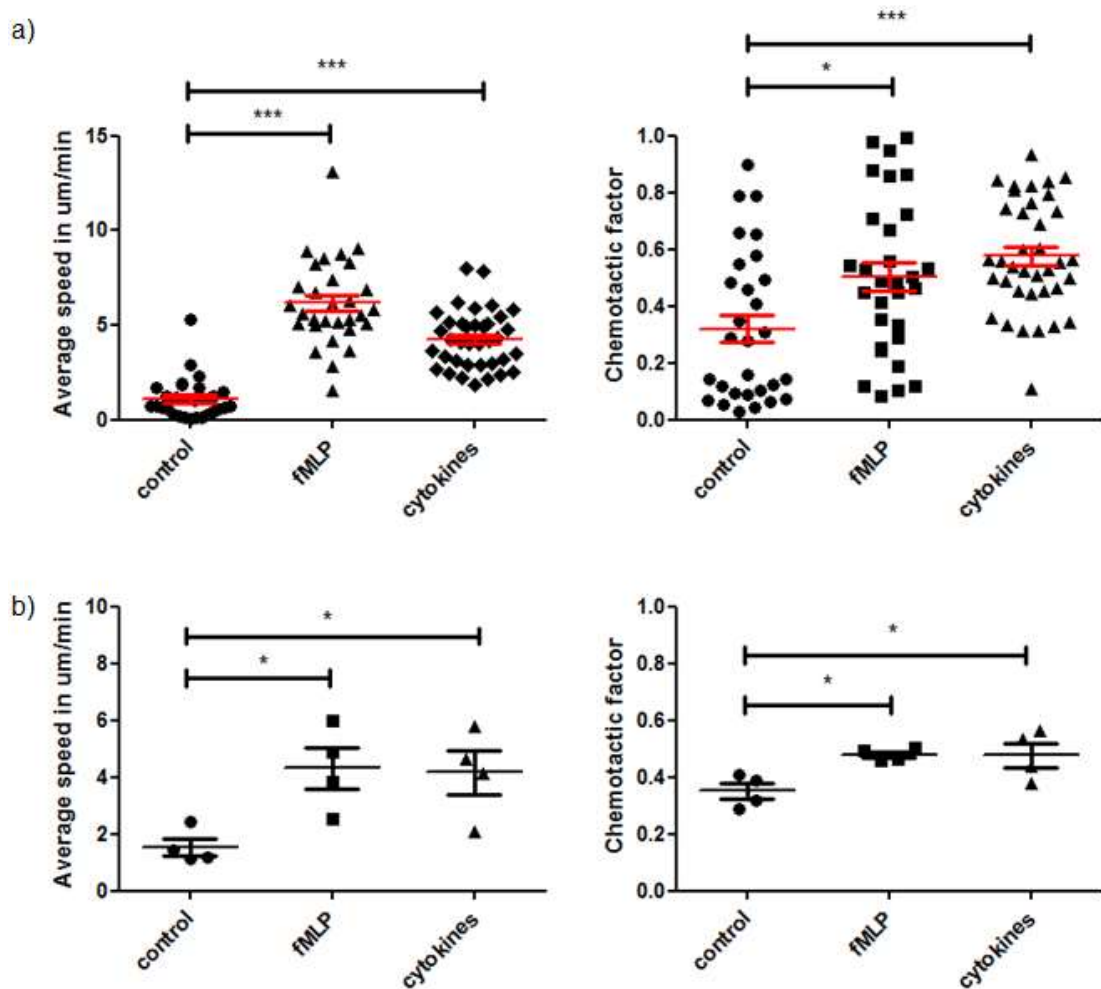


**Figure 38: Neutrophil migration towards different chemoattractants**

Neutrophil migration from Dunn chambers was tracked using Icy. Shown is quantification for migration for one donor (a) where each point represents one cell and the mean values of individual donors (b) where each dot represents one donor. “Control” = no chemoattractant, “cytokines” = cocktail of 10  $\mu\text{g}/\text{ml}$  Gro- $\alpha$ , 3  $\mu\text{g}/\text{ml}$  IL-8 and 1  $\mu\text{g}/\text{ml}$  Mip-3 $\alpha$ , fMLP was used at 100 nM as a positive control, error bars are mean  $\pm$  SEM, \* $p < 0.05$ , \*\*\* $p < 0.001$ , Kruskal-Wallis test, followed by Dunn’s multiple comparison test,  $n = 4$ .

## **6.6 Dendritic cell migration is stimulated by IL-8, Mip-3 $\alpha$ and Gro- $\alpha$**

After seeing a positive effect on neutrophil migration using of IL-8, Gro- $\alpha$  and Mip-3 $\alpha$ , we went on to test migration of DCs cells towards these cytokines.

DCs were generated from CD14+ positive cells (see 2.2.1.15) and used for migration experiments using the Chemotaxis Slide from Ibidi. Migration was manually tracked using ImageJ (see 2.2.1.19).

For this experiment, we again used the levels of cytokines released from control cells after stimulation with IL-15 (Gro- $\alpha$ : 10  $\mu$ g/ml, IL-8: 3  $\mu$ g/ml and Mip-3 $\alpha$ : 1  $\mu$ g/ml). This time, we compared them to the levels of cytokines released from KD cells stimulated with IL-15 (Gro- $\alpha$ : 5  $\mu$ g/ml, IL-8: 1.5  $\mu$ g/ml and Mip-3 $\alpha$ : 0.5  $\mu$ g/ml) which were approximately equivalent to half quantities released from IL-15 stimulated control cells. As DCs migrate slower than neutrophils, images were taken every five minutes and acquired overnight.

The higher concentrations of IL-8, Gro- $\alpha$  and Mip-3 $\alpha$  used induced a significant increase in DC migratory speed whereas the lower concentrations of the chemokines did not. Directionality of migration was not changed for either condition (Figure 39).

This suggests that in initial stages of infection, DCs might not be recruited as efficiently to the site of infection in X-SCID patients compared to healthy individuals resulting in an ineffective initial response to infection.

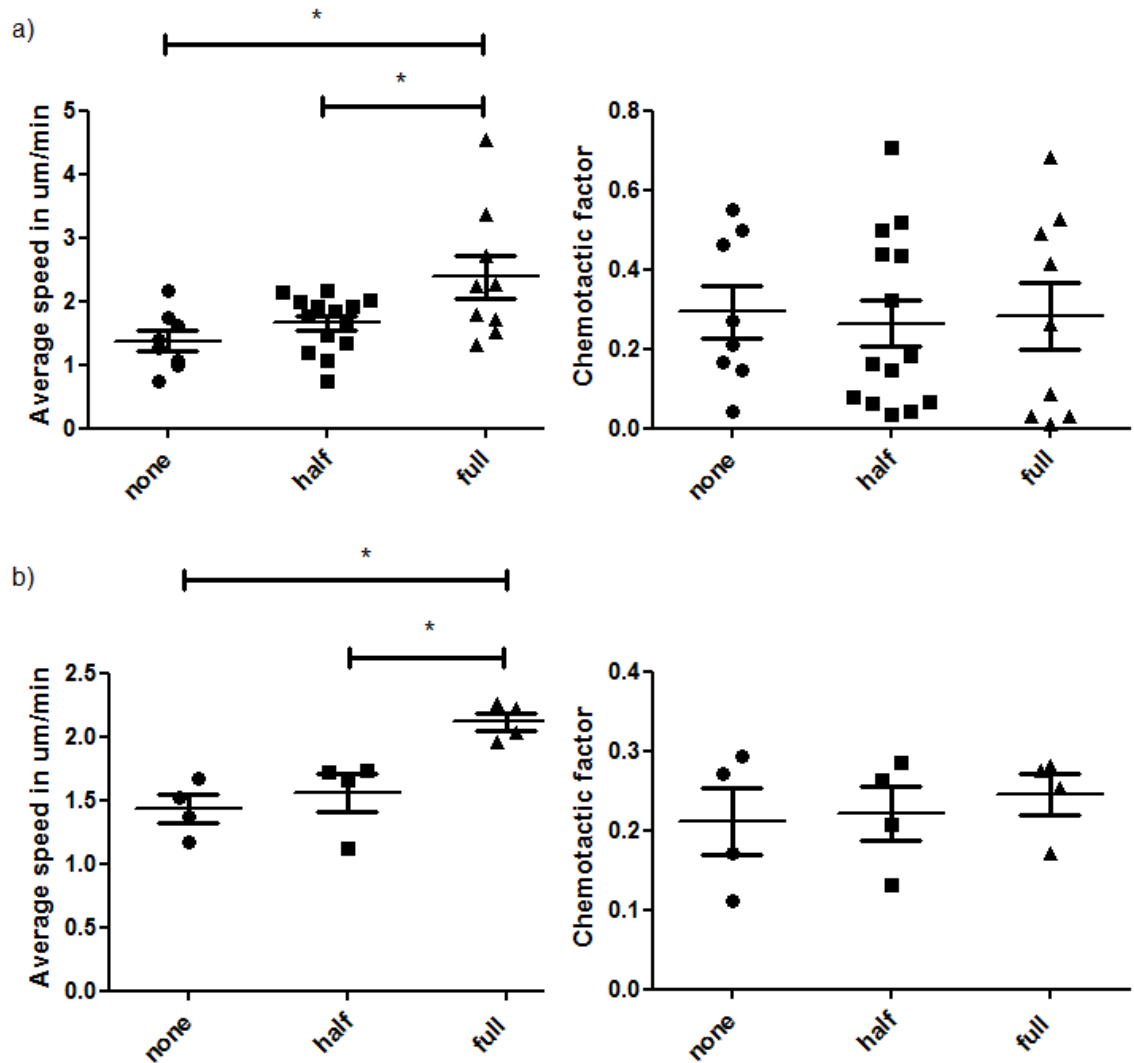


**Figure 39: Dendritic cell migration towards Gro- $\alpha$ , IL-8 and Mip-3 $\alpha$**

DCs were generated from CD14+ positive cells and used for migration experiments using Chemotaxis Slides from Ibidi. Cells were imaged every five minutes overnight, cell migration was manually tracked using ImageJ, shown is quantification for migration for one donor (a) where each dot represents one cell tracked and the means of all donors (b) where each dot represents results from an individual. “None” = no chemoattract, “half” = cytokine cocktail of 5  $\mu\text{g}/\text{ml}$  Gro- $\alpha$ , 1.5  $\mu\text{g}/\text{ml}$  IL-8 and 0.5  $\mu\text{g}/\text{ml}$  Mip-3 $\alpha$ , “full” = cytokine cocktail of 10  $\mu\text{g}/\text{ml}$  Gro- $\alpha$ , 3  $\mu\text{g}/\text{ml}$  IL-8 and 1  $\mu\text{g}/\text{ml}$  Mip-3 $\alpha$ , error bars are mean  $\pm$  SEM, \* $p < 0.05$ , Kruskal-Wallis test, followed by Dunn’s multiple comparison test,  $n = 4$ .

## **6.7 IL-8, Mip-3 $\alpha$ and Gro- $\alpha$ are able to attract CD4+ T cells**

After seeing a positive effect of IL-8, Mip-3 $\alpha$  and Gro- $\alpha$  on the migration of both DCs and neutrophils, we next wanted to look at CD4+ T cells. Most animal models describe mainly an influx of CD4+ T cells to sites of PV infection compared to CD8+ T cells which are present in lower numbers (133-135, 144, 151).

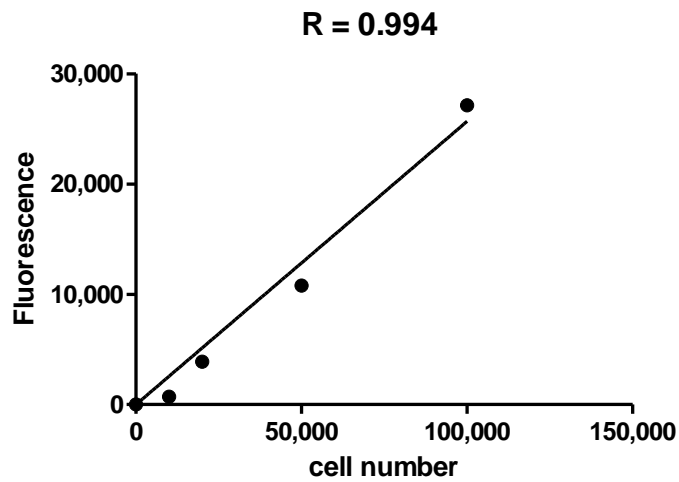
As Dunn Chamber and Chemotaxis Slides from Ibidi can only be used with adherent cells, transwell migration assays were used to examine T cell migration instead.

As for DCs, we compared the use of 10  $\mu$ g/ml Gro- $\alpha$ , 3  $\mu$ g/ml IL-8 and 1  $\mu$ g/ml Mip-3 $\alpha$  to half these concentrations to attract CD4+ T cells. Fractalkine was used as a positive control. CD4+ T cells were isolated from healthy donor blood and directly used for migration experiments using transwell inserts with 5.0  $\mu$ m pores. Migration was carried out for 2 hours at 37 °C and cell number determined using the CyQuant NF Cell Proliferation Assay which measures fluorescence depending on DNA content (see 2.2.1.20).

A clear correlation between the cell number tested with the intensity of the fluorescence detected were confirmed initially (Figure 40a) indicating a direct correlation of the fluorescence intensity to the amount of cells present. Using the cytokine mix, we saw a significant increase in migration only with the full concentration of the three chemokines compared to the negative control but not with half the concentration. Half the concentration induced a small increase in migration which was not significant (Figure 40 b).

These results together with data from the neutrophil and DC migration experiments suggest that migration of several immune cell types towards  $\gamma$ -chain deficient keratinocytes might be reduced as a result of reduced chemokine secretion following IL-15 stimulation. This is especially relevant as IL-15 is upregulated in models for epithelial wounding and microwounds are necessary for entry of HPV (298).

a)



b)

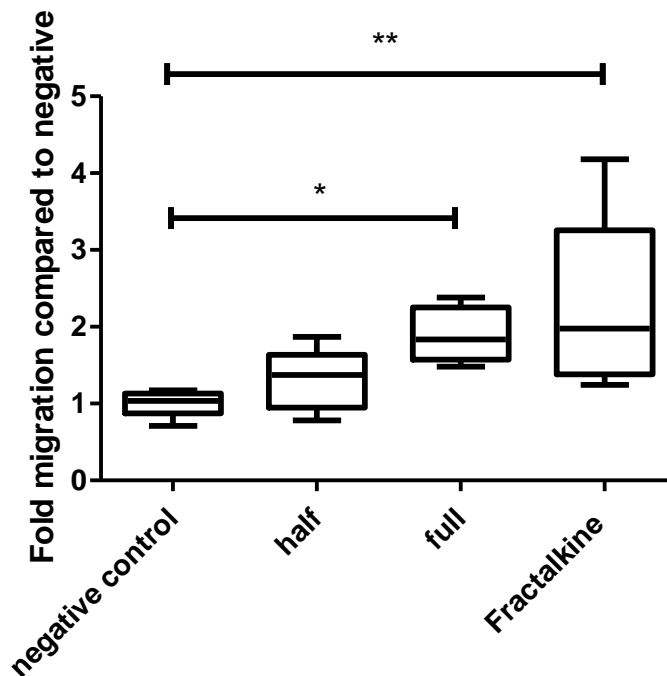


**Figure 40: CD4+ T cell migration towards different cytokines**

CD4+ T cells were isolated from whole blood and used for transwell migration assays using transwells with a 5.0  $\mu\text{m}$  polycarbonate membrane.  $1 - 2 \times 10^5$  cells were used per transwell, migration was carried out for 2 h at 37 °C, cell number was determined using the CyQuant NF Cell Proliferation Assay, standard curve for the assay showing regression between cell number used and fluorescence detected (a) and results of migration assays (b), “half” = cytokine cocktail of 5  $\mu\text{g}/\text{ml}$  Gro- $\alpha$ , 1.5  $\mu\text{g}/\text{ml}$  IL-8 and 0.5  $\mu\text{g}/\text{ml}$  Mip-3 $\alpha$ , “full” = cytokine cocktail of 10  $\mu\text{g}/\text{ml}$  Gro- $\alpha$ , 3  $\mu\text{g}/\text{ml}$  IL-8 and 1  $\mu\text{g}/\text{ml}$  Mip-3 $\alpha$ , Fractalkine was used as a positive control at 40  $\mu\text{g}/\text{ml}$ ; \* $p < 0.05$ , \*\* $p < 0.01$ , Kruskal-Wallis test, followed by Dunn’s multiple comparison test,  $n = 3$ , run in triplicate.

## **6.8 Gro- $\alpha$ secretion is increased in HPV18 positive control cells but not in $\gamma$ -chain deficient cells**

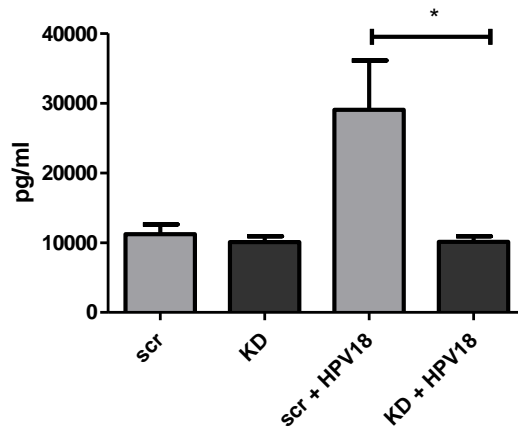
In order to identify, whether there are differences in cytokine secretion in cells that are stably expressing HPV18, we used HPV18 transfected cells (see Chapter 5.3). This would be representative of the situation in later stages of infection where HPV is stably maintained in keratinocytes. As we previously identified Gro- $\alpha$ , IL-8 and Mip-3 $\alpha$  as potential targets that are influenced by the absence of  $\gamma$ -chain, we selected these three chemokines for analysis.

Supernatants were collected from scr control and KD cells stably transfected with HPV18 after 24 hours in culture and used for Luminex bead array to detect the expression of Gro- $\alpha$ , IL-8 and Mip-3 $\alpha$ .

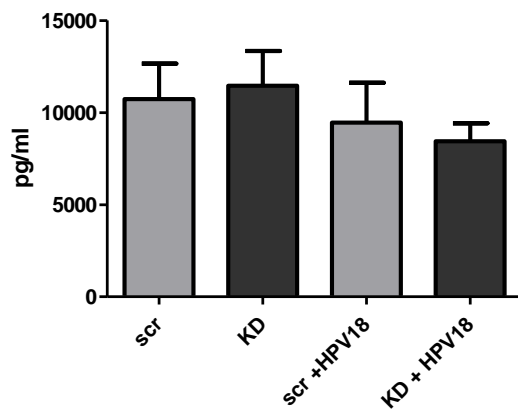
Gro- $\alpha$  was the only one of the three chemokines that was affected by the presence of HPV18. Control cells transfected with HPV18 secreted significantly more Gro- $\alpha$  than KD cells transfected with HPV18 and untransfected control and KD cells. In contrast, there were no differences in secretion for IL-8 and Mip-3 $\alpha$  (Figure 41).

This suggests, that Gro- $\alpha$  might be a potential chemokine that could influence migration of immune cells in the later stages of infection.

a) Gro- $\alpha$



b) IL-8



c) Mip-3 $\alpha$

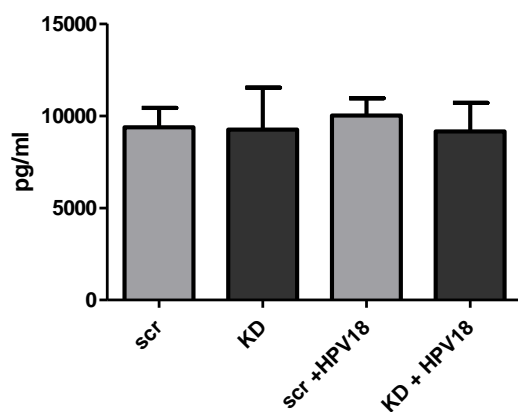


**Figure 41: Secretion of Gro- $\alpha$ , IL-8 and Mip-3 $\alpha$  in HPV18 positive NIKS**

Supernatants from scr control and KD NIKS with and without HPV18 were collected after 24 hours in culture and analysed for the expression of Gro- $\alpha$  (a), IL-8 (b) and Mip-3 $\alpha$  (c) using a Luminex bead assay, mean  $\pm$  SEM, \* $p$ <0.05, Kruskal-Wallis test, followed by Dunn's multiple comparison test,  $n = 4$ .

## **6.9 Higher Gro- $\alpha$ concentrations attract less CD4+ T cells**

As secretion of Gro- $\alpha$  was increased in scr control cells transfected with HPV18 but not in KD cells transfected with HPV18, we wanted to test whether different concentrations of Gro- $\alpha$  are able to attract different amounts of CD4+ T cells. Only T cells were used for this experiment as it is thought that T cells more important in the later stages of infection than antigen-presenting cells and cells of the innate immune system.

CD4+ T cells were isolated from healthy donor blood and used for transwell migration experiments as before. Gro- $\alpha$  was used at 10  $\mu\text{g/ml}$  (as secreted by KD + HPV18 and untransfected cells) and 30  $\mu\text{g/ml}$  (as secreted by scr + HPV18 cells).

A significant increase in the number of CD4+ T cells that migrated could be seen with both concentrations of Gro- $\alpha$ . Interestingly, however, using Gro- $\alpha$  at 10  $\mu\text{g/ml}$  lead to a significantly higher migration of CD4+ T cells than the higher Gro- $\alpha$  concentration of 30  $\mu\text{g/ml}$  (Figure 42).

This result suggests that under these conditions higher levels of Gro- $\alpha$  lead to a reduction in CD4+ T cell migration. With this analysis, we were unable to support a simple mechanism whereby reduction in Gro- $\alpha$  alone by  $\gamma$ -chain deficiency leads to reduced CD4+ T cell recruitment.

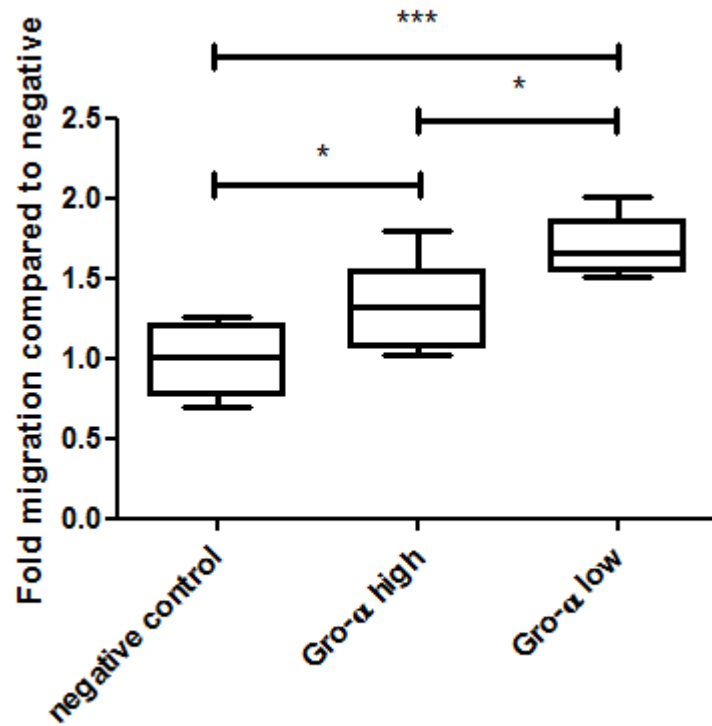


**Figure 42: Migration of CD4+ T cells towards different concentrations of Gro- $\alpha$**

CD4+ T cells were isolated from whole blood and used for transwell migration assays using transwells with a 5.0  $\mu\text{m}$  polycarbonate membrane.  $1 - 2 \times 10^5$  cells were used per transwell, migration was carried out for 2 h at 37  $^{\circ}\text{C}$ , cell number was determined using the CyQuant NF Cell Proliferation Assay, shown are results of migration assays with “Gro- $\alpha$  high” at 30  $\mu\text{g}/\text{ml}$ , “Gro- $\alpha$  low” at 10  $\mu\text{g}/\text{ml}$ ; \* $p < 0.05$ , \*\*\* $p < 0.001$ , Kruskal-Wallis test, followed by Dunn’s multiple comparison test,  $n = 3$ , run in triplicate.

## **6.10 HPV18 presence in control but not in $\gamma$ -chain deficient cells leads to increased attraction of CD4+ T cells**

In our Luminex experiments, we only measured a certain subset of cytokines which came up as potential hits from the cytokine array and then used these levels of exogenous cytokines to attract immune cells. In these assays the potential synergistic or inhibitory effects of all cytokines secreted by keratinocytes cannot be accounted for. Therefore, in the final migration experiments using transwells, we used supernatants collected from keratinocytes after 24 hours in culture to attract T cells as a more biologically relevant target.

CD4+ T cells were isolated as in previous experiments (see 2.2.1.20 and Chapter 6.7) and then they were resuspended in keratinocyte growth medium and filled into the inserts of the transwell plate. The collected supernatant was filled into the bottom of the transwells to attract the CD4+ T cells.

For controls cells, stable transfection with HPV18 led to an increase in the attraction of CD4+ T cells compared to untransfected cells. While KD cells showed an increase chemoattraction at baseline compared to control cells, no increase in chemoattraction was seen after HPV transfection (Figure 43).

This result suggests that only in control cells the presence of HPV18 leads to an increase in CD4+ T cell migration which does not occur for KD cells. The implication of this in a clinical setting could be that HPV infection in X-SCID patients does not lead to an increase in CD4+ T cells attraction compared to basal levels so that the infection response in these patients would not be as effective as in healthy individuals. This might be an important factor to explain the increased susceptibility to HPV infection seen in X-SCID patients.

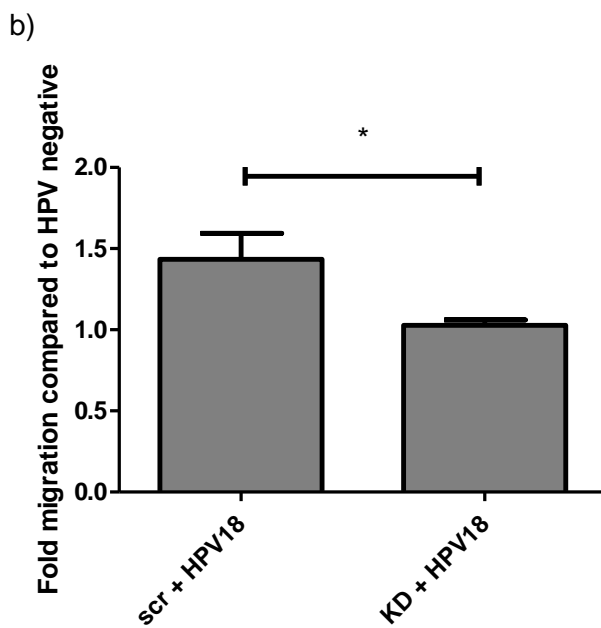
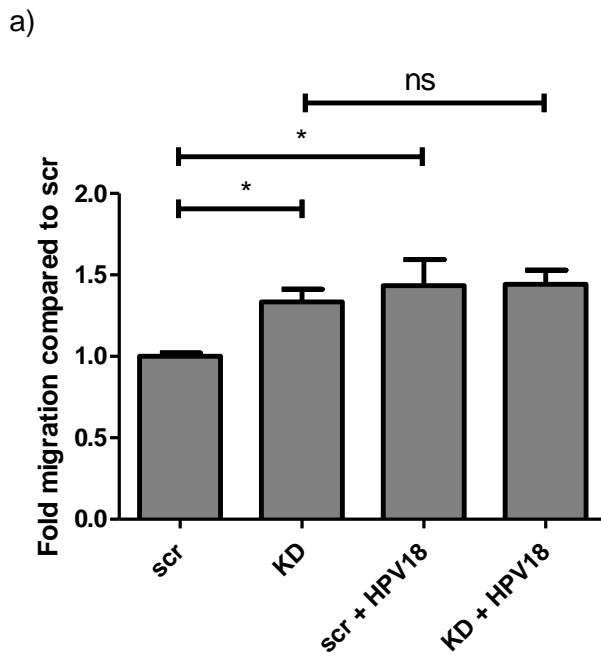


**Figure 43: CD4+ T cell migration towards supernatants from HPV positive and negative NIKS**

CD4+ T cell were isolated from whole blood and used for transwell migration assays using transwells with a 5.0  $\mu\text{m}$  polycarbonate membrane.  $1 - 2 \times 10^5$  cells were used per transwell, migration was carried out for 2 h at 37 °C, cell number was determined using the CyQuant NF Cell Proliferation Assay, migration was measured towards supernatants harvested from scr control and KD cells with and without HPV18, migration compared to scr (a) and normalised to HPV18 negative samples (b), mean  $\pm$  SEM, \*p < 0.05, measured with four different sets of supernatants and two different blood donors, everything run in duplicate.

## **6.11 HPV18 presence only in $\gamma$ -chain deficient but not in control cells leads to increased attraction of CD8+ T cells**

After seeing differences in migration of CD4+ T cells to supernatants of HPV negative and HPV18 positive control and  $\gamma$ -chain knock-down cells, we went on to repeat the experiments with CD8+ T cells as both T cell subsets have distinct roles in fighting infections.

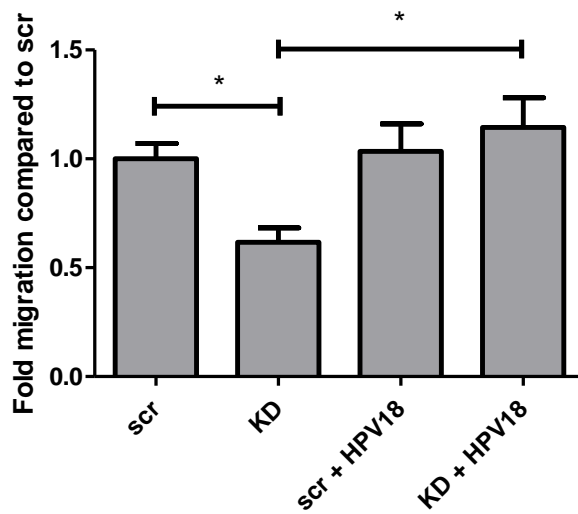
CD8+ T cells were isolated from PBMCs in a similar way to the isolation of CD4+ T cells for previous experiments. The migration experiment using collected supernatants was carried out as for CD4+ T cells.

Interestingly, the results obtained with CD8+ T cells seemed to be the reverse to the results obtained with CD4+ T cells.

The levels of attracted CD8+ T cells were lower using KD cell supernatant compared to control cell supernatant from HPV negative cells. For scr control cells, no difference in CD8+ T cell attraction was seen between HPV negative and HPV18 positive cells. Here, KD supernatants showed a significantly increased attraction of CD8+ T cells when they were HPV18 positive compared to HPV negative samples. The fold increase in chemoattraction between HPV negative and HPV18 positive cells was significantly higher in KD cells compared to scr control cells (Figure 44).

This means that only in  $\gamma$ -chain deficient cells the presence of HPV18 leads to an increase in CD8+ T cell migration which is exactly the opposite result than the one seen with CD4+ T cells. *In vivo*, this could mean that X-SCID patient demonstrate an increase in CD8+ T cell recruitment to wart lesion and a decrease in CD4+ T cell recruitment.

a)



b)

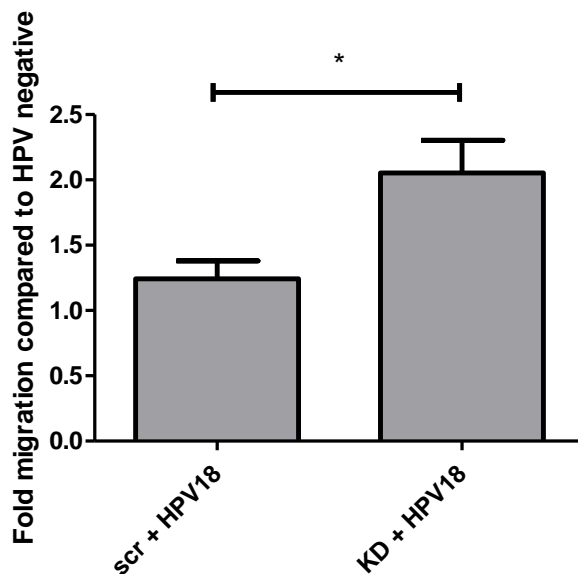


**Figure 44: CD8+ T cell migration towards supernatants from HPV positive and negative NIKS**

CD8+ T cell were isolated from whole blood and used for transwell migration assays using transwells with a 5.0  $\mu\text{m}$  polycarbonate membrane.  $1 - 2 \times 10^5$  cells were used per transwell, migration was carried out for 2 h at 37  $^{\circ}\text{C}$ , cell number was determined using the CyQuant NF Cell Proliferation Assay, migration was measured towards supernatants harvested from scr control and KD cells with and without HPV18, migration compared to scr (a) and normalised to HPV18 negative samples (b), mean  $\pm$  SEM, \* $p < 0.05$ , measured with four different sets of supernatants and two different blood donors, everything run in duplicate.

## 6.12 Discussion

X-SCID patients are affected by severe HPV infections of the skin that normally do not regress over time and are extremely difficult to treat. The pathomechanism for the increased susceptibility, heightened disease severity and impaired immune response is currently unknown.

In this chapter, we examined cytokine secretion from keratinocytes after infection with quasivirions, after stimulation with  $\gamma$ -chain cytokines and in cells stably transfected with HPV18 genomes.

After infection with HPV quasivirions, we did not observe any changes in the secretion of the cytokines tested. Not many experiments have been done looking at cytokine secretion after infection with PVs. In one study, canine keratinocytes were infected with CPV-2. No changes in the mRNA expression of IFN- $\beta$ , IL-6 and TNF- $\alpha$  or the pattern recognition receptors RIG-I, IFI16 and MDA5 were observed either 24 hours or 4 days post-infection (300). In another report by the same group comparing keratinocytes from normal and X-SCID dogs, no changes in the mRNA levels for the same targets were observed after stimulation with either poly(dA:T) or CPV-2 at 2 and 6 days. There was reduced expression of TNF- $\alpha$  and IFN- $\kappa$  at 4 days after challenge with CPV-2 but no difference between X-SCID and control canine keratinocytes (265). These observations suggest that initial virus infection has either no significant influence on cytokine and chemokine secretion or that the appropriate chemokines and cytokines or time points were not analysed. Moreover, in natural infection with PV other factors, such as the necessity for micro-trauma, also play a role meaning that infecting monolayers of keratinocytes does not sufficiently mimic natural infection.

Therefore, we next looked at the secretion of chemokines after stimulation with IL-7 and IL-15 as the latter one is induced in epithelial wounding (298). A significant increase in the levels of Gro- $\alpha$ , Mip-3 $\alpha$  and IL-8 was observed after stimulation with IL-15 in control cells. The levels of these cytokines were physiologically relevant inducing migration of neutrophils, DCs and CD4+ T cells. Moreover, the cytokine levels released from IL-15 stimulated control cells induced significantly higher migration of DCs and CD4+ T cells than those released from knock-down cells stimulated with IL-15 suggesting that after epithelial wounding more immune cells are recruited in healthy individuals than in X-SCID patients. Together these results suggest that following microwounding and initial HPV infection fewer immune cells may be recruited in X-SCID patients.

Chemokines are important in the host defence because of their chemoattractant properties. They are involved in recruiting neutrophils, monocytes and lymphocytes. Chemokines are small 8 – 10 kDa molecules that are classified in four distinct families according to their sequence homologies: CC, CXC, CX3C and C. IL-8 (CXCL8) and Gro- $\alpha$  (CXCL1) are CXC chemokines that transmit their signals via CXCR1 and CXCR2 receptors. Mip-3 $\alpha$  (CCL20/LARC) is a CC chemokine which binds and activates CCR6 (44).

CXCR1 or CXCR2 are expressed on neutrophils, T cells, NK cells, monocytes and DCs (301-303). Therefore, Gro- $\alpha$  and IL-8 should theoretically be able to attract all these cell types. Gro- $\alpha$  and IL-8 are very well known chemoattractants for neutrophils and IL-8 has also been shown to be able to attract T cells (304, 305). For Gro- $\alpha$ , attraction of NK cells and CXCR2 positive T cells was shown (306, 307). The data about the effect of IL-8 on DC migration is limited. One study showed no effect of IL-8 on the migration of DCs but in another study blocking IL-8 using a neutralising antibody led to a reduction of DC migration (303, 308). In the same study, blocking Gro- $\alpha$  had no effect on DC migration. CCR6 – the receptor for Mip-3 $\alpha$  – is expressed memory T cells and DCs and Mip-3 $\alpha$  is a known chemoattractant for these cells (309-311).

Most of these studies used higher concentrations of the chemokines (usually around 100 ng/ml) than we did, however, our results showed that lower chemokine levels – equivalent to those released from keratinocytes – were sufficient to attract immune cells. One publication showed that administrating Gro- $\alpha$  and IL-8 together led to an add-on effect of the chemoattracting properties towards macrophages showing that these cytokines can interact which is potentially true here as well (312).

Our study is the first one to show that IL-15 can induce the secretion of IL-8, Gro- $\alpha$  and Mip-3 $\alpha$  by keratinocytes and that this induction is  $\gamma$ -chain dependent. We also showed for the first time that relatively low concentrations of these chemokines are sufficient to attract immune cells.

To further show that these chemokines in the concentrations released from keratinocytes after IL-15 stimulation are important for immune cell recruitment, these experiments should be repeated using supernatants from keratinocytes instead of exogenously supplying chemokines. In addition, migration experiments using blocking antibodies for IL-8, Gro- $\alpha$  and Mip-3 $\alpha$  should be performed in future. These blocking antibodies should be used both separately and in combination to identify whether just one of the cytokines is important for the effect or whether the changes in all three are necessary to induce changes in immune cell migration.

After modelling the initial infection, we next looked at cells stably transfected with HPV18 to analyse later stages of infection. We analysed supernatants from cells transfected with HPV18 for the secretion of IL-8, Mip-3 $\alpha$  and Gro- $\alpha$ . Only Gro- $\alpha$  was increased in HPV18 positive cells but under the conditions used, higher levels of Gro- $\alpha$  led to a reduction in CD4+ T cell migration. A simple mechanism whereby lower levels of Gro- $\alpha$  alone lead to reduced CD4+ T cell recruitment could not be supported.

Therefore, we used supernatants collected from keratinocytes to attract T cells. In control cells, presence of HPV18 led to an increase in CD4+ T cell attraction with no changes in CD8+ T cell attraction. In contrast, for  $\gamma$ -chain deficient cells, transfection with HPV18 did not lead to changes in CD4+ T cell attraction but increased CD8+ T cell attraction.

In the literature, CD4+ T cells are generally the cell type that is regarded to be the most important for regression of PV induced lesions but the role of CD8+ T cells is less clear. For example, in multiple studies looking at cervical intraepithelial neoplasia, E7-specific CD4+ T cells responses were associated with regression whereas the data on CD8+ T cells was less clear or did not show any association with regression (295-297, 313).

In this aspect, our data is interesting as we saw that stable maintenance of HPV18 in control cells resulted in an increased migration of CD4+ T cells which was not seen for  $\gamma$ -chain deficient cells. This indicates that in X-SCID patients less CD4+ T cells might be recruited to the site of infection. As they are the main cell type found initially regression, wart lesion regression in X-SCID patients may be impaired. The data for the CD8+ T cells in this aspect was more surprising as they are also found in regressing lesions but in lower numbers and we saw a significant increase in CD8+ T cells migrating towards HPV positive  $\gamma$ -chain deficient cells compared to HPV negative ones. However, it is not clear yet which balance of CD8+ to CD4+ T cells is needed for regression or whether CD4+ T cell help is required for CD8+ T cell function in this setting. It is therefore possible, that the defect in X-SCID patients is due to an imbalance of infiltrating T cells due to changes in chemokine secretion.

These results provided a possible explanation for the susceptibility of X-SCID to severe cutaneous HPV infections, however, so far this data was only gained with *in vitro* techniques. In future, it will be needed to use animal models to confirm these results. Another limitation of this work is that we used cells transfected with HPV18 which is a high risk  $\alpha$ -HPV type but warts in X-SCID patients are formed by other HPV types. Use of other HPV types is technically challenging as transfection has only been established

using the high-risk  $\alpha$ -types HPV16, 18 and 31 and for other types often only limited maintenance is observed. Moreover, further studies are needed into which cytokines are responsible for the differences in T cells recruitment seen between the control and  $\gamma$ -chain deficient cells. As we identified Gro- $\alpha$  as changed between control and  $\gamma$ -chain deficient cells transfected with HPV18, the migration experiments should be repeated using neutralising antibodies to Gro- $\alpha$ . In the experiments performed so far with Gro- $\alpha$  synergistic effects with other chemokines cannot be accounted for. Therefore, even though initial experiments did not seem to show that Gro- $\alpha$  is accountable for the changes seen in this model, this remains to be tested in detail.

In conclusion, our data suggests that alterations in cytokine secretion and the resulting reduction in recruitment of immune cells is a significant contributory factor to the increased HPV susceptibility seen in X-SCID patients.

## **7. Final Discussion**

## **7.1 The absence of the common $\gamma$ -chain affects HPV infection at multiple stages**

X-SCID is caused by mutations in the common  $\gamma$ -chain and leads to an absence of T and NK cells. B cells are present but they are not functional. This leads to a complete absence of the adaptive immune system and therefore inability to fight infections. The disease can only be cured using bone marrow transplantation or gene therapy which has been done very successfully in the recent years with ever increasing survival rates (225).

However, it was shown that a discrete immunodeficiency remains leaving the patients susceptible to severe cutaneous infections with HPV with approximately 50% of patients suffering from infections. The resulting warts are often impossible to eradicate with current treatments. Both through cosmetic effects and impairment of hand and foot function, this disease has a great impact on the quality of life of the affected patients. In the two main studies, the heightened susceptibility was not associated with any immunological or transplant specific factors (236, 237).

In this thesis, we examined the possibility that  $\gamma$ -chain deficiency in keratinocytes is the reason for the remaining immunodeficiency. Keratinocytes are not replaced by the available treatment options and HPV exclusively infects them making them a likely candidate. This theory is further supported by the fact that they are immune sentinels which are able to detect infection, attract immune cells via the secretion of chemokines and cytokines and that they have antigen-presenting abilities. Prior to the start of this project, limited amounts of information about  $\gamma$ -chain and its expression and function in the skin were available. As a result of this work, we showed that

- a)  $\gamma$ -chain is expressed in keratinocytes
- b) most of its co-receptors are expressed in keratinocytes including IL-15R $\alpha$  and IL-2R $\beta$ ; only IL-2R $\alpha$  was not expressed
- c) signals are transmitted via the  $\gamma$ -chain leading to increases in phosphorylation of AKT and small changes of STAT5 phosphorylation

As discussed in previous chapters, our results agreed with previously available literature and extended these findings by systematically examining  $\gamma$ -chain and its co-receptors in one study.

We hypothesized that the lack of the  $\gamma$ -chain could influence HPV infection at multiple stages, e.g. initial infection resulting in a higher permissiveness of cells to HPV infection, alterations in the viral life cycle once infection has been established leading to

hyperproliferation and changes in secretion of cytokines and chemokines decreasing the chemoattraction of professional immune cells.

Our study is the first one to look in detail at the role of the common  $\gamma$ -chain in skin immunity and to provide detail about how keratinocyte  $\gamma$ -chain might contribute to the specific HPV immunity.

We found effects of  $\gamma$ -chain deficiency in keratinocytes on all aspects examined:

- a)  $\gamma$ -chain deficient keratinocytes were more easily infected than control keratinocytes
- b) organotypic rafts made with  $\gamma$ -chain deficient, HPV positive cells displayed an increased suprabasal synthesis and changes in keratin-10 expression even though HPV life cycle markers were not affected
- c) chemokine secretion from  $\gamma$ -chain deficient cells was reduced after IL-15 stimulation leading to reduced migration of neutrophils, DCs and CD4+ T cells
- d) supernatants from HPV18 positive,  $\gamma$ -chain deficient cells attracted different amounts of CD4+ and CD8+ T cells compared to control cells

While future work is required, we propose that the effect of the  $\gamma$ -chain on HPV infections is a multi-step process. Based on our experimental data, we propose a model of HPV infection in the context of  $\gamma$ -chain deficiency (Figure 45). In this model, firstly, more virus can enter the cell which is then not combatted as effectively because immune cells are not recruited as efficiently in the early stages. This leads to establishment of infection at a greater level than in healthy individuals. Secondly, once the virus has established infection it has a greater influence on the cells leading to more proliferation and therefore increased disease severity. Thirdly, due to changes in chemokine secretion of still unknown nature the balance of CD4+ and CD8+ T cells which are recruited to the site of infection is disturbed leading to reduced resolution of the disease and therefore lack of regression.

Some of the changes, e.g. the effect on suprabasal DNA synthesis, we saw were relatively small but they are potentially cumulative (suprabasal proliferation follows higher infection rate etc.) so that multiple changes amount to the severe phenotype seen in patients.

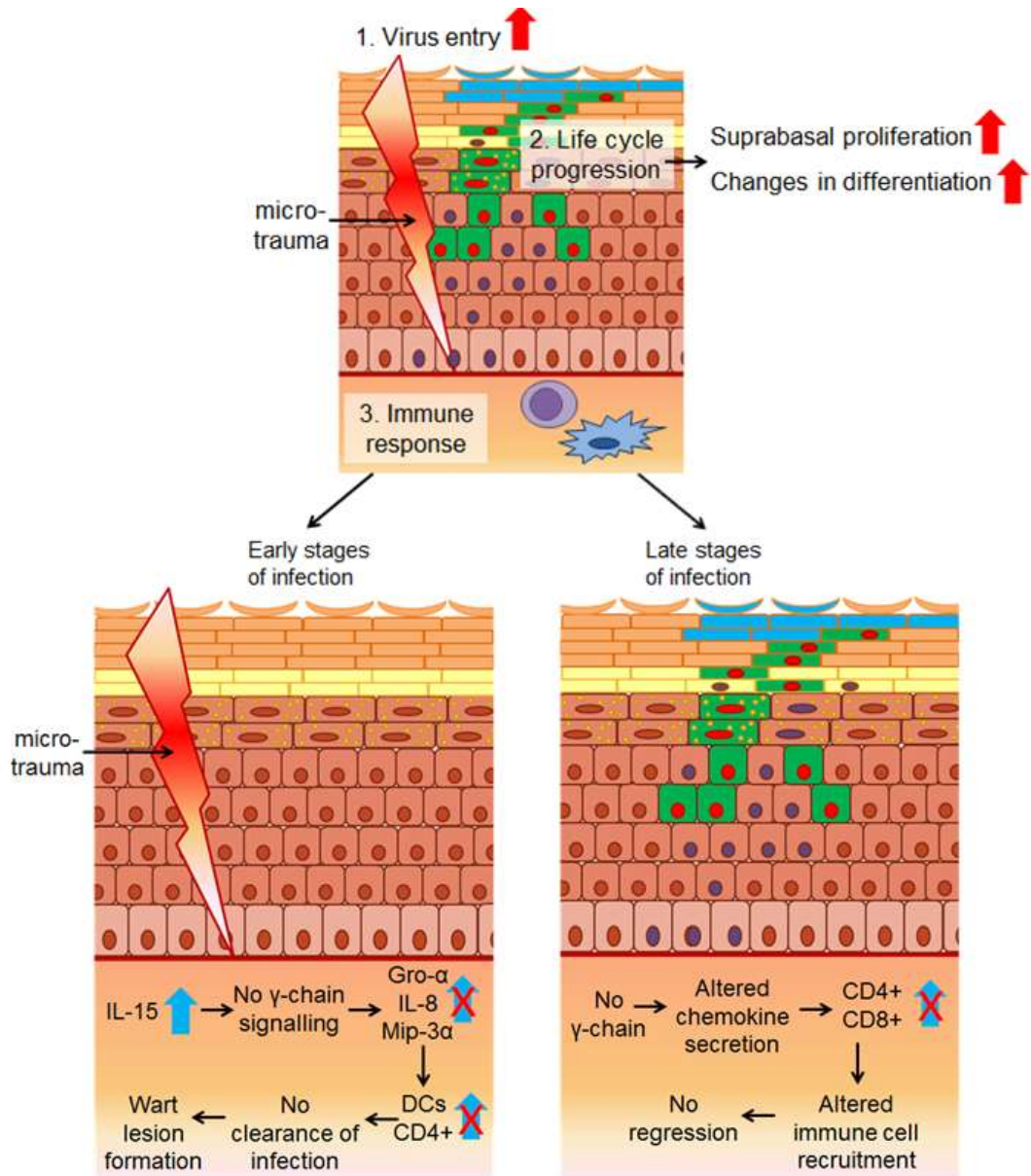


**Figure 45: Model for the effect of  $\gamma$ -chain deficiency on HPV infection**

The absence of the common  $\gamma$ -chain has an impact on HPV progression at multiple stages of infection. It enhances viral entry and leads to an increase in suprabasal proliferation when the infection is established and alters the immune response in two phases. In the early stage of infection, IL-15 is released after wounding. As there is no  $\gamma$ -chain dependent signalling, chemokines such as Gro- $\alpha$ , IL-8 and Mip-3 $\alpha$  are not induced and immune cells such as DCs and CD4+ T cells are not recruited. Therefore the infection is not cleared resulting in wart lesion formation. In the later stages, when the infection is already established, alterations in chemokine secretion lead to reduced CD4+ and increased CD8+ T cell migration. Due to the resulting imbalances in the T cell subsets, warts do not regress.

Even though we found evidence that the absence of  $\gamma$ -chain can have an effect on multiple stages of HPV infection, we favour that the influence on cytokine secretion is the main effect leading to increased HPV susceptibility. The reasons for this are that a) our experimental data is most robust for this and b) an alteration of the immune response can explain the clinical phenotype seen: the high incidence, the disease severity and lack of regression. Thirdly, we know that the immune response is key for HPV regression. Different strategies activating the immune response by different mechanisms can all be effective against HPV infections, e.g. using Candida Antigen or Contact Allergen Immunotherapy to non-specifically activate cell-mediated immune responses or using Imiquimod to induce cytokine secretion (314). The success of these therapies shows the importance of activating the immune system to fight HPV infections for the resolution of warts.

Another question is why not all X-SCID patients present with warts even though they would all suffer from reduced anti-HPV responses due to  $\gamma$ -chain deficiency in keratinocytes. It seems unlikely that some individuals have no HPV colonisation however the virulence and pathogenicity of different HPV types may play a role. For others viruses such as EBV over 90% of individuals are infected but not everyone in the adult population (315).

An additional factor that was proposed during the time frame of this work is that reduced NK cell reconstitution is responsible for the HPV infections (238). This observation was not made in other studies, however, there might have been slight variations in NK cell populations which did not reach statistical significance but might be biologically relevant. As reconstitution of NK cells is variable, this might also explain why not all X-SCID patients develop the severe HPV infections. It is interesting that CXCR1 and CXCR2, the receptors for both IL-8 and Gro- $\alpha$ , are also expressed on NK cells and Gro- $\alpha$  was shown to be a chemoattractant for NK cells (306). It is therefore tempting to speculate that NK cell recruitment is impaired in  $\gamma$ -chain deficient skin but this was not specifically tested here. As we are proposing a multi-step process for the effect of  $\gamma$ -chain deficiency on HPV infection, this might be another step predisposing patients. We could extend our proposed model that the heightened susceptibility of X-SCID patients to HPV infections is due to an imbalance of immune cells infiltrates enhanced both via the inability of keratinocytes to secrete the right amounts of chemokines as well as variations in the available immune cells such as NK cells.

## 7.2 Potential treatment options of X-SCID

Our findings raise the question how X-SCID patients can be treated as it has been proven to be difficult to eradicate the warts once established. BMT for X-SCID patients is usually performed without conditioning leading to incomplete reconstitution of the myeloid compartment, e.g. LCs and a proportion of dermal DCs stay of host origin (29, 226, 248). As it has also been postulated that the absence of  $\gamma$ -chain in DCs/LCs could be responsible for the heightened susceptibility observed, it has been proposed that conditioning regimes should be amended for X-SCID patients to achieve myeloid engraftment and thereby reducing the likeliness of them developing HPV induced warts. However, given our results and the results from the NK cell study, it seems less likely that DCs and LCs play a role and therefore conditioning would not lead to an improvement of the clinical phenotype. As conditioning is associated with higher mortality, it is preferable to avoid it if it is not necessary for transplant success.

The question then remains of how treatment for X-SCID patients might be improved. Usually destructive surgery such as using salicylic acid, cryotherapy or surgical removal are temporarily providing clinical benefits but as the infection is not cleared warts tend to form again quickly. Using immune stimulants such as Imiquimod is often not successful at inducing to wart regression, however, this might be due to the size of the wart.

Imiquimod was approved by the FDA in the US in 1997 for the treatment of external genital and perianal warts. It does not have direct anti-viral effects but rather acts an immune stimulating agent via activating TLR7 and 8. This leads to activation of the innate immune system resulting in cytokine release (keratinocytes upregulate IFN- $\alpha$ , IL-6 and IL-8), co-stimulatory molecule expression and T cell activation (316, 317).

Imiquimod is used topically as a cream and it penetrates the top layers of the wart and therefore might not reach the lower, basal layers where an immune response would need to be induced. It might therefore be necessary to combine multiple measures for successful treatment of the wart lesions of X-SCID patients, e.g. first surgical removal of the wart followed by application of Imiquimod to induce clearance of infection. However, Imiquimod could stimulate the keratinocytes to release factors needed for immune cell stimulation and infiltration. We cannot exclude that  $\gamma$ -chain deficient keratinocytes display defects in chemokine and cytokine secretion in general that might impair the use of TLR ligands.

It might be possible to use intralesional injections of cytokines to induce regression. As cytokines and chemokines are our suspected reason for the lack of regression seen,

replacing them might lead to the necessary immune cell attraction and therefore resolution of infection.

In support of this concept, the use of cytokines has been shown to induce the resolution of HPV lesions in sporadic studies in immunocompromised patients. In one patient suffering from chronic lymphocytic leukaemia (CLL), HPV-induced lesions in the perianal area were treated using high-dose IL-2 ( $5 \times 10^6$  U) injected subcutaneously once daily in combination with topical cidofovir (3%) – a virus static agent. He did not develop new warts and generally reacted well to the treatment. Previously, the warts would regrow within 2 weeks of surgical removal, however after the high-dose IL-2 treatment the patient did not show signs of regression after several months of follow-up (318). In another patient with CLL with HPV induced viral warts, IL-2 was also used successfully in therapy. The patient presented with extensive warts on hands, feet and knees which did not resolve in over six years. He was injected for 2 weeks once daily subcutaneously with  $5 \times 10^6$  U of IL-2 and 24 days later, his warts regressed. The warts did not recur in the nine years of follow-up (319).

These two studies indicate that administration of IL-2 to activate an immune response near the site of infection can be successful in treating HPV induced lesions. As IL-2 is already approved in clinic it might be a potential treatment for X-SCID patients. IL-2 is a  $\gamma$ -chain dependent cytokine but as its addition leads to activation of T cells which have been either replaced by BMT or corrected by GT use of this strategy could be successful even in X-SCID patients.

However, as the cellular response of keratinocytes to micro-trauma and HPV infection cannot be corrected, it will only be possible to treat the disease once it occurs, e.g. when warts start to form, but a preventive therapy might not be possible. It will therefore remain to be tested if in X-SCID patients a long-lasting cellular response to HPV can be induced after infection, e.g. via the production of anti-HPV antibodies by stimulated B cells or using vaccines to reduce the risk of reactivation of disease. However, the currently available vaccines only protect against mucosal HPV types and not the types which are usually found in wart lesions. If X-SCID patients also display a higher susceptibility to mucosal HPV types is currently unknown but one patient with JAK3 deficiency in our cohort developed HPV related cervical neoplasia in early adulthood. It would seem a reasonable precaution to administer currently available HPV vaccines to reduce the risk of mucosal HPV infections.

### 7.3 Future experiments

Our results suggest multiple reasons for the increased susceptibility of X-SCID patients to HPV infections. However, further experiments are needed to confirm our findings and to gain deeper understanding of the mechanisms involved. Some of these future experiments have already been described in previous chapters.

As all our experiments were carried out using cell lines it will be useful to confirm the results using primary cells. However, due to the small number of X-SCID patients it is difficult to obtain sufficient amounts of material for studies using human primary cells especially as these cells have a limited life span. Another possibility would be to use primary mouse keratinocytes which can be isolated from tail skin and grown under low calcium conditions without the use of feeder cells (320). Preparation of MmuPV1 VLPs *in vitro* has also been performed and was successfully used to infect mice *in vivo* (321). However, until now no studies have been published using primary murine keratinocytes for infection studies using MmuPV1 particles *in vitro*. We have tried to infect a mouse keratinocyte cell line using MmuPV1 particles harvested from nude mice and were able to detect MmuPV1 E1<sup>4</sup> mRNA several days after infection (unpublished data). If the results from the initial infectivity studies can be confirmed using primary mouse keratinocytes, both these cells and the NIKS cell lines could then be used to identify why there was a change in infectivity, e.g. using super resolution microscopy and FC techniques (also see Chapter 4.7).

In addition, HPV18 was used in most experiments which is a high risk mucosal and not a cutaneous HPV type which affects X-SCID patients. The effects, the use of this HPV type on the results might have, were discussed in detail in Chapters 4.7 and 5.7. In summary, cutaneous types generally have a less potent effect on cells than high risk mucosal HPV types and therefore, effects are probably less pronounced in a patient setting. Therefore, certain experiments should be repeated. It is possible to make HPV VLP using pShell plasmids for the cutaneous types HPV5 and 8 and other mucosal types such as HPV26, 51 and 58 even though they show sometimes limited infectivity (279, 321). Therefore, other types of packaging plasmids should also be used to confirm the results seen using HPV18 quasivirions. Similar experiments would in theory be possible for the raft studies. However, NIKS do not always maintain low risk HPV types when they are transfected and therefore, raft cultures are often not possible using these types (personal communication P.F. Lambert). In addition, protocols have not been established to make organotypic rafts using primary murine keratinocytes. It will, therefore, be challenging to confirm the results obtained in Chapter 5 with currently available techniques.

Even though the results obtained for the infectivity and life cycle are interesting and might give further insight into the regulation of HPV, the more important studies would be to further examine the cytokine and chemokine secretion and their influence on immune cell migration. Studies using animal models for PV infection have not yet shown a role for NK cells, but as the reconstitution of these cells has been implied to be correlated to HPV disease in X-SCID patients, migration studies *in vitro* should be carried out using NK cells. Further studies into which cytokines might be important for the changes in immune cell recruitment seen in cells stably transfected with HPV18 will be important to find out which cytokines and chemokines are leading to the differential recruitment of CD4+ and CD8+ T cells in our experiments. More cytokine arrays, ELISAs and Luminex assays will need to be carried out to this end. Mass spectrometry approaches may also be possible if larger amounts of supernatant protein can be obtained. Again, studies using cells transfected with other HPV types but HPV18 should be performed but – as previously described – these are also impacted by the difficulty of maintaining cutaneous HPV types in NIKS cells.

In addition, it would be interesting to see whether keratinocytes release factors that can activate immune cells, especially using cells transfected with HPV, as activation status can impact migration. We would propose analysing activation markers, e.g. co-stimulatory and MHC molecules, on immune cells, such as DCs, T and NK cells, following incubation with supernatants collected from  $\gamma$ -chain deficient and control cells with and without HPV.

The best way to confirm the results of this thesis would be to carry out *in vivo* experiments. A few of the issues were discussed in previous chapters (see Chapter 8.5) such as the problem of creating a model where only the keratinocytes are  $\gamma$ -chain deficient. We discussed the pros and cons of using either BMT or skin engraftment studies. Both models have drawbacks and the ideal solution would be the creation of a skin-specific knock-out model, e.g. using a K14 specific promoter, to generate a mouse with  $\gamma$ -chain deficiency limited to keratinocytes.

Using this knock-out model, it would be possible to examine the release of inflammatory molecules by keratinocytes after a) wounding, b) infection and in c) stable infection/wart lesions. As immune cells would be present, immune cell recruitment could be tracked over the course of time to identify infiltrating immune cell subsets and the differences seen between skin  $\gamma$ -chain knock-out and control mice. Furthermore, the mouse model could be used to test the different proposed treatment strategies, e.g. either injecting chemokines close to wart lesions or using IL-2 injections as these seemed to help in certain patients.

## **7.4 Relevance of this project to patients**

This project has originally arisen from the clinical problem of persistent warts after BMT and gene therapy for in X-SCID patients who have a ~50% chance of developing severe cutaneous HPV infections around 10 years after BMT. The resulting warts have a substantial impact on the quality of life of affected patients.

Even though, this project has aimed to identify the underlying reasons for the increased susceptibility to HPV infection, many questions remain unanswered. Therefore further research is needed to be able to feed back to the clinic and to inform patient care. As there are still multiple hypothesis as to which cell type is main driver for the clinical phenotype, understanding whether HPV infection in  $\gamma$ -chain deficiency results from defects of haematopoietic cells or intrinsic keratinocyte defects will determine whether refinement of bone marrow transplant protocols, development of immune modulation treatments or new antiviral agents are the most appropriate avenue for better treatment of this disabling condition.

In addition, the immune response to HPV responsible for latency or wart regression is poorly understood. Rare monogenic primary immunodeficiencies where severe HPV infection is a prominent feature provide a unique opportunity to study the importance of specific immune components for HPV control. Therefore, continuing this project will have importance for a) understanding skin immunology especially in relation to HPV and b) enabling the development of better future therapies for HPV. Given the high prevalence of cutaneous HPV infections in other immunosuppressed patient groups and the general population, further research might potentially have great impact.

**8. Appendix – Using MmuPV1 in  $\gamma$ -chain deficient mice to study infection**

## 8.1 Introduction

It has been suggested that PVs are ubiquitously present in all amniotes, therefore, it was not surprising when MmuPV1 was found, the first PV that is able to infect laboratory mice (146). In the past years, advances have been made in order to characterise the tissue tropism of MmuPV1 and the susceptibility of different mouse strains to MmuPV1 infection.

Lack of available animal models has impeded the study of PV infection *in vivo* using an X-SCID specific model. With the discovery of MmuPV1, studies about the role of  $\gamma$ -chain have become possible as MmuPV1 can be used to infect X-SCID mouse models.

X-SCID patients are commonly infected with cutaneous  $\beta$ -type HPVs. MmuPV1 – at the current state of research – most closely resembles  $\beta$ -type HPVs (151) and therefore it would be a suitable model to examine the reasons for increased susceptibility to HPV infections in X-SCID patients.

In this chapter, a preliminary study of MmuPV1 infection using the C57/BL6  $\gamma$ -chain knock-out strain B6.129S4-*Il2rg*<sup>tm1Wjl</sup>/J is presented. Experiments were performed at Prof. Paul Lambert's lab, using the animal facilities of the University of Wisconsin-Madison with the help and supervision of Aayushi Uberoi and Amy Liem under the licence held by Prof. Paul Lambert.

## 8.2 MmuPV1 infection can successfully be established in $\gamma$ -chain KO mice

In order to check whether MmuPV1 was able to induce wart formation in  $\gamma$ -chain knock-out mice, both KO mice and wild type animals were infected with MmuPV1 at a concentration of  $1 * 10^8$  vge/site (“viral genome equivalents” as determined by Southern blot) and lesion formation was monitored once a week.

Around 3 – 4 weeks after inoculation with the virus, 80% of KO animals had developed lesions. None of the lesions spontaneously regressed. In contrast, none of the WT animals developed lesions after infection with MmuPV1.

This preliminary result suggests that MmuPV1 can be used to infect  $\gamma$ -chain knock-out mice which can be further used to examine the defects seen in X-SCID patients.

**Table 17: Formation of wart lesions in mice**

| <b>Genotype</b> | <b>Application</b> | <b>Animals tested</b> | <b>Animals developing lesions</b> |
|-----------------|--------------------|-----------------------|-----------------------------------|
| IL2RG -/-       | MmuPV1             | 5                     | 4                                 |
| WT BL6          | MmuPV1             | 3                     | 0                                 |
| WT BL6          | PBS                | 2                     | 0                                 |

### 8.3 Skin grafting model for studying HPV infection in X-SCID skin

Infecting  $\gamma$ -chain knock-out mice does not accurately reflect the situation in X-SCID patients post-BMT. Human patients are only lacking  $\gamma$ -chain in the skin as T cell immunity has been successfully restored. To further mimic the clinical setting, we aimed to develop a murine model in which  $\gamma$ -chain is only lacking in the skin.

There are two different possibilities: a) transplanting bone marrow from WT mice into  $\gamma$ -chain knock-out mice; b) grafting  $\gamma$ -chain knock-out mouse skin onto WT mice. As transplanting bone marrow in mice results in variable reconstitution of cellular immunity, we decided to employ a skin graft model. In addition, whether a skin graft is successful can be easily detected by just examining the transplanted skin patch, rather than analysing the blood of the mice as needed when doing BMT.

Different parts of the mouse skin show different susceptibilities to MmuPV1 infection. Whereas tail, ears and muzzle are easily infected, trunk skin is not (150). In this study, ear skin from  $\gamma$ -chain knock-out mice was transplanted onto the trunk of WT mice. Each mouse was transplanted with two ear skin pieces, one from a  $\gamma$ -chain knock-out and one from an age-matched WT mouse as control (Figure 46).

The engraftment of skin was checked one week after transplant by visual examination. Most grafts were successful; however, a few animals (~10%) did not survive the overall transplantation process.



**Figure 46: Successful skin transplant on a mouse**

Ear skin of donor mice was fitted onto a rectangular size patch onto the back of WT C57/BL6 mice. One donor skin patch was fitted to each site, with total of two grafts per animal. The image shows the successfully engrafted skin a week after transplantation.

#### **8.4 No lesions develop using the initial skin graft model for MmuPV1 infection studies**

Following successful skin transplantation of skin from  $\gamma$ -chain knock-out mice on WT mice, the grafted mice were infected with MmuPV1 a month post transplantation at the concentration of  $1 * 10^8$  vge/site as used in the previous experiment. The transplanted skin was carefully scarified and then virus was applied. None of the mice developed wart lesions even multiple months after virus inoculation.

In an unpublished study from the Lambert lab, it was shown that 60% of immunocompetent FVB/NJ and Balb/c mice developed wart lesions at tails and ears after 3 months when they were subjected to UVB irradiation at  $300 \text{ mJ/cm}^2$  before infection with MmuPV1. Of these warts, a certain percentage regressed over time.

Based on this, the mice engrafted with  $\gamma$ -chain knock-out mouse skin were treated with UVB at the dose of  $300 \text{ mJ/cm}^2$  and then infected with MmuPV1. However, there was no wart lesion formation in these transplanted animals treated with UVB.

These results suggest that in order for us to use a transplantation model, it will be necessary to find conditions in which wart lesion formation is possible.

## 8.5 Discussion

The discovery of MmuPV1 has had a big impact on the field of PV research as it allows for the development of new mouse models to study PV infection *in vivo*. To date, there are limited publications using this model to study the immune response to PV infections. We performed preliminary studies to show that  $\gamma$ -chain knock-out mice could be infected with MmuPV1 and that lesions formed in most animals. This result is not that surprising as these mice have a reduction in the absolute number of lymphocytes, limited numbers of mature B and T cells and completely lack NK cells (322) and as absence of T cells is associated with wart formation after MmuPV1 inoculation (151, 153). It is, however, worth noticing that the remaining T cell populations in  $\gamma$ -chain knock-out mice are not sufficient to combat MmuPV1 infection.

As X-SCID patients are only deficient for  $\gamma$ -chain in the skin, we aimed to create a skin graft model to mimic this situation. Grafting procedures were successful; however, none of the infected animals developed lesions even after UVB treatment. There are a number of possible reasons for this. As mentioned previously, the location of the inoculation with MmuPV1 is an important factor for the establishment of wart lesions with the back being one of the sites where lesions usually do not form. It has been hypothesized that this is due to unknown region-specific intracellular factors that influence the infection (150). Interestingly, a similar phenomenon was observed in X-SCID patients. Certain areas of the body are more commonly infected than others. Nearly all patients display warts on their hands, with face and feet also being a common location for wart formation. In contrast, neck, back and trunk are only affected in a few patients (236).

This site-specific susceptibility might also be accountable for the absence of lesion formation in our experiments. Full thickness skin from the ear of  $\gamma$ -chain knock-out mice was transplanted on the back of WT mice. It has been suggested that that region-specific gene expression in the skin can be regulated by the dermal fibroblasts and by the hypodermis which is located underneath the dermis (151). As only the epidermis and dermis were transplanted, factors coming from the hypodermis could potentially still play a role and affect viral life cycle progression. There is, however, no other area on the animal that is large enough to place a potential transplant which is the limiting factor for this model.

An alternative reason for the lack of wart formation could be the background mouse strain. The mice used were of the C57/BL6 background, which were the least susceptible mouse strain to MmuPV1 infection in different studies following partial immunosuppression or UVB treatment ((151) and unpublished data from the Lambert

lab).  $\gamma$ -chain knock-out mice are also available on a Balb/c background so it might be better to use this mouse strain as it has a higher susceptibility.

In conclusion, these preliminary results will help to inform future experiments with MmuPV1 in  $\gamma$ -chain knock-out mice. If it is not possible to modify the graft model to achieve wart formation, bone marrow transplantation is an alternative model to analyse the defects seen in X-SCID patients.

## 9. References

1. Fuchs E & Raghavan S (2002) Getting under the skin of epidermal morphogenesis. *Nature reviews. Genetics* 3(3):199-209.
2. Proksch E, Brandner JM, & Jensen J-M (2008) The skin: an indispensable barrier. *Experimental dermatology* 17(12):1063-1072.
3. Ross MHP, W. (2015) *Histology: A Text and Atlas* (Wolter Kluwer Health) 7th Ed.
4. Munde PB, Khandekar SP, Dive AM, & Sharma A (2013) Pathophysiology of merkel cell. *Journal of oral and maxillofacial pathology : JOMFP* 17(3):408-412.
5. Agar N & Young AR (2005) Melanogenesis: a photoprotective response to DNA damage? *Mutation research* 571(1-2):121-132.
6. Clausen BE & Kel JM (2010) Langerhans cells: critical regulators of skin immunity? *Immunology and cell biology* 88(4):351-360.
7. Nestle FO, Di Meglio P, Qin JZ, & Nickoloff BJ (2009) Skin immune sentinels in health and disease. *Nature reviews. Immunology* 9(10):679-691.
8. Rowden G (1975) Ultrastructural studies of keratinized epithelia of the mouse. III. Determination of the volumes of nuclei and cytoplasm of cells in murine epidermis. *The Journal of investigative dermatology* 64(1):1-3.
9. Fuchs E & Green H (1980) Changes in keratin gene expression during terminal differentiation of the keratinocyte. *Cell* 19(4):1033-1042.
10. Fuchs E (1990) Epidermal differentiation. *Current opinion in cell biology* 2(6):1028-1035.
11. Moll R, Divo M, & Langbein L (2008) The human keratins: biology and pathology. *Histochemistry and cell biology* 129(6):705-733.
12. Nelson WG & Sun TT (1983) The 50- and 58-kdalton keratin classes as molecular markers for stratified squamous epithelia: cell culture studies. *The Journal of cell biology* 97(1):244-251.
13. Eichner R & Kahn M (1990) Differential extraction of keratin subunits and filaments from normal human epidermis. *The Journal of cell biology* 110(4):1149-1168.
14. Fuchs E (1993) Epidermal differentiation and keratin gene expression. *Journal of cell science. Supplement* 17:197-208.
15. Eckhart L, Lippens S, Tschachler E, & Declercq W (2013) Cell death by cornification. *Biochimica et biophysica acta* 1833(12):3471-3480.
16. Mehrel T, et al. (1990) Identification of a major keratinocyte cell envelope protein, loricrin. *Cell* 61(6):1103-1112.
17. Rice RH & Green H (1979) Presence in human epidermal cells of a soluble protein precursor of the cross-linked envelope: activation of the cross-linking by calcium ions. *Cell* 18(3):681-694.
18. Eckert RL & Green H (1986) Structure and evolution of the human involucrin gene. *Cell* 46(4):583-589.
19. Resing KA, al-Alawi N, Blomquist C, Fleckman P, & Dale BA (1993) Independent regulation of two cytoplasmic processing stages of the intermediate filament-associated protein filaggrin and role of Ca<sup>2+</sup> in the second stage. *The Journal of biological chemistry* 268(33):25139-25145.
20. Manabe M, Sanchez M, Sun TT, & Dale BA (1991) Interaction of filaggrin with keratin filaments during advanced stages of normal human epidermal differentiation and in ichthyosis vulgaris. *Differentiation; research in biological diversity* 48(1):43-50.
21. Presland RB, Haydock PV, Fleckman P, Nirunsuksiri W, & Dale BA (1992) Characterization of the human epidermal profilaggrin gene. Genomic organization and identification of an S-100-like calcium binding domain at the amino terminus. *The Journal of biological chemistry* 267(33):23772-23781.
22. Blanpain C & Fuchs E (2009) Epidermal homeostasis: a balancing act of stem cells in the skin. *Nat Rev Mol Cell Biol* 10(3):207-217.

23. Fuchs E & Chen T (2013) A matter of life and death: self-renewal in stem cells. *EMBO Rep* 14(1):39-48.
24. Hsu YC, Li L, & Fuchs E (2014) Emerging interactions between skin stem cells and their niches. *Nature medicine* 20(8):847-856.
25. Mascré G, *et al.* (2012) Distinct contribution of stem and progenitor cells to epidermal maintenance. *Nature* 489(7415):257-262.
26. Di Meglio P, Perera GK, & Nestle FO (2011) The multitasking organ: recent insights into skin immune function. *Immunity* 35(6):857-869.
27. Chorro L, *et al.* (2009) Langerhans cell (LC) proliferation mediates neonatal development, homeostasis, and inflammation-associated expansion of the epidermal LC network. *The Journal of experimental medicine* 206(13):3089-3100.
28. Hoeffel G, *et al.* (2012) Adult Langerhans cells derive predominantly from embryonic fetal liver monocytes with a minor contribution of yolk sac-derived macrophages. *The Journal of experimental medicine* 209(6):1167-1181.
29. Merad M, *et al.* (2002) Langerhans cells renew in the skin throughout life under steady-state conditions. *Nature immunology* 3(12):1135-1141.
30. Kissenpfennig A, *et al.* (2005) Dynamics and function of Langerhans cells in vivo: dermal dendritic cells colonize lymph node areas distinct from slower migrating Langerhans cells. *Immunity* 22(5):643-654.
31. Kupper TS & Fuhlbrigge RC (2004) Immune surveillance in the skin: mechanisms and clinical consequences. *Nature reviews. Immunology* 4(3):211-222.
32. Bobr A, *et al.* (2010) Acute ablation of Langerhans cells enhances skin immune responses. *J Immunol* 185(8):4724-4728.
33. Gomez de Agüero M, *et al.* (2012) Langerhans cells protect from allergic contact dermatitis in mice by tolerizing CD8(+) T cells and activating Foxp3(+) regulatory T cells. *The Journal of clinical investigation* 122(5):1700-1711.
34. Malissen B, Tamoutounour S, & Henri S (2014) The origins and functions of dendritic cells and macrophages in the skin. *Nature reviews. Immunology* 14(6):417-428.
35. Liu K, *et al.* (2009) In vivo analysis of dendritic cell development and homeostasis. *Science* 324(5925):392-397.
36. Geissmann F, *et al.* (2010) Development of monocytes, macrophages, and dendritic cells. *Science* 327(5966):656-661.
37. Tamoutounour S, *et al.* (2013) Origins and functional specialization of macrophages and of conventional and monocyte-derived dendritic cells in mouse skin. *Immunity* 39(5):925-938.
38. Kobayashi M, *et al.* (2009) Expression of toll-like receptor 2, NOD2 and dectin-1 and stimulatory effects of their ligands and histamine in normal human keratinocytes. *The British journal of dermatology* 160(2):297-304.
39. Harder J & Nunez G (2009) Functional expression of the intracellular pattern recognition receptor NOD1 in human keratinocytes. *The Journal of investigative dermatology* 129(5):1299-1302.
40. Kalali BN, *et al.* (2008) Double-stranded RNA induces an antiviral defense status in epidermal keratinocytes through TLR3-, PKR-, and MDA5/RIG-I-mediated differential signaling. *J Immunol* 181(4):2694-2704.
41. Baker BS, Ovigne JM, Powles AV, Corcoran S, & Fry L (2003) Normal keratinocytes express Toll-like receptors (TLRs) 1, 2 and 5: modulation of TLR expression in chronic plaque psoriasis. *The British journal of dermatology* 148(4):670-679.
42. Lebre MC, *et al.* (2007) Human keratinocytes express functional Toll-like receptor 3, 4, 5, and 9. *The Journal of investigative dermatology* 127(2):331-341.

43. Gutowska-Owsiak D & Ogg GS (2012) The epidermis as an adjuvant. *The Journal of investigative dermatology* 132(3 Pt 2):940-948.
44. Uchi H, Terao H, Koga T, & Furue M (2000) Cytokines and chemokines in the epidermis. *Journal of dermatological science* 24 Suppl 1:S29-38.
45. Tokura Y, Kobayashi M, & Kabashima K (2008) Epidermal chemokines and modulation by antihistamines, antibiotics and antifungals. *Experimental dermatology* 17(2):81-90.
46. Grone A (2002) Keratinocytes and cytokines. *Veterinary immunology and immunopathology* 88(1-2):1-12.
47. Locksley RM, Killeen N, & Lenardo MJ (2001) The TNF and TNF receptor superfamilies: integrating mammalian biology. *Cell* 104(4):487-501.
48. Schroder K, Hertzog PJ, Ravasi T, & Hume DA (2004) Interferon-gamma: an overview of signals, mechanisms and functions. *Journal of leukocyte biology* 75(2):163-189.
49. Francisco-Cruz A, *et al.* (2014) Granulocyte-macrophage colony-stimulating factor: not just another haematopoietic growth factor. *Med Oncol* 31(1):774.
50. Basham TY, Nickoloff BJ, Merigan TC, & Morhenn VB (1984) Recombinant gamma interferon induces HLA-DR expression on cultured human keratinocytes. *The Journal of investigative dermatology* 83(2):88-90.
51. Black AP, *et al.* (2007) Human keratinocyte induction of rapid effector function in antigen-specific memory CD4+ and CD8+ T cells. *European journal of immunology* 37(6):1485-1493.
52. Wakem P, *et al.* (2000) Allergens and irritants transcriptionally upregulate CD80 gene expression in human keratinocytes. *The Journal of investigative dermatology* 114(6):1085-1092.
53. Symington FW & Santos EB (1991) Lysis of human keratinocytes by allogeneic HLA class I-specific cytotoxic T cells. Keratinocyte ICAM-1 (CD54) and T cell LFA-1 (CD11a/CD18) mediate enhanced lysis of IFN-gamma-treated keratinocytes. *J Immunol* 146(7):2169-2175.
54. Kim BS, *et al.* (2009) Keratinocytes function as accessory cells for presentation of endogenous antigen expressed in the epidermis. *The Journal of investigative dermatology* 129(12):2805-2817.
55. Doorbar J, *et al.* (2012) The biology and life-cycle of human papillomaviruses. *Vaccine* 30 Suppl 5:F55-70.
56. Peretti A, FitzGerald PC, Bliskovsky V, Buck CB, & Pastrana DV (2015) Hamburger polyomaviruses. *The Journal of general virology*.
57. Bravo IG, de Sanjose S, & Gottschling M (2010) The clinical importance of understanding the evolution of papillomaviruses. *Trends in microbiology* 18(10):432-438.
58. Bernard HU, *et al.* (2010) Classification of papillomaviruses (PVs) based on 189 PV types and proposal of taxonomic amendments. *Virology* 401(1):70-79.
59. de Villiers EM, Fauquet C, Broker TR, Bernard HU, & zur Hausen H (2004) Classification of papillomaviruses. *Virology* 324(1):17-27.
60. Schiffman M, Castle PE, Jeronimo J, Rodriguez AC, & Wacholder S (2007) Human papillomavirus and cervical cancer. *Lancet* 370(9590):890-907.
61. Smith JS, *et al.* (2007) Human papillomavirus type distribution in invasive cervical cancer and high-grade cervical lesions: a meta-analysis update. *International journal of cancer. Journal international du cancer* 121(3):621-632.
62. Watson M, *et al.* (2008) Using population-based cancer registry data to assess the burden of human papillomavirus-associated cancers in the United States: overview of methods. *Cancer* 113(10 Suppl):2841-2854.
63. Doorbar J (2005) The papillomavirus life cycle. *Journal of clinical virology : the official publication of the Pan American Society for Clinical Virology* 32 Suppl 1:S7-15.

64. Harwood CA, *et al.* (2004) Increased risk of skin cancer associated with the presence of epidermodysplasia verruciformis human papillomavirus types in normal skin. *The British journal of dermatology* 150(5):949-957.
65. Bouwes Bavinck JN, *et al.* (2010) Multicenter study of the association between betapapillomavirus infection and cutaneous squamous cell carcinoma. *Cancer research* 70(23):9777-9786.
66. Heilman CA, Law MF, Israel MA, & Howley PM (1980) Cloning of human papilloma virus genomic DNAs and analysis of homologous polynucleotide sequences. *Journal of virology* 36(2):395-407.
67. Ustav M, Ustav E, Szymanski P, & Stenlund A (1991) Identification of the origin of replication of bovine papillomavirus and characterization of the viral origin recognition factor E1. *The EMBO journal* 10(13):4321-4329.
68. McBride AA (2008) Replication and partitioning of papillomavirus genomes. *Advances in virus research* 72:155-205.
69. Baker TS, *et al.* (1991) Structures of bovine and human papillomaviruses. Analysis by cryoelectron microscopy and three-dimensional image reconstruction. *Biophysical journal* 60(6):1445-1456.
70. Buck CB, *et al.* (2008) Arrangement of L2 within the papillomavirus capsid. *Journal of virology* 82(11):5190-5197.
71. Duensing S & Munger K (2004) Mechanisms of genomic instability in human cancer: insights from studies with human papillomavirus oncoproteins. *International journal of cancer. Journal international du cancer* 109(2):157-162.
72. Dyson N, Howley PM, Munger K, & Harlow E (1989) The human papilloma virus-16 E7 oncoprotein is able to bind to the retinoblastoma gene product. *Science* 243(4893):934-937.
73. Lee JO, Russo AA, & Pavletich NP (1998) Structure of the retinoblastoma tumour-suppressor pocket domain bound to a peptide from HPV E7. *Nature* 391(6670):859-865.
74. Schulze A, *et al.* (1995) Cell cycle regulation of the cyclin A gene promoter is mediated by a variant E2F site. *Proceedings of the National Academy of Sciences of the United States of America* 92(24):11264-11268.
75. Zerfass K, *et al.* (1995) Sequential activation of cyclin E and cyclin A gene expression by human papillomavirus type 16 E7 through sequences necessary for transformation. *Journal of virology* 69(10):6389-6399.
76. Funk JO, *et al.* (1997) Inhibition of CDK activity and PCNA-dependent DNA replication by p21 is blocked by interaction with the HPV-16 E7 oncoprotein. *Genes & development* 11(16):2090-2100.
77. Zerfass-Thome K, *et al.* (1996) Inactivation of the cdk inhibitor p27KIP1 by the human papillomavirus type 16 E7 oncoprotein. *Oncogene* 13(11):2323-2330.
78. Scheffner M, Werness BA, Huibregtse JM, Levine AJ, & Howley PM (1990) The E6 oncoprotein encoded by human papillomavirus types 16 and 18 promotes the degradation of p53. *Cell* 63(6):1129-1136.
79. Scheffner M, Huibregtse JM, Vierstra RD, & Howley PM (1993) The HPV-16 E6 and E6-AP complex functions as a ubiquitin-protein ligase in the ubiquitination of p53. *Cell* 75(3):495-505.
80. Stanley MA & Sterling JC (2014) Host responses to infection with human papillomavirus. *Current problems in dermatology* 45:58-74.
81. Egawa N, Egawa K, Griffin H, & Doorbar J (2015) Human Papillomaviruses; Epithelial Tropisms, and the Development of Neoplasia. *Viruses* 7(7):3863-3890.
82. Schiller JT, Day PM, & Kines RC (2010) Current understanding of the mechanism of HPV infection. *Gynecologic oncology* 118(1 Suppl):S12-17.
83. Roberts JN, *et al.* (2007) Genital transmission of HPV in a mouse model is potentiated by nonoxynol-9 and inhibited by carrageenan. *Nature medicine* 13(7):857-861.

84. Boxman IL, *et al.* (1997) Detection of human papillomavirus DNA in plucked hairs from renal transplant recipients and healthy volunteers. *The Journal of investigative dermatology* 108(5):712-715.
85. Combita AL, *et al.* (2001) Gene transfer using human papillomavirus pseudovirions varies according to virus genotype and requires cell surface heparan sulfate. *FEMS microbiology letters* 204(1):183-188.
86. Johnson KM, *et al.* (2009) Role of heparan sulfate in attachment to and infection of the murine female genital tract by human papillomavirus. *Journal of virology* 83(5):2067-2074.
87. Richards KF, Mukherjee S, Bienkowska-Haba M, Pang J, & Sapp M (2014) Human papillomavirus species-specific interaction with the basement membrane-resident non-heparan sulfate receptor. *Viruses* 6(12):4856-4879.
88. Giroglou T, Florin L, Schafer F, Streeck RE, & Sapp M (2001) Human papillomavirus infection requires cell surface heparan sulfate. *Journal of virology* 75(3):1565-1570.
89. Richards RM, Lowy DR, Schiller JT, & Day PM (2006) Cleavage of the papillomavirus minor capsid protein, L2, at a furin consensus site is necessary for infection. *Proceedings of the National Academy of Sciences of the United States of America* 103(5):1522-1527.
90. Day PM & Schelhaas M (2014) Concepts of papillomavirus entry into host cells. *Current opinion in virology* 4:24-31.
91. Schelhaas M, *et al.* (2012) Entry of human papillomavirus type 16 by actin-dependent, clathrin- and lipid raft-independent endocytosis. *PLoS pathogens* 8(4):e1002657.
92. Spoden G, *et al.* (2008) Clathrin- and caveolin-independent entry of human papillomavirus type 16--involvement of tetraspanin-enriched microdomains (TEMs). *PloS one* 3(10):e3313.
93. Bergant Marusic M, Ozbun MA, Campos SK, Myers MP, & Banks L (2012) Human papillomavirus L2 facilitates viral escape from late endosomes via sorting nexin 17. *Traffic* 13(3):455-467.
94. Ustav M & Stenlund A (1991) Transient replication of BPV-1 requires two viral polypeptides encoded by the E1 and E2 open reading frames. *The EMBO journal* 10(2):449-457.
95. Chiang CM, *et al.* (1992) Viral E1 and E2 proteins support replication of homologous and heterologous papillomaviral origins. *Proceedings of the National Academy of Sciences of the United States of America* 89(13):5799-5803.
96. Ilves I, Kivi S, & Ustav M (1999) Long-term episomal maintenance of bovine papillomavirus type 1 plasmids is determined by attachment to host chromosomes, which is mediated by the viral E2 protein and its binding sites. *Journal of virology* 73(5):4404-4412.
97. Lorenz LD, Rivera Cardona J, & Lambert PF (2013) Inactivation of p53 rescues the maintenance of high risk HPV DNA genomes deficient in expression of E6. *PLoS pathogens* 9(10):e1003717.
98. Bedell MA, *et al.* (1991) Amplification of human papillomavirus genomes in vitro is dependent on epithelial differentiation. *Journal of virology* 65(5):2254-2260.
99. Buck CB, Thompson CD, Pang YY, Lowy DR, & Schiller JT (2005) Maturation of papillomavirus capsids. *Journal of virology* 79(5):2839-2846.
100. Day PM, Roden RB, Lowy DR, & Schiller JT (1998) The papillomavirus minor capsid protein, L2, induces localization of the major capsid protein, L1, and the viral transcription/replication protein, E2, to PML oncogenic domains. *Journal of virology* 72(1):142-150.
101. Griffin H, *et al.* (2012) E4 antibodies facilitate detection and type-assignment of active HPV infection in cervical disease. *PloS one* 7(12):e49974.

102. Kanodia S, Fahey LM, & Kast WM (2007) Mechanisms used by human papillomaviruses to escape the host immune response. *Current cancer drug targets* 7(1):79-89.
103. Rudolf MP, *et al.* (1999) Induction of HPV16 capsid protein-specific human T cell responses by virus-like particles. *Biological chemistry* 380(3):335-340.
104. Le Bon A & Tough DF (2002) Links between innate and adaptive immunity via type I interferon. *Current opinion in immunology* 14(4):432-436.
105. Diamond MS & Farzan M (2013) The broad-spectrum antiviral functions of IFIT and IFITM proteins. *Nature reviews. Immunology* 13(1):46-57.
106. Nees M, *et al.* (2001) Papillomavirus type 16 oncogenes downregulate expression of interferon-responsive genes and upregulate proliferation-associated and NF-kappaB-responsive genes in cervical keratinocytes. *Journal of virology* 75(9):4283-4296.
107. Tummers B & Burg SH (2015) High-risk human papillomavirus targets crossroads in immune signaling. *Viruses* 7(5):2485-2506.
108. Hasan UA, *et al.* (2007) TLR9 expression and function is abolished by the cervical cancer-associated human papillomavirus type 16. *J Immunol* 178(5):3186-3197.
109. Reiser J, *et al.* (2011) High-risk human papillomaviruses repress constitutive kappa interferon transcription via E6 to prevent pathogen recognition receptor and antiviral-gene expression. *Journal of virology* 85(21):11372-11380.
110. Um SJ, *et al.* (2002) Abrogation of IRF-1 response by high-risk HPV E7 protein in vivo. *Cancer letters* 179(2):205-212.
111. Park JS, *et al.* (2000) Inactivation of interferon regulatory factor-1 tumor suppressor protein by HPV E7 oncoprotein. Implication for the E7-mediated immune evasion mechanism in cervical carcinogenesis. *The Journal of biological chemistry* 275(10):6764-6769.
112. Li S, *et al.* (1999) The human papilloma virus (HPV)-18 E6 oncoprotein physically associates with Tyk2 and impairs Jak-STAT activation by interferon-alpha. *Oncogene* 18(42):5727-5737.
113. Sunthamala N, *et al.* (2014) E2 proteins of high risk human papillomaviruses down-modulate STING and IFN-kappa transcription in keratinocytes. *PloS one* 9(3):e91473.
114. Rincon-Orozco B, *et al.* (2009) Epigenetic silencing of interferon-kappa in human papillomavirus type 16-positive cells. *Cancer research* 69(22):8718-8725.
115. Stanley MA (2012) Epithelial cell responses to infection with human papillomavirus. *Clinical microbiology reviews* 25(2):215-222.
116. Barnard P & McMillan NA (1999) The human papillomavirus E7 oncoprotein abrogates signaling mediated by interferon-alpha. *Virology* 259(2):305-313.
117. Perea SE, Massimi P, & Banks L (2000) Human papillomavirus type 16 E7 impairs the activation of the interferon regulatory factor-1. *Int J Mol Med* 5(6):661-666.
118. Havard L, Rahmouni S, Boniver J, & Delvenne P (2005) High levels of p105 (NFKB1) and p100 (NFKB2) proteins in HPV16-transformed keratinocytes: role of E6 and E7 oncoproteins. *Virology* 331(2):357-366.
119. Spitkovsky D, Hehner SP, Hofmann TG, Moller A, & Schmitz ML (2002) The human papillomavirus oncoprotein E7 attenuates NF-kappa B activation by targeting the Ikappa B kinase complex. *The Journal of biological chemistry* 277(28):25576-25582.
120. Tummers B, *et al.* (2015) The interferon-related developmental regulator 1 is used by human papillomavirus to suppress NFkappaB activation. *Nat Commun* 6:6537.

121. Franchi L, Warner N, Viani K, & Nunez G (2009) Function of Nod-like receptors in microbial recognition and host defense. *Immunological reviews* 227(1):106-128.
122. Karim R, *et al.* (2011) Human papillomavirus deregulates the response of a cellular network comprising of chemotactic and proinflammatory genes. *PLoS one* 6(3):e17848.
123. Niebler M, *et al.* (2013) Post-translational control of IL-1beta via the human papillomavirus type 16 E6 oncoprotein: a novel mechanism of innate immune escape mediated by the E3-ubiquitin ligase E6-AP and p53. *PLoS pathogens* 9(8):e1003536.
124. Huang SM & McCance DJ (2002) Down regulation of the interleukin-8 promoter by human papillomavirus type 16 E6 and E7 through effects on CREB binding protein/p300 and P/CAF. *Journal of virology* 76(17):8710-8721.
125. Sperling T, *et al.* (2012) Human papillomavirus type 8 interferes with a novel C/EBPbeta-mediated mechanism of keratinocyte CCL20 chemokine expression and Langerhans cell migration. *PLoS pathogens* 8(7):e1002833.
126. Larsen CG, Anderson AO, Appella E, Oppenheim JJ, & Matsushima K (1989) The neutrophil-activating protein (NAP-1) is also chemotactic for T lymphocytes. *Science* 243(4897):1464-1466.
127. Leong CM, Doorbar J, Nindl I, Yoon HS, & Hibma MH (2010) Loss of epidermal Langerhans cells occurs in human papillomavirus alpha, gamma, and mu but not beta genus infections. *The Journal of investigative dermatology* 130(2):472-480.
128. Georgopoulos NT, Proffitt JL, & Blair GE (2000) Transcriptional regulation of the major histocompatibility complex (MHC) class I heavy chain, TAP1 and LMP2 genes by the human papillomavirus (HPV) type 6b, 16 and 18 E7 oncoproteins. *Oncogene* 19(42):4930-4935.
129. Ashrafi GH, Haghshenas MR, Marchetti B, O'Brien PM, & Campo MS (2005) E5 protein of human papillomavirus type 16 selectively downregulates surface HLA class I. *International journal of cancer. Journal international du cancer* 113(2):276-283.
130. Zhou F, Chen J, & Zhao KN (2013) Human papillomavirus 16-encoded E7 protein inhibits IFN-gamma-mediated MHC class I antigen presentation and CTL-induced lysis by blocking IRF-1 expression in mouse keratinocytes. *The Journal of general virology* 94(Pt 11):2504-2514.
131. Zhang B, *et al.* (2003) The E5 protein of human papillomavirus type 16 perturbs MHC class II antigen maturation in human foreskin keratinocytes treated with interferon-gamma. *Virology* 310(1):100-108.
132. Maglennon GA & Doorbar J (2012) The biology of papillomavirus latency. *The open virology journal* 6:190-197.
133. Nicholls PK, *et al.* (2001) Regression of canine oral papillomas is associated with infiltration of CD4+ and CD8+ lymphocytes. *Virology* 283(1):31-39.
134. Wilgenburg BJ, Budgeon LR, Lang CM, Griffith JW, & Christensen ND (2005) Characterization of immune responses during regression of rabbit oral papillomavirus infections. *Comparative medicine* 55(5):431-439.
135. Knowles G, O'Neil BW, & Campo MS (1996) Phenotypical characterization of lymphocytes infiltrating regressing papillomas. *Journal of virology* 70(12):8451-8458.
136. Coleman N, *et al.* (1994) Immunological events in regressing genital warts. *American journal of clinical pathology* 102(6):768-774.
137. Selvakumar R, Schmitt A, Iftner T, Ahmed R, & Wettstein FO (1997) Regression of papillomas induced by cottontail rabbit papillomavirus is associated with infiltration of CD8+ cells and persistence of viral DNA after regression. *Journal of virology* 71(7):5540-5548.

138. Savani BN, *et al.* (2008) Increased risk of cervical dysplasia in long-term survivors of allogeneic stem cell transplantation--implications for screening and HPV vaccination. *Biology of blood and marrow transplantation : journal of the American Society for Blood and Marrow Transplantation* 14(9):1072-1075.
139. Moscicki AB, *et al.* (2000) Prevalence of and risks for cervical human papillomavirus infection and squamous intraepithelial lesions in adolescent girls: impact of infection with human immunodeficiency virus. *Archives of pediatrics & adolescent medicine* 154(2):127-134.
140. Torres M, *et al.* (2015) Prevalence of beta and gamma human papillomaviruses in the anal canal of men who have sex with men is influenced by HIV status. *Journal of clinical virology : the official publication of the Pan American Society for Clinical Virology* 67:47-51.
141. Maglennon GA, McIntosh P, & Doorbar J (2011) Persistence of viral DNA in the epithelial basal layer suggests a model for papillomavirus latency following immune regression. *Virology* 414(2):153-163.
142. Amella CA, *et al.* (1994) Latent infection induced with cottontail rabbit papillomavirus. A model for human papillomavirus latency. *The American journal of pathology* 144(6):1167-1171.
143. Hibma MH (2012) The immune response to papillomavirus during infection persistence and regression. *The open virology journal* 6:241-248.
144. Okabayashi M, Angell MG, Christensen ND, & Kreider JW (1991) Morphometric analysis and identification of infiltrating leucocytes in regressing and progressing Shope rabbit papillomas. *International journal of cancer. Journal international du cancer* 49(6):919-923.
145. Nasir L & Campo MS (2008) Bovine papillomaviruses: their role in the aetiology of cutaneous tumours of bovids and equids. *Veterinary dermatology* 19(5):243-254.
146. Ingle A, *et al.* (2011) Novel laboratory mouse papillomavirus (MusPV) infection. *Veterinary pathology* 48(2):500-505.
147. Schulz E, *et al.* (2012) Isolation of three novel rat and mouse papillomaviruses and their genomic characterization. *PLoS one* 7(10):e47164.
148. Joh J, *et al.* (2011) Genomic analysis of the first laboratory-mouse papillomavirus. *The Journal of general virology* 92(Pt 3):692-698.
149. Joh J, *et al.* (2012) Molecular diagnosis of a laboratory mouse papillomavirus (MusPV). *Experimental and molecular pathology* 93(3):416-421.
150. Handisurya A, *et al.* (2013) Characterization of Mus musculus papillomavirus 1 infection in situ reveals an unusual pattern of late gene expression and capsid protein localization. *Journal of virology* 87(24):13214-13225.
151. Handisurya A, *et al.* (2014) Strain-specific properties and T cells regulate the susceptibility to papilloma induction by Mus musculus papillomavirus 1. *PLoS pathogens* 10(8):e1004314.
152. Cladel NM, *et al.* (2013) Secondary infections, expanded tissue tropism, and evidence for malignant potential in immunocompromised mice infected with Mus musculus papillomavirus 1 DNA and virus. *Journal of virology* 87(16):9391-9395.
153. Sundberg JP, *et al.* (2014) Immune status, strain background, and anatomic site of inoculation affect mouse papillomavirus (MmuPV1) induction of exophytic papillomas or endophytic trichoblastomas. *PLoS one* 9(12):e113582.
154. Cladel NM, *et al.* (2015) A novel pre-clinical murine model to study the life cycle and progression of cervical and anal papillomavirus infections. *PLoS one* 10(3):e0120128.
155. Noguchi M, Adelstein S, Cao X, & Leonard WJ (1993) Characterization of the human interleukin-2 receptor gamma chain gene. *The Journal of biological chemistry* 268(18):13601-13608.

156. Takeshita T, Asao H, Suzuki J, & Sugamura K (1990) An associated molecule, p64, with high-affinity interleukin 2 receptor. *International immunology* 2(5):477-480.
157. Takeshita T, *et al.* (1992) An associated molecule, p64, with IL-2 receptor beta chain. Its possible involvement in the formation of the functional intermediate-affinity IL-2 receptor complex. *J Immunol* 148(7):2154-2158.
158. Takeshita T, *et al.* (1992) Cloning of the gamma chain of the human IL-2 receptor. *Science* 257(5068):379-382.
159. Wang X, Rickert M, & Garcia KC (2005) Structure of the quaternary complex of interleukin-2 with its alpha, beta, and gammac receptors. *Science* 310(5751):1159-1163.
160. Rickert M, Boulanger MJ, Goriatcheva N, & Garcia KC (2004) Compensatory energetic mechanisms mediating the assembly of signaling complexes between interleukin-2 and its alpha, beta, and gamma(c) receptors. *Journal of molecular biology* 339(5):1115-1128.
161. Noguchi M, *et al.* (1993) Interleukin-2 receptor gamma chain: a functional component of the interleukin-7 receptor. *Science* 262(5141):1877-1880.
162. Russell SM, *et al.* (1993) Interleukin-2 receptor gamma chain: a functional component of the interleukin-4 receptor. *Science* 262(5141):1880-1883.
163. Giri JG, *et al.* (1994) Utilization of the beta and gamma chains of the IL-2 receptor by the novel cytokine IL-15. *The EMBO journal* 13(12):2822-2830.
164. Kimura Y, *et al.* (1995) Sharing of the IL-2 receptor gamma chain with the functional IL-9 receptor complex. *International immunology* 7(1):115-120.
165. Asao H, *et al.* (2001) Cutting edge: the common gamma-chain is an indispensable subunit of the IL-21 receptor complex. *J Immunol* 167(1):1-5.
166. Habib T, Senadheera S, Weinberg K, & Kaushansky K (2002) The common gamma chain (gamma c) is a required signaling component of the IL-21 receptor and supports IL-21-induced cell proliferation via JAK3. *Biochemistry* 41(27):8725-8731.
167. Giri JG, *et al.* (1995) Identification and cloning of a novel IL-15 binding protein that is structurally related to the alpha chain of the IL-2 receptor. *The EMBO journal* 14(15):3654-3663.
168. Rochman Y, Spolski R, & Leonard WJ (2009) New insights into the regulation of T cells by gamma(c) family cytokines. *Nature reviews. Immunology* 9(7):480-490.
169. Miyazaki T, *et al.* (1994) Functional activation of Jak1 and Jak3 by selective association with IL-2 receptor subunits. *Science* 266(5187):1045-1047.
170. Chen M, *et al.* (1997) The amino terminus of JAK3 is necessary and sufficient for binding to the common gamma chain and confers the ability to transmit interleukin 2-mediated signals. *Proceedings of the National Academy of Sciences of the United States of America* 94(13):6910-6915.
171. Rodig SJ, *et al.* (1998) Disruption of the Jak1 gene demonstrates obligatory and nonredundant roles of the Jaks in cytokine-induced biologic responses. *Cell* 93(3):373-383.
172. Leonard WJ (2001) Cytokines and immunodeficiency diseases. *Nature reviews. Immunology* 1(3):200-208.
173. Leonard WJ & O'Shea JJ (1998) Jaks and STATs: biological implications. *Annual review of immunology* 16:293-322.
174. Ahmed NN, Grimes HL, Bellacosa A, Chan TO, & Tsichlis PN (1997) Transduction of interleukin-2 antiapoptotic and proliferative signals via Akt protein kinase. *Proceedings of the National Academy of Sciences of the United States of America* 94(8):3627-3632.
175. Migone TS, *et al.* (1998) Functional cooperation of the interleukin-2 receptor beta chain and Jak1 in phosphatidylinositol 3-kinase recruitment and phosphorylation. *Molecular and cellular biology* 18(11):6416-6422.

176. Song G, Ouyang G, & Bao S (2005) The activation of Akt/PKB signaling pathway and cell survival. *Journal of cellular and molecular medicine* 9(1):59-71.
177. Ravichandran KS & Burakoff SJ (1994) The adapter protein Shc interacts with the interleukin-2 (IL-2) receptor upon IL-2 stimulation. *The Journal of biological chemistry* 269(3):1599-1602.
178. Murata T, Noguchi PD, & Puri RK (1996) IL-13 induces phosphorylation and activation of JAK2 Janus kinase in human colon carcinoma cell lines: similarities between IL-4 and IL-13 signaling. *J Immunol* 156(8):2972-2978.
179. Murata T, Noguchi PD, & Puri RK (1995) Receptors for interleukin (IL)-4 do not associate with the common gamma chain, and IL-4 induces the phosphorylation of JAK2 tyrosine kinase in human colon carcinoma cells. *The Journal of biological chemistry* 270(51):30829-30836.
180. Dubois S, Mariner J, Waldmann TA, & Tagaya Y (2002) IL-15Ralpha recycles and presents IL-15 In trans to neighboring cells. *Immunity* 17(5):537-547.
181. Olsen SK, *et al.* (2007) Crystal Structure of the interleukin-15.interleukin-15 receptor alpha complex: insights into trans and cis presentation. *The Journal of biological chemistry* 282(51):37191-37204.
182. Morgan DA, Ruscetti FW, & Gallo R (1976) Selective in vitro growth of T lymphocytes from normal human bone marrows. *Science* 193(4257):1007-1008.
183. Taniguchi T, *et al.* (1983) Structure and expression of a cloned cDNA for human interleukin-2. *Nature* 302(5906):305-310.
184. Trinchieri G, *et al.* (1984) Response of resting human peripheral blood natural killer cells to interleukin 2. *The Journal of experimental medicine* 160(4):1147-1169.
185. Zubler RH, *et al.* (1984) Activated B cells express receptors for, and proliferate in response to, pure interleukin 2. *The Journal of experimental medicine* 160(4):1170-1183.
186. Liao W, Lin JX, & Leonard WJ (2011) IL-2 family cytokines: new insights into the complex roles of IL-2 as a broad regulator of T helper cell differentiation. *Current opinion in immunology* 23(5):598-604.
187. Liao W, *et al.* (2008) Priming for T helper type 2 differentiation by interleukin 2-mediated induction of interleukin 4 receptor alpha-chain expression. *Nature immunology* 9(11):1288-1296.
188. Sakaguchi S, Yamaguchi T, Nomura T, & Ono M (2008) Regulatory T cells and immune tolerance. *Cell* 133(5):775-787.
189. Ahmadzadeh M & Rosenberg SA (2006) IL-2 administration increases CD4+ CD25(hi) Foxp3+ regulatory T cells in cancer patients. *Blood* 107(6):2409-2414.
190. Antony PA, *et al.* (2006) Interleukin-2-dependent mechanisms of tolerance and immunity in vivo. *J Immunol* 176(9):5255-5266.
191. Sadlack B, *et al.* (1995) Generalized autoimmune disease in interleukin-2-deficient mice is triggered by an uncontrolled activation and proliferation of CD4+ T cells. *European journal of immunology* 25(11):3053-3059.
192. Horak I (1995) Immunodeficiency in IL-2-knockout mice. *Clinical immunology and immunopathology* 76(3 Pt 2):S172-173.
193. Paul WE (1991) Interleukin-4: a prototypic immunoregulatory lymphokine. *Blood* 77(9):1859-1870.
194. Thurner B, *et al.* (1999) Generation of large numbers of fully mature and stable dendritic cells from leukapheresis products for clinical application. *Journal of immunological methods* 223(1):1-15.
195. Kuhn R, Rajewsky K, & Muller W (1991) Generation and analysis of interleukin-4 deficient mice. *Science* 254(5032):707-710.

196. Metwali A, *et al.* (1996) The granulomatous response in murine Schistosomiasis mansoni does not switch to Th1 in IL-4-deficient C57BL/6 mice. *J Immunol* 157(10):4546-4553.
197. Jankovic D, *et al.* (1999) Schistosome-infected IL-4 receptor knockout (KO) mice, in contrast to IL-4 KO mice, fail to develop granulomatous pathology while maintaining the same lymphokine expression profile. *J Immunol* 163(1):337-342.
198. Namen AE, *et al.* (1988) Stimulation of B-cell progenitors by cloned murine interleukin-7. *Nature* 333(6173):571-573.
199. Chazen GD, Pereira GM, LeGros G, Gillis S, & Shevach EM (1989) Interleukin 7 is a T-cell growth factor. *Proceedings of the National Academy of Sciences of the United States of America* 86(15):5923-5927.
200. Mazzucchelli R & Durum SK (2007) Interleukin-7 receptor expression: intelligent design. *Nature reviews. Immunology* 7(2):144-154.
201. Link A, *et al.* (2007) Fibroblastic reticular cells in lymph nodes regulate the homeostasis of naive T cells. *Nature immunology* 8(11):1255-1265.
202. Alves NL, van Leeuwen EM, Derks IA, & van Lier RA (2008) Differential regulation of human IL-7 receptor alpha expression by IL-7 and TCR signaling. *J Immunol* 180(8):5201-5210.
203. von Freeden-Jeffry U, *et al.* (1995) Lymphopenia in interleukin (IL)-7 gene-deleted mice identifies IL-7 as a nonredundant cytokine. *The Journal of experimental medicine* 181(4):1519-1526.
204. Peschon JJ, *et al.* (1994) Early lymphocyte expansion is severely impaired in interleukin 7 receptor-deficient mice. *The Journal of experimental medicine* 180(5):1955-1960.
205. Van Snick J, *et al.* (1989) Cloning and characterization of a cDNA for a new mouse T cell growth factor (P40). *The Journal of experimental medicine* 169(1):363-368.
206. Uyttenhove C, Simpson RJ, & Van Snick J (1988) Functional and structural characterization of P40, a mouse glycoprotein with T-cell growth factor activity. *Proceedings of the National Academy of Sciences of the United States of America* 85(18):6934-6938.
207. Renauld JC, Goethals A, Houssiau F, Van Roost E, & Van Snick J (1990) Cloning and expression of a cDNA for the human homolog of mouse T cell and mast cell growth factor P40. *Cytokine* 2(1):9-12.
208. Hauber HP, Bergeron C, & Hamid Q (2004) IL-9 in allergic inflammation. *International archives of allergy and immunology* 134(1):79-87.
209. Dugas B, *et al.* (1993) Interleukin-9 potentiates the interleukin-4-induced immunoglobulin (IgG, IgM and IgE) production by normal human B lymphocytes. *European journal of immunology* 23(7):1687-1692.
210. Townsend JM, *et al.* (2000) IL-9-deficient mice establish fundamental roles for IL-9 in pulmonary mastocytosis and goblet cell hyperplasia but not T cell development. *Immunity* 13(4):573-583.
211. Grabstein KH, *et al.* (1994) Cloning of a T cell growth factor that interacts with the beta chain of the interleukin-2 receptor. *Science* 264(5161):965-968.
212. Carson WE, *et al.* (1997) A potential role for interleukin-15 in the regulation of human natural killer cell survival. *The Journal of clinical investigation* 99(5):937-943.
213. Sato N, Patel HJ, Waldmann TA, & Tagaya Y (2007) The IL-15/IL-15Ralpha on cell surfaces enables sustained IL-15 activity and contributes to the long survival of CD8 memory T cells. *Proceedings of the National Academy of Sciences of the United States of America* 104(2):588-593.
214. Lodolce JP, *et al.* (1998) IL-15 receptor maintains lymphoid homeostasis by supporting lymphocyte homing and proliferation. *Immunity* 9(5):669-676.

215. Kennedy MK, *et al.* (2000) Reversible defects in natural killer and memory CD8 T cell lineages in interleukin 15-deficient mice. *The Journal of experimental medicine* 191(5):771-780.
216. Parrish-Novak J, *et al.* (2000) Interleukin 21 and its receptor are involved in NK cell expansion and regulation of lymphocyte function. *Nature* 408(6808):57-63.
217. Recher M, *et al.* (2011) IL-21 is the primary common gamma chain-binding cytokine required for human B-cell differentiation in vivo. *Blood* 118(26):6824-6835.
218. Yi JS, Du M, & Zajac AJ (2009) A vital role for interleukin-21 in the control of a chronic viral infection. *Science* 324(5934):1572-1576.
219. Elsaesser H, Sauer K, & Brooks DG (2009) IL-21 is required to control chronic viral infection. *Science* 324(5934):1569-1572.
220. Yano S, Komine M, Fujimoto M, Okochi H, & Tamaki K (2003) Interleukin 15 induces the signals of epidermal proliferation through ERK and PI 3-kinase in a human epidermal keratinocyte cell line, HaCaT. *Biochem Biophys Res Commun* 301(4):841-847.
221. Caruso R, *et al.* (2009) Involvement of interleukin-21 in the epidermal hyperplasia of psoriasis. *Nature medicine* 15(9):1013-1015.
222. Heufler C, *et al.* (1993) Interleukin 7 is produced by murine and human keratinocytes. *The Journal of experimental medicine* 178(3):1109-1114.
223. Hong CH, Chang KL, Wang HJ, Yu HS, & Lee CH (2015) IL-9 induces IL-8 production via STIM1 activation and ERK phosphorylation in epidermal keratinocytes: A plausible mechanism of IL-9R in atopic dermatitis. *Journal of dermatological science* 78(3):206-214.
224. Kovanen PE & Leonard WJ (2004) Cytokines and immunodeficiency diseases: critical roles of the gamma(c)-dependent cytokines interleukins 2, 4, 7, 9, 15, and 21, and their signaling pathways. *Immunological reviews* 202:67-83.
225. Buckley RH (2004) Molecular defects in human severe combined immunodeficiency and approaches to immune reconstitution. *Annual review of immunology* 22:625-655.
226. Gaspar HB, *et al.* (2013) How I treat severe combined immunodeficiency. *Blood* 122(23):3749-3758.
227. Antoine C, *et al.* (2003) Long-term survival and transplantation of haemopoietic stem cells for immunodeficiencies: report of the European experience 1968-99. *Lancet* 361(9357):553-560.
228. Gaspar HB, *et al.* (2004) Gene therapy of X-linked severe combined immunodeficiency by use of a pseudotyped gammaretroviral vector. *Lancet* 364(9452):2181-2187.
229. Hacein-Bey-Abina S, *et al.* (2008) Insertional oncogenesis in 4 patients after retrovirus-mediated gene therapy of SCID-X1. *The Journal of clinical investigation* 118(9):3132-3142.
230. Hacein-Bey-Abina S, *et al.* (2014) A modified gamma-retrovirus vector for X-linked severe combined immunodeficiency. *The New England journal of medicine* 371(15):1407-1417.
231. Roifman CM (2000) Human IL-2 receptor alpha chain deficiency. *Pediatric research* 48(1):6-11.
232. Caudy AA, Reddy ST, Chatila T, Atkinson JP, & Verbsky JW (2007) CD25 deficiency causes an immune dysregulation, polyendocrinopathy, enteropathy, X-linked-like syndrome, and defective IL-10 expression from CD4 lymphocytes. *The Journal of allergy and clinical immunology* 119(2):482-487.
233. Kotlarz D, *et al.* (2013) Loss-of-function mutations in the IL-21 receptor gene cause a primary immunodeficiency syndrome. *The Journal of experimental medicine* 210(3):433-443.
234. Horev L, *et al.* (2015) Generalized verrucosis and HPV-3 susceptibility associated with CD4 T-cell lymphopenia caused by inherited human interleukin-

- 7 deficiency. *Journal of the American Academy of Dermatology* 72(6):1082-1084.
235. Neven B, *et al.* (2009) Long-term outcome after hematopoietic stem cell transplantation of a single-center cohort of 90 patients with severe combined immunodeficiency. *Blood* 113(17):4114-4124.
236. Laffort C, *et al.* (2004) Severe cutaneous papillomavirus disease after haemopoietic stem-cell transplantation in patients with severe combined immune deficiency caused by common gamma cytokine receptor subunit or JAK-3 deficiency. *Lancet* 363(9426):2051-2054.
237. Gaspar HB, Harwood C, Leigh I, & Thrasher AJ (2004) Severe cutaneous papillomavirus disease after haematopoietic stem-cell transplantation in patients with severe combined immunodeficiency. *British journal of haematology* 127(2):232-233.
238. Kamili QU, *et al.* (2014) Severe cutaneous human papillomavirus infection associated with natural killer cell deficiency following stem cell transplantation for severe combined immunodeficiency. *The Journal of allergy and clinical immunology* 134(6):1451-1453 e1451.
239. Schmalstieg FC & Goldman AS (2002) Immune consequences of mutations in the human common gamma-chain gene. *Molecular genetics and metabolism* 76(3):163-171.
240. Frucht DM, *et al.* (2001) Unexpected and variable phenotypes in a family with JAK3 deficiency. *Genes and immunity* 2(8):422-432.
241. Pullen RP, Somberg RL, Felsburg PJ, & Henthorn PS (1997) X-linked severe combined immunodeficiency in a family of Cardigan Welsh corgis. *Journal of the American Animal Hospital Association* 33(6):494-499.
242. Jezyk PF, Felsburg PJ, Haskins ME, & Patterson DF (1989) X-linked severe combined immunodeficiency in the dog. *Clinical immunology and immunopathology* 52(2):173-189.
243. Henthorn PS, *et al.* (1994) IL-2R gamma gene microdeletion demonstrates that canine X-linked severe combined immunodeficiency is a homologue of the human disease. *Genomics* 23(1):69-74.
244. Felsburg PJ, Somberg RL, Hartnett BJ, Henthorn PS, & Carding SR (1998) Canine X-linked severe combined immunodeficiency. A model for investigating the requirement for the common gamma chain (gamma c) in human lymphocyte development and function. *Immunologic research* 17(1-2):63-73.
245. Felsburg PJ, *et al.* (1999) Canine X-linked severe combined immunodeficiency. *Veterinary immunology and immunopathology* 69(2-4):127-135.
246. Hartnett BJ, *et al.* (1999) Bone marrow transplantation for canine X-linked severe combined immunodeficiency. *Veterinary immunology and immunopathology* 69(2-4):137-144.
247. Goldschmidt MH, *et al.* (2006) Severe papillomavirus infection progressing to metastatic squamous cell carcinoma in bone marrow-transplanted X-linked SCID dogs. *Journal of virology* 80(13):6621-6628.
248. Bogunovic M, *et al.* (2006) Identification of a radio-resistant and cycling dermal dendritic cell population in mice and men. *The Journal of experimental medicine* 203(12):2627-2638.
249. Merad M, Collin M, & Bromberg J (2007) Dendritic cell homeostasis and trafficking in transplantation. *Trends in immunology* 28(8):353-359.
250. Kanitakis J, Petruzzo P, & Dubernard JM (2004) Turnover of epidermal Langerhans' cells. *The New England journal of medicine* 351(25):2661-2662.
251. Beilin C, *et al.* (2013) Dendritic cell-expressed common cytokine receptor gamma-chain is essential for effective IL-15 transpresentation to CD4+T cells at the immunological synapse. *Immunology* 140:156-156.

252. Choudhuri K, *et al.* (2013) Dendritic cell-expressed common gamma-chain recruits IL-15 for trans-presentation at the immunological synapse. *Journal of Immunology* 190.
253. Arima N, *et al.* (1992) Pseudo-high affinity interleukin 2 (IL-2) receptor lacks the third component that is essential for functional IL-2 binding and signaling. *The Journal of experimental medicine* 176(5):1265-1272.
254. Ishii N, *et al.* (1994) Impairment of ligand binding and growth signaling of mutant IL-2 receptor gamma-chains in patients with X-linked severe combined immunodeficiency. *J Immunol* 153(3):1310-1317.
255. Allen-Hoffmann BL, *et al.* (2000) Normal growth and differentiation in a spontaneously immortalized near-diploid human keratinocyte cell line, NIKS. *The Journal of investigative dermatology* 114(3):444-455.
256. Todaro GJ & Green H (1963) Quantitative studies of the growth of mouse embryo cells in culture and their development into established lines. *The Journal of cell biology* 17:299-313.
257. de Chaumont F, *et al.* (2012) Icy: an open bioimage informatics platform for extended reproducible research. *Nature methods* 9(7):690-696.
258. Record J, *et al.* (2015) Immunodeficiency and severe susceptibility to bacterial infection associated with a loss-of-function homozygous mutation of MKL1. *Blood*.
259. Yano S, Komine M, Fujimoto M, Okochi H, & Tamaki K (2003) Interleukin 15 induces the signals of epidermal proliferation through ERK and PI 3-kinase in a human epidermal keratinocyte cell line, HaCaT. *Biochemical and Biophysical Research Communications* 301(4):841-847.
260. Raingeaud J & Pierre J (2005) Interleukin-4 downregulates TNFalpha-induced IL-8 production in keratinocytes. *FEBS Lett* 579(18):3953-3959.
261. Nishio H, Matsui K, Tsuji H, Tamura A, & Suzuki K (2001) Immunolocalisation of the janus kinases (JAK)--signal transducers and activators of transcription (STAT) pathway in human epidermis. *Journal of anatomy* 198(Pt 5):581-589.
262. Kagami S, *et al.* (2005) Interleukin-4 and interleukin-13 enhance CCL26 production in a human keratinocyte cell line, HaCaT cells. *Clinical and experimental immunology* 141(3):459-466.
263. Zhang SQ, *et al.* (2008) Autoinhibition of IL-15 expression in KC cells is ERK1/2 and PI3K dependent. *Scandinavian journal of immunology* 68(4):397-404.
264. Distler JH, *et al.* (2005) Expression of interleukin-21 receptor in epidermis from patients with systemic sclerosis. *Arthritis and rheumatism* 52(3):856-864.
265. Luff JA, *et al.* (2014) Keratinocyte antiviral response to Poly(dA:dT) stimulation and papillomavirus infection in a canine model of X-linked severe combined immunodeficiency. *PloS one* 9(7):e102033.
266. Lindemann MJ, Benczik M, & Gaffen SL (2003) Anti-apoptotic signaling by the interleukin-2 receptor reveals a function for cytoplasmic tyrosine residues within the common gamma (gamma c) receptor subunit. *The Journal of biological chemistry* 278(12):10239-10249.
267. Johnson SE, Shah N, Panoskaltsis-Mortari A, & LeBien TW (2005) Murine and human IL-7 activate STAT5 and induce proliferation of normal human pro-B cells. *J Immunol* 175(11):7325-7331.
268. Lin JX, *et al.* (1995) The role of shared receptor motifs and common Stat proteins in the generation of cytokine pleiotropy and redundancy by IL-2, IL-4, IL-7, IL-13, and IL-15. *Immunity* 2(4):331-339.
269. Barrera-Oro JG, Smith KO, & Melnick JL (1962) Quantitation of papova virus particles in human warts. *Journal of the National Cancer Institute* 29:583-595.
270. Boyle WF, Riggs JL, Oshiro LS, & Lennette EH (1973) Electron microscopic identification of papova virus in laryngeal papilloma. *The Laryngoscope* 83(7):1102-1108.

271. Stauffer Y, Raj K, Masternak K, & Beard P (1998) Infectious human papillomavirus type 18 pseudovirions. *Journal of molecular biology* 283(3):529-536.
272. Unckell F, Streeck RE, & Sapp M (1997) Generation and neutralization of pseudovirions of human papillomavirus type 33. *Journal of virology* 71(4):2934-2939.
273. Zhao KN, Sun XY, Frazer IH, & Zhou J (1998) DNA packaging by L1 and L2 capsid proteins of bovine papillomavirus type 1. *Virology* 243(2):482-491.
274. Meyers C, Frattini MG, Hudson JB, & Laimins LA (1992) Biosynthesis of human papillomavirus from a continuous cell line upon epithelial differentiation. *Science* 257(5072):971-973.
275. Meyers C, Mayer TJ, & Ozbun MA (1997) Synthesis of infectious human papillomavirus type 18 in differentiating epithelium transfected with viral DNA. *Journal of virology* 71(10):7381-7386.
276. Ozbun MA (2002) Infectious human papillomavirus type 31b: purification and infection of an immortalized human keratinocyte cell line. *The Journal of general virology* 83(Pt 11):2753-2763.
277. Buck CB, Pastrana DV, Lowy DR, & Schiller JT (2004) Efficient intracellular assembly of papillomaviral vectors. *Journal of virology* 78(2):751-757.
278. Buck CB & Thompson CD (2007) Production of papillomavirus-based gene transfer vectors. *Current protocols in cell biology / editorial board, Juan S. Bonifacino ... [et al.]* Chapter 26:Unit 26 21.
279. Kwak K, *et al.* (2014) Impact of inhibitors and L2 antibodies upon the infectivity of diverse alpha and beta human papillomavirus types. *PLoS one* 9(5):e97232.
280. Warren CJ, *et al.* (2014) The antiviral restriction factors IFITM1, 2 and 3 do not inhibit infection of human papillomavirus, cytomegalovirus and adenovirus. *PLoS one* 9(5):e96579.
281. Pyeon D, Pearce SM, Lank SM, Ahlquist P, & Lambert PF (2009) Establishment of human papillomavirus infection requires cell cycle progression. *PLoS pathogens* 5(2):e1000318.
282. Griffin LM, Cicchini L, & Pyeon D (2013) Human papillomavirus infection is inhibited by host autophagy in primary human keratinocytes. *Virology* 437(1):12-19.
283. Ruckert R, *et al.* (2000) Inhibition of keratinocyte apoptosis by IL-15: a new parameter in the pathogenesis of psoriasis? *J Immunol* 165(4):2240-2250.
284. Boukamp P, *et al.* (1988) Normal keratinization in a spontaneously immortalized aneuploid human keratinocyte cell line. *The Journal of cell biology* 106(3):761-771.
285. Schelhaas M, *et al.* (2008) Human papillomavirus type 16 entry: retrograde cell surface transport along actin-rich protrusions. *PLoS pathogens* 4(9):e1000148.
286. Flores ER, Allen-Hoffmann BL, Lee D, Sattler CA, & Lambert PF (1999) Establishment of the human papillomavirus type 16 (HPV-16) life cycle in an immortalized human foreskin keratinocyte cell line. *Virology* 262(2):344-354.
287. Lambert PF, *et al.* (2005) Using an immortalized cell line to study the HPV life cycle in organotypic "raft" cultures. *Methods in molecular medicine* 119:141-155.
288. Peh WL, *et al.* (2002) Life cycle heterogeneity in animal models of human papillomavirus-associated disease. *Journal of virology* 76(20):10401-10416.
289. Middleton K, *et al.* (2003) Organization of human papillomavirus productive cycle during neoplastic progression provides a basis for selection of diagnostic markers. *Journal of virology* 77(19):10186-10201.
290. Flores ER, Allen-Hoffmann BL, Lee D, & Lambert PF (2000) The human papillomavirus type 16 E7 oncogene is required for the productive stage of the viral life cycle. *Journal of virology* 74(14):6622-6631.

291. Merrick DT, Blanton RA, Gown AM, & McDougall JK (1992) Altered expression of proliferation and differentiation markers in human papillomavirus 16 and 18 immortalized epithelial cells grown in organotypic culture. *The American journal of pathology* 140(1):167-177.
292. Jones DL, Alani RM, & Munger K (1997) The human papillomavirus E7 oncoprotein can uncouple cellular differentiation and proliferation in human keratinocytes by abrogating p21Cip1-mediated inhibition of cdk2. *Genes & development* 11(16):2101-2111.
293. Westphal K, Akgul B, Storey A, & Nindl I (2009) Cutaneous human papillomavirus E7 type-specific effects on differentiation and proliferation of organotypic skin cultures. *Cellular oncology : the official journal of the International Society for Cellular Oncology* 31(3):213-226.
294. Chenoweth MJ, et al. (2012) IL-15 can signal via IL-15Ralpha, JNK, and NF-kappaB to drive RANTES production by myeloid cells. *J Immunol* 188(9):4149-4157.
295. Tong WW, et al. (2015) Human papillomavirus 16-specific T-cell responses and spontaneous regression of anal high-grade squamous intraepithelial lesions. *The Journal of infectious diseases* 211(3):405-415.
296. Hopfl R, et al. (2000) Spontaneous regression of CIN and delayed-type hypersensitivity to HPV-16 oncoprotein E7. *Lancet* 356(9246):1985-1986.
297. Peng S, et al. (2007) HLA-DQB1\*02-restricted HPV-16 E7 peptide-specific CD4+ T-cell immune responses correlate with regression of HPV-16-associated high-grade squamous intraepithelial lesions. *Clinical cancer research : an official journal of the American Association for Cancer Research* 13(8):2479-2487.
298. Kennedy-Crispin M, et al. (2012) Human keratinocytes' response to injury upregulates CCL20 and other genes linking innate and adaptive immunity. *The Journal of investigative dermatology* 132(1):105-113.
299. McDermott DH, et al. (2015) Chromothriptic cure of WHIM syndrome. *Cell* 160(4):686-699.
300. Luff JA, et al. (2013) Canine keratinocytes upregulate type I interferons and proinflammatory cytokines in response to poly(dA:dT) but not to canine papillomavirus. *Veterinary immunology and immunopathology* 153(3-4):177-186.
301. Chuntharapai A, Lee J, Hebert CA, & Kim KJ (1994) Monoclonal antibodies detect different distribution patterns of IL-8 receptor A and IL-8 receptor B on human peripheral blood leukocytes. *J Immunol* 153(12):5682-5688.
302. Lippert U, Zachmann K, Henz BM, & Neumann C (2004) Human T lymphocytes and mast cells differentially express and regulate extra- and intracellular CXCR1 and CXCR2. *Experimental dermatology* 13(8):520-525.
303. Sozzani S, et al. (1997) Receptor expression and responsiveness of human dendritic cells to a defined set of CC and CXC chemokines. *J Immunol* 159(4):1993-2000.
304. Wang JM, Xu L, Murphy WJ, Taub DD, & Chertov O (1996) IL-8-Induced T-Lymphocyte Migration: Direct as Well as Indirect Mechanisms. *Methods* 10(1):135-144.
305. Oppenheim JJ, Zachariae CO, Mukaida N, & Matsushima K (1991) Properties of the novel proinflammatory supergene "intercrine" cytokine family. *Annual review of immunology* 9:617-648.
306. Inngjerdigen M, Damaj B, & Maghazachi AA (2001) Expression and regulation of chemokine receptors in human natural killer cells. *Blood* 97(2):367-375.
307. Kershaw MH, et al. (2002) Redirecting migration of T cells to chemokine secreted from tumors by genetic modification with CXCR2. *Human gene therapy* 13(16):1971-1980.

308. Scimone ML, *et al.* (2005) Migration of polymorphonuclear leucocytes is influenced by dendritic cells. *Immunology* 114(3):375-385.
309. Hieshima K, *et al.* (1997) Molecular cloning of a novel human CC chemokine liver and activation-regulated chemokine (LARC) expressed in liver. Chemotactic activity for lymphocytes and gene localization on chromosome 2. *The Journal of biological chemistry* 272(9):5846-5853.
310. Liao F, *et al.* (1999) CC-chemokine receptor 6 is expressed on diverse memory subsets of T cells and determines responsiveness to macrophage inflammatory protein 3 alpha. *J Immunol* 162(1):186-194.
311. Greaves DR, *et al.* (1997) CCR6, a CC chemokine receptor that interacts with macrophage inflammatory protein 3alpha and is highly expressed in human dendritic cells. *The Journal of experimental medicine* 186(6):837-844.
312. Yang HT, Cohen P, & Rousseau S (2008) IL-1beta-stimulated activation of ERK1/2 and p38alpha MAPK mediates the transcriptional up-regulation of IL-6, IL-8 and GRO-alpha in HeLa cells. *Cellular signalling* 20(2):375-380.
313. Ovestad IT, *et al.* (2011) The impact of epithelial biomarkers, local immune response and human papillomavirus genotype in the regression of cervical intraepithelial neoplasia grades 2-3. *Journal of clinical pathology* 64(4):303-307.
314. Kollipara R, *et al.* (2015) Advancements in Pharmacotherapy for Noncancerous Manifestations of HPV. *Journal of clinical medicine* 4(5):832-846.
315. Hislop AD (2015) Early virological and immunological events in Epstein-Barr virus infection. *Current opinion in virology* 15:75-79.
316. Bilu D & Sauder DN (2003) Imiquimod: modes of action. *The British journal of dermatology* 149 Suppl 66:5-8.
317. Schon MP & Schon M (2007) Imiquimod: mode of action. *The British journal of dermatology* 157 Suppl 2:8-13.
318. Nambudiri VE, *et al.* (2013) Successful treatment of perianal giant condyloma acuminatum in an immunocompromised host with systemic interleukin 2 and topical cidofovir. *JAMA dermatology* 149(9):1068-1070.
319. Hamblin TJ (2007) Long-lasting response of therapy-resistant viral warts to treatment with interleukin-2 in a patient with chronic lymphocytic leukemia (CLL) and profound immunodeficiency. *Leukemia research* 31(3):413-414.
320. Lichti U, Anders J, & Yuspa SH (2008) Isolation and short-term culture of primary keratinocytes, hair follicle populations and dermal cells from newborn mice and keratinocytes from adult mice for in vitro analysis and for grafting to immunodeficient mice. *Nature protocols* 3(5):799-810.
321. Handisurya A, *et al.* (2012) Murine skin and vaginal mucosa are similarly susceptible to infection by pseudovirions of different papillomavirus classifications and species. *Virology* 433(2):385-394.
322. Cao X, *et al.* (1995) Defective lymphoid development in mice lacking expression of the common cytokine receptor gamma chain. *Immunity* 2(3):223-238.